



University
of Glasgow

Alkhaldi, Abdulsalam Abdulhadi (2012) *Drug development against kinetoplastid parasites*. PhD thesis.

<http://theses.gla.ac.uk/3637/>

Copyright and moral rights for this thesis are retained by the author

A copy can be downloaded for personal non-commercial research or study

This thesis cannot be reproduced or quoted extensively from without first obtaining permission in writing from the Author

The content must not be changed in any way or sold commercially in any format or medium without the formal permission of the Author

When referring to this work, full bibliographic details including the author, title, awarding institution and date of the thesis must be given

Drug Development against Kinetoplastid Parasites

Abdulsalam Abdulhadi Alkhaldi

This Thesis is submitted in fulfilment of the requirements for the
degree of Doctor of Philosophy

**Institute of Infection, Immunity & Inflammation
College of Medical, Veterinary & Life Sciences
University of Glasgow**

September 2012

Abstract

Human African trypanosomiasis and leishmaniasis are caused by parasites belonging to the genera *Trypanosoma* and *Leishmania*, respectively. Significant numbers of people are affected by these diseases worldwide, which are fatal if untreated. Animals can also be infected, posing agricultural and economic hindrances, especially in poor countries. Although chemotherapy can be used for treatment, many problems are associated with it, including drug toxicity, resistance, lack of guaranteed supply, and high treatment cost. Therefore, there is an urgent need for new treatment approaches. Here, we aim to examine the *in vitro* efficacy of curcumin and phosphonium compounds against these parasites, assay their toxicity to human kidney cells *in vitro*, and investigate the mechanism of antiparasite activity of curcumin.

The Alamar blue assay was used to test 158 curcumin analogues against *Leishmania major* promastigotes and *Leishmania mexicana* promastigotes and axenic amastigotes to obtain *in vitro* EC₅₀ values. Many curcumin compounds such as AS-HK122 and AS-HK126 exhibited anti-leishmanial activities similar to or better than the current clinical drug pentamidine. Similarly, EC₅₀ values of 83 phosphonium compounds against *Trypanosoma brucei brucei* bloodstream forms were determined. More than 20% of the tested compounds were found to be more active than the standard veterinary drug diminazene aceturate. Multi-drug resistant strains were used to determine that there is no cross-resistance between the tested compounds and the diamidine or melaminophenyl arsenical classes of trypanocides.

Structure activity relationship (SAR) analysis revealed that mono-*O*-demethylated curcumin compounds showed 10-fold higher activity against the parasites than curcumin. The addition of one or two pentyl pyridinium (C₁₀H₁₅N) groups on specific positions of the aromatic ring also increased the activity of these compounds. Furthermore, curcumin compounds with an isoxazole ring instead of the diketo motif showed higher activity and the lowest EC₅₀ values. Similarly, pentyl bromide (OC₅H₁₀Br) substitutions on the phenyl rings improved the antiparasitic activity. Curcuminoids with trienone linkers showed increased antiparasitic activity against all parasites tested.

Eighty-three phosphonium analogues were tested against *T. brucei brucei*. SAR analysis indicated that the bulky substituents surrounding the bisphosphonium cations led to strong antiparasitic activity while the nature of the linker had less effect on the activity. Some monophosphonium analogues registered the lowest EC₅₀ values of all the phosphonium compounds.

The toxicity of the curcumin and phosphonium analogues to HEK cells was analysed *in vitro*. All curcumin and phosphonium compounds demonstrated lower toxicity to HEK cells than to the parasites. Of the 83 phosphonium compounds, 60 displayed >200-fold *in vitro* selectivity index (SI).

We also investigated the mode of antiparasitic activity of curcumin compounds. Preliminary toxicity tests had revealed that AS-HK014 caused rapid depletion of glutathione content in rat hepatocytes. Therefore, we tested AS-HK014 activity in the presence of different concentrations of L-glutathione, and AS-HK014 activity was found to decrease with increased L-glutathione concentrations, strongly suggesting that glutathione reacted with the active compound. Indeed, a chemical adduct was observed between the two compounds and identified through mass spectrometry.

A trypanosome cell line (TA014) adapted to AS-HK014 was produced. TA014 and wild-type *T. brucei brucei* were treated with AS-HK014 and compared with each other and with untreated controls. The glutathione and trypanothione levels were lower in the treated WT cells than in the untreated cells. However, there was no change in the glutamate, ornithine, or spermidine levels, providing no evidence for the inhibition of trypanothione synthesis, suggesting that the effect is probably not metabolic but chemical.

AS-HK014 did not significantly affect thiol levels in TA014; this might reflect a higher level of trypanothione synthesis through increased glutathione synthetase (GS) and/or γ -glutamylcysteine synthetase (γ -GCS) expression. Therefore, we analysed the protein levels using western blotting, and sequenced the encoding genes in both WT and TA014 to identify any mutations in the open reading frames (ORFs). However, we found no changes in the GS and γ -GCS protein levels in resistant trypanosomes and no mutations were found in the GS and γ -GCS ORFs. It is clear that the resistance is to the reactive enone motif of AS-

HK014 rather than to curcumin and curcuminoids in general, since TA014 only displayed resistance to AS-HK014 analogues bearing the enone motif while sensitivity to curcumin remained unchanged, confirming that this motif is responsible for the higher activity of AS-HK014 compared to curcumin.

The effects of bisphosphonium analogues on *T. brucei brucei* bloodstream forms were investigated to identify the target. All tested analogues rapidly reduced the *T. brucei brucei* mitochondrial membrane potential Ψ_m and decreased the intracellular ATP level after one hour of incubation, suggesting that the compounds may be targeting the mitochondria. The intracellular Ca^{2+} levels increased gradually after eight hours, suggesting that the damaged mitochondria are unable to retain the stored Ca^{2+} as their membrane potential dissipates.

We also studied the trypanosome cell cycle after incubating the parasites with bisphosphonium compounds. The cell cycle defects became apparent after eight hours of incubation: DNA synthesis could not be initiated, leading to a dramatic reduction of cells in the S phase. This result was also confirmed by fluorescence microscopic assessment of DNA configuration. After eight hours of incubation with the bisphosphonium compound CD38, the number of 2K1N cells significantly decreased as compared with the control. There may be a causal relationship between mitochondrial damage and cell cycle defects. Transmission electron microscopy images of the cells obtained after 12 h of exposure to CD38 also revealed the presence of mitochondrial damage.

We tested whether bisphosphonium compounds can induce programmed cell death in trypanosomes. A TUNEL assay was used to detecting DNA fragmentation; the results showed increased DNA fragmentation after 24-h treatment with two different bisphosphonium compounds, CD38 and EFpI7. This result indicates is consistent with apoptosis occurring in treated cells but there was no evidence suggesting that bisphosphonium-induced cell death in trypanosomes is dependent on new protein synthesis.

In conclusion, curcumin and phosphonium analogues exhibit promising antiparasitic activity, and some analogues could be optimised for in vivo evaluation. Further investigations on the site of action of phosphonium compounds in the mitochondrion are in progress.

Table of Contents

1	CHAPTER ONE: Introduction	1
1.1	Human African Trypanosomiasis (HAT)	2
1.1.1	Disease	2
1.1.2	Morphology	4
1.1.3	Life Cycle	5
1.1.4	Clinical manifestations of the disease	7
1.1.5	Diagnosis	7
1.1.6	The control of HAT	8
1.1.7	Treatment of HAT	9
1.1.8	Drug Resistance	14
1.2	Leishmaniasis	15
1.2.1	Disease	16
1.2.2	Morphology	17
1.2.3	Life cycle	18
1.2.4	Clinical Disease	19
1.2.5	Diagnosis	21
1.2.6	The control of Leishmaniasis	21
1.2.7	Treatment of leishmaniasis	22
1.2.8	Drug Resistance	27
1.3	Transporters in kinetoplastids and their importance in drugs development	27
1.4	Trypanosome metabolism	29
1.4.1	Thiol metabolism	29
1.4.2	The role of mitochondria in bloodstream form <i>T. b. brucei</i>	30
1.5	Trypanosome signalling pathways	31
1.5.1	cAMP	31
1.5.2	Calcium Ions	32
1.6	Mode of Action Studies	33
1.7	New drugs for protozoa	34
1.8	Treatment of protozoan infections by natural products and their derivatives	35
1.8.1	Quinolines in malaria	37
1.8.2	Antibiotics	38
1.8.3	Curcumin	39
1.8.4	Artemisinin	41
1.9	Aims	42
2	Chapter two: Material and Methods	43
2.1	Cell culture	44
2.1.1	<i>Trypanosoma brucei</i> blood stream forms (BSF) in-vitro:	44
2.1.2	<i>Leishmania mexicana</i> & <i>Leishmania major</i> Promastigotes:	44
2.1.3	<i>Leishmania mexicana</i> amastigotes:	44
2.1.4	Human embryonic kidney (HEK) cells (strain 293T):	45
2.1.5	Bacterial strains:	45
2.2	Preparation of stabilates	46
2.3	Drug sensitivity using Alamar blue	46
2.3.1	Drug sensitivity using Alamar Blue assay in bloodstream forms of <i>T. b. brucei</i>	47
2.3.2	Drug sensitivity using Alamar Blue assay in <i>Leishmania mexicana</i> amastigotes	48
2.3.3	Drug sensitivity using Alamar Blue assay in <i>L. mexicana</i> and <i>L. major</i> promastigotes	48

2.3.4	Alamar Blue assay in Human Embryonic Kidney (HEK) Cells.....	49
2.4	Drug sensitivity using Cell count	50
2.5	Drug sensitivity using Propidium Iodide assay	50
2.6	Determination of the mitochondrial membrane potential by flow cytometry	51
2.7	Cell cycle using flow cytometry	51
2.8	Measurement of intracellular calcium level	52
2.9	DNA configuration assessment using fluorescence microscopy	53
2.10	Giemsa Staining	53
2.11	Live Cell Imaging	53
2.12	Transmission Electron Microscopy	54
2.13	Scanning Electron Microscopy	55
2.14	ATP Determination.....	55
2.15	TUNEL Assay	56
2.16	Counting Cells treated with Cycloheximide (CHX)	57
2.16.1	Pulse Labelling of Protein Pool in <i>T. b. brucei</i>	57
2.17	Induction of <i>T. b. brucei</i> cell lines resistant to AS-HK014 and curcumin 58	58
2.18	Metabolism of Curcumin in Trypanosomes	58
2.19	Measurement of Plasma Membrane Potential (V_m).....	59
2.20	Molecular techniques	60
2.20.1	Extraction of Genomic DNA.....	60
2.20.2	Polymerase Chain Reaction for DNA.....	60
2.20.3	Agarose Gel Electrophoresis of DNA.....	61
2.20.4	A-overhang of PCR product	62
2.20.5	Ligation into pGEMT-Easy Vector	62
2.20.6	Transformation of Escherichia Coli	62
2.20.7	PCR for Screening of Colonies.....	63
2.20.8	Plasmid DNA Purification.....	63
2.20.9	DNA Sequencing	63
2.21	Western Blotting	64
3	Chapter Three: Antiparasitic activity of curcumin analogues	65
3.1	Introduction	66
3.2	Results	67
3.3	Multi-drug resistant strains of <i>T. b. brucei</i> are not cross-resistant with curcumin analogues	91
3.4	Structural determinants of curcumin analogues important for antileishmanial activity - comparison with <i>T. b. brucei</i>	94
3.5	Selectivity of curcuminoids: therapeutic index relative to Human Embryonic Kidney cells	95
3.6	Discussion.....	99
4	Chapter four: Investigation into the mechanism of the trypanocidal activity of curcumin analogues bearing the enone motif.....	102
4.1	Introduction	103
4.2	Effect of curcuminoids on intracellular cAMP levels in trypanosomes..	105
4.3	Modulation of plasma membrane potential and intracellular calcium by curcuminoids	106
4.3.1	Effect of curcumin compounds on membrane potential.....	106
4.3.2	Effect of curcumin compounds on intracellular calcium level.....	107
4.4	Extracellular L-glutathione affects the trypanocidal activity AS-HK001 and AS-HK014.....	108
4.5	Induction of <i>T. b. brucei</i> cell lines resistant to AS-HK014 and to curcumin 110	110

4.6	Assessment of cross-resistance between <i>T. b. brucei</i> -WT and TA014 cell lines	111
4.7	Resistance profile of the ASHK014-adapted line TA014 and effect of L-glutathione on resistance.....	113
4.8	AS-HK014 makes a chemical adduct with glutathione	114
4.9	Metabolomic assessment of ASHK014 action on <i>T. b. brucei</i>	115
4.9.1	Experimental design.....	115
4.9.2	Metabolism of curcumin AS-HK014 in trypanosome: possible reactions with glutathione.....	117
4.10	Analysis of the protein expression levels of glutathione synthetase and γ -glutamylcysteine synthetase in wild-type and TA014 trypanosomes	125
4.11	Identification of Tb427.10.12370 and Tb427.07.4000 genes	126
4.11.1	Polymerase chain reaction.....	127
4.11.2	Sequence analysis	127
4.1	Discussion	129
5	CHAPTER Five: Phosphonium salts compounds as novel trypanocidel agents	133
5.1	Introduction	134
5.2	Assessment of the activity of phosphonium compounds on wild-type and multi-drug resistant trypanosome lines; determination of in vitro therapeutic index	136
5.2.1	In vitro activity on <i>T. b. brucei</i> bloodstream form	136
5.2.2	Assessment of cross-resistance	142
5.2.3	Cytotoxic activity of phosphonium compounds on Human Embryonic Kidney (HEK) cells and Therapeutic index values	142
5.3	Analysis of structural determinants of phosphonium analogues contributing to trypanocidal activity	143
5.4	Effect of test compounds on trypanosome proliferation after limited exposure	148
5.5	Monitoring the speed of action of test compound on Trypanosomes by using propidium iodide.....	150
5.6	Discussion.....	152
6	CHAPTER Six: Investigation into the mode of action of Bisphosphonium compounds in <i>T. b. brucei</i> bloodstream form.....	156
6.1	Introduction	157
6.2	Effect of test compounds on trypanosome growth	158
6.3	Bisphosphonium compounds strongly affect mitochondrial membrane potential (Ψ_m).....	161
6.4	Effects of bisphosphonium compounds on ATP levels in <i>T. b. brucei</i> ...	162
6.5	Effects of bisphosphonium compounds on intracellular calcium levels	165
6.6	Cell cycle analysis in bisphosphonium-exposed cells.....	166
6.7	Analysis of the effect of bisphosphonium compounds on DNA configuration using fluorescence microscopy.....	170
6.8	Microscopical investigation of cellular morphology after treatment with selected bisphosphonium analogues	173
6.8.1	Using Giemsa staining.....	173
6.8.2	Life cells images	174
6.9	Electron microscopy of trypanosomes exposed to bisphosphonium compounds (TEM and SEM)	176
6.9.1	Transmission electron microscopy (TEM).....	176
6.9.2	Scanning electron microscopy (SEM).....	181
6.10	Bisphosphonium-induced cell death in trypanosomes does not require protein synthesis.....	182

6.11	TUNEL assay.....	186
6.12	Discussion	189
7	Chapter Seven: General Discussion	193

List of Tables

Table 1.1. Major species and location of Leishmania which cause different types of the disease	15
Table 3.1. Structure and antileishmanial activity of curcumin analogues with a 3, 5-diketo, 1,6-diheptene linker. EC ₅₀ values are the average and SEM of at least three independent determinations.....	73
Table 3.2. Antileishmanial activity of some tetrahydro curcumin compounds, with saturated C ₇ linkers.	75
Table 3.3. The activity of hexahydro and octahydro curcumin analogues against <i>Leishmania</i> promastigotes and amastigotes.	75
Table 3.4. The activity of isoxazole curcumin compounds.....	77
Table 3.5. The activity of isoxazole curcumin compounds.....	79
Table 3.6. The activity of mono keto curcumin analogues.....	82
Table 3.7. The EC ₅₀ values of different curcumin analogues after introduction and reduction some chemical groups.	83
Table 3.8. . Anti-leishmanial activity of imine analogues of AS-HK014.	84
Table 3.9. Anti-leishmanial activity of AS-HK014 analogue with a different olefinic position.	85
Table 3.10. The effect of the dienone and trienone curcumin compounds	89
Table 3.11. Average EC ₅₀ values for curcumin compounds against <i>T. b. brucei</i> wild type, TbAT1- knockout and B48 blood stream form.	94
Table 3.12. : Average EC ₅₀ values for curcumin compounds against <i>T. b. brucei</i> wild type blood stream form, <i>L. mexicana</i> amastigotes.....	96
Table 4.1. Average EC ₅₀ values of some curcumin compounds and trypanocides as determined by Alamar Blue assay in bloodstream-form Tb427-WT and TA014.....	113
Table 5.1. Average EC ₅₀ values for phosphonium compounds against <i>T. b. brucei</i> wild type, TbAT1- knockout, and B48 bloodstream form plus standard errors.....	141
Table 5.2. Antitrypanosomal activity of bisphosphonium salts..	144
Table 5.3. Antitrypanosomal activity of bisphosphonium salts having substituted phenyl substituents..	145
Table 5.4. Antitrypanosomal activity of bisphosphonium salts having aryl groups or heterocycle substituents..	146
Table 5.5. Antitrypanosomal activity of monophosphonium salts.....	147

List of Figures

Figure 1.1. Distribution of human African trypanosomiasis (Brun <i>et al.</i> , 2010).....	3
Figure 1.2. The structure of <i>Trypanosoma brucei</i>	5
Figure 1.3. Life cycle of Trypanosomiasis.	6
Figure 1.4. Chemical Structures of drugs used against Trypanosomiasis.	14
Figure 1.5. Leishmaniasis is endemic in tropical, Asian and southern European countries.	16
Figure 1.6. The main intracellular organelles Leishmania Promastigote (left) and amastigote (right) (Besteiro <i>et al.</i> , 2007)	17
Figure 1.7. Life cycle of Leishmaniasis.....	19
Figure 1.8. Chemical structures of drugs used against Leishmaniasis.	26
Figure 2.1. explains the way drugs are doubly diluted down two rows across the plate. Indicates the drug free wells	48
Figure 3.1. Three dimensional structure of curcumin, and the corresponding isoxazole and Isoxazoline ring anaologues..	79
Figure 3.2. 3D structure of compounds 53 and 59, modelled with Chem3D Ultra (CambridgeSoft), (arrows indicate double bonds).	85
Figure 3.3. The effect of some curcumin compounds on bloodstream forms of three <i>T.</i> <i>b. brucei</i> strains, Tb427-WT (A), TbAT1-KO (B) and B48 (C) by using Alamar blue assay.....	92
Figure 4.1. Average intracellular cAMP in bloodstream-form <i>T. b. brucei</i>	105
Figure 4.2. Effect of curcumin compounds on the fluorescence of bisoxonol in bloodstream-form <i>T. b. brucei</i>	107
Figure 4.3. Effect of curcumin compounds on the intracellular calcium level in bloodstream-form <i>T. b. brucei</i>	108
Figure 4.4. EC ₅₀ values for AS-HK001 and AS-HK014 in the presence of various concentrations of glutathione.	109
Figure 4.5. Creation of the TA014 cell line. The drug concentration steadily increased for a period of about 11 months.	110
Figure 4.6. Average EC ₅₀ values of the clonal lines that were long-term exposed to AS- HK001 (A) or AS-HK014 (B) compared with wild-type <i>T. b. brucei</i> bloodstream forms.	111
Figure 4.7. Growth rates of WT 427 and TA014 trypanosomes.	111
Figure 4.8. EC ₅₀ values for curcumin AS-HK014 with various concentrations of glutathione.	114
Figure 4.9. Chemical reaction between curcumin AS-HK014 and glutathione (performed by Apichart Suksamrarn). 1: AS-HK014 and 2: adduct.	115

Figure 4.10. Effect of different concentrations of AS-HK014 on the growth curve of bloodstream form <i>T. brucei brucei</i> WT and TA014 resistance lines.	116
Figure 4.11. Dose response curve of the AS-HK014 compound for bloodstream-form <i>T. b. brucei</i> and TA014 resistance line..	117
Figure 4.12. Relative abundance of 915 putative metabolites from cells treated with ASHK-014 relative to untreated cells.....	118
Figure 4.13. Trypanothione pathway.....	119
Figure 4.14. Metabolomic analysis of the AS-HK014 compound in the <i>T. b. brucei</i> -WT and TA014 resistance line.	121
Figure 4.15. Spermidine pathway.....	122
Figure 4.16. Adduct levels of Trypanothione and Glutathione	124
Figure 4.17. Levels of AS-HK014 in WT s427 and TA014 trypanosomes as determined in a metabolomic experiment performed without mBBr treatment.....	125
Figure 4.18. Western blot of the <i>T. b. brucei</i> -WT and TA014 resistance lines.....	126
Figure 4.19. PCR amplification of G1 (γ -GCS) and G2 (GS) for both strains of bloodstream-form <i>T. b. b.</i> WT and TA014 resistance line.....	127
Figure 5.1. General structure of benzophenone-derived bisphosphonium salt derivatives with antileishmanial and antitrypanosomal	135
Figure 5.2. 1 Effect of bisphosphonium compounds AHI15 (A) and AHI16 (B) on the growth curve of the <i>T. b. b.</i> bloodstream	148
Figure 5.3. Effect of bisphosphonium compounds AHI15 (A) and AHI16 (B) on Tb427 wild type bloodstream form trypanosome proliferation.....	149
Figure 5.4. Dose response curve of the CD38 compound for the bloodstream form of various strains of <i>T. b. brucei</i>	151
Figure 6.1. Effect of different concentrations of four bisphosphonium compounds on the growth of bloodstream form <i>T. brucei brucei</i> WT over 96 h.....	160
Figure 6.2. Effect of Bisphosphonium compounds on mitochondrial membrane potential (Ψ_m).	162
Figure 6.3. ATP standard curve. A standard curve was generated by serial dilutions of ATP.	163
Figure 6.4. ATP concentration was measured using the ATP Determination Kit (Invitrogen) as described in section 2.12. 1×10^6 cells/ml of untreated and treated <i>T. b. brucei</i> bloodstream forms.	164
Figure 6.5. Effect of Bisphosphonium compounds on intracellular calcium levels of WT s427 bloodstream-form <i>T. brucei brucei</i>	166
Figure 6.6. An example for flow cytometry analysis of the DNA content of bloodstream-form	167

Figure 6.7. An example of flow cytometry analysis of DNA content by Modfit LT software for two samples, drug-free and CD38 (0.7 μ M), which were incubated for 16 hrs.	168
Figure 6.8. FACS analysis of DNA content of BSF <i>T. b. b.</i> for untreated and treated cells with bisphosphonium compounds.	169
Figure 6.9. Percentage of wild type Tb427 populations in each stage of the cell cycle, with and without incubation with CD38 (0.7 μ M) over 24 h.....	172
Figure 6.10. shows the cells under bright field light microscopy with the visualisation of BSF <i>T. b. b.</i> stained with Giemsa stain.....	174
Figure 6.11. shows the images of live WT-s427 trypanosome cell samples..	175
Figure 6.12. Transmission electron micrograph of an untreated bloodstream-form Tb427 wild type trypanosome..	176
Figure 6.13. Transmission electron micrograph of a wild type bloodstream-form Tb427 trypanosome. Control images taken at 0 h	177
Figure 6.14. Transmission electron micrograph of a wild type bloodstream-form Tb427 Trypanosome. Cells treated with 1 μ M CD38 and incubated for 12 hrs (image A) and 16 hrs (image B and C).....	178
Figure 6.15. Transmission electron micrograph of an untreated bloodstream-form Tb427 Trypanosome. Cells were treated with 1 μ M CD38 and incubated for 12 h.	179
Figure 6.16. Transmission electron micrograph of a wild type bloodstream-form Tb427 trypanosome. Cells were treated with 1 μ M CD38 and incubated for 16 h.	179
Figure 6.17. Transmission electron micrograph of a wild type bloodstream-form Tb427 trypanosome. Cells were treated with 1 μ M of CD38 and incubated for 16 h.	180
Figure 6.18. Transmission electron micrograph of a wild type bloodstream-form Tb427 trypanosome. Cells were treated with 1 μ M CD38 and incubated for 16 h.	181
Figure 6.19. Scanning electron microscopy of bloodstream-form <i>T. b. brucei</i> that were incubated for 20 h. A: Drug free; B, C and D incubated for 20 h with 1 μ M CD38.	182
Figure 6.20. Effect of different concentrations of bisphosphonium compounds on the growth curve of bloodstream-form <i>T. brucei brucei</i> WT over 24 hrs..	184
Figure 6.21. The graph shows the radioactivity count of a 10 ml culture of bloodstream-form <i>T. b. b.</i> at 5×10^6 cells/ml, which were incubated with (+CHX) and without (-CHX) 10 μ g/ml cycloheximide.	185
Figure 6.22. TUNEL assay of apoptotic cells of bloodstream-form <i>T. b. b.</i> that were treated with different compounds or left untreated and incubated for 24 h..	187
Figure 6.23. . TUNEL assay of DNA fragmentation cells of bloodstream-form <i>T. b. b.</i> that were treated with different compounds or left untreated.....	188

Acknowledgements

First of all, I acknowledge and thank God for his blessing, insight and support, which insure my success.

I gratefully acknowledge my supervisor, Dr. Harry de Koning, for his trust, guidance, encouragement and suggestions throughout these four years of work and study on my PhD. He provided me with the finest scientific counselling and guidance that I could ever wish for.

I also would like to thank my assessors, Dr. Tannsy Hammarton and Prof. Sylke Muller, for their advice and support, and all the people who contributed to this project.

I would like to thank all our collaborators: Dr. Christophe Dardonville, Dr. Chatchawan Changtam and Prof. Apichart Sukamran.

Very special thanks to my parents and all the members of my family back in Saudi Arabia for their support during my study, and to my beloved wife Maram Alolime, for her support and for being patient (especially for the long nights I spent away at work). Most importantly, appreciation is due my children, Motaz, Login, Bayan and Faris for the laughter and great times I had with them. Also, many thanks to my wife's family for their support.

I would also like to thank all my fellow students and the staff of GBRC, Level 5 and Level 6, Division of Infection, Immunity & Inflammation (University of Glasgow), in particular those in the Harry de Koning group (previous and current members): Ibrahim, Hasan, Mohammed, Juma, Antonius, Gordon, Matt, Jane and Neils for their support and encouragement.

Many thanks to Mike Barrett's group and those I shared the office with: Edward, Sultan, Nushin, Federica, Hyun, Isabel, Cora, Roy, David, Abhinav, Harshal and Suliman.

Special thanks to Dr. Darren Creek for his help with the metabolomics work, Dr. Laurence Tetley for helping in TEM and SEM work and Ms. Diane Vaughan for her help in FACS work.

This work received financial support from Aljouf University in the Kingdom of Saudi Arabia.

Author's declaration

I declare that the results presented in this thesis are my own work and that, to the best of my knowledge, it contains no material previously substantially overlapping with material submitted for the award of any other degree at any institution, except where due acknowledgment is made in the text.

Abdulsalam Alkhaldi

Aug 2012

List of Abbreviations

ABC	ATP- binding cassette
AC	Adenylyl cyclase
ApoL1	Apolipoprotein L1
ATP	Adenosine triphosphate
BBB	Blood brain barrier
bp	base pairs
BSF	Bloodstream form
Ca ²⁺	Calcium ion
cAMP	cyclic adenosine monophosphate
CATT	card agglutination trypanosomiasis test
CHX	cycloheximide
CIATT	card indirect agglutination trypanosomiasis test
CL	cutaneous leishmaniasis
CNS	central nervous system
CoMFA	Comparative molecular field analysis
CSF	cerebrospinal fluid
DAPCO	4-diazabicyclo[2.2.2]octane
DAPI	6-diamidino-2-phenylindole
DAT	Direct agglutination test
DCL	Diffuse cutaneous leishmaniasis
DDT	dichlorodiphenyltrichloroethane
DFMO	-alpha-difluoromethylornithine
DMSO	methyl sulphoxide
DNA	deoxyribonucleic acid
<i>E. coli</i>	<i>Escherichia coli</i>
EC ₅₀	effective concentration inhibiting 50% cell proliferation
EDTA	ethylenediamine tetra acetic acid
ELISA	enzyme-linked immunosorbence assay
Et	ethyl
EtoH	ethanol
FACS	fluorescence activated cell sorting
FCS	fetal calf serum

GS	glutathione synthetase
HAPT1	High-affinity pentamidine transporter
HAT	Human African Trypanosome
HCL	Hydrochloric acid
HEK	Human embryonic kidney
HMI9	Hirumi medium 9
HRP	Haptoglobin-related protein
h	hour
IC ₅₀	50% inhibitory concentration
IFAT	Immunofluorescence test
kDa	kilodalton
kDNA	kinetoplast DNA
KO	knockout
K	kinetoplast
LAPT1	low affinity pentamidine transporter
LDLs	low density lipoproteins
MCL	mucocutaneous leishmaniasis
Me	methane
MeT	melarsen-trypanothione adduct
ml	millilitre
ND	not determined
NG	negative control
nM	nanomolar
NS	not significant
N	nucleus
ODC	ornithine decarboxylase
ORF	open reading frame
P2	aminopurine transporter 2
PAO	Phenyl Arsine Oxide
PBS	phosphate-buffered saline
PCF	procyclic form
PCR	polymerase chain reaction
Ph	phenyl
PI	propidium iodide
PKDL	post-kala azar dermal leishmaniasis

Pr	propane
rpm	revolutions per minutes
SAR	structure activity relationship
SDM	schneider's drosophila medium
SDS	sodium dodocyl sulphate
SEM	scanning electron microscopy
SIT	sterile insect technique
TA014	resistant line of AS-HK014 compound
TAE	Tris-acetate buffer
TAO	Trypanosome alternative oxidase
TBS /T	Tris-base buffered saline + tween20
TCA	Trichloroacetic acid
TDR	Tropical diseases research
TEM	transmission electron microscopy
THC	tetrahydro curcumin
TI	therapeutic index
TLF	Trypanosome Lytic Factor
TMRE	Tetramethylrhodamine ethyl ester
TrypSyn	trypanothine synthetase
TryR	trypanothine reductase
TSH	trypanothione
TUNEL	Terminal deoxynucleotide transferase dUTP nick end labeling
UV	ultraviolet
VL	visceral leishmaniasis
V _m	Plasma Membrane Potential
VSG	variable surface glycoprotein
WHO	World Health Organisation
WT	wild type
γ-GCS	gamma-glutamylcysteine synthetase
μl	microlitre
μg	microgram
μM	micromolar

1 CHAPTER ONE: Introduction

People all over the world suffer from innumerable types of diseases, with many different causes. One frequent cause of disease is infection with microscopic organisms; namely, viruses, fungi, bacteria and protozoa. Protozoa come in a variety of forms; among them are *Trypanosoma* and *Leishmania*, both of which are transmitted by insect bites and affect many people in large geographical areas.

Sleeping sickness (Human African trypanosomiasis; HAT) and leishmaniasis are caused by species of protozoa called *Trypanosoma* and *Leishmania*, respectively, and are among the major tropical and subtropical diseases (Newton, 1974). These parasites both belong to the Trypanosomatidae family, which is responsible for a large number of diseases in both humans and animals. They share the same organelle, known as a kinetoplast; consequently, they fall into the Kinetoplastida order, a subdivision of the Zoomastigophora class.

1.1 Human African Trypanosomiasis (HAT)

1.1.1 Disease

Human African trypanosomiasis (HAT); or sleeping sickness, is one of the world's most neglected infectious diseases. It is caused by the protozoan parasite *Trypanosoma brucei*, which has three subspecies, *T. b. gambiense*, *T. b. rhodesiense*, and *T. b. brucei*. Each subspecies causes a distinct pathology (Barrett, 1999). The tsetse flies that transmit *T. b. gambiense* parasites are found in West and Central Africa, whereas *T. b. rhodesiense* is spread in East Africa. *T. b. brucei* is present throughout sub-Saharan Africa where tsetse flies are prevalent. *T. b. gambiense* causes the chronic form of sleeping sickness in humans, but is not thought to infect many animal species. *T. b. rhodesiense* leads to acute sleeping sickness in humans, developing very rapidly. This species is zoonotic, with a significant animal reservoir. *T. b. brucei* infects domestic and wild animals and is unable to infect to human due to Trypanosome Lytic Factor (TLF), which is found in human serum (Molina Portela *et al.*, 2000). There are two TLF, haptoglobin-related protein (HRP) and apolipoprotein L1 (ApoL1) (Drain *et al.*, 2001). By contrast, *T. b. gambiense* and *T. b. rhodesiense* are resistant to TLF and, as a result are infectious to humans (Molina Portela *et al.*,

2000). It is well known that certain species of tsetse flies (*Glossina*) act as intermediaries in the transfer of trypanosomiasis. The species responsible for *T. b. rhodesiense* is *Glossina morsitans*, whereas *Glossina palpalis* is the main carrier of *T. b. gambiense* (Garcia, 2007).

There are 36 countries in sub-Saharan African at risk from human African trypanosomiasis, and it is thus a threat to about 60 million people in these countries (Garcia, 2007). According to Barrett *et al* (Barrett *et al.*, 2003), the number of people infected with human African trypanosomiasis is around 500,000, resulting in 50,000 deaths per year. There were roughly 10,000 new cases of African trypanosomiasis in 2009 (Simarro *et al.*, 2011).

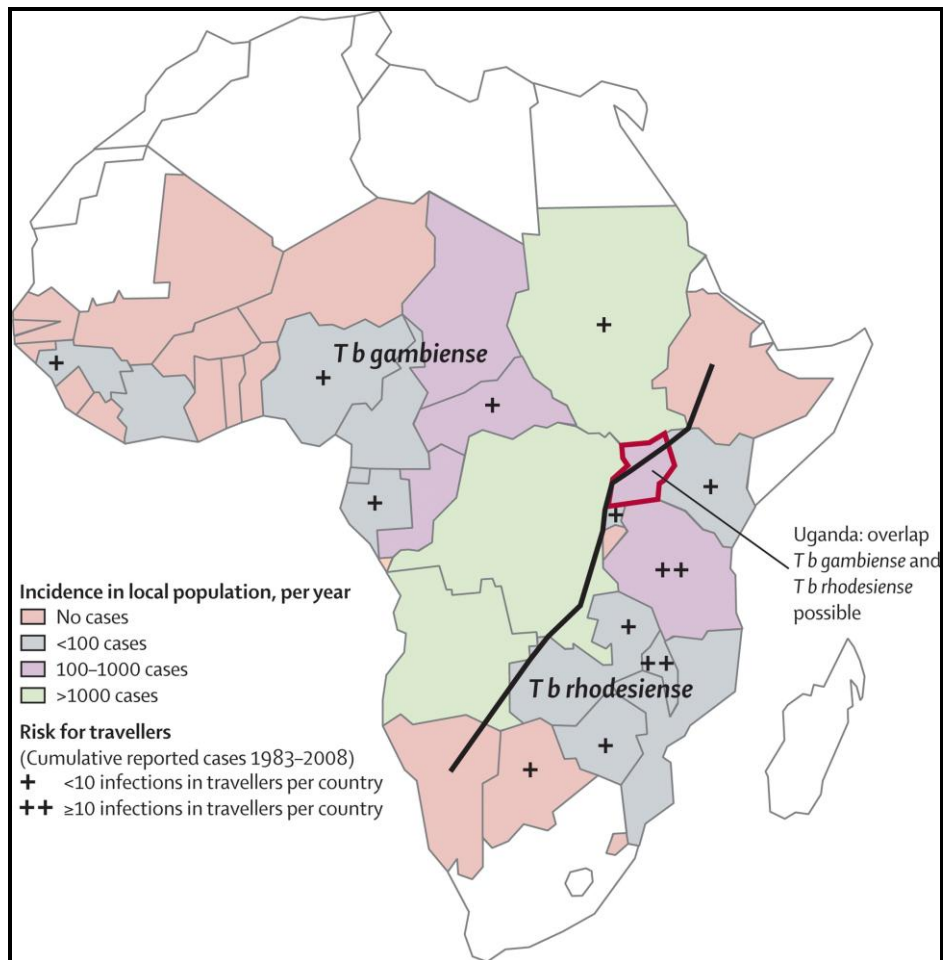


Figure 1.1. Distribution of human African trypanosomiasis (Brun *et al.*, 2010)

1.1.2 Morphology

Trypanosomes are eukaryotic cells, which belong to the order Kinetoplastida because they contain kinetoplasts. These cells have all the usual eukaryotic organelles, i.e. the nucleus, mitochondrion, endoplasmic reticulum, Golgi apparatus, lysosomes, and cell membrane. The trypanosome cell has is asymmetric, with clearly different anterior and posterior ends. Trypanosomes pass through five distinct forms during their life cycles in mammals and tsetse flies (Matthews, 2005). The origin of the flagellum is close to the posterior end of the cell, near the basal body, and passes along the cell, holding together a thin layer known as the undulating membrane, which connects the cell body and much of the flagellum. The kinetoplast is connected to the basal body. Trypanosomes have a fixed and flexible form and this contributes to the structure of the pellicle (Vickerman, 1974). The cell membrane consists of phospholipids, proteins, cholesterol, and glycolipids. In the bloodstream, a dense coat of variable surface glycoproteins (VSG) covers the trypanosome surface to protect it from the mammalian immune response (Garcia, 2007). The morphology of the two human-infective African trypanosomes is very similar and it can be difficult to differentiate between them on this basis alone. According to Hide and Tilley (Hide & Tilley, 2001) the different species of trypanosomes can best be distinguished from their DNA sequences.

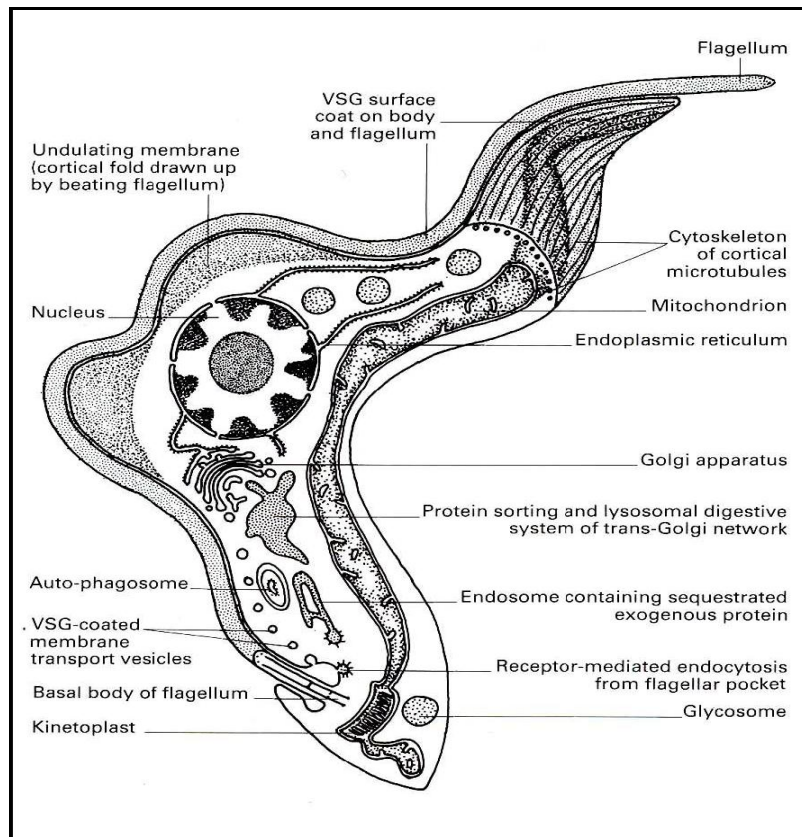


Figure 1.2. The structure of *Trypanosoma brucei*

Reproduced from (Vickerman *et al.*, 1993)

1.1.3 Life Cycle

The life cycle of a trypanosome has two stages, their time in a vertebrate host (human or animal) and that in an invertebrate vector (tsetse fly). Morphological transformations and biochemical changes are seen as the life cycle progresses. These changes affect the morphology of the parasite, including the position of the kinetoplast in relation to the nucleus. The life cycle begins when the metacyclic trypomastigote is ingested by the tsetse fly when feeding on host blood. The metacyclic trypomastigote has a long, slender cell body (14-30 μm long and 1.5 - 3.5 μm wide) alongside the flagellum. The basal body and kinetoplast are near the posterior end (Garcia, 2007; Matthews, 2005). The cell, in this form, is divided by binary fission in the blood and lymph nodes. After many divisions, its long slender form is transformed into a stumpy form that is shorter and thicker. At this stage, the stumpy form can infect the vector. Thus, when the tsetse fly takes a blood meal, the stumpy trypomastigote passes into

its digestive canal and reaches the mid-gut. In the mid-gut, the stumpy trypomastigote again undergoes morphological changes and some organellar changes as the binary fission transforms it into its procyclic trypomastigote form. These changes include a loss of the Variable Surface Glycoproteins (VSG) surface coat, and a much more developed mitochondrion (Matthews, 2005). After approximately two weeks, the procyclic form migrates to the salivary glands via the hypo pharynx. In the salivary glands, the procyclic trypomastigote transforms to its epimastigote form, which has the nucleus at the posterior end, while the kinetoplast and the basal body are at the anterior end. In addition, it develops a long flagellum, which is attached along the length of the cell body. After two to five days of growth by binary fission, the epimastigote form develops into the metacyclic trypomastigote form; at which point, it is ready to infect the vertebrate host. The tsetse fly that has trypanosomes in metacyclic form remains infected for the rest of its life (Garcia, 2007). The life cycle of the tsetse fly lasts about three weeks, while the life cycle of the trypanosome from its entry into a vertebrate host to its re-entry takes 18-34 days (Garcia, 2007; Jeffrey & Leach, 1966).

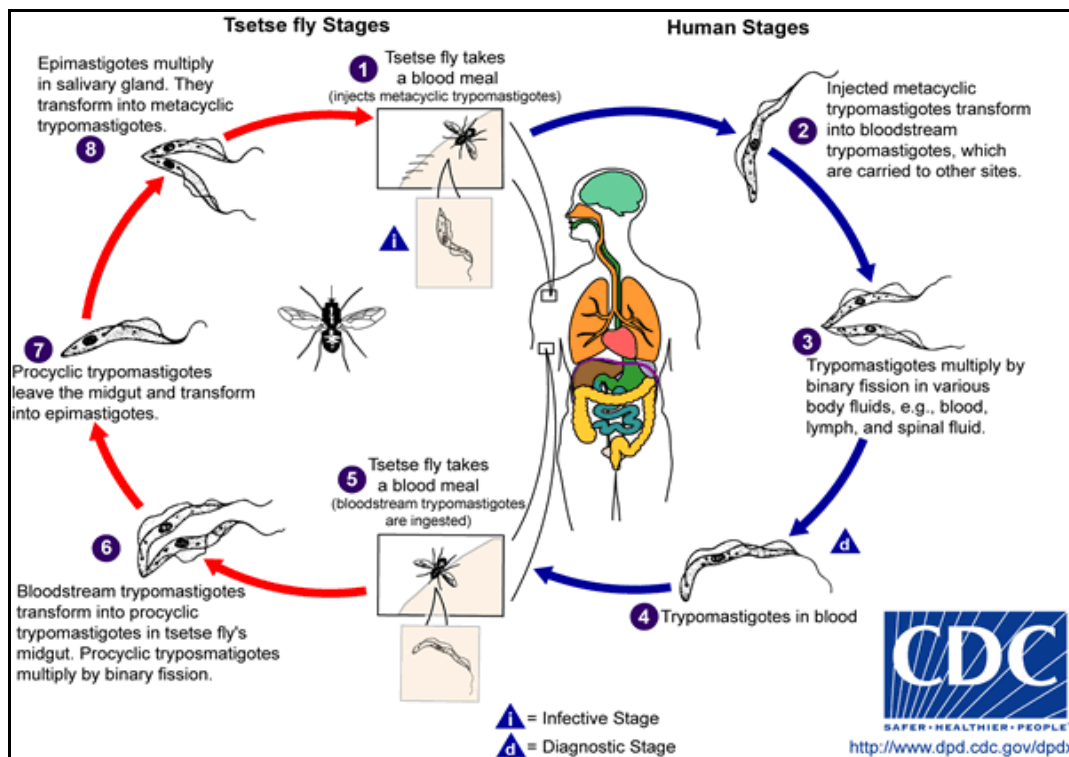


Figure 1.3. Life cycle of Trypanosomiasis.

<http://www.dpd.cdc.gov/dpdx/html/trypanosomiasisafrican.htm>

1.1.4 Clinical manifestations of the disease

The clinical progression of sleeping sickness depends on the type of trypanosome infection. There are two kinds of disease known as: the acute disease that results from *T. b. rhodesiense* and leads to Rhodesian sleeping sickness, and the chronic disease caused by *T. b. gambiense* and leads to Gambian sleeping sickness. The incubation period for Rhodesian sleeping sickness is two to three weeks, and death generally occurs within a year; Gambian sleeping sickness has an incubation period of several days to some weeks (Markell *et al.*, 1999). The duration of infection for Rhodesian sleeping sickness is about six months, whereas it is about two years in Gambian sleeping sickness (Welburn *et al.*, 2001). In general, there are two stages of sleeping sickness, which are classified according to the presence of parasites in the central nervous system (CNS) (Barrett *et al.*, 2003; Garcia, 2007). In the first stage of the disease, the parasites multiply under the skin, leading to a nodule or ulcer. After several weeks, the parasites begin to spread through the body and attack lymph nodes; they then enter the bloodstream. At this point, common symptoms begin to appear, such as headache, fever with night sweats, malaise, and weakness. Lymphadenopathy is the main indication of Gambian sleeping sickness, because the lymph nodes will swell along the back of the neck. This swelling is known as Winterbottom's sign (Barrett *et al.*, 2003; Markell *et al.*, 1999). However, in Rhodesian sleeping sickness, this swelling may not be present. The second stage of the disease begins when parasites penetrate the Central Nervous System (CNS). In *T. b. rhodesiense*, this occurs a few weeks after infection, while it can be several months to a year with *T. b. gambiense*. At this stage, headaches become harsh and the sleep disorder becomes noticeable. There are personality changes and apathy and, finally, the patient falls into coma and, if not treated, will then die (Barrett *et al.*, 2003; Garcia, 2007; Markell *et al.*, 1999).

1.1.5 Diagnosis

The diagnosis of trypanosomiasis initially depends on noticing the symptoms of disease, such as irregular fever and swelling of lymph nodes (Winterbottom's sign). Thereafter, a number of methods can be used to accurately diagnose trypanosomiasis in humans. In the past, enlargement of the lymph nodes in the

back of the neck was the main method used to identify the disease in slaves in the late 18th century (Barrett *et al.*, 2003). An examination of fluid taken from the lymph node, using stains to discover the metacyclic trypomastigote can now verify this diagnosis. The blood sample is the easiest technique although it has some problems. The blood is placed on slides and stained, after which metacyclic trypomastigotes can be detected in the blood using a microscope. However, the parasites can be difficult to detect during the afebrile phase because, in this period, there are few parasites in the blood (Garcia, 2007;Markell *et al.*, 1999). In addition, cerebrospinal Fluid (CSF) can also be collected for diagnosis of trypomastigote, primarily in the second stage of disease. The CSF must be centrifuged and stained in order to find trypomastigotes. Another method, Antigen Detection, an enzyme-linked immunosorbent assay (ELISA) method is used to detect antigens in the CSF and serum. Briefly: a special card, called the card indirect agglutination trypanosomiasis test (CIATT) is used to detect circulating antigens in a person who has African trypanosomiasis. Moreover, Antibody Detection, the card agglutination trypanosomiasis test (CATT) can be applied to blood, serum or plasma, and CSF to discover antibodies against *T. brucei*. Increased levels of IgG are a clear sign of the disease (Garcia, 2007;Markell *et al.*, 1999). Furthermore, as differentiation among species of trypanosomiasis is very difficult, DNA diagnosis can be important in deciding the species of trypanosomiasis, as treatment differs for the two species. However, the geographical location is usually a sufficient indicator of species.

1.1.6 The control of HAT

The control of the disease can be achieved two ways: the control of disease by minimising transmission of the parasites by their vector, or by using medicinal treatments to kill parasites within the mammalian host. The development of an effective vaccine against any African trypanosome remains unlikely in the foreseeable future, mainly due to the antigenic variation in their surface coat (Stuart *et al.*, 2008).

Trypanosomes parasites are transmission by the tsetse fly, which is distributed in sub-Sahara Africa in the size of areas more than 8.5 million km². Controlling the

flies is an important choice for reducing the disease burden. During the early 20th century, animals were killed and massive areas of forests destroyed to deprive flies of habitat and food; however this method is unacceptable because of the massive environmental damage (Allsopp, 2001). It is true that insecticides such as DDT can be used to eliminate the flies, however this method also has disadvantages. For instance, the flies become resistant to insecticides and the chemicals led to pollution of the environment and food chain (Aksoy, 2003). Another method that has been used is a bait technique that depends on attracting tsetse into fabric traps. This method is effective (and not harmful to the environment), particularly where these traps are placed near cattle pens, where the tsetse takes its meal (Allsopp, 2001). Recently, sterile insect technique (SIT) has been used to decrease the population of flies which could help to decrease the disease level in long-term. Using sterile male insects is a successful method and is environmentally friendly, but it is criticized for its high cost (Aksoy *et al.*, 2001).

1.1.7 Treatment of HAT

According to Jordan (Jordan, 1986), using drugs to treat sleeping sickness is an easier and cheaper means of overcoming trypanosomiasis than killing all tsetse flies. There are five drugs available for the treatment of sleeping sickness. Pentamidine and suramin are used in first stage of disease, while melarsoprol, eflornithine, and nifurtimox treat the second stage.

1.1.7.1 Pentamidine

Pentamidine is a drug known for its medical significance and its structure, which contains two benzamidine groups (figure 1.4). It is used in the treatment of *T. b. gambiense* infections because of its therapeutic efficacy, and also exhibits prophylactic activity (Bacchi, 1993). At the molecular level, this drug interacts with minor grooves of DNA where the concentrations of adenine and thymine are high and this features allow the multifactorial impact of the drug on cellular processes (Moreno *et al.*, 2010). The ionic form of each of the amidine moieties at physiological pH is a single positive charge and pentamidine is therefore a dication. This renders the drug incapable of crossing the blood brain barrier (BBB) and other bio-membranes and it is found to be physiologically effective only

during the initial stages of sleeping sickness (Denise & Barrett, 2001). The concentration of Pentamidine achieved within parasites residing inside the host cell is believed to reach millimolar levels, due to the involvement of several transport proteins in the trypanosome's plasma membrane (de Koning, 2008). The P2 aminopurine transporter contributes approximately 50% of Pentamidine uptake by *T. b. brucei* (depending on concentration); the drug is further transported by the High Affinity Pentamidine Transporter (HAPT1) and the Low Affinity Pentamidine Transporter (LAPT1) (de Koning, 2001b). The action of pentamidine is likely to be multi factorial. One contributing mechanisms is its binding to the minor groove of DNA (Moreno *et al.*, 2010). Destruction of the kinetoplast by Pentamidine was also observed as the drug has the ability to interact with the small circular DNA that comprise kinetoplast also known as kDNA (Tevis *et al.*, 2009). The mitochondria membrane potential is rapidly affected by pentamidine which may means that the mitochondria are a target of the pentamidine (Lanteri *et al.*, 2008) Dosage is 4 mg/kg per day by intramuscular injection for 7-10 days (Legros *et al.*, 2002;Markell *et al.*, 1999). Side effects, however, consist of nausea, vomiting, and hypotension (Garcia, 2007;Markell *et al.*, 1999).

1.1.7.2 Suramin

Suramin is a derivative of naphthalene and has a polysulphonated structure (figure 1.4). It is used for the treatment of the surra disease in camels, which is caused by *T. evansi* (Zhou *et al.*, 2004). It was discovered in 1916 by two scientists working for Bayer, Richard Kothe and Oskar Dressel (Haberkorn *et al.*, 2001). In humans it is used in the treatment regime of the initial stages of infections caused by *T. b. rhodesiense* but almost never for *T. b. gambiense* (WHO, 1995). Its side-effects have been found to be stronger more severe than with pentamidine, when used for infections of *T. b. gambiense* (Pepin & Milord, 1994). At physiological pH it exhibits 6 negative charges and this highly charged molecule is therefore unable to cross membranes by diffusion (Delespaux & de Koning, 2007). Suramin binds firmly to low density lipoproteins (LDLs); these are plasma proteins in the mammalian bloodstream and are considered as the sole source of sterols in trypanosomes. *T. b. brucei* plasma membranes contain receptors that are responsible for endocytosis of LDL, and this overall process facilitates the uptake of Suramin into the cell (Bacchi, 2009;Barrett *et al.*,

2007). In a very recent study Alsford and colleagues have introduced a new versatile tool termed RNA interference target sequencing (RIT-seq) for the purpose of functional analyses at molecular level to identify drug target (Alsford *et al.*, 2012). However, this study showed that a different protein, ISG75, may be involved in the endocytosis of suramin. This study further succeeded in identifying good candidates for the pentamidine transporters, and confirmed the role of the trypanothione pathway in susceptibility to arsenical drugs.

A test dose is recommended, followed by five injections of 20 mg/kg per day over 5-7 days (Jannin & Cattand, 2004). Side effects that have been noted include anaphylactic shock, nausea, vomiting, loss of consciousness, pruritus, oedema, and renal failure (Garcia, 2007; Legros *et al.*, 2002).

1.1.7.3 Melarsoprol

One of the members of the melaminophenyl family named Melarsoprol (structure shown in figure 1.4) is a drug that exhibits a therapeutic effect against second stage infection with *T. b. gambiense* or *T. b. rhodesiense*. Clinical trials results showed that 5% of patients who received treatment regime of Melarsoprol died from its high toxicity (Blum *et al.*, 2001), yet the drug has also been used to treat leukaemia patients (Soignet *et al.*, 1999). One explanation for the poor outcome is the formation of reactive arsenical encephalopathy. The toxic impact of Melarsoprol on trypanosomes is still not clear but studies suggest that it forms stable adducts with thiols, most probably with dihydrotrypanothione to form MelT (Fairlamb *et al.*, 1989). However, this is likely to be a defence mechanism of the cell rather than its mode of action.

Melarsoprol as a treatment against infections caused by *T. b. gambiense* has recently become less efficacious, with a high failure rate especially in areas with high epidemic profile such as the Democratic Republic of Congo, Southern Sudan, Uganda and Angola. It seems highly likely that this increase in failure rate is the result of drug resistance in the parasites (Delespaux & de Koning, 2007). The recommended dose is 2.2 mg/kg per day for ten days. Possible side effects include nausea, vomiting, and encephalopathy (Garcia, 2007; Jannin & Cattand, 2004; Legros *et al.*, 2002).

1.1.7.4 Eflornithine (DFMO)

α -Difluoromethylornithine, also known as Eflornithine (structure in figure 1.4), is used in the treatment of Melarsoprol-refractory gambiense sleeping sickness in humans; it is not effective against *T. b. rhodesiense* infections (Delespaux & de Koning, 2007). There are fewer adverse side effects of this drug because it is generally less toxic compared to Melarsoprol. Once it was licensed for human subjects, it was used for the first time in treatment of HAT (1990) caused by *T. b. gambiense* and it was found to be physiologically active in last stage of infection. DFMO acts as an inhibitor of the enzyme Ornithine Decarboxylase (ODC), a key enzyme in the synthesis of the polyamines spermidine, spermine, and putrescine that are essential for cell proliferation (Burri & Brun, 2003). Studies have shown that DFMO efficiency inhibits ODC in both trypanosomes and humans. However, the selectivity of effect for this drug is the result of differences in human and trypanosome ODC. The human cells are able to replace their ODC enzyme much more rapidly than the trypanosome (Iten *et al.*, 1997; Tabor & Tabor, 1984).

Oral administration of the Eflornithine is impractical because of bio-availability, and administration by intravenous infusion is generally recommended, although efforts to develop an oral formulation are ongoing (Manson-Bahr, 1974). Until recently it was believed that DFMO might enter trypanosomes by passive diffusion (de Koning, 2001a; Denise & Barrett, 2001). However, it was recently found independently by several groups that DFMO uptake in fact requires the expression of the amino acid transporter TbAAT6 (Baker *et al.*, 2011; Schumann *et al.*, 2011; Vincent *et al.*, 2010). Recent reports show that resistance against DFMO can be developed easily in trypanosomes. Results of one study show that a high level of resistance against DFMO in *T. b. brucei* strain 427 bloodstream forms was developed within 60 days. This study employed the approach of culturing sensitive cells in higher concentrations of the drug and linked resistance to the loss of the AAT6 gene (Vincent *et al.*, 2010).

The protocol for treatment is 100 mg/kg every six hours for two weeks via slow intravenous infusion. Side effects can include pancytopenia, diarrhoea, and anaemia (Garcia, 2007; Jannin & Cattand, 2004; Legros *et al.*, 2002; Markell *et al.*, 1999).

1.1.7.5 Nifurtimox

This drug is a member of the 5-nitrofuran family (for structure see figure 1.4) and it is well known for its anti-protozoal action. It has been used for this purpose since the 1960s. It is used to treat the acute form of protozoal infections including Chagas disease in South America and was recently introduced for the treatment of late-stage infection caused by *T. b. gambiense* in a combination formulation with eflornithine. The benefits of using this drug are that its oral administrable forms are available and not expensive. It also doesn't display cross resistance when administered with other drugs. However, it is ineffective as monotherapy, with the dosage and duration of treatment being restricted by unacceptable levels of toxicity. To avoid such instances of toxicity in patients, lower drug dosages of drug are recommended for a short duration, which is possible when combined with Eflornithine (Delespaux & de Koning, 2007; Lutje *et al.*, 2010; Yun *et al.*, 2010), as the drugs appear to act synergistically. Currently, a combination therapy of Eflornithine and nifurtimox is replacing the monotherapy of Eflornithine (Opigo & Woodrow, 2009; Priotto *et al.*, 2009).

The recommended dose of nifurtimox is 15 mg/kg per day in three doses over two weeks for children and 20 mg/kg per day in 3 doses for two weeks for adults. Side effects may include confusion, weight loss, tremors, and vertigo (Garcia, 2007; Legros *et al.*, 2002).

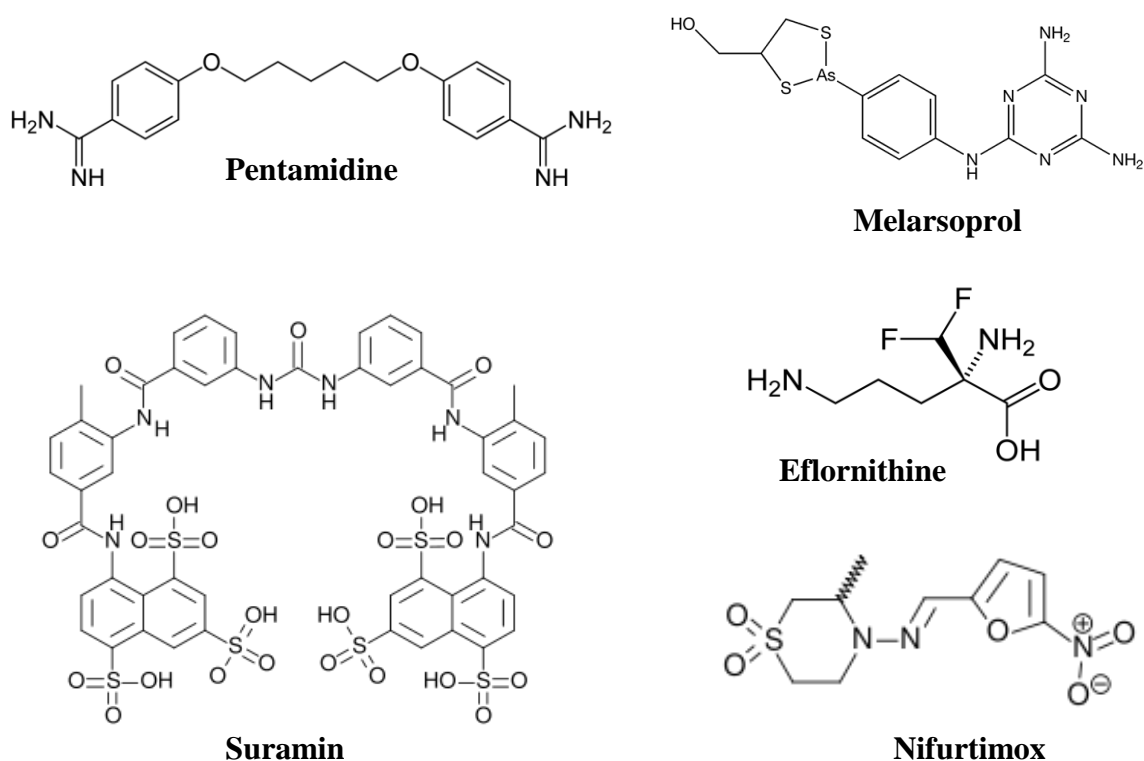


Figure 1.4. Chemical Structures of drugs used against Trypanosomiasis.

1.1.8 Drug Resistance

Of the several problems that surround the chemotherapy of Human African Trypanosomiasis, drug resistance is one of the primary reasons for treatment failure and has led to difficulty in the control of this disease. Although there has been long-term use of different kinds of drugs for treating trypanosomiasis, the mechanism of resistance is unclear (Ross *et al.*, 1997). Delespaux and De Koning (Delespaux & de Koning, 2007) reported that one of the most important reasons for drug resistance is due to the shortage of drug accumulation into the trypanosome. Furthermore, decreasing uptake of the drug by the trypanosome is frequently connected with drug resistance (de Koning, 2001b). In particular, De Koning (de Koning, 2001a) mentioned that loss of the purine transporter TbAT1/P2 leads to resistance. However, when two drugs share in the same mode of uptake through the P2 transporter, this leads to cross-resistance (de Koning *et al.*, 2004). There are many examples of resistance to trypanosomiasis drugs. Resistance to melarsoprol has been reported (Legros *et al.*, 1999). In Uganda, resistance of *T. b. rhodesiense* to DFMO has been reported (Iten *et al.*, 1995).

1.2 Leishmaniasis

Leishmania spp. are protozoa of the Trypanosomatidae family and are transmitted to mammalian hosts by sand flies. Two subgenera divide the genus *Leishmania*, and this divide centres on the site of the parasite's development in the sand fly's body. In the subgenus *Leishmania*, the parasite grows in the frontal portion of the alimentary area, whereas in the subgenus *Viannia*, it develops in the mid-gut and hindgut (Garcia, 2007). There are more than 30 species of *Leishmania* distributed across the world, which are found in two main regions: the Old World and the New World. Endemic areas of the Old World include Africa, Southern Europe, Asia, the Middle East, and India, while the New World endemic regions consist of Central and South America. According to WHO (2010), there are many of *Leishmania* species are responsible for most of the parasitic disease burden (Table 1.1).

<i>Species</i>	<i>Region</i>	<i>Disease</i>
<i>L. donovani</i>	Old World	Visceral Leishmaniasis (VL) & Cutaneous Leishmaniasis (CL) & PKDL
<i>L. major</i>	Old World	Cutaneous Leishmaniasis (CL) & Visceral Leishmaniasis (VL) & Mucocutaneous Cutaneous Leishmaniasis (MCL)
<i>L. tropica</i>	Old World	Cutaneous Leishmaniasis (CL) & Mucocutaneous Cutaneous Leishmaniasis (MCL)
<i>L. aethiopica</i>	Old World	Cutaneous Leishmaniasis (CL) & Mucocutaneous Cutaneous Leishmaniasis (MCL)
<i>L. mexicana</i>	New World	Diffuse Cutaneous Leishmaniasis (DCL)
<i>L. brasiliensis</i>	New World	Cutaneous Leishmaniasis (CL) & Mucocutaneous Cutaneous Leishmaniasis (MCL)
<i>L. amazonensis</i>	New World	Cutaneous Leishmaniasis (CL) & Mucocutaneous Cutaneous Leishmaniasis (MCL) & Diffuse Cutaneous Leishmaniasis (DCL)
<i>L. infantum</i>	New World	Visceral Leishmaniasis (VL) & Cutaneous Leishmaniasis (CL)

Table 1.1. Major species and location of *Leishmania* which cause different types of the disease

1.2.1 Disease

There are four types of leishmaniasis: visceral leishmaniasis (VL) (also known as kala azar or dum dum fever), cutaneous leishmaniasis (CL), diffuse cutaneous leishmaniasis (DCL), and mucocutaneous leishmaniasis (MCL) (Table 1). According to the World Health Organization (WHO, 2007), more than 12 million people are currently infected and there are two million new cases every year, with around 350 million people at risk. This disease affects the poorest populations in 88 countries, the majority of which are developing countries in Asia and South America (Garcia, 2007; Matlashewski, 2001; WHO, 2007). VL is found in 70 countries, with an estimated 500,000 new cases per year, whereas CL is present in 82 countries with annual estimates of 1.5 million cases per year (Desjeux, 2004; Garcia, 2007; WHO, 2007). Around 90% of CL cases are concentrated in seven countries: Afghanistan, Algeria, Brazil, Iran, Peru, Saudi Arabia, and Syria; while, about 60% of VL cases occur in three countries: Bangladesh, India and Nepal (TDR, 2009). Leishmaniasis is transmitted by female sandflies. There are 30 known species of sand fly. Of these, the *Phlebotomus* genus is found only in the Old World and the *Lutzomyia* genus is found only in the New World. Leishmania species could be transferred via leishmaniasis-contaminated blood (Markell *et al.*, 1999), potentially spreading species to new areas.

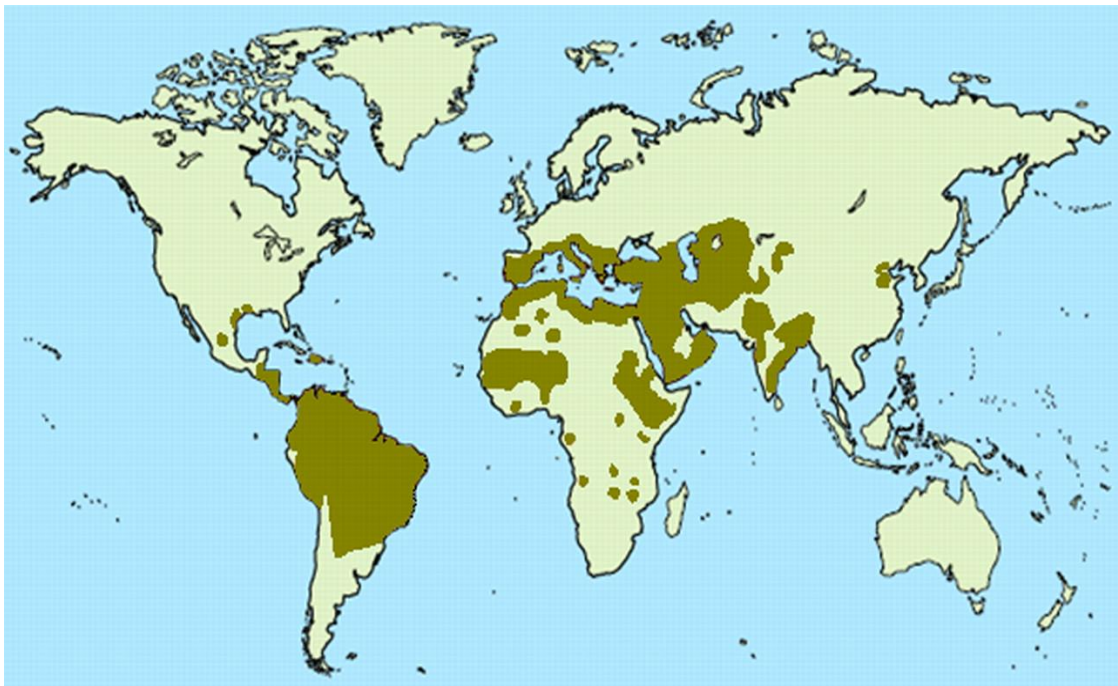


Figure 1.5. Leishmaniasis is endemic in tropical, Asian and southern European countries.

1.2.2 Morphology

Leishmania are protozoan parasites belonging to the Kinetoplastida order because they contain a kinetoplast in all cells. There are two main forms of *Leishmania*: amastigotes and promastigotes. Amastigote forms live in macrophages in blood hosts, whereas promastigote forms live in sandflies. Both forms have all the major cell organisms, i.e. nucleus, kinetoplast, mitochondrion, Golgi apparatus, flagellar pocket, endoplasmic reticulum, and glycosome (Besteiro *et al.*, 2007). The amastigotes are small and circular (3-5 μm in diameter), while the promastigotes are extended (1.5-3.5 by 15-20 μm) with one flagellum of 15-28 μm (Besteiro *et al.*, 2007; Garcia, 2007).

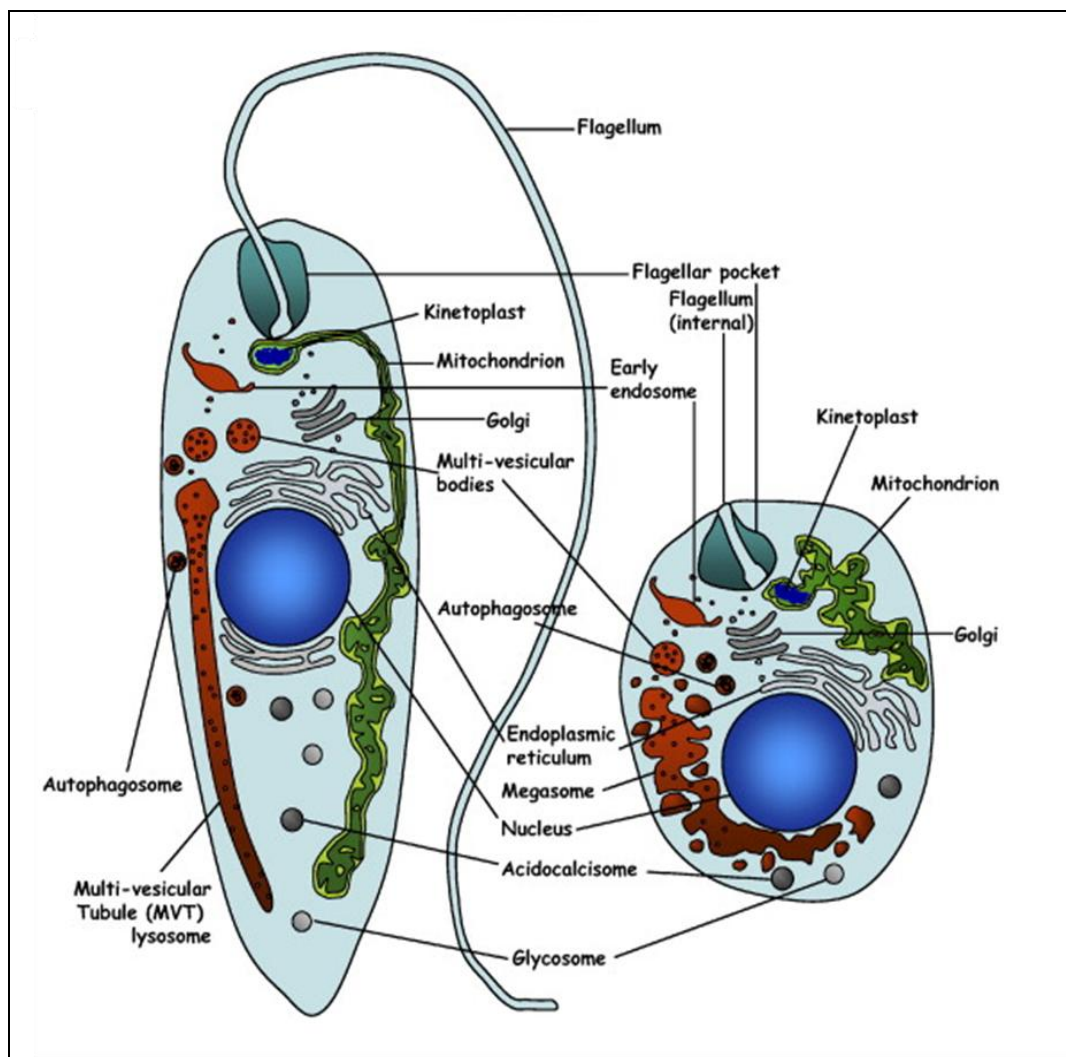


Figure 1.6. The main intracellular organelles *Leishmania* Promastigote (left) and amastigote (right) (Besteiro *et al.*, 2007)

1.2.3 Life cycle

Leishmaniasis is transmitted by the bite of sand flies that are at the infectious stage and so transmit metacyclic promastigotes. When sandflies feed on the blood of a host, the metacyclic promastigotes are passed to the host. The promastigotes are taken up by the macrophage where they quickly transform into their amastigote form in the phagolysosome and lose their flagella. The amastigotes multiply within the macrophages via binary fission until the cells are damaged, causing the amastigotes to be released for invasion of other macrophages (Chappuis *et al.*, 2007). What follows at this point depends on the species of leishmaniasis, In CL, the amastigotes appear in the skin and causes chronic infection in parts of the body such as the hands, face, feet, arms, and legs. In VL, they pass to deeper organs, for instance, the spleen, liver, and bone marrow. When new sandflies feed on the blood of mammals that have amastigotes in the macrophages of their blood, the macrophages are ingested and amastigotes are released in the sandfly's mid-gut. They then transform into promastigotes and multiply by longitudinal fission in metacyclic promastigote form. The metacyclic promastigotes are highly mobile and migrate to the hypostome of the fly. Metacyclic promastigotes are then found in the mouthparts, where they are ready to infect vertebrate hosts during the fly's next blood meal. The life cycle of the sand fly depends on the species, but ranges between four and eighteen days (Garcia, 2007).

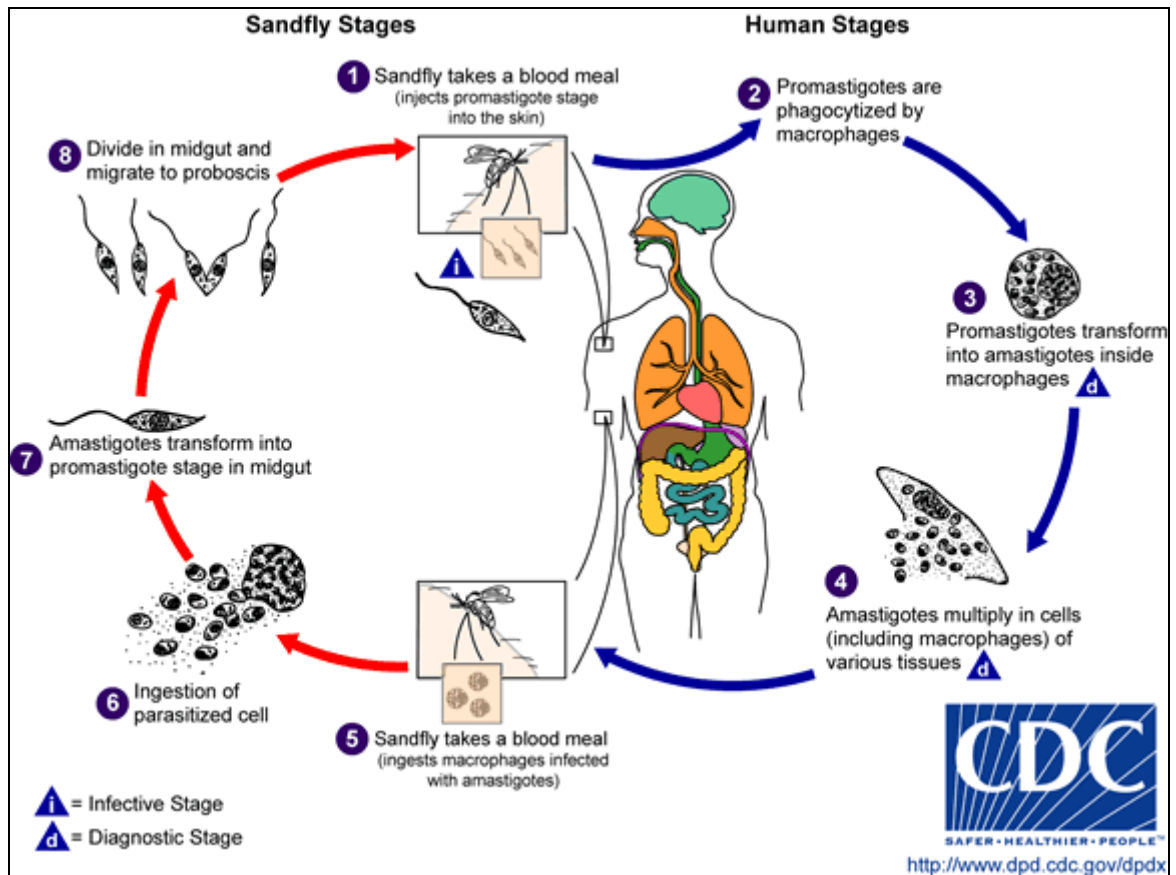


Figure 1.7. Life cycle of Leishmaniasis.

Reproduced from <http://dpd.cdc.gov/dpdx/html/Leishmaniasis.htm>

1.2.4 Clinical Disease

There are four types of leishmaniasis disease are different for different species that causes the disease.

1.2.4.1 Cutaneous Leishmaniasis (CL)

The incubation period of CL is two to eight weeks and may extend to a couple of years (Garcia, 2007;Markell *et al.*, 1999). The first symptoms of cutaneous disease are lesions at the point of entry where the bite of the sandfly occurred. This point is initially painless but soon becomes itchy. These lesions normally appear on parts of the body that are more frequently uncovered, such as the face, arms, and legs. The disease can go on to create a great number of lesions. These can further develop into ulcers covered by a scab and containing exudates. Other symptoms depend on species. For example, in *L. major* the

lesions have inflammation and crusting and are necrotic and exudative. In *L. tropica*, the lesions are less necrotic but exhibit greater swelling and a thicker crust (Garcia, 2007;WHO, 2007).

1.2.4.2 Mucocutaneous Leishmaniasis (MCL)

The disease usually begins after an early cutaneous infection. Cutaneous lesions develop and can become very large. MCL causes infection of mucosal surfaces with lesions that can lead to destruction of one side or all of the mucous membranes of the mouth and nose. Others symptoms include fever, anaemia, and weight loss. Failure to treat this disease is likely to lead to the loss of all of the soft parts of the nose, palate, and lips. In the Old World, MCL are related to *L. tropica* and *L. major*, whereas in the New World they are linked to *L. braziliensis* and *L. guyanensis* (Desjeux, 2004;Markell *et al.*, 1999).

1.2.4.3 Diffuse Cutaneous Leishmaniasis (DCL)

Diffuse cutaneous leishmaniasis (DCL) is an uncommon manifestation of cutaneous leishmaniasis. According to Desjeux (Desjeux, 2004), “This occurs in individuals with defective cell-mediated immune response. Its severity is due to disseminated lesions that resemble those of lepromatous leprosy”. These lesions are usually scaly with numerous nodules and can occur over the whole of body (Garcia, 2007). Several *Leishmania* species cause diffuse cutaneous leishmaniasis. In the Old World, *L. aethiopica*, and, in the New World, *L. pifanoi*, *L. amazonensis*, and *L. mexicana* cause DCL (Garcia, 2007).

1.2.4.4 Visceral Leishmaniasis (VL)

The incubation period of VL is usually between two and six months (Chappuis *et al.*, 2007;Garcia, 2007). This is the most dangerous of the leishmaniasis diseases and leads to death if not treated (Matlashewski, 2001). The main symptom of VL patients is fever, which is accompanied by weight loss, chills, weakness, anaemia, swelling of the spleen and liver, diarrhoea, and enlarged lymph nodes. In addition, VL patients can sometimes develop another disease after the VL has been treated, known as post-kala azar dermal leishmaniasis (PKDL). In India, more than 20% of patients treated for VL develop PKDL, and this figure rises to

50% in Sudanese VL patients. PKDL is a cutaneous disease but quite different from CL, and much more diffuse. In the beginning, macules form near the mouth. These then spread to the face and continue to the arms, the trunk, and the legs (Garcia, 2007). VL is caused by *L. donovani* and *L. infantum*, in the Old World and *L. chagasi* and *L. amazonensis* in the New World (Garcia, 2007;Markell *et al.*, 1999).

1.2.5 Diagnosis

Diagnosis of leishmaniasis can usually be undertaken by general practitioners, but this depends on the symptoms, and on how common the disease is in a given area. However, in parts of the world where leishmaniasis disease is rare, diagnosis depends on the appearance of amastigotes or promastigotes in samples (Garcia, 2007). Parasitology and serology are very important to the diagnosis of leishmaniasis (Manson-Bahr, 1987). Parasitological diagnosis relies on detection of the parasites in the blood, skin, lymph nodes, experimental animals, spleen, liver, and bone marrow using blood films, needle biopsies, and biopsies (Garcia, 2007;Kreier, 1987;Manson-Bahr, 1987). Serological diagnosis on the other hand, is usually based on the presence of *Leishmania* antibodies in the blood (Jhingran *et al.*, 2008). Many serological methods are used to detect leishmaniasis, including direct agglutination tests (DAT), immunofluorescence tests (IFAT), and enzyme-linked immunosorbent assays (ELISA) (Garcia, 2007;Jhingran *et al.*, 2008;Manson-Bahr, 1987).

1.2.6 The control of Leishmaniasis

It could be said that control of leishmaniasis depends on three strategies: vector control, treatment and vaccines. Vector control to minimize or interrupt disease transmission takes many forms. For example, using insecticides like DDT although it has disadvantages is a good choice. In India, The use of DDT is part of the plan to eliminate Visceral Leishmaniasis by 2015 (Killick-Kendrick, 2010). There are several types of insecticides that can be used such as malathion, propoxur and deltamethrin (WHO, 2010). In addition, bed nets and wearing clothing to cover arms are effective for reducing the disease by decrease exposure to the bites of flies.

Using vaccines is not yet a means for the prevention of leishmaniasis. To date, in spite of efforts to design vaccines, no vaccine can be used because the problem is limited by the necessary attempt to translate the successful use of vaccines in experimental animals to humans, and to translate those results into practical field applications, rather than just laboratory tests (Kedzierski, 2010).

1.2.7 Treatment of leishmaniasis

As with many protozoan diseases, there are many problems associated with the therapy of leishmaniasis. Despite the fact that humans recover from CL without assistance, over a period of a few months to several years (Garcia, 2007), the use of drugs for rapid treatment is still much preferable due to the disfiguring nature of the lesions and the potential for secondary infections. There are five main drugs used in the chemotherapy of leishmaniasis: pentavalent antimonials, amphotericin B, miltefosine, paromomycin, and pentamidine. The most effective treatment of leishmaniasis depends on the species and the clinical manifestation (Peters & Killick-Kendrick, 1987).

1.2.7.1 Pentavalent antimonial

Since 1947 the treatment of leishmaniasis includes the use of antimonial drugs for the reduction of visceral and cutaneous leishmaniasis. There are two such drug preparations that are available for antimonial therapy, i.e. Pentostam and Glucantime. Figure 1.8 shows the Pentostam structure as sodium stibogluconate; Glucantime is known as Meglumine antimoniate. Some of the clinical symptoms that arise from pentavalent antimonial toxicity are malaise, vomiting and anorexia (Chang *et al.*, 1985; Kreier, 1987). Cases of visceral leishmaniasis were found to be responded by antimony therapy. Relapse may occur over the patient's life time and its treatment often involves the second line therapy of amphotericin B or Pentamidine (Olliario *et al.*, 2002). Unfortunately, half of the patients who received this treatment regime were found to have VL disease (Ganguly, 2002). Initially WHO approved 20 mg of antimonial per kg per day for treating Leishmaniasis and later its recommended up to 850 mg / per kg of body for 28 days (Balana-Fouce *et al.*, 1998).

Intracellular ATP level is decreased due to the metabolic action of this drug as it interferes with glycolysis and with β -oxidation of fatty acids in amastigotes of many species of *Leishmania* (Van Voorhis, 1990). Oral administration of pentavalent antimonial is reported to be possible, and the drug can be developed (Frezard *et al.*, 2008) from a complex of meglumine antimoniate (MA), β -cyclodextrin (β -CD), and pentavalent antimonial (Sb) (NMG-Sb- β -CD-Sb-NMG). This drug enters through the gastrointestinal epithelium by simple diffusion. Clinical manifestations upon high drug dosages include myalgia, hepatotoxicity, and malaise (Hepburn *et al.*, 1993), headache, anorexia, nausea, cardiotoxicity and phlebitis (Navin *et al.*, 1992). The few other symptoms that appear with high dosages are fever, skin rash, gastrointestinal irritation, and cough (Warren & Mahmoud, 1984) and pancreatitis (Gasser, Jr. *et al.*, 1994). However, in some cases treatment is ineffective due to the resistance by parasites against the administered antimonial; approximately 10 to 25 % of the cases who received the treatment are reported to have frequent relapse in the former disease condition (Opperdoes & Michels, 2008). This treatment is considered as the first line drug against Leishmaniasis while the second line treatment regime includes Pentamidine, Amphotericin B alone and the formulation of amphotericin B encapsulated in liposomes (AmBisome) (WHO, 2007).

1.2.7.2 Amphotericin B

This drug is also employed as second line treatment of different types of Leishmaniasis and studies have shown that this drug has a positive physiological impact in patients who have VL relapses (Olliaro & Bryceson, 1993) but some disadvantages of using this drug are its high toxicity and cost. However, some lipid formulations of this drug have been prepared to overcome such issues, including cholesterol sulphate amphotericin B liposomes (Amphocil), distearylphosphatidyl amphotericin B complex (AmBisome) and abeleet. These lipids formulations offer less toxicity and are more efficient in bringing about VL and ML remission (Yardley & Croft, 2000). In studies employing VL and CL experimental models, amphotericin B and its liposomic form were observed to be active in abating the infection intensity (Croft *et al.*, 2005). Amphotericin B (AmpB) is reported to prevent binding of *L. donovani* with macrophages, thus limiting macrophage infection. AmpB is thought to interact with cholesterol of

the host macrophages and ergosterol of the parasite (Paila *et al.*, 2010). Countries like India and Nepal recommend this drug in Leishmaniasis infection and its dosage period is extended if the infection process has spread to splenic smears and marrow.

Dose range of this drug varies from 0.5 to 1 mg/Kg of body weight. High drug doses are prohibited because of its toxic metabolic impact at this concentration. Side effects at high doses include hepatotoxicity, hypomagnesaemia, fever, hypokalemia, renal dysfunction, myociditis, sudden death and bone marrow suppression (Balana-Fouce *et al.*, 1998;Sundar, 2001).

In *Leishmania* and fungi, the mode of action of amphotericin B involves sterol metabolism as it acts on a sterol called 24-ergosterol, the main sterol in their plasma membranes. Amphotericin B binding to ergosterol causes parasite death because of increased membrane permeability (Balana-Fouce *et al.*, 1998;Singh *et al.*, 2006).

1.2.7.3 Miltefosine

The best feature of this drug is that its oral administrable form is available in the market, which has a high impact on remitting VL (Fischer *et al.*, 2001;TDR, 2002). It is also active in reducing CL infections (Croft *et al.*, 2005). This drug was proven to be therapeutically effective against VL in studies conducted in Bihar, India with 94% potential of disease treatment (Singh *et al.*, 2006). Besides this, researches conducted in Africa and Columbia showed similar results against CL (Oppendoes & Michels, 2008). Acting at a cellular level, Miltefosine induces the production of inducible nitric oxide synthase 2 (iNOS2), thus catalysing the production of nitric oxide within macrophages and killing parasites (Wadhone *et al.*, 2009). Range of optimum dosages for Miltefosine is recommended to be 2.5 mg/kg of body weight in a day for a period of four weeks (Jha *et al.*, 1999;Sundar *et al.*, 2002). Side effect associated with Miltefosine include only minor symptoms such as gastrointestinal disturbances including vomiting (40% cases) and 20% of the patients complained about diarrhoea (Singh *et al.*, 2006). Some other concerns raised in using this treatment regime are its long half-life which makes the drug available for enough time to have resistance developing against it (Singh *et al.*, 2006). In order to decrease the potential for resistance

several combinations with other drugs have been investigated (Seifert & Croft, 2006); specifically combinations miltefosine with Paromomycin, Sitamaquine, Pentostam or amphotericin B were tested. Among all these combinations, the most effective combination therapies were the ones employing amphotericin B and Paromomycin.

1.2.7.4 Paromomycin

The structure of this drug is presented in figure 1.8. It is widely employed in the treatment of bacterial and intestinal parasitic infections e.g. VL. Cases with reported antimonial resistance are recommended to take this therapy and its added benefits are low cost, high efficiency and authorization (Olliaro *et al.*, 2002;Sundar, 2001). This treatment is declared to be safe and it has replaced amphotericin B in VL, as that drug is costly and toxic. Formulations for oral administration and topical use have been prepared and they are effective against enteric protozoa and old world CL (Flanigan *et al.*, 1996). However, topical paromomycin formulations are still undergoing clinical trial and have yet to be approved. Optimum dosage for this drug ranges from 14 to 16 mg/kg thrice a week and the maximum amount of this drug given can reach 1 g. Side effects associated with this drug include nephrotoxicity (Sundar, 2001). In central Tunisia, topical Paromomycin prescriptions are given because it is active against *Leishmania major* which causes zoonotic CL in that country. Observations of this study showed that it is ineffective in this type of Leishmaniasis (Ben *et al.*, 1995). Paromomycin led to inhibition of protein synthesis in the promastigote stage of *L. mexicana* and reduced proliferation but had little effect on mammalian cells. This drug strongly interacts with parasites, whereas it does not bind to mammalian cells (Fernandez *et al.*, 2011). Studies have been conducted to determine the therapeutic effect of combination of Paromomycin and antimonial in old and new type of Leishmaniasis (Jha *et al.*, 1999;Thakur *et al.*, 2000).

1.2.7.5 Pentamidine

Diagram 1.8 shows the structure of Pentamidine. This drug is employed as a second line treatment regime of antimony-relapsed visceral leishmaniasis. It displays relatively high toxicity and cost, but is reportedly a quite effective

antileishmanial agent. In general, pentamidine is not considered a major drug for treating leishmaniasis. In some cases—mostly after treatment failure with pentavalent antimonials—pentamidine is used as a second line drug. However, in a few countries such as Suriname, pentamidine is used as a first line drug for CL (Van Der Meide *et al.*, 2009). Its route of administration is intramuscular and the injections contain drug dosage in range of 2-4 mg/kg body weight. The drug is administered thrice a week for a period of 3-4 weeks (Balana-Fouce *et al.*, 1998). 30 to 50% of the patients who received this therapy were reported to have side effects including hyperglycemia, hypoglycemia, sterile injection abscess (Sundar, 2001) and sudden shock, anemia, nephrotoxicity, hepatic enzymes induction, and skin rashes (Balana-Fouce *et al.*, 1998; Sundar, 2001) while 10% of the cases developed diabetes mellitus manifestations (Ganguly, 2002).

The drug enters the cell via active transportation, possibly using the arginine and polyamine transport system (Basselin *et al.*, 1996). The exact metabolic mechanism through which it kills parasite is still unknown but it is suggested that it affects mitochondrial membrane potential and this rendering it non-functional (Basselin *et al.*, 1996; Mukherjee *et al.*, 2006).

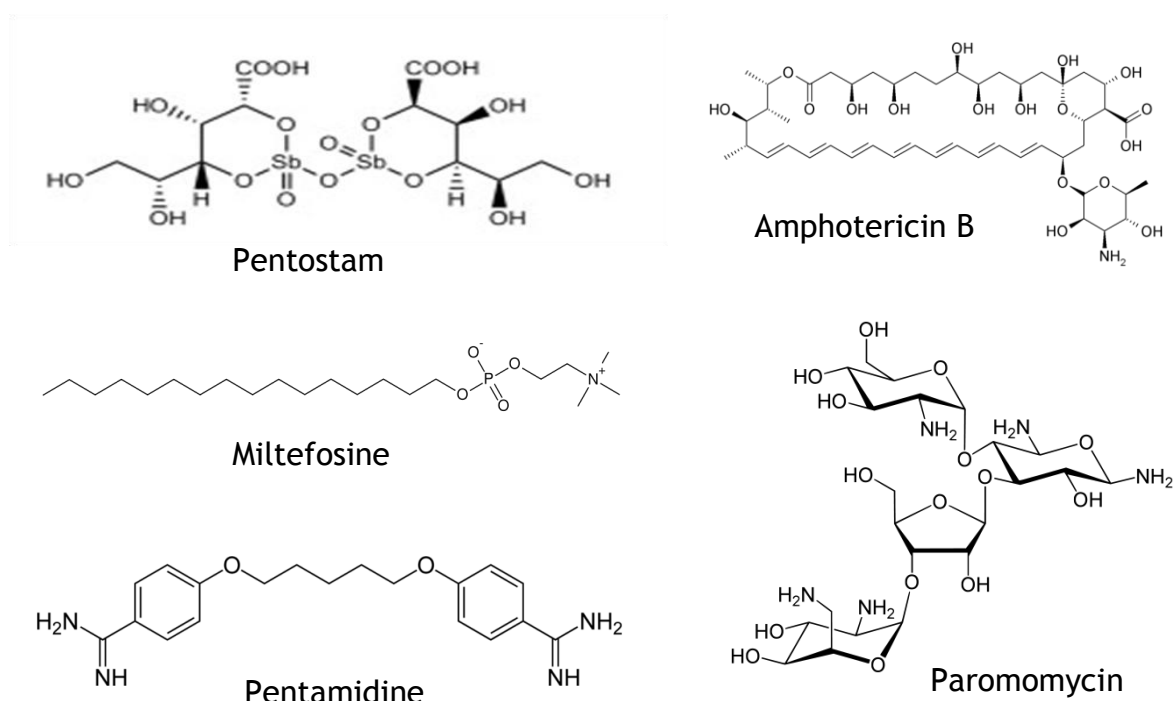


Figure 1.8. Chemical structures of drugs used against Leishmaniasis.

1.2.8 Drug Resistance

Recently, resistance to drugs has emerged as a major problem in the control of *Leishmania* parasites, which has serious impact on community health in endemic areas. According to Croft and Coombs (Croft & Coombs, 2003), many *Leishmania* species, including *L. donovani* and *L. tropica*, are zoonotic and consequently increases in drug resistance are less probable unless there is also substantial human to human transmission. The reduced benefit of pentavalent antimony for treating of VL is due to drug resistance (Sundar *et al.*, 2008), which has added another dimension to this matter. Moreover, in India, the use of pentamidine for some parasites has been stopped due to resistance (Sundar, 2001). Despite the fact that mechanisms of resistance are not well understood, some explanations have been put forward regarding this issue. For example, underdosing may lead to resistance (Polonio & Efferth, 2008). On the other hand, Brochu *et al* (Brochu *et al.*, 2003) have suggested that reduced accumulation of a drug can lead to resistance.

1.3 Transporters in kinetoplastids and their importance in drugs development

Kinetoplastids are obligatory parasites that are completely dependent on the host environment to obtain the necessary materials for their cellular functions. Cell membranes of all cells have many roles, and one of these is to control the movement of materials into and out of the cell. Membrane transporters are responsible for the movement of necessary nutrients, the regulation of physiological concentrations, cellular communication, and elimination of waste products. Controlling the molecular traffic across the cell membrane is performed through five methods: simple diffusion, facilitated diffusion, active transport, endocytosis, and exocytosis (Mohammed, 2000). Drug therapy is one of the ways by which parasites are controlled and their numbers reduced, and as most drug targets are intracellular, drugs must pass through the parasite membranes. Thus, transport processes play key roles in not only maintaining the life of cells but also in the action of anti-infective agents.

Among many other necessary materials for the life of the parasite, nucleosides and nucleobases, which are essential for nucleic acid synthesis, must pass through the membrane. Purines and pyrimidines are necessary for synthesis of nucleic acids in all cells. All protozoan parasites are incapable of *de novo* purine biosynthesis, and they depend on their hosts to obtain purines (de Koning *et al.*, 2005). In contrast, *de novo* synthesis of pyrimidine rings occurs in all protozoan parasites, except for *Giardia lamblia*, *Tritrichomonas foetus* and *Tritrichomonas vaginalis* (Hassan & Coombs, 1988).

Many proteins are associated with the cell surface and assist in the passage of materials across the cell membrane. In eukaryotes, there are two known families of mammalian transport proteins that help to move free nucleosides and nucleobases through the cell membrane. These are non-homologous and classified based on mechanism of translocation of substrate. The first family is the Equilibrative Nucleoside Transporter (ENT) family that enables the movement of these molecules down concentration gradients into or out of cells (facilitated diffusion) (Baldwin *et al.*, 2004). However, some protozoan transporters of the ENT family have been shown to be energy dependent, using the proton gradient across the plasma membrane to efficiently transport substrate (de Koning *et al.*, 2005). The second family is the Concentrative Nucleoside Transporter (CNT) family that uses a co-transport mechanism for sodium ions (Gray *et al.*, 2004). The CNT family consists of three subtypes of sodium-dependent transporters: CNT1 or (SLC28A1) which transports pyrimidine nucleosides, CNT2 or (SLC28A2) which is responsible for purine nucleoside transport, and CNT3 (also referred to as SLC28A3) which transports both pyrimidine and purine nucleosides (Gray *et al.*, 2004). However, no members of this transporter family have been detected in protozoa, although ENT transporters do not account for all known nucleobase transport activities, especially those mediating pyrimidine uptake (de Koning, 2007).

Apart from selective uptake through unique protozoan transporters, antiparasitic drugs rely for their selective action on unique targets not present, or sufficiently different, in the human host. Therefore, new drug development programmes commonly seek to target pathways or enzymes that do not exist in host cells. One example is trypanothione, which is essential to trypanosomatids and found only in kinetoplastid parasites. Another example is ornithine decarboxylase

(ODC), which although essential in both humans and *T. b. gambiense*, is sufficiently different between the two species to be a good drug target (Delespaux & de Koning, 2007).

1.4 Trypanosome metabolism

Many studies have been conducted on trypanosome metabolic processes, particularly with emphasis on glycolysis (Albert *et al.*, 2005; Haanstra *et al.*, 2008; Visser & Opperdoes, 1980) and trypanothione synthesis (Fairlamb *et al.*, 1987; Xiao *et al.*, 2009). The biochemical pathways were investigated using HPLC, NMR and classical techniques of biochemistry and enzymology. Quantification of phosphorylated compounds in the bloodstream and procyclic of *T. brucei* was performed via NMR (Moreno *et al.*, 2000) and also for performing analysis in enzyme inhibition process in the same organism (Coustou *et al.*, 2005). However, the in-depth analysis of some pathways such as glycolysis and mitochondrial functions have left other aspects of kinetoplastid biochemistry relatively under-explored. The application of systems biology and metabolomics to this problem is starting to address some of the gaps, however. For instance, analysis of alterations in procyclic trypanosome metabolism after change of carbon source from glucose to proline was performed through Hydrophilic Interaction Chromatography (HILIC)-Orbitrap mass spectrometry (Kamleh *et al.*, 2008). In the case of this energy metabolism shift, this highlights a number of other metabolite changes, e.g. glutamate, 5-carboxypyrroline and glutathione in cells cultured in proline rich media (Kamleh *et al.*, 2008), in turn identifying biochemical pathways being activated or inhibited by the change in medium.

1.4.1 Thiol metabolism

Mammalian cells contain high concentrations of glutathione and at physiological pH it serves as a sulfhydryl buffer. Besides this, it is involved in many cellular metabolic processes including DNA & protein synthesis, amino acids importation and detoxification of oxidative species (Hayes & McLellan, 1999; Meister, 1981). The molecular structure of glutathione consists of a tri-peptide thiol. Clarity in the host and parasite metabolic processes and the variation between them is essential for the development of effective treatment regimes against

trypanosome infections (Wang, 1995). Glutathione metabolism is different in trypanosome and mammals because the former involves the contribution of the glutathione and spermidine conjugate named trypanothione that is responsible for thiol pool availability for further metabolic processes (Fairlamb *et al.*, 1997). The biosynthesis of trypanothione (and glutathione) starts with the synthesis of glutamylcysteine from glutamic acid and cysteine by the catalytic action of γ -glutamylcysteine synthetase (γ -GCS) (Griffith & Mulcahy, 1999). This enzyme is rate limiting in mammalian species (Griffith, 1999) whereas the homologous enzyme catalyzes trypanothione in the trypanosomatid *Leishmania tarentolae* (Grondin *et al.*, 1997). The synthesis of glutathione is completed by the addition of the third amino acid, glycine, by glutathione synthase (GS). Two glutathione residues are then coupled to spermidine to yield one molecule of trypanothione, in a reaction mediated by trypanothione synthetase (TrypSyn).

There are several different mechanisms through which trypanothione metabolism can be targeted. The first one involves the inhibition of trypanothione reductase (TryR) by specific inhibitors such as those of the pyrimidinobenzothiazepine and thiaisoalloxazine scaffolds (Galarreta *et al.*, 2008). Secondly, inhibition of trypanothione synthetase itself is possible and a recent report from the Fairlamb group describes a series of potent quinol inhibitors for this enzyme (König *et al.*, 2011). In addition, drugs like DFMO are found to be effective in inhibiting trypanothione synthesis by inhibiting putrescine and spermidine production (Vincent *et al.*, 2012).

1.4.2 The role of mitochondria in bloodstream form *T. b. brucei*

One of the major organelles present in a trypanosome is the mitochondrion, which is singular and it requires the cell division cycle to duplicate. 10-20% of the total DNA of the *T. brucei* is present in the mitochondrion of the cell, which contains its own genome, which is not uniform in shape because the shape of the genome is dependent on the stage of the cell cycle. The mitochondrion does not fully mature in the bloodstream form (BSF) and contains singular canal without of inner membrane folding. The mitochondrion of bloodstream forms lacks both Krebs cycle and the classical respiratory chain, whereas both the respiratory chain and Krebs cycle are present in the procyclic forms (PCF). The

mitochondrion is present in the form of a network with inner membrane folding (van Weelden *et al.*, 2003; Vickerman, 1985).

Both morphological and functional changes to the mitochondria take place during the process of differentiation of *T. brucei* between the distinct life-cycle stages, as the source of the energy of the parasite changes from amino acid to glucose oxidation (Vickerman, 1985). Via the glycolytic pathway the BSF cells make use of the sugar-rich environment of the mammalian bloodstream for their energy metabolism (Bienen *et al.*, 1993). There is no cytochrome-mediated respiratory chain in the BSF cells; rather they contain the glycerol-3-phosphate dehydrogenase and the salicylic hydroxamic acid (SHAM)-sensitive alternative oxidase which is a significant electron transport chain present in the mitochondria, also known as the trypanosome alternative oxidase (TAO) (Chaudhuri *et al.*, 2006). A mitochondrial membrane potential is preserved regardless of the absence of complete cytochrome-containing complexes III and IV in BSF trypanosomes, driven by ATP hydrolysis of the FoF1-ATP synthase complex, which exports portions from the mitochondrial matrix (Schnauffer *et al.*, 2005).

1.5 Trypanosome signalling pathways

There are several types of signals that regulate cellular processes including gene expression patterns in response to extracellular triggers. These signals are called second messengers and include cAMP and calcium ions (Ca^{2+}), which in turn activate effector proteins such as Protein Kinase A and other protein kinases, Calmodulin, ion channels and other pathways in many cell types.

1.5.1 cAMP

In this case the role of second messenger is played by cyclic adenosine monophosphate (cAMP), which is involved in many biological processes. The discovery of the Adenylyl cyclase (AC) activity in trypanosomes took place in 1974 in *Trypanosoma gambiense* (Walter *et al.*, 1974), which led to estimating cAMP levels in different life-cycle stages of *Trypanosoma lewisi*, and it was discovered that in the non-reproducing state, the cAMP concentration was

around twice that of the reproducing form (Strickler & Patton, 1975). As the parasitaemia in rats increased so did the cAMP concentration in the parasites suggesting a role in quorum sensing and possibly in differentiation to short-stumpy forms or exchanges of the VSG coat; similar alterations were seen in the strains that caused a relapsing parasitaemia (Mancini & Patton, 1981). Interest in the cAMP-dependent pathways has recently peaked with reports showing that cAMP phosphodiesterases TbPDEB1/B2 and some adenylyl cyclases are essential and potential drug targets (de Koning *et al.*, 2012; Salmon *et al.*, 2012).

1.5.2 Calcium Ions

Calcium ions (Ca^{2+}) plays a crucial role as omnipresent messengers in the cell, and facilitate many cellular responses such as proliferation, contraction, secretion, differentiation and cell division. In parasites, Ca^{2+} plays a vital role in their interaction with host cells. There are two intracellular Ca^{2+} transport systems in *Trypanosoma brucei*, one of them in mitochondria and the other in the endoplasmic reticulum (Moreno *et al.*, 1992). For *Trypanosoma cruzi*, there is also a relationship with increased virulence of parasites as well as their penetration into the host cell (Docampo & Moreno, 1996).

Intracellular Ca^{2+} can be released to the cytosol from numerous organelles, including endoplasmic reticulum, mitochondria and acidocalcisomes. Apart from its physiological role as a regulator, extracellular Ca^{2+} plays an important role in the action of several trypanocidal drugs, for instance potentiating the effect of melarsoprol (Clarkson Jr & Amole, 1982).

Until now there has been no evidence of the existence of voltage-dependent Ca^{2+} channels in parasitic protozoa (Moreno & Docampo, 2003). However, Ca^{2+} entry into *Trypanosoma brucei* can be stimulated by Phospholipase A2 activity, which releases arachidonic acid and is itself Ca^{2+} -regulated (Eintracht *et al.*, 1998).

The concentration of intracellular Ca^{2+} and its homeostasis in the cell is very important. Any changes might lead to a failure in metabolism and cell death. Importantly, mitochondrial calcium release has also been implicated in programmed cell death (Fidalgo & Gille, 2011). Therefore, studying intracellular

Ca^{2+} in trypanosomes and the effect of different drugs on intracellular Ca^{2+} could help to understand the mode of action for some of the lead compounds that are under development against trypanosomiasis.

1.6 Mode of Action Studies

The process of drug development is very expensive and early investigation of a potential lead compound's mode of action (MoA) can either help advancing the project through target-based optimisation and improved assays, or help dismiss the scaffold early if it is found that the MoA is inappropriate. Possibly the most powerful tool for lead compound optimisation is medicinal chemistry based on analysis of a proper structure-activity relationship (SAR) of structural analogues interacting with a single protein target. This allows for the rational optimisation of the lead compound structure towards desirable qualities such as higher affinity, higher specificity, metabolic stability, oral absorption etc. For this to be possible MoA studies are required in order to identify the target of antiparasitic agents with promising activity and selectivity discovered through screening in whole-cell assays.

Initially, the active compound led to drug discovery with information regarding mode of action coming much later, now, attempts are being made to discover if it can be drawn from the discovery of a good metabolic target. To examine a drug's effect on the tiny metabolites present within a cell population, a new method called Metabolomics is considered very beneficial because it eases up the process of licensing and cost of drug discovery.

There are two pathways of metabolomics-based mode of action, initially, the alterations after drug induction are observed using metabolic fingerprint, and then the metabolome is compared with drugs that have known modes of action using multivariate statistical analysis (Yi *et al.*, 2007). However, there are few trypanocides with known mode of action, although examples exist, such as Eflornithine and the new N-myristoyltransferase (NMT) inhibitors. But is unlikely that a novel compound of unknown trypanocidal mode of action would exactly mimic the actions of ether eflornithine or NMT inhibitors, thus unbiased approach to mode of action discovery is necessary. The second pathway is more

consistent because it focuses more on the separate metabolite abundance changes which take place after adding the drug (Le Roch *et al.*, 2008) and this permits the discovery of new modes of action and also prediction of off-target effects.

1.7 New drugs for protozoa

Currently, chemotherapy is still important for the control of most parasitic diseases, such as trypanosomiasis and leishmaniasis. However, problems associated with treatment of these diseases include drug toxicity, resistance, a lack of guaranteed supply, and high cost. In addition, at present, with the rapid development of the world in all fields, the numbers of people who have parasitic diseases are extreme. For example, more than 12 million people are presently infected by leishmaniasis and 50,000 new cases per year of African trypanosomiasis are reported. Obviously these numbers do not include the large numbers of people in remote areas that are never formally diagnosed with the disease. Furthermore, a large number of antiparasitic drugs have been only experimentally tested in animal models, so little is known about their efficacy on parasitic hosts (el Kouni, 2003).

According to DNDi in 2012 (<http://dndi.org/press-releases/1207-astellas-and-dndi.html>) the newest drugs used for the treatment of HAT and VL are nifurtimox-eflornithine combination therapy (NECT) and sodium stibogluconate and paromomycin (SSG&PM) combination therapy, respectively.

Currently, there are several compounds under consideration for the treatment of HAT and Leishmaniasis. In addition, Fexinidazole is one new drug that is being developed against HAT; it shows ability to kill the parasites of both species that caused HAT *in vitro* and *in vivo* (Kaiser *et al.*, 2011). Another very promising new class of compounds is the oxaboroles (Maser *et al.*, 2012), which is being developed by DNDi and Scynexis. The lead oxaborole SCYX-7158 is active in both acute and cerebral mouse models of trypanosomiasis, and has now started Phase I clinical trials (Nare *et al.*, 2010).

Despite the improved pipeline for antiparasitic drug development it is essential that efforts continue to identify new, unrelated lead compounds, as experience

shows that many preclinical candidates will not in the end be approved for human use. Consequently, this study will focus on several promising lead compounds to study their effects on pathogenic parasites.

1.8 Treatment of protozoan infections by natural products and their derivatives

Only a very restricted number of drugs are licensed and used as antiparasitic agents due to the development of drug resistance, which causes most of the drugs to become dormant or less active against the parasites. This has led to the discontinuation of the use of many compounds that were once highly efficacious, like chloroquine for malaria. In the disease endemic countries, issues such as toxicity, price and accessibility are also major factors affecting the use of antiparasitic drugs. One possible approach to improve this situation is to screen for antiprotozoal activities in natural resources, such as plants, microorganisms (bacteria, fungi), marine organisms, sponges and invertebrates. These provide an enormous diversity of potent bio-active compounds that may be amenable for clinical application (Kayser *et al.*, 2003).

More than 20,000 species of plants are being used to produce traditional medical treatments for a plethora of diseases and ailments (Phillipson, 1994). It has been estimated that around 6.1 billion people in the world (66%) trust traditional medicines more than pharmaceutical drugs, despite limited knowledge about their toxicity and efficacy, due to issues such as restriction in accessibility, and/or the increased costs of pharmaceutical drugs (Tagboto & Townson, 2001). Consequently, the use of these traditional medicines has contributed to many deaths, despite the great value in some of natural and herbal medicines.

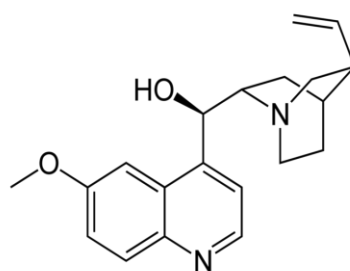
Foxglove, ephedra, and morphine are the first three natural sources derived from plants for use in traditional medicines. These drugs can be used in the treatment of heart disease, respiratory disorders, and produces an effective analgesic effect, respectively (Tagboto & Townson, 2001). For the production of

new anti-infective agents with reduced toxicity and higher efficacy natural products are often used as starting point.

Further detail regarding many natural antiparasitics is being given below. For the treatment of malaria, quinine and artemisinin are used and to confront several parasitic and non-parasitic diseases, curcumin is used. Antibiotics are widely used against many infectious agents, prominently including infections of bacterial origin but in specific cases also protozoan disease.

1.8.1 Quinolines in malaria

Quinine is a natural white crystalline alkaloid compound (see below), which is derived from the bark of *Cinchona* trees. It was initially discovered in South America for the treatment of tropical fevers. Nowadays, it is being used to treat malaria caused by *P. falciparum* and also as an analgesic and anti-inflammatory agent.



The quinine base is found in 5 states, namely: quinine dihydrochloride, quinine hydrochloride, quinine sulfate and quinine gluconate. All these quinine bases can be administered in doses of 8 mg/kg of quinine base three times a day either orally or by intravenous injection. Furthermore, it can also be administered rectally or intramuscularly every 12 hours in doses of 20 mg per kg or 12.5 mg/kg of quinine base, as mentioned by Barennes and colleagues (Barennes *et al.*, 2006).

Even though the mode of action of quinine against malaria parasites is still under examination, it is believed to be similar to chloroquine; causing cytotoxicity by inhibiting the polymerisation of haem into haemozoin, resulting in free haem which is toxic for the parasite (Yakuob *et al.*, 1995). Quinine and its chemical quinoline analogues accumulate in the parasite's food vacuole into which they freely diffuse prior to being trapped by protonation. It is this accumulation that leads to a sufficiently high local concentration to interfere with haem polymerisation.

Cinchonism, heart attack, stroke, cardiac arrhythmias, hearing loss, cardiovascular problems, nausea, headach and visual loss are some of the side effects observed after Quinine administration (Bodenhamer & Smilkstein, 1993; Boland *et al.*, 1985; Jung *et al.*, 1993; Smilkstein *et al.*, 1987; Wolf *et al.*, 1992). Despite various studies on the use of quinine, very few studies have

studied the effect of this compound on trypanosomes *in vitro*. Merschjohann and co-workers did one of these studies, which measured the efficacy of this drug together with 33 other alkaloids on two species of Trypanosoma: *T. b. brucei* and *T. congolense* (Merschjohann *et al.*, 2001). As a result, the IC₅₀ value of quinine on *T. b. brucei* was determined about 5 µM.

1.8.2 Antibiotics

Antibiotics are of course known as antibacterials, and are used for treatment of infection caused by bacteria, but ‘antibiotics’ are an extremely diverse category of compounds and are used to treat many diseases that are caused by different organisms such as fungi and protozoa.

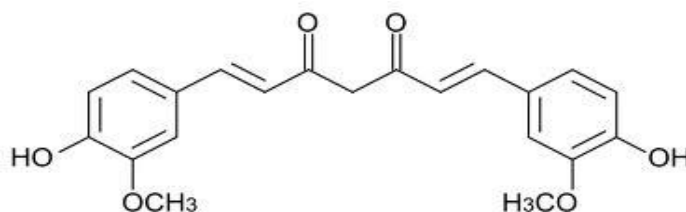
One of the famous antibiotics used for treatment malaria is tetracycline (IMBODEN, Jr. *et al.*, 1950), Ruiz-Sanchez *et al* (RUIZ *et al.*, 1952) effectively used tetracycline to treat malaria which is caused by *P. falciparum* and *P. vivax*, although its effect as an antimalarial is slow (Dahl *et al.*, 2006). This antibiotic acts on the ribosome of bacterial origin that is located within the *Plasmodium* plastid and thus inhibits protein biosynthesis within this organelle (Connell *et al.*, 2003)

There are many efforts to discover new antibiotics against trypanosomes. For instance, Ishiyama and his colleges (Ishiyama *et al.*, 2008) have found two antibiotics that have a strong antitrypanosomal effect *in vitro* and *in vivo*: KS-505a and Alazopeptin display *in vitro* IC₅₀ values in the range 1.6 to 0.5 µg/ml against *T. b. brucei* and *T. b. rhodesiense*, which is almost the same IC₅₀ as for registered HAT drugs suramin and eflornithine. In addition, nine antimicrobial peptides were tested on African trypanosomes bloodstream and Procyclic forms and the results shows that the antibiotic BMAP-27 inhibited 100% of growth at low concentrations (2 µM and 9 µM for bloodstream and procyclic respectively). Five of the nine antimicrobial peptides inhibited the growth of both lifecycle stages, highlighting the possibility of development of those antibiotics as chemotherapy for trypanosomes (Haines *et al.*, 2003).

Antibiotics are also used to treat Leishmaniasis, and this includes one of the most important antileishmanial drugs, Amphotericin B. More details about this antibiotic have already been given in (section 1.2.7.2).

1.8.3 Curcumin

Curcumin (structure see below) is a phenolic compound, and a natural yellow dye, which is derived from the roots and rhizomes of different species of *Curcuma* plants, called Zingiberaceae (Perez-Arriaga *et al.*, 2006). Another plant of this species is the *Curcuma longa* Linn (turmeric) which is considered a significant medicinal plant which can also be used to give colour, spice and flavour to foods (Iqbal *et al.*, 2003; Pan *et al.*, 1999a; Sharma *et al.*, 2005a). There are three main components of *Curcuma* spp, the first is essential oils e.g. zingiberene, turmerones and atlantones, second is turmerin (a water soluble peptide) and the third is curcuminoids e.g. curcumin and its immediate derivatives (Sharma *et al.*, 2005a).



Aside from water, Curcumin has the ability to dissolve in acetone, ethanol and dimethylsulphoxide (Sharma *et al.*, 2005a). It was also suggested by Wang *et al.* (Wang *et al.*, 1997) that curcumin is not stable in the neutral and basic pH because it disintegrates into feruloyl-methane and ferulic acid. There is evidence to suggest that the main curcumin metabolites are the oxidation products dihydrocurcumin and tetrahydrocurcumin, which are further metabolised to monoglucuronide conjugates (Maheshwari *et al.*, 2006; Pan *et al.*, 1999b). Holder and his co-workers also suggested that the main metabolites of curcumin are glucuronide conjugates of tetrahydrocurcumin (THC) and hexahydrocurcumin (Holder *et al.*, 1978).

1.8.3.1 Curcumin use in medicine

Curcumin has been used to treat many medical problems and it has long been used as a traditional medicine in India (Sharma *et al.*, 2005b). Curcumin has been reported as having anti-microbial, anti-inflammatory, anti-mutagenic, and anti-oxidant activities, as well as wound-healing abilities (Maheshwari *et al.*, 2006; Sharma *et al.*, 2005b). In addition, curcumin has been reported to have anti-cancer properties (Sharma *et al.*, 2005; Iqbal *et al.*, 2003; Koide *et al.*, 2002).

Inflammation plays an important role in chronic diseases such as asthma, and curcumin, as mentioned before, is an effective anti-inflammatory agent. For example, curcumin downregulates the expression of the enzyme COX-2 that is correlated with many types of inflammation (Lee *et al.*, 2005). Curcumin also inhibits the action of TNF, which is one of the most pro-inflammatory cytokines (Gulcubuk *et al.*, 2006). Furthermore, curcumin has been shown to guard against several inflammatory diseases such as colitis (Sugimoto *et al.*, 2002), arthritis (Joe *et al.*, 1997), pancreatitis (Gulcubuk *et al.*, 2006; Masamune *et al.*, 2006) and allergies .

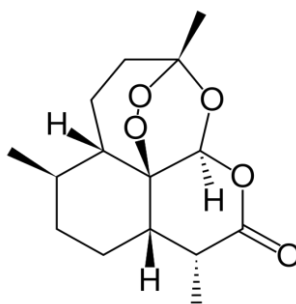
Oxidative stress also plays an important role in the pathogenesis of many diseases such as cerebral ischemia-reperfusion injury, myocardial ischemia, cancer and hypoxia (Maheshwari *et al.*, 2006). Curcumin has been reported to aid in the defence of different cells from oxidative stress (Atsumi *et al.*, 2005).

Curcumin has been shown potent against many types of cancer such as skin (Kuttan *et al.*, 1987), liver (Notarbartolo *et al.*, 2005), prostate (Imaida *et al.*, 2001), breast (Choudhuri *et al.*, 2002), colon (Chen *et al.*, 1999) and lung cancer (Radhakrishna Pillai *et al.*, 2004). Many studies have demonstrated that curcumin inhibits chemical carcinogenesis in animal models.

In addition, curcumin has been shown to have anti-parasitic effects with parasites such as *Trypanosoma* (Nose *et al.*, 1998), *Leishmania* species (Gomes *et al.*, 2002; Koide *et al.*, 2002; Saleheen *et al.*, 2002) and *P. falciparum* (Mishra *et al.*, 2008). Recently, curcumin was also shown to be effective against *Trypanosoma cruzi*; it caused reduced parasitemia in infected mice and killed the parasites *in vitro* (Nagajyothi *et al.*, 2012).

1.8.4 Artemisinin

The herb *Artemisia annua* produces a compound called Artemisinin (structure see below)(Ferreira & Janick, 1996). This compound was identified in the 1960s by Chinese biologist Tu Youyou who named it Qinghaosu in Chinese. This compound is made from natural herbs which are used to cure various conditions such as skin diseases, malaria, parasitic infections such as *Schistosoma mansoni*, *S. japonicum* and *Clonorchis sinensis* (Hien & White, 1993), leukaemia and colon cancer (Efferth *et al.*, 2001). Other than this, it is also used for the cure and prevention of breast cancer (Rowen, 2002) because it regulates hormones. In the 1970s, the compound was also given the title of a multi-drug resistance drug for the treatment of *P. falciparum* malaria (Arnold *et al.*, 1990).



Artemether, artesunate, arteether and artelinate are a few chemical derivatives of artemisinin and these compounds have the ability transform into an active plasma metabolite state called, dihydroartemisinin, and this is the actual state which has the anti-malarial activity (Wilairatana *et al.*, 1998). The safe dose of artemisinin that can be administered for treatment of the disease is 3 g for around 3-5 days (about 50 mg per kg bodyweight), but it is advised to use this with other antimalarial drugs having a longer half life because the derivative compounds have a short half-life (White, 2004).

Despite limited knowledge regarding the specific mechanism of action of artemisinin, a study was conducted in 2005 using a yeast model and it was seen that this drug initially acts on the electron transport chain and releases local reactive oxygen species which in turn results in depolarization of the mitochondrial membrane (Li *et al.*, 2005). One study suggested that the one of the mode of action of artemisinin is dose alkylation of heme to form adduct from reaction between artemisinin and heme (O'Neill *et al.*, 2010).

Artemisinin did not harm the human body despite a high dosage in a 70 mg/kg body weight per day (Rowen, 2002). But there was a case study which showed that in a subject receiving a high dose (120 mg/kg) of artemisinin over 3 days (Hien & White, 1993), the concentrations of serum aspartate aminotransferase (AST) were increased and this could be indicative of acute or mild hepatotoxicity.

1.9 Aims

This thesis will aim to investigate these points:

1. To identify new curcumin analogues with activity against *Leishmania* spp and African trypanosomes *in vitro*.
2. To identify new phosphonium salts with activity against African trypanosomes *in vitro*.
3. To analyse the structure activity relationship (SAR) for curcumin compounds on *Leishmania* spp and phosphonium compounds on African trypanosomes.
4. To study the mode of action of the most promising curcumin compound.
5. To identify the target of phosphonium analogues.

2 Chapter two: Material and Methods

2.1 Cell culture

2.1.1 *Trypanosoma brucei* blood stream forms (BSF) in-vitro:

Three strains of bloodstream form (BSF) of *Trypanosoma brucei* were used in this study: (A) *Trypanosoma brucei brucei* wild type strain (s427-WT), (B) TbAT1 knock out (KO) is derived from the s427-WT strain by the deletion of both alleles coding for the TbAT1/P2 transporter. This leads to resistance to diminazene aceturate and low levels of resistance to several other drugs including pentamidine and melarsen oxide (Matovu *et al.*, 2003); (C) TbAT1-B48 is derived from TbAT1-KO by increasing their exposure to pentamidine, which causes a high resistance to diminazene, pentamidine and melaminophenyl arsenicals. Consequently, these cells do not have the TbAT1/P2 transporter or the high affinity pentamidine transporter (HAPT) (Bridges *et al.*, 2007). The standard culture medium that has been used for three strains is HMI-9 medium (Hirumi & Hirumi, 1989) with 10% heat-inactivated Fetal Calf Serum (FCS) and 14 µl of β-mercaptoethanol (Sigma) per litre of medium, with pH adjustment with HCl or NaOH to 7.4. The medium was sterilized inside a flow cabinet by filtration through 0.22 µm Millipore Express PLUS membranes (PES) filters. The parasites were cultured and incubated at 37 °C under 5% CO₂ atmosphere and were passaged three times per week in vented flasks.

2.1.2 *Leishmania mexicana* & *Leishmania major* Promastigotes:

Leishmania mexicana (MNYC/BZ/62/M379 strain) and *Leishmania major* (Friedlin strain) were grown in HOMEM medium (pH 7.4) with 10% heat-inactivated Fetal Calf Serum (FCS) in plastic flasks at 25°C. Cultures were passaged into fresh medium three times per week.

2.1.3 *Leishmania mexicana* amastigotes:

Axenic *Leishmania mexicana* amastigotes cultures were maintained in 80% Schneider's Drosophila Medium, complemented with 20% heat-inactivated FCS

with 0.3% Gentamycin (G 1272) for each ml of medium, and 10 μ l of 1.0 M HCl for every 1 ml of medium to adjust to pH 5.5. The medium was sterilized inside a flow cabinet by filtration through 0.22 μ m Millipore Express PLUS membranes (PES) filters, then stored at 4°C. The parasites were cultured and incubated at 32 °C under 5% CO₂ and were passaged twice a week in vented flasks by adding 1 ml from the original culture to 10 ml fresh medium with the observation that the cells of *L. mexicana* amastigotes grow in the form of colonies. As a result, cells were withdrawn using a syringe with the needle against the side of the flask, to ensure that all of the cells were separated before passage.

2.1.4 Human embryonic kidney (HEK) cells (strain 293T):

Human Embryonic Kidney Cells were grown in a standard culture that included 500 ml Dulbecco's Modified Eagle's Medium-DMEM (Sigma), 50 ml newborn Calf Serum (NBCS) (Gibco), 5 ml Penicillin/Streptomycin (Gibco) and 5 ml L-Glutamax (200 mM, Gibco). All constituents were mixed under sterile conditions in a 500 ml bottle of DMEM, then kept medium at 4°C.

The cells were cultured and incubated at 37°C + 5% CO₂ and were passaged three times per week when they reached 80-85% confluence in passage ratio in vented flasks. Flasks are incubated on their sides (horizontally) to expose a larger surface in order to allow cells adherence, which is essential for the cell growth as a monolayer.

2.1.5 Bacterial strains:

XL1 strain of *Escherichia coli* was used for routine cloning of *T. b. brucei* genomic sequences. *E. coli* cells were kept as glycerol stabulates at -80 °C. Cells were moved and grown in LB broth (sigma) that was supplemented with 100 μ g/ml of ampiciline (sigma) at 37 °C under vigorous shaking (250 rpm) overnight.

2.2 Preparation of stabilates

Stabilates were manufactured from the different strains that we used on a daily basis. A cell suspension of to 2×10^6 cells/ml in HMI-9 (10% FCS) was diluted 1:1 with HMI-9 containing 30% of glycerol. Immediately after the preparation of dilutions, samples kept in vials were transferred to a -80°C freezer and stored for 24 h prior to transfer to liquid nitrogen for permanent storage.

Stabilates were taken out from liquid nitrogen and brought to room temperature by simply thawing. Harvesting of cells was performed by centrifugation at a speed of $3000 \times g$ for 10 minutes at 21°C and the cells were resuspended in normal HMI-9/FCS.

2.3 Drug sensitivity using Alamar blue

Alamar Blue is used as an indicator of metabolic cell function. The dye (Resazurin sodium salt) is added to a cell culture containing a test drug solution to determine the *in vitro* drug sensitivity of African trypanosomes (Raz *et al.*, 1997) and *Leishmania* spp (Fumarola *et al.*, 2004) to the drug.. Alamar blue is used to measure cell proliferation or cell viability depending on the metabolic activity of cells. Live cells will metabolise resazurin (blue and nonfluorescent) to resorufin (pink and highly fluorescent), whereas metabolic activity stops with cell death and the resazurin does not change. By using special software, the EC_{50} can be determined for different concentrations of the drug.

An Alamar Blue solution was prepared by dissolving 12.5 mg Resazurin sodium salt (Sigma) in 100 ml of Phosphate Buffered Saline (PBS) and adjusting the pH to 7.4. The solution was sterilized inside a flow cabinet by filtration through a $0.22 \mu\text{m}$ Millipore Express PLUS membrane (PES) filter. This dye solution can be stored at 4°C away from the light for several weeks or frozen for longer storage (Raz *et al.*, 1997).

All drugs dilutions are freshly prepared in the individual medium on the same day of the assay, ensuring that the final concentration of solvent (usually DMSO) does not surpass 1%, as higher levels will affect trypanosome growth.

2.3.1 Drug sensitivity using Alamar Blue assay in bloodstream forms of *T. b. brucei*

Stock solutions of drugs were typically prepared at 20 mM or 40 mM in DMSO and diluted to 200 μ M with HMI-9 medium + 10% FCS; 200 μ l of this was added to the first well of rows (A), (C), (E) and (G) of a 96-well plate, setting up for doubling dilutions of 4 different drugs, each over two rows of a 96-well plate (Figure 1). Diminazene or/and Pentamidine are used as positive controls for each experiment. 100 μ l of HMI-9 medium is pipetted into all remaining wells. 100 μ l of a drug preparation are taken by a multichannel pipettor from the first column in rows (A), (C), (E) and (G) and mixed gently with the medium in the wells of the second column, then another 100 μ l from second column wells are added to third column wells and so on, creating a doubling dilution. The last column of the plate (which is the first column in rows B, D, F and H) does not receive any drug solution, because this is the drug free control.

Cell counts were performed (haemocytometer) and cells density adjusted to the desired concentration of 2×10^5 cells/ml of which 100 μ l was added to all of the wells in the plate, resulting in 1×10^5 cells/ml for all wells. The plates were incubated at 37°C + 5% CO₂ for 48 hours after which 20 μ l sterile Alamar Blue solution was added to every well, followed by a further incubation of 24 h. The fluorescence of the wells was read by a FLUOstar OPTIMA Fluorimeter (BMG Labtech) at wavelengths 530 nm for excitation and 590 nm for emission. The fluorescence values were analysed via GraphPad Prism5 software, plotting the data to an equation for a sigmoid curve and to determine the EC₅₀ values.

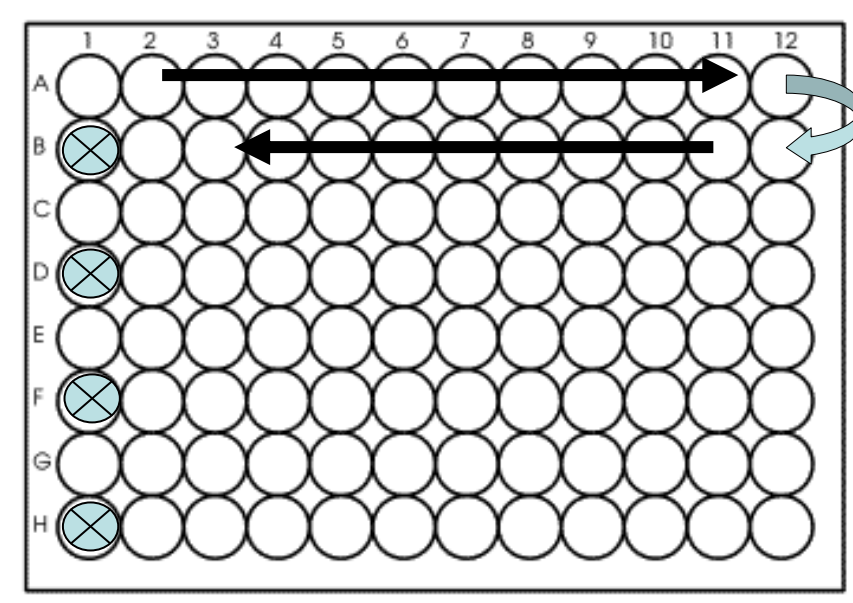


Figure 2.1. explains the way drugs are doubly diluted down two rows across the plate. Indicates the drug free wells 

2.3.2 Drug sensitivity using Alamar Blue assay in *Leishmania mexicana* amastigotes

The Alamar Blue assay for *Leishmania mexicana* amastigotes is similar to that for *Trypanosoma brucei brucei*, with the following exceptions, A- 80% Schneider's Drosophila Medium (SDM), with 20% FCS and 0.3% Gentamycin was used. B- The final density of cells in all wells was 1×10^6 cells/ml. C- When the cells were counted, the cells were first separated using a syringe as described above.

The plates were incubated at $32^\circ\text{C} + 5\% \text{CO}_2$ for 72 hours after which 20 μl Alamar Blue solution was added to all wells, and the plate was incubated for an additional 48 h, after which fluorescence was determined in a fluorimeter.

2.3.3 Drug sensitivity using Alamar Blue assay in *L. mexicana* and *L. major* promastigotes

The Alamar Blue assay for *L. mexicana* and *L. major* promastigotes is also the same way as in *Trypanosoma brucei brucei* except: A- Using HOMEM medium (pH 7.4) with 10% heat-inactivated Fetal Calf Serum (FCS). B-The final density of

cells in each well was 1×10^6 cells/ml. C- The plate is incubated at $25^\circ\text{C} + 5\% \text{CO}_2$ for 72 hours after which 20 μl Alamar Blue solution is added to every well and the plate incubated for a further 48 hours.

2.3.4 Alamar Blue assay in Human Embryonic Kidney (HEK) Cells

Passaging the cells is done through several steps, which are summarised as follows: The medium is removed from vented culture flask by withdraw it and 2 ml of pre-warmed 37°C 0.25% Trypsin-EDTA solution (Sigma) are added to the flask and left for 5 minutes after which 8 ml of medium (pre-warmed to 37°C) is added, and the suspension is mixed and transferred to a sterile 15 ml centrifuge tube, and the cells are spun down at 1200 rpm for 5 min at room temperature. The supernatant is decanted and the cells re-suspended in 10 ml of medium. 1 ml of cell suspension is added to a vented flask with 10 ml of medium and the flask is incubated at $37^\circ\text{C} + 5\% \text{CO}_2$.

Cell counts are performed by pipetting 10 μl of cell suspension (after mixing) into the haemocytometer counting chamber. Cell suspensions could be used for the Alamar Blue assay as well. Cells are counted and adjusted to a density of the desired concentration (3×10^5 cells/ml). 100 μl of this suspension is added to each well of a 96-well plate, so every well contains 3×10^4 cells. The plate is incubated at $37^\circ\text{C} + 5\% \text{CO}_2$ for 3 hours to allow the cells to adhere to the bottom of the plate. Drug stocks are prepared at 800 μM (two times concentration) by diluting them in DMEM medium. Phenyl arsine oxide (PAO) is prepared at 200 μM as a positive control. Using a separate 96-well plate, 260 μl of the drug stock is pipetted into the first column in rows (A), (C), (E) and (G) of 96-wells plates (figure 1), so that two rows are used for every drug. 130 μl of DMEM medium is pipetted into all remaining wells. 130 μl of drug is taken by multichannel from the first column in rows (A), (C), (E) and (G) and mixed gently with the medium in the wells of second column, then another 100 μl from the second column wells are added to third column wells and so on, the last column of the plate (which is the first column in rows B, D, F and H) does not receive any drug solution, because this is the drug free control. After of incubating the plate that has HEK cells for 3 hours, 100 μl /well of the plate that contains the

drug dilution series is transferred to the opposite well on the plate that contains the HEK cells, using a multichannel pipette. The result is a final concentration of drug in the first wells of 400 μM (for PAO this is 100 μM). The plate is then incubated at 37 °C + 5% CO_2 for 16 hours followed by the addition of 20 μl of Alamar Blue solution to every well and incubation at 37 °C + 5% CO_2 for a further 24 hours. The fluorescence of the plate is read on a Fluorimeter at wavelengths 530 nm for excitation and 590 nm for emission. The data are then analysed using GraphPad Prism4 software to draw the graph and determine the EC_{50} values.

2.4 Drug sensitivity using Cell count

A set of compounds with different concentrations was tested on trypanosomes for monitoring *in vitro* cell growth using cell count. The parasites were taken from cultures at the late logarithmic phase of growth and cell density was determined using a haemocytometer. Cell density was adjusted to the desired concentration and diluted with fresh HMI-9/FCS medium. The cell count was taken in triplicate at four time points (0, 4, 8 and 12h) on each day for each concentration of the compounds, for 72 h.

2.5 Drug sensitivity using Propidium Iodide assay

This procedure is used in order to monitor the speed of action of test compounds on trypanosomes in real time. Cells become fluorescent as PI enters the cell and binds to nucleic acids. This occurs only upon breach of the plasma membrane, i.e. loss of cellular integrity. In this method, 100 μl of HMI-9/FCS was added to each well of a 96-well plate and 200 μl from different compounds of the appropriate concentration, also in HMI-9, was added to the first column, whereas the last wells of each column received only media and served as drug free controls. 100 μl of the drug solution was taken by a multichannel pipettor from the first column and mixed gently with the medium in the wells of the second column, then another 100 μl from second column wells are added to third column wells, and so on, to make a doubling drug dilution. Cell density was adjusted to a suspension of $1 \times 10^7 \text{ ml}^{-1}$ in the presence of 18 μM of PI. In addition,

18 μM of PI without cells was prepared for the negative control, which is the same doubling drug dilution series in the absence of cells. The plates were then incubated in a FLUOstar OPTIMA fluorimeter (BMG Labtech) at 37 °C with 5% CO_2 , and the fluorescence was observed at 544 nm excitation and 620 nm emission for up to 8 hours, with absorbance values analysed using GraphPad Prism 5 software to plot the data.

2.6 Determination of the mitochondrial membrane potential by flow cytometry

The mitochondrial membrane potential of treated and untreated cells was assessed by using Tetramethylrhodamine ethyl ester (TMRE) (Denninger *et al.*, 2007; Figarella *et al.*, 2006). The cell density was adjusted to 1×10^6 cells/ml with and without test compounds for the start of the experiment. 1 ml of sample was transferred at each time point into a microfuge tube and centrifuged at 2500 rpm for 10 min at 4 °C, and was then resuspended in 1 ml PBS containing 25 nM of TMRE, and cells were incubated at 37 °C for 30 minutes. In addition, 100 nM of valinomycin and 10 μM of troglitazone were used as controls, as they are known to induce mitochondrial membrane depolarisation and hyperpolarisation, respectively (Denninger *et al.*, 2007). All samples were analysed by flow cytometry using a FL2-height detector and CellQuest software.

2.7 Cell cycle using flow cytometry

Flow cytometry was used as described by (Hammarton *et al.*, 2003) to study the effects of test compounds on DNA content in *Trypanosoma brucei brucei*. The cell density was adjusted to 1×10^6 cells/ml with and without test compounds for the duration of the experiment. 1 ml of sample was transferred at each time point into microfuge tubes and centrifuged at 2500 rpm for 10 min at 4 °C, then resuspended and fixed in 1 ml of 70% methanol and 30% PBS and left at 4 °C overnight. After storage, the samples were washed twice with 1 ml of PBS and subsequently resuspended in 1 ml PBS containing propidium iodide and RNase A

(both at 10 µg/ml), and incubated at 37 °C for 45 minutes while protected from light. Samples were analysed by Becton Dickinson FACSCalibur using the FL2-Area detector and CellQuest software. ModFit LT software was used to quantify the flow cytometry results.

2.8 Measurement of intracellular calcium level

Intracellular Calcium level was measured using the Screen Quest™ Fluo-8 Calcium Kit produced by ABD Bioquest (Ibrahim *et al.*, 2011). *Trypanosoma brucei brucei*-WT cells were used in this experiment and grown in HMI-9/FCS in vented flasks incubated at 37°C + 5% CO₂ for 48 h. The cells were then centrifuged at 2500 × g for 10 min at 4 °C, and re-suspended to a final density of 4 × 10⁶ cells/ml in the Fluo-8 dye-loading solution and further incubated at 37 °C for 30 min. The cells were then washed twice with assay buffer to remove any extracellular dye-loading solution. 90 µl of cells were added to each well in a black-bottomed 96-well plate. The positive control (Calcium ionophore A23187 (Sigma) 10 µM) and the negative control (assay buffer) were prepared. The plate was then incubated in a FLUOstar OPTIMA fluorimeter at 37°C, and the fluorescence was observed for two minutes at 485 nm excitation and 520 nm emission. The fluorimeter was stopped while different concentrations of the compound and positive and negative controls were added. The fluorescence was observed for a further 15 minutes (250 cycles - 4 sec/cycle). Finally, the absorbance values were analysed using GraphPad Prism 5 software to plot the data. However, for some compounds there was no short-term response in Intracellular Calcium level which was therefore also determined at 0, 4, 8 and 12 hours. During this time the cells were grown in HMI-9 medium + 10% FCS in vented flasks with and without test compounds. At the beginning of the experiment, a predetermined amount of cells from each flask (treated and control) was removed to microfuge tubes, centrifuged for 10 min (2500 × g, 4 °C) and re-suspended to a final density of 4 × 10⁶ cells/ml in the Fluo-8 dye-loading solution, and intracellular calcium was determined as above.

2.9 DNA configuration assessment using fluorescence microscopy

DNA configuration from nuclei and kinetoplast were assessed using the dye 4,6-diamidino-2-phenylindole (DAPI), which fluoresces when bound with DNA. 50 μ l of cells at $\sim 5 \times 10^5$ cells/ml were spread onto a glass microscope slide, left to air dry and fixed in methanol overnight at -20 °C. The slides were rehydrated with 1 ml of BPS for 10 minutes which was allowed to evaporate (without completely dry). 50 μ l of PBS containing 1 μ g /ml DAPI and 1% of 1,4-diazabicyclo [2.2.2] octane (DAPCO) was added to the slides and spread by coverslip. Slides were observed under UV light on a Zeiss Axioplan microscope using a Hamamatsu digital camera and Openlab software. 500 cells were recorded for each sample, and scored for DNA configuration following these groups: 1N1K, 1N2K, 2N2K (Early) and 2N2K (Late) (N, nucleus; K, kinetoplast). The effect of test compounds on DNA configuration was determined at 0, 8, 12, 16 and 24 h; untreated cultured served as control.

2.10 Giemsa Staining

Giemsa stain was used to detect overt morphological changes in cells exposed to test compounds. The cell density was adjusted to 1×10^6 cells/ml with and without test compounds for the start of the experiment and at each time point, 1.5 ml of culture was centrifuged at 2500 rpm at room temperature for 10 min. Smears were made by resuspending the pellet in 75 μ l of HMI 9 + 20% FCS and using 25 μ l of this suspension. The smear was then air dried and fixed with 100% of methanol for 2 min. Staining was performed for 30 minutes with 10% Giemsa solution After which the slides were washed with water and air dried. A Zeiss Axioskop Mk1 microscope with an oil emersion $\times 63$ objective lens was used for observing the slide. For imaging Cooplux, CCD coloured camera was used and Rimage and tsivision software was used for editing the images.

2.11 Live Cell Imaging

A cell culture with the density of 1×10^6 cells/ml was made applying the same method as described in section 2.10. At each time point 50 μ l of culture was

taken and covered with a cover slip and observed under Axioplan 2 imaging light microscope with resolution of $\times 100$ oil immersion objective lens. A Hamamatsu camera was used for taking the images and Openlab and Volocity software were used for editing.

2.12 Transmission Electron Microscopy

Transmission Electron Microscopy was used to assess the action of test compounds on *Trypanosoma brucei brucei* ultrastructure. The cell density was 1×10^6 cells/ml. Two 10 ml samples were transferred to 15 ml centrifuge tubes and to one of them 1 μ M CD38 was added. Cells were centrifuged at 2600 rpm for 10 min at room temperature and the pellet contained the supernatant was discarded. A 0.5 ml solution of 2.5% of Glutaraldehyde was prepared in 0.1 M phosphate buffer (pH 7.4) and added gently to the centrifuge tubes from the side wall to avoid pellet resuspension. The solution was left undisturbed for 10 min. The pellet was then gently agitated in the fixative and again left undisturbed for half an hour. The fixative was sucked back by pipette and 0.5 ml of the 0.1 M phosphate buffer was introduced into the tubes to dissolve the remaining Glutaraldehyde in the tube and sample was left at 4 °C overnight.

1 mm of pellet was taken and then remaining aldehyde was removed by rinsed it in fix buffer twice. 1% osmium tetra oxide was used as a fixative to fix the cells and after its addition the cell was left undisturbed for an hour. Distilled water washes were performed to remove excess osmium tetra oxide. Then cells were kept in the 0.5% Uranyl acetate solution for almost 30 minutes and washing was performed with distilled water after it. Different concentrations of alcohol were used to wash and dehydrated the cells (30, 50, 70, 90 and 100% ethanol). After all the procedures cell infiltration was performed utilizing Epon/Araldite epoxy resin. The suspension was kept overnight, rotating at 200 °C. Polymerization of cells in the silicon block moulds was done after embedding it in the fresh resin. The temperature used for polymerization of cells was 600 °C. The size of the section that we used for analysis in Transmission Electron Microscopy was 60-80 nm. Lead and Uranyl solutions were used to stain the cells and then the sections were observed in Zeiss 912 Energy filtering TEM at 120 kv.

2.13 Scanning Electron Microscopy

To check the impact of the CD38 compound on the structure of *Trypanosoma brucei brucei* we employed the Scanning Electron Microscopy. Cells were cultured to a concentration of 1×10^6 cells/ml and two separate 10 ml aliquots were prepared (1 μ M CD38 and control) in 15 ml of centrifuge tubes which were spun at 2600 rpm for 10 min at room temperature. The supernatant was discarded with great caution without disturbing the pellet. Glutaraldehyde solution was prepared with a concentration of 2.5% in PBS and added to the cell pellet. The mixture was left at room temperature for an hour after which the fixative was removed by washing with 0.5 ml 0.1 M PBS (pH 7.4).

The samples were fixed in a solution of 1% osmium tetroxide for one hour, washed with distilled water and then dehydrated by using a series of increasing concentration of acetone (30, 50, 70, 90 and 100 % acetone; 10 min per treatment). A Critical Point Dryer was then used to dry the samples. Mounting was performed employing silver paint and double sided copper tape. Samples were then coated with palladium gold and its thickness was about 20nm and then samples were observed in the scanning electron microscope (JEOL 6400).

2.14 ATP Determination

ATP was measured using an ATP Determination Kit (Invitrogen) which has D-Luciferin and Luciferase (firefly recombinant). Briefly, 1×10^7 cells of both treated and untreated *Trypanosoma brucei brucei* were collected by centrifugation at 4 °C for 10 min at 2800 rpm. The pellet was washed twice in 200 μ l of 50 mM Tris-HCl, pH 7.4, containing 0.1 mM DTT. The cells were lysed by sonication on ice (twice for 10 s separated by 30 s in), using a Soniprep 150 at 8 μ amplitude. Then they were centrifuged at 14000 rpm for 10 min at 4 °C. The supernatant was immediately frozen in liquid nitrogen and stored in -80 °C. ATP levels were determined using the contents of the kit, and the standard reaction solution was prepared for a 10 ml volume from 8.9 ml dH₂O, 0.5 ml 20 \times reaction buffer, 0.1 ml of 0.1 M DTT, 0.5 ml of 10 mM D-luciferin, and 2.5 μ l firefly luciferase (5 mg/ml). 90 μ l reaction solution was added to each well and the

background luminescence was recorded in a FLUOstar OPTIMA fluorimeter; 10 μ l of each sample was added to the well and the luminescence was recorded. A standard curve was prepared using different concentrations of ATP (1 μ M-1 nM) to calculate the ATP concentrations in the samples.

2.15 TUNEL Assay

DNA fragmentation after exposure with different compounds was assessed by TUNEL assay. APO-BrdUTM TUNEL Assay Kit (Invitrogen) was used in the detection of DNA fragmentation. The cell density of *Trypanosoma brucei brucei* was adjusted to 1×10^6 cells/ml and incubated with and without test compounds for the duration of the experiment. After the specified incubation time the cells initially underwent fixation: 2×10^6 cells were suspended in 500 μ l of PBS, and 5 ml of 1% (w/v) paraformaldehyde in PBS was added to the sample and placed on ice for 15 min. The sample was then centrifuged at 2000 rpm for 5 min, and the cells were washed twice in 5 ml PBS before they were resuspended in 500 μ l PBS. Finally, 5 ml of 70% of ethanol was added to the sample and it was stored in a -20 °C freezer. After storage, the sample was centrifuged for 5 min at 2000 rpm to remove the ethanol. The cells were resuspended in 1 ml of wash buffer and centrifuged again for 5 min at 2000 rpm; this step was repeated. Then 50 μ l of DNA-labelling solution (10 μ l of the reaction buffer, 0.75 μ l of Terminal deoxynucleotidyl transferase (TdT) enzyme, 8 μ l of BrdUTP, and 31.25 μ l dH₂O) was added followed by incubation at 37 °C for an hour (with the sample shaken every 15 min). At the end of the incubation time, 1 ml of the rinse buffer was added to the sample and spun at 2000 rpm for 5 min, and this step was repeated, with the supernatants removed. Then 100 μ l of antibody staining solution (5 μ l of the Alexa Fluor 488 dye-labelled anti-BrdU antibody and 95 μ l of the rinse buffer) was added to each sample and incubated at room temperature for 30 min in the dark. Finally, 500 μ l of propidium iodide/RNase was added to each sample and the samples were incubated for 30 min at room temperature with the sample protected from light. Finally, the sample was analysed by flow cytometry using both FL3-width and Anti-BrdU FITC detectors and CellQuest software.

2.16 Counting Cells treated with Cycloheximide (CHX)

CHX was used as a protein synthesis inhibitor and used to investigate whether protein synthesis is necessary for CD38-induced cell death in *T. brucei*. A number of culture flasks were set up with 5×10^5 cells/ml with or without 10 µg/ml of CHX; preincubation with CHX was 1 h (37 °C, 5% CO₂). Four groups were set up for each concentration of compound:

1. - CHX, - Compound
2. + CHX, - Compound
3. - CHX, + Compound
4. + CHX, + Compound

Growth was monitored using manual cell counts after 0, 4, 8, 12, and 24 hours.

2.16.1 Pulse Labelling of Protein Pool in *T. b. brucei*

In order to confirm that CHX did indeed inhibit protein synthesis in *T. b. brucei* under the conditions used, proteins were pulse-labelled in the presence or absence of CHX. Cells were cultured to 5×10^6 cells/ml and divided over two flasks into which either CHX (10 µg/ml) was added or the same volume of DMSO (solvent) followed by a 1 h incubation at 37 °C and 5% CO₂. To each flask 25 µCi of [³H]-Lysine was then added followed by a further incubation of 3 h. After which cultures were centrifuged at 2800 rpm for 10 minutes at 4 °C. The cell pellet was solubilised in 1% Sodium dodecyl sulphate (SDS) and the suspension was centrifuged to pellet cell debris, which was placed on ice. To the supernatant Trichloroacetic acid (TCA) was added to a final concentration of 10% after which the solution was centrifuged again (10 min, room temp., 13,000 × g). The resulting protein pellet was washed with 10% ice-cold TCA 4 °C and transferred to a scintillation tube. The tube was left for incubation for half an hour at room temperature after the addition of 2% SDS (200 µl).

2.17 Induction of *T. b. brucei* cell lines resistant to AS-HK014 and curcumin

Two resistant cell lines were established for AS-HK001 (curcumin) and AS-HK014 to be used as a model to study drug uptakes levels and other adaptations in comparison to the parental cell line. In addition, a new resistant line could help in the understanding of mechanism of action that compound. Compounds AS-HK001 and AS-HK 014 were added to cultures of 5×10^4 cells/ml bloodstream form trypanosomes at different concentrations in HMI9/FCS medium. The adaptation was started using a range of test compound concentrations, ranging from $2 \times EC_{50}$ to $\frac{1}{4} \times EC_{50}$, with cells grown in a 24-well plate at 37 °C with 5% CO₂. 48 hours after incubation, a new 24-well plate was prepared, and the same concentration of compounds and 50 µl of cells were transferred from each well to the new plate where they were left for another 48-hour incubation in the same conditions, then the 24-well plate was observed by light microscopy. The maximum concentration at which the parasites were still observed to multiply was chosen as the initial maximum tolerated concentration. In this experiment, the initial concentrations were 5 µM and 0.25 µM for AS-HK001 and AS-HK 014, respectively. The trypanosomes were next passaged into a 24-well plate with fresh medium only as a control, fresh medium with initial concentration and fresh medium with double the initial concentration, and incubated for 48h. The cultures were observed every 48h, and the concentrations increased gradually depending on the cells' viability.

2.18 Metabolism of Curcumin in Trypanosomes

A metabolomic approach was used to examine the effect of some curcumin compounds on the bloodstream forms of *Trypanosoma brucei brucei*. Parasites were harvested in normal conditions and were taken at the late logarithmic phase before centrifugation at 2600 rpm for 10 min. The cell density was adjusted to 2×10^6 cells/ml in fresh HMI-9/FCS medium. Both adapted and wild-type cells were used, and incubated with and without the specified concentration of the compounds for the duration of the experiment. At the specified time of incubation, 25 ml of the cells were taken and directly quenched on a dry ice/ethanol bath to decrease the temperature to 4 °C; in

some cases the compound was added to other untreated cells after quenching. The cells were spun at 2600 rpm for 10 min at 4 °C. Then 5 µl of the supernatants (no cells) was taken and stored for analysis before removing all supernatants, but the pellet was kept. Next, 50 µl of 40 mM EPPS (4-(2-Hydroxyethyl) Piperazine-1-Propanesulfonic acid) + 2 mM EDTA and another 50 µl of 2 mM monobromobimane were added to each cell pellet and vigorously mixed; the mixture was added to the samples that have no cells as well. Then the samples were incubated in a water bath at 70 °C for 5 min. They were briefly cooled in ice before 100 µl of Acetonitrile (100%) was added, followed by incubation on ice for an additional 10 min. Finally, the samples were centrifuged at 14,000 rpm for 10 min at 4 °C, and then the supernatants were taken and stored at -80 °C until analysis using Orbitrap Mass Spectrometry and IDEOM software was used to analyse the metabolomic dataset (Creek et al., 2012). Further, 5 µl from the medium and from chemical reagents used in the experiment were taken and tested for double-checking if they had any metabolic content.

2.19 Measurement of Plasma Membrane Potential (V_m)

The membrane potential of trypanosomes was determined by using a fluorescent dye, bisoxonol, as described (de Koning & Jarvis, 1997). *T. b. brucei* were cultured, harvested and washed in assay buffer. The final concentration of cells was maintained at a concentration of 10^7 cells/ml. After bringing the cells to room temperature, a 100 µl aliquot was added to 2.9 ml of 0.1 µM bisoxonol. The fluorimeter cuvette had a path length of 1 cm and the temperature was set to 25 °C. The fluorescent intensity was observed at an excitation wavelength of 540 nm with bandwidths of 4 nm where emission wavelength size was 580 nm with bandwidths of 10 nm. The fluorescent intensity was found to be directly proportional to the cell concentration and we added 30 µl of compounds to be tested 140 s after cells were added to the cuvette. This allowed the recording of stable base lines before and after addition of the cells and the accurate recording of the compound's effect on the membrane potential. Control traces were recorded using the same scheme in the absence of cells in order to compensate for dilutions and any effect of the test compound on the read-out by

quenching or innate fluorescence. The positive control was Gramicidin and the negative control was either assay buffer or 1% ethanol (solvent control).

2.20 Molecular techniques

2.20.1 *Extraction of Genomic DNA*

Wild-type and the AS-HK014-adapted cell line TA014 were re-cloned by limiting dilution; TA014 was cloned out in the presence of 4.5 μ M AS-HK014. Genomic DNA was isolated from both strains as follows.

The cells were centrifuged at 2600 rpm for 10 minutes and cell pellets resuspended, and washed in PBS buffer and finally resuspended in 500 μ l of the NTE buffer (Appendix A) along with 25 μ l 10% SDS and 50 μ l of 10 mg/ml RNase A (Sigma). The mixture was incubated at 37 °C for 5 min. After a gentle stirring it was then allowed to stand undisturbed for 30 min at 37 °C. After the addition of 25 μ l of 20 mg/ml Pronase the sample was incubated overnight at 37 °C after which 600 μ l of phenol:chloroform:isoamyl alcohol 25:24:1 (Sigma) was added. The tube was centrifuged at 12,000 rpm for five min to get a clear top phase which was moved to a sterile centrifuge tube and the same volume of the same mixture was added followed by another centrifugation. Again the upper phase was transferred to another sterile tube and mixed with 600 μ l of chloroform and centrifuged at 12,000 rpm for five minutes. Again the resultant upper phase was transferred to a new sterile polystyrene tube and 2.5 ml of 100% ethanol was introduced in the sample for the DNA precipitation. DNA was washed with 70% ethanol after being transferred to a new tube. Centrifugation at maximum speed was performed and the DNA pellet was air-dried before being dissolved in 50 μ l TE buffer and the DNA sample was stored until use at 4 °C.

2.20.2 *Polymerase Chain Reaction for DNA*

Genomic DNA of *T. brucei* was amplified by using PCR with specific primers. From the databases we obtained gene ID numbers along with the published sequences of *Trypanosoma brucei* strain TREU927 from GeneDB as a reference

sequence. Unique 26 base pair upstream and downstream sequences were identified used for primer design. Sequences for forwards and reverse primers for the amplification of γ -GCS gene were 5' ggatccATGGGTCTTCTAACCACTGG 3' and 5' aagcttTCACCCTTCGCGTTGTCTTT 3' respectively (Eurofins MWG Operon). For GS gene the reverse primer sequence was 5' aagcttTTACGGTACAACCGCTAAGG 3' and 5' gctagcATGGTGTTAAATTGTTGCT 3' was the primer sequence for forward primer. The Phusion High-Fidelity proofreading polymerase (NEB) was used to improve reliability of the PCR. The PCR mix contained 15 μ l nuclease free water, 5 μ l fusion HF buffer, 0.5 μ l dNTPs, 1.25 μ l forward primer (10 μ M), 1.25 reverse primer (10 μ M), 0.75 μ l DMSO along with 0.25 μ l of DNA polymerase and 1 μ l of genomic DNA. A negative control was included, which contained all the components of the PCR mix except genomic DNA. The programme of the thermal cycler (PTC200 DNA Engine Thermal Cycler, MJ Research Incorporated, USA) was used for running the PCR reaction was as follows:

Cycle 1: Hot start denaturation at 98 °C for 30 seconds

Subsequent cycles: 32 cycles of

Denaturation: 98 °C for 10 seconds

Annealing: 58 °C for 30 seconds

Extension: 72 °C for one minute

At the end of cycles, final extension at 72 °C for 10 minute

After the reaction, agarose gel of 1% was run to observe the PCR products. Correct size fragments were extracted and purified for further proceedings.

2.20.3 Agarose Gel Electrophoresis of DNA

Agarose gel was prepared for the analysis of DNA that was isolated by the established protocol. 1% agarose was dissolved in 1 × TAE buffer and the solution was boiled until it became clear signifying that agar was dissolved in the TAE buffer. After cooling the solution Ethidium bromide (0.5 μ g/ ml) was added. Gels

were run at 100-120 Volts and the bands were observed on the UV transilluminator.

The bands containing the required DNA fragment were cut out with a scalpel and transferred to a micro-centrifuge tube. DNA was extracted using a Gel purification kit from Qiagen according to manufacturer's instructions (Qiagen).

2.20.4 *A-overhang of PCR product*

Blunt ends were obtained after performing PCR, so the generation of adenosine overhangs in the sides of PCR product was necessary for cloning into the vector pGEM-T Easy and this was done using Taq polymerase. The reaction mix was prepared by mixing 45 µl of gel purified product with 12 µl GoTaq reaction buffer, 0.5 µl GoTaq polymerase and 1 µl of dATP. The mixture was incubated for 30 minutes at 72 °C.

2.20.5 *Ligation into pGEMT-Easy Vector*

pGEMT-Easy was used for the cloning of amplified PCR product, using a Promega Vector System 1 kit. PCR products with an A overhang were ligated to the pGEMT vector system using a mix comprised of 5 µl 2× rapid ligation buffer, 1 µl pGEMT-Easy, 1 µl T4 DNA Ligase and 3 µl of the purified PCR products with A overhangs. The mixture was left overnight at 4 °C.

2.20.6 *Transformation of Escherichia Coli*

XL1 strain *E. coli* were transformed with the pGEMT-Easy-based constructs using the heat shock method. A 50 µl aliquot of bacteria was thawed at low temperature, 5 µl of ligation mix was added and it was kept on ice for half an hour. Heat shock was given to the cells at 42 °C for 60 seconds after which it was kept on ice for two more minutes. 1 ml of SOC medium was added to the mixture which was subsequently incubated in a shaking incubator at 37°C for half

an hour. The mixture was then plated onto LB agar containing ampicillin and incubated overnight at 37 °C.

2.20.7 *PCR for Screening of Colonies*

Bacterial colonies were grown on selective media containing ampicillin allowing growth of colonies containing the desired construct. For the confirmation of plasmid with insert in those bacteria we conducted a PCR reaction. In a total volume of 25 µl (16.3 µl nuclease free water, 5 µl Green GoTaq reaction buffer, 1 µl dNTPs (10mM), 0.75 µl forward primer and 0.75 µl reverse primer along with 0.2 µl GoTaq DNA polymerase). Colonies were introduced in this mixture contained in a PCR tube by the help of a sterilized tip. The remainder of those colonies were added to LB broth and incubated overnight at 37 °C.

2.20.8 *Plasmid DNA Purification*

A single colony was grown up in LB medium (37 °C, O/N) in a shaking incubator and cells were harvested by centrifugation at 1250 × g for 10 minutes at room temperature. A QIAprep spin miniprep kit was used for plasmid purification follow the manufacturer's instructions.

2.20.9 *DNA Sequencing*

Samples were sent for sequencing and it was found that a 900-1000 bp read was the maximum to be obtained with acceptable quality. γ- Glutamylcysteine synthetase has a size of 2040 base pairs and was sequenced using internal primers as well as the primers targeting the 3' and 5' flanking regions described above. The forward primer sequence was 5'CACCATGGAGAGGACGGTAG 3' (20bp) and the reverse primer sequence was 5'CGTAGATGACAAGAGGGTCT 3' (20pb). Nine colonies each were sequenced for γ-GCS and for GS for each of the strains Tb427 and TA014.

2.21 Western Blotting

After harvesting and washing of *Trypanosoma brucei*, cells were transferred into fresh HMI-9 media at a concentration of 1×10^6 cells/ml and then transferred to PBS. Cell lysis was performed in 300 μ l lysis buffer (20 mM MOPS, pH 8.0, 10 mM NaCl, 4 mM $MgCl_2$ + 1 tablet of cOmplete Lysis Kits -Roche diagnostics_ in 10 ml for Protease inhibitor -Roche). The mixture was then mixed vigorously and transferred to a 1.5 ml tube. The suspension was flash frozen with liquid nitrogen and then thawed in a water bath at 37 °C, and this cycle was repeated three times. Lysate was centrifuged to remove cell debris (13,000 x g, room temperature, 3 min). The Bradford method was employed to determine the protein concentration and 40 μ g was boiled after assay with mixture 4 \times SDS sample buffer (80% of 4 \times SDS -Invitrogen, 20% of 0.1 mM DTT) at 98 °C for five minutes. 15 μ l of each sample was separated on a 4-12% NuPAGE Novex Bis-Tris gradient gel using MES SDS running buffer (20 \times), both Invitrogen, at 180 V. The proteins were then transferred by blotting to a nitrocellulose membrane (Hybond-ECL, Amersham) at 70 V (2h, 4 °C). The transfer buffer contained 25 mM Tris-base, 192 mM Glycine, 20% ethanol. 5% of milk was used as a blocking agent along with TBS/T (20 mM Tris-base, 137 mM NaCl - pH 7.4-+ 0.1% (v/v) Tween 20). The membrane was washed three times with TBS/T, and incubated for 2 hours at room temperature with primary antibody (either with Rabbit polyclonal anti-gamma GCS antibody or with Rabbit polyclonal anti-GS; both antibodies were obtained from Phillips Lab, UT Southwestern Medical Center) that was diluted at 1:2000 in 5% milk with TBS/T. Washing with TBS/T was performed after incubation with antibodies three times and for 5 min each and the blot was incubated with a secondary antirabbit horseradish peroxidase antibody (Amersham Biosciences) for 1 hour at room temperature diluted in the same mixture used for the primary antibody (dilution 1:1000). The membrane was washed three times 5 min with TBS/T and observed on X-ray film after the addition of chemiluminescence substrate.

3 Chapter Three: Antiparasitic activity of curcumin analogues

3.1 Introduction

Curcumin, a polyphenolic compound obtained from the nutritional spice turmeric, is derived from the rhizome and roots of the plant *Curcuma longa* (Ammon & Wahl, 1991). It is found in South and South East tropical Asia and is generally used as an herb for adding spice, colour and flavour to food (Iqbal *et al.*, 2009; Sharma *et al.*, 2005). In addition, curcumin is used as a traditional medicine in India (Sharma *et al.*, 2005). There are three active compound classes in *Curcuma* spp. namely, the curcuminoids, the essential oils (atlantones, zingiberene and turmerones) and turmerin (a water-soluble peptide) (Sharma *et al.*, 2005).

Curcumin has been reported as having anti-microbial, anti-inflammatory, anti-mutagenic, and anti-oxidant activity, as well as wound-healing abilities (Maheshwari *et al.*, 2006; Sharma *et al.*, 2005). In addition, curcumin has been shown to have anti-parasitic effects against *Trypanosoma* (Nose *et al.*, 1998) and *Leishmania* species (Koide *et al.*, 2002).

Chemotherapy is still important for the control of most parasitic diseases, such as trypanosomiasis and leishmaniasis. However, problems associated with treatment of these diseases include drug toxicity, resistance, a lack of guaranteed supply, and high cost. With the present rapid rate of development in the world, the number of people who have parasitic diseases is extreme. Consequently, new drugs are urgently needed for the most neglected diseases.

158 curcumin analogues that have been synthesized as anti-leishmanial drugs were tested on *L. major* promastigotes, *L. mexicana* promastigotes and *L. mexicana* amastigotes. 157 of those analogues exhibit a general structure which has a 7-carbon spacer between aromatic rings with the remaining compound involving only a 5-carbon spacer (AS-HK129). The first three compounds are the parent of the analogues curcumin AS-HK001, demethoxycurcumin AS-HK002 and bisdemethoxycurcumin AS-HK003 (Changtam *et al.*, 2010a).

The antiparasitic effects of curcumin analogues were investigated using the *in vitro* Alamar blue viability assay, which is based on the blue and non-fluorescent dye alamar blue (resazurin)(Raz *et al.*, 1997), which is metabolised to resorufin (pink and fluorescent) by live cells only (Gonzalez & Tarloff, 2001). This procedure has been used to quantify the sensitivity to different chemical entities in many cell types such as, African trypanosomes (Raz *et al.*, 1997) and *Leishmania* spp (Fumarola *et al.*, 2004;Al-Salabi & de Koning, 2005).

Each compound was tested in triplicate against *Leishmania* species to identify the EC₅₀. Half of those analogues were more active than curcumin itself against the *L. major* promastigote, a third of them were considerably more active than curcumin in the *L. mexicana* promastigote, and almost half of them had an EC₅₀ less than that of curcumin against the *L. mexicana* amastigote.

In this study, the structure-activity relationship (SAR) of curcumin analogues as compounds against *Leishmania* species will be investigated.

3.2 Results

Alamar blue assays were used to obtain the EC₅₀ values for curcumin analogues in at least three independent determinations. All results of curcumin compounds 001-098 were determined by my colleague Hasan Ibrahim (Ibrahim, 2009) whereas I determined the values for compounds 100-158 and present here the analysis of the full dataset for structural insights. In the below analysis curcumin (AS-HK001) is consistently used as reference compound, unless specifically stated otherwise.

Curcumin analogues were divided into ten groups according to type of aromatic ring substituents. Curcumin is a symmetrical molecule and has one methoxy (positions 2 and 6) and one hydroxyl group (positions 3 and 7) on each aromatic ring (Table 3.1). The contribution of the methoxy substituents to antileishmanial activity was investigated. Compound AS-HK002, identical to curcumin except for

the demethylation at position 6 was equally active as curcumin (AS-HK001). Additional demethylation at position 2 (AS-HK032) also did not substantially change the antileishmanial activity, whereas the complete loss of methoxy at position 2 resulted in loss of activity (AS-HK003). ASHK019, which has no methoxy substituents but hydroxyl groups at positions 2, 3 and 7, has similar activity as curcumin. The methylation of curcumin hydroxyl groups at positions 3 and 7 (AS-HK073) did increase the activity against *L. major* almost 10-fold, but only in the continued presence of the 6-methoxy (see AS-HK074 and AS-HK075) group and the effects on *L. mexicana* were much less pronounced. The importance of the 6-methoxy substitution for high antiparasitic activity was also evident from AS-HK033, which has hydroxyl groups on the 2,3 and 7 positions but the best antileishmanial activity from this series of close curcumin analogues, with a better than 8-fold increased activity against *L. major* promastigotes.

To determine the effect of higher alkyl ether analogues on the activity of the parasites, curcuminoids bearing an *n*-propyl ether (AS-HK079), allyl ethers (AS-HK044 and AS-HK045), 3,3-dimethylallyl ethers (AS-HK76, AS-HK077 and AS-HK078) and 2-hydroxyethyl ethers (AS-HK023, AS-HK024 and AS-HK081) were tested. These compounds were less active or similar to the parent compound AS-HK001 for *Leishmania* species, except AS-HK044 and AS-HK077, which demonstrated modestly increased activity by 6 and 4.3-fold against *L. major* promastigotes, respectively. This improvement was not observed against *L. mexicana* promastigotes and amastigotes.

The introduction of a polar group on the aromatic ring, such as nitro at position 4 in the AS-HK041 analogue, was evaluated for anti *Leishmania* species activity. It was found that the activity was similar to that of the parent compound AS-HK001 for *L. major* promastigotes and *L. mexicana* amastigotes, whereas the compound was less active against *L. mexicana* promastigotes. Introduction of (different) charged groups on other ring positions was not explored in the current series. However, a series of ester analogues including the acetates AS-

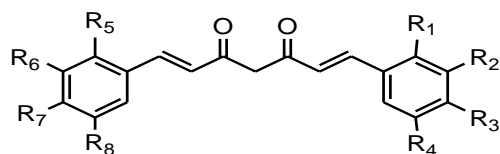
HK025, AS-HK026 and AS-HK027, and the benzoates AS-HK028, AS-HK029, AS-HK065 and AS-HK066 were tested on *Leishmania* species. The acetates showed less activity than AS-HK001 against *Leishmania* species, except in the case of AS-HK027, which was 2-fold more active against *L. mexicana* amastigotes. The benzoate analogues (compounds 28, 29, 65 and 66) had no discernable effect on *L. mexicana* promastigotes or amastigotes up to the highest concentration tested (100 μ M) and only moderate effects on *L. major* promastigotes. Adding an ethylacetate group to positions 3 and 7 (AS-HK101) had little effect on the activity of curcumin against promastigotes of both *Leishmania* species but, interestingly, increased its activity 8-fold against axenic amastigotes, suggesting perhaps a selective uptake system expressed at this lifecycle stage.

Other sizeable ester or ether ring substitutions at positions 3 and 7 showed a similar pattern. The introduction of cyanomethyl ethers (OCH_2CN) (AS-HK080) completely abolished activity for *Leishmania* species but replacing the two curcumin hydroxyl groups with two groups of O-biotin (AS-HK100) or one or two of methacrylic acid (AS-HK102 - 106) substitutions resulted in generally poor activity against promastigotes (a bit better for *L. major* than *L. mexicana*) but much better activity against *L. mexicana* amastigotes. The introduction of 5-bromopentane ethers ($\text{O}(\text{CH}_2)_5\text{Br}$) at positions 3 and/or 7 (ASHK-108 - 113) further solidified this trend, with activity against *L. mexicana* amastigotes 3-6-fold higher as against promastigotes of the same species. Replacing the end bromo for azide (5-azylpentoxy ether ($\text{O}(\text{CH}_2)_5\text{N}_3$), as in AS-HK116 resulted in the loss of residual activity to promastigotes while retaining low micromolar activity against amastigotes, reinforcing the conclusion that this sub-class of curcuminoids either acts through a different mechanism or a different uptake system on amastigotes than on promastigotes.

In contrast, substitutions of one or two pentyl pyridinium ethers ($\text{O}(\text{CH}_2)_5(\text{NC}_5\text{H}_5)$) on positions 3 and/or 7 (AS-HK119 - 124) led to a similarly increased activity (up to 20-fold) against promastigotes and amastigotes. The increased activity was

particularly strong for the di-substituted analogues AS-HK119 and AS-HK122 but it could be speculated that the apparently different action by pyridinium-substitutes curcuminoids, compared to uncharged substitutions described above, has more to do with the alkyl pyridinium moieties than with curcumin itself. We have recently reported a separate series of alkyl pyridinium alkaloids with similar anti-leishmanial activity, with uncharged pyridine analogues being inactive compared to positively-charged pyridinium compounds (Rodenko *et al.*, 2011).

The alteration of the two keto groups in the linker chain of the parent compound AS-HK001 to two methoxy imines (=N-OCH₃), as found in AS-HK012, did not change the activity against *Leishmania*, whereas modification of these keto groups to hydroxyl imine (=N-OH), as in AS-HK042, dramatically reduced the anti-leishmanial activity.



Compound	EC ₅₀ (μM) of <i>L. major</i> promastigote	EC ₅₀ (μM) of <i>L. mexicana</i> promastigote	EC ₅₀ (μM) of <i>L. mexicana</i> amastigote
 AS-HK012	19.2 ± 2	18 ± 1	27 ± 2
 AS-HK042	77 ± 30	> 100	> 100

AS-HK	R ₁	R ₂	R ₃	R ₄	R ₅	R ₆	R ₇	R ₈	EC ₅₀ (μM) of <i>L. major</i> promastigote	EC ₅₀ (μM) of <i>L. mexicana</i> promastigote	EC ₅₀ (μM) of <i>L. mexicana</i> amastigote
001	H	O-CH ₃	OH	H	H	O-CH ₃	OH	H	33 ± 4	26 ± 0.6	16 ± 3
002	H	O-CH ₃	OH	H	H	H	OH	H	37 ± 1	46 ± 0.5	37 ± 4
003	H	H	OH	H	H	H	OH	H	72 ± 3	>100	63 ± 3
019	H	OH	OH	H	H	H	OH	H	22±2	26±5	21 ± 2
020	H	H	O-CH ₃	H	H	H	OH	H	87 ± 5	73 ± 20	32 ± 2
023	H	O-CH ₃	O-C ₂ H ₄ OH	H	H	O-CH ₃	O-C ₂ H ₄ OH	H	33 ± 8	27±4	37 ± 5
024	H	O-CH ₃	OH	H	H	O-CH ₃	O-C ₂ H ₄ OH	H	22±4	33 ± 3	30 ± 4
025	H	O-CH ₃	OC(O)CH ₃	H	H	O-CH ₃	OC(O)CH ₃	H	73 ± 20	>100	34 ± 4
026	H	O-CH ₃	OC(O)CH ₃	H	H	H	OC(O)CH ₃	H	>100	>100	43 ± 7
027	H	H	OC(O)CH ₃	H	H	H	OC(O)CH ₃	H	66 ± 10	32 ± 10	7.1 ± 1
028	H	O-CH ₃	OH	H	H	O-CH ₃	OC(O)-C ₆ H ₅	H	9.3 ± 1	>100	76 ± 10
029	H	O-CH ₃	OH	H	H	H	OC(O)-C ₆ H ₅	H	20 ± 1	>100	>100
032	H	OH	OH	H	H	OH	OH	H	26 ± 0.1	29 ± 2	12 ± 3
033	H	OH	OH	H	H	O-CH ₃	OH	H	4.3 ± 0.5	6.2 ± 0.2	3.2 ± 0.5
041	H	O-CH ₃	OH	NO ₂	H	O-CH ₃	OH	H	28 ± 3	>100	14 ± 4
044	H	O-CH ₃	O-C ₃ H ₅	H	H	O-CH ₃	OH	H	5.7 ± 0.7	35 ± 0.8	12 ± 4

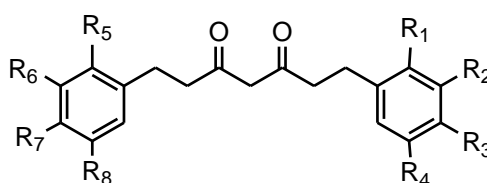
045	H	O-CH ₃	O-C ₃ H ₅	H	H	O-CH ₃	O-C ₃ H ₅	H	25 ± 9	>100	>100
065	H	H	OH	H	H	O-CH ₃	OC(O)-C ₆ H ₅	H	42 ± 10	>100	>100
066	H	H	OH	H	H	H	OC(O)-C ₆ H ₅	H	60 ± 10	>100	>100
073	H	O-CH ₃	O-CH ₃	H	H	O-CH ₃	O-CH ₃	H	2.8 ± 0.4	18 ± 5	10 ± 1
074	H	O-CH ₃	O-CH ₃	H	H	H	O-CH ₃	H	23 ± 6	65 ± 20	61 ± 3
075	H	O-CH ₃	O-CH ₃	H	H	H	OH	H	23 ± 3	50 ± 3	38 ± 6
076	H	O-CH ₃	O-C ₅ H ₉	H	H	O-CH ₃	O-C ₅ H ₉	H	>100	>100	27 ± 0.8
077	H	O-CH ₃	OH	H	H	O-CH ₃	O-C ₅ H ₉	H	7.6 ± 0.7	27 ± 4	21 ± 4
078	H	O-CH ₃	O-C ₅ H ₉	H	H	H	O-C ₅ H ₉	H	48 ± 9	55 ± 0.4	27 ± 7
079	H	O-CH ₃	O-C ₃ H ₇	H	H	O-CH ₃	O-C ₃ H ₇	H	28 ± 2	60 ± 30	34 ± 0.2
080	H	O-CH ₃	O-CH ₂ CN	H	H	O-CH ₃	O-CH ₂ CN	H	>100	>100	>100
081	H	O-CH ₃	OH	H	H	H	O-C ₂ H ₄ OH	H	42 ± 10	>100	>100
100	H	O-CH ₃	O-biotin	H	H	O-CH ₃	O-biotin	H	>100	>100	9.2 ± 2
101	H	O-CH ₃	OCH ₂ C(O)OEt	H	H	O-CH ₃	OCH ₂ C(O)OEt	H	21 ± 3	43 ± 2	2.0 ± 0.3
102	H	O-CH ₃	OC(O)C(CH ₂) CH ₃	H	H	O-CH ₃	OC(O)-C(CH ₂) CH ₃	H	28 ± 2.6	>100	17.3±1.7
103	H	O-CH ₃	OC(O)C(CH ₂) CH ₃	H	H	O-CH ₃	OH	H	9.6 ± 1.8	42 ± 9	5.5 ± 1.2
104	H	O-CH ₃	OC(O)C(CH ₂) CH ₃	H	H	H	OH	H	16.6 ± 1.4	57 ± 2.6	6.7 ± 1.4
105	H	O-CH ₃	OC(O)C(CH ₂) CH ₃	H	H	H	OC(O)C(CH ₂) CH ₃	H	31 ± 0.4	>100	11.6 ± 2.4

106	H	H	OC(O)C(CH ₂) CH ₃	H	H	H	OC(O)C(CH ₂) CH ₃	H	>100	>100	11.7±2.1
108	H	O-CH ₃	O-C ₅ H ₁₀ Br	H	H	O-CH ₃	O-C ₅ H ₁₀ Br	H	55 ± 10	75 ± 13	2.5 ± 0.3
109	H	O-CH ₃	O-C ₅ H ₁₀ Br	H	H	O-CH ₃	OH	H	15.7 ± 4.3	24 ± 6	3.9 ± 0.5
111	H	O-CH ₃	O-C ₅ H ₁₀ Br	H	H	H	OH	H	16.7 ± 6.3	24 ± 0.6	5.1 ± 0.6
112	H	O-CH ₃	OH	H	H	H	O-C ₅ H ₁₀ Br	H	72 ± 10	>100	10.4 ± 1.6
113	H	O-CH ₃	O-C ₅ H ₁₀ Br	H	H	H	O-C ₅ H ₁₀ Br	H	41 ± 7.4	32 ± 3.6	3.3 ± 0.4
116	H	O-CH ₃	O-(CH ₂) ₅ -N ₃	H	H	O-CH ₃	O-(CH ₂) ₅ -N ₃	H	>100	>100	5.6 ± 0.8
119	H	O-CH ₃	O(CH ₂) ₅ -N-pyridine	H	H	O-CH ₃	O(CH ₂) ₅ -N-pyridine	H	1.6 ± 0.4	4.5 ± 1.4	9.5 ± 1
120	H	O-CH ₃	O(CH ₂) ₅ -N-pyridine	H	H	O-CH ₃	OH	H	19.3 ± 1.8	36 ± 10	16.8 ± 4.5
122	H	O-CH ₃	O(CH ₂) ₅ -N-pyridine	H	H	H	O(CH ₂) ₅ -N-pyridine	H	1.4 ± 0.3	1.7 ± 0.1	6.5 ± 1.8
123	H	O-CH ₃	OH	H	H	H	O(CH ₂) ₅ -N-pyridine	H	6.5 ± 0.8	15.3 ± 1.7	7.4 ± 2
124	H	O-CH ₃	O(CH ₂) ₅ -N-pyridine	H	H	H	OH	H	8.8 ± 0.5	12.2 ± 0.2	15.6 ± 4.2
Pentamidine									5.1 ± 1.1	3.1 ± 0.7	4.3 ± 0.8

Table 3.1. Structure and antileishmanial activity of curcumin analogues with a 3, 5-diketo, 1,6-diheptene linker. EC₅₀ values are the average and SEM of at least three independent determinations.

The next analogues that were evaluated against the *Leishmania* species were the tetrahydro analogues AS-HK007, AS-HK008, AS-HK009, AS-HK085 and AS-HK087, where the double bonds in the C₇ linker were saturated (Table 3.2). All these analogues display less activity than their parent compounds, except AS-HK085, which was more active than the original compound AS-HK001 by 2 to 3-fold against *L. mexicana* and *L. major* promastigotes, and equally against *L. mexicana* amastigotes. On the other hand, exchanging the two keto groups in analogue AS-HK009 with two hydroxyl imine (=N-OH), as in AS-HK047, did not measurably change the activity relative to the parent compound AS-HK003 for the *L. major* promastigote. This is similar to the hydroxyl imine substitution in ASHK-042 depicted in Table 3.2 with the original, unsaturated curcumin linker.

Further reduction to hexahydro and octahydro analogues AS-HK030, AS-HK031 and AS-HK082, AS-HK084 and AS-HK086 displayed very low, if any, activity. Indeed, some of these compounds had no affect at 100 μ M on *Leishmania* species. The number and position of hydroxyl and methoxy groups on the rings had little influence on the activities, confirming that the increased saturation of the linker caused the loss of antileishmanial activity. It is instructive to compare these compounds directly with the corresponding curcumin analogues with the original conjugated di-ketone linker. For example, AS-HK086 was 9 to 25-fold less active against *Leishmania* species than the corresponding ‘conjugated’ compound AS-HK033 (Table 3.3).



Compound	EC ₅₀ (μ M) of <i>L. major</i> promastigote	EC ₅₀ (μ M) of <i>L. mexicana</i> promastigote	EC ₅₀ (μ M) of <i>L. mexicana</i> amastigote
 AS-HK047	75 \pm 30	ND	ND
 AS-HK085	11 \pm 1	14 \pm 0.7	16 \pm 3

AS-HK	R ₁	R ₂	R ₃	R ₄	R ₅	R ₆	R ₇	R ₈	EC ₅₀ (μM) of <i>L. major</i> promastigote	EC ₅₀ (μM) of <i>L. Mexicana</i> promastigote	EC ₅₀ (μM) of <i>L. Mexicana</i> amastigote
007	H	O-CH ₃	OH	H	H	O-CH ₃	OH	H	90 ± 20	59	43 ± 9
008	H	O-CH ₃	OH	H	H	H	OH	H	>100	>100	>50 ¹
009	H	H	OH	H	H	H	OH	H	80 ± 10	>100	64 ± 10
083	H	O-CH ₃	OH	H	H	H	OH	H	>100	57±30	82±7
087	H	OH	OH	H	H	OH	OH	H	>100	>100	53±3

Table 3.2. Antileishmanial activity of some tetrahydro curcumin compounds, with saturated C₇ linkers.

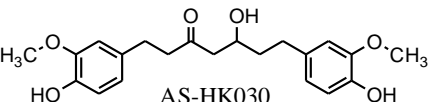
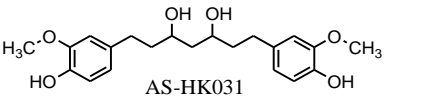
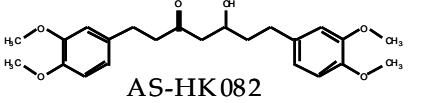
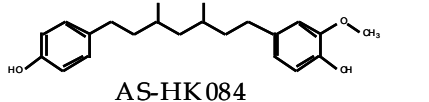
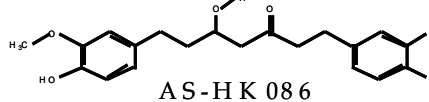
Compound	EC ₅₀ (μM) of <i>L. major</i> promastigote	EC ₅₀ (μM) of <i>L. mexicana</i> promastigote	EC ₅₀ (μM) of <i>L. mexicana</i> amastigote
 AS-HK030	>100	>100	>100
 AS-HK031	>100	>100	>100
 AS-HK082	41 ± 10	>100	>100
 AS-HK084	>100	>100	>100
 AS-HK086	>100	55 ± 3	40 ± 5

Table 3.3. The activity of hexahydro and octahydro curcumin analogues against *Leishmania* promastigotes and amastigotes.

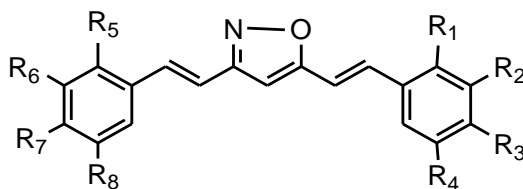
Isoxazole and Isoxazoline analogues:

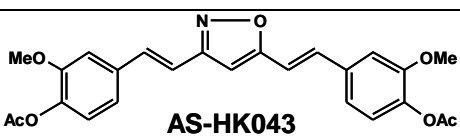
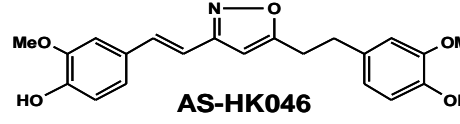
Exchanging the keto groups in the aromatic ring in parent compounds 1, 2 and 3 with an isoxazole ring did not change the overall anti-leishmanial activity relative to the corresponding compounds with original linkers (Table 3.4). Activity increased slightly for compound AS-HK004 for *Leishmania* species

(relative to curcumin), whereas the activity was slightly reduced for AS-HK005 and AS-HK006 compared with their parent compounds (AS-HK002 and 003, respectively). Acetylation of the position 3 and 7 hydroxyl groups of AS-HK004 to the di-acetyl ester (AS-HK043) had no significant effect on activity, but the monopentyl ether (position 3) of AS-HK022, displayed 2-fold improved activity, consistent with similar observations made with the original linker series (compare Table 3.1). Also consistent with those observations, loss of conjugation (AS-HK046) led to reduced anti-leishmanial activity, especially against *L. mexicana*.

Introducing an methacrylic acid group at positions 3 and 7 to analogue AS-HK004, which gave AS-HK107, led to a >3-fold increase in activity against *L. mexicana* amastigotes, and an apparent decline in activity against the *L. mexicana* promastigote. Similarly, AS-HK115, which is created from AS-HK004 by introducing one group of bromopentane ($C_5H_{10}Br$) at position 3, was 8-fold more active against *L. mexicana* amastigotes, and significantly less active against the *L. mexicana* promastigote. Substitutions of one or two pentyl pyridinium ethers ($O(CH_2)_5(NC_5H_5)$) on positions 3 and/or 7 also increased anti-leishmanial activity, particularly against promastigotes of both species, with EC_{50} values from 0.8 to 2.1 μM (Table 3.4).

It is very clear that curcuminoids with isoxazole linkers are almost indistinguishable from their counterparts with the original conjugated di-keto linkers, and that the anti-leishmanial activity can be modulated in much the same way, by the same substitutions, for both sets of analogues. No doubt this reflects the same overall, rigid structure with a straight C_7 linker between the identical aromatic rings. However, the isoxazole ring is much more stable than the di-keto motif, where the linker stabilisation is dependent on keto-enol tautomerism to produce a semi-conjugated π -electron structure (Figure 3.1). It follows that it is the precise structure rather than a reaction of curcumin or its analogues that is responsible for its antiprotozoal activity.



Compound	EC ₅₀ (μM) of <i>L. major</i> promastigote	EC ₅₀ (μM) of <i>L. mexicana</i> promastigote	EC ₅₀ (μM) of <i>L. mexicana</i> amastigote
 AS-HK043	19 ± 5	27 ± 0.3	10 ± 4
 AS-HK046	13 ± 0.7	>100	20 ± 5

AS-HK	R ₁	R ₂	R ₃	R ₄	R ₅	R ₆	R ₇	R ₈	EC ₅₀ (μM) of <i>L. major</i> promastigote	EC ₅₀ (μM) of <i>L. Mexicana</i> promastigote	EC ₅₀ (μM) of <i>L. Mexicana</i> amastigote
004	H	O-CH ₃	OH	H	H	O-CH ₃	OH	H	20 ± 0.8	20 ± 0.3	18 ± 3
005	H	O-CH ₃	OH	H	H	H	OH	H	61 ± 3	>100	54 ± 8
006	H	H	OH	H	H	H	OH	H	>100	81 ± 30	>100
022	H	O-CH ₃	O-C ₅ H ₁₁	H	H	H	OH	H	16 ± 0.2	16 ± 0.8	8.1 ± 2
107	H	O-CH ₃	C ₄ H ₈ O ₂	H	H	O-CH ₃	C ₄ H ₈ O ₂	H	8±0.4	>100	5.3±0.5
115	H	O-CH ₃	O-C ₅ H ₁₀ Br	H	H	O-CH ₃	OH	H	6.5±1.7	35±5.6	2±0.2
125	H	O-CH ₃	OC ₁₀ H ₂₀ BrN	H	H	O-CH ₃	OC ₁₀ H ₂₀ BrN	H	0.8±0.2	1.3±0.1	10±2.5
126	H	O-CH ₃	OC ₁₀ H ₂₀ BrN	H	H	O-CH ₃	OH	H	2.1±0.2	2.1±0.2	3.7±1

Table 3.4. The activity of isoxazole curcumin compounds

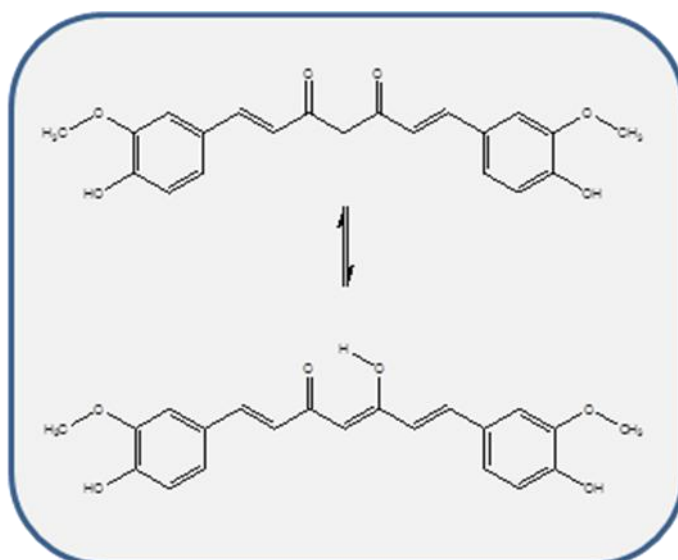
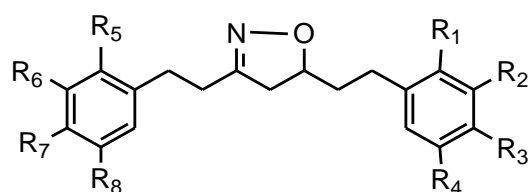


Figure 3.1. The curcumin linker is stabilised by keto-enol tautomerism

It follows that significant bending of the linker chain would be expected to abolish most of the anti-leishmanial activity of the curcumin analogues. This was accomplished by replacing the isoxazole ring with an isoxazoline ring in a saturated C_7 linker (Table 3.5), which causes a stable bend of almost 90° in the linker (Figure 3.2), greatly distorting the 3D structure, although all ring-substituents were the same. Compounds AS-HK088 - AS-HK090 correspond to compounds AS-HK004-AS-HK006 in Table 3.4. These are unfortunately not the most active compounds themselves, but the activity of the analogues with the bend linker does appear reduced, and indeed is virtually absent - similarly for AS-HK091, which has an additional ethyl ether substituent on positions 3 and 7. However, the isobutyryl ether or pentyl pyridinium substitutions would have been more informative comparisons as these are very active compounds with either the original or isoxazole linkers.



AS-HK	R ₁	R ₂	R ₃	R ₄	R ₅	R ₆	R ₇	R ₈	EC ₅₀ (μM) of <i>L. major</i> promastigote	EC ₅₀ (μM) of <i>L. mexicana</i> promastigote	EC ₅₀ (μM) of <i>L. mexicana</i> amastigote
088	H	O-CH ₃	OH	H	H	O-CH ₃	OH	H	75 ± 0.8	89 ± 4	43 ± 6
089	H	O-CH ₃	OH	H	H	H	OH	H	70 ± 30	56 ± 30	>100
090	H	H	OH	H	H	H	OH	H	>100	>100	>100
091	H	O-CH ₃	O-C(O)CH ₃	H	H	O-CH ₃	O-C(O)CH ₃	H	66 ± 20	>100	45 ± 8

Table 3.5. The activity of isoxazole curcumin compounds

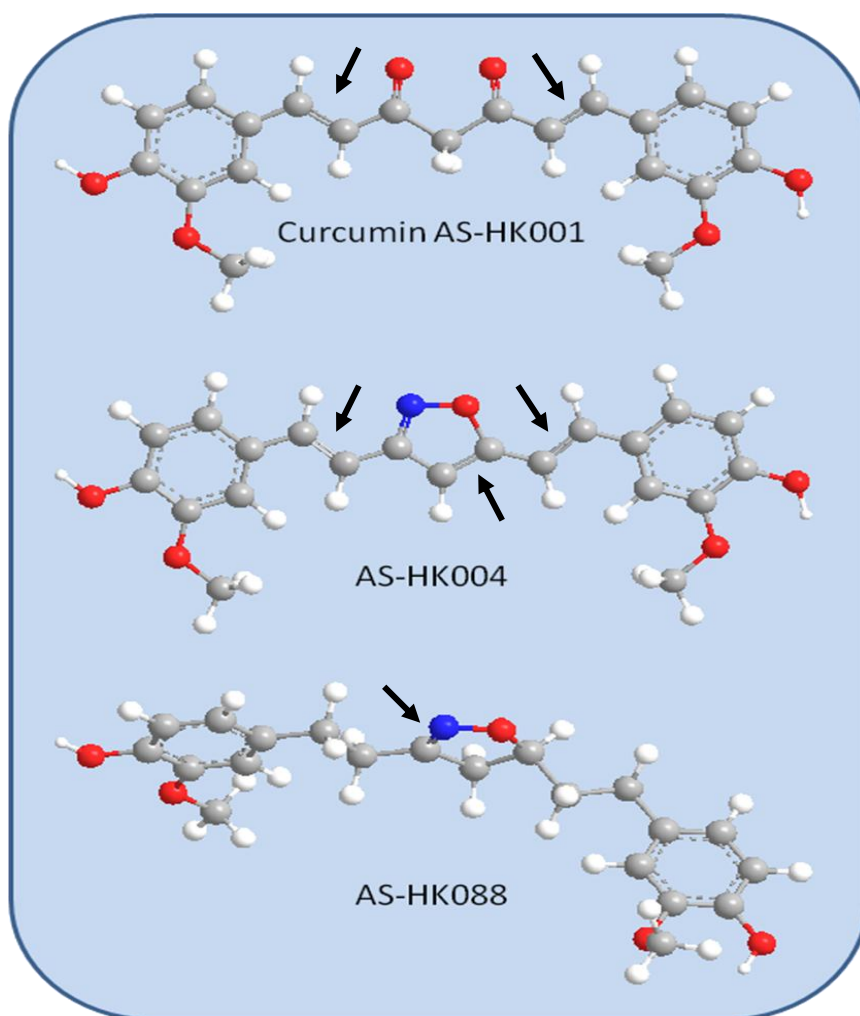


Figure 3.2. Three dimensional structure of curcumin, and the corresponding isoxazole and Isoxazoline ring analogues. The structures were generated using ChemDraw 3D Ultra version 10.0 (CambridgeSoft) using energy minimisation, (arrows indicate double bonds).

Monoketo analogs:

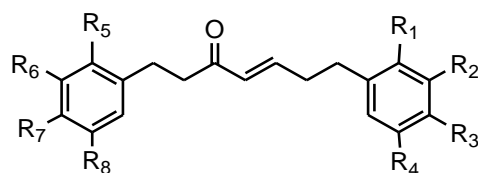
The monoketo analogue AS-HK014 was prepared by the dehydration of analogue AS-HK030. This monoketo analogue appeared to be 3 to 12-fold more active against *Leishmania* species than AS-HK030. However, its activity did not really change in comparison with compound AS-HK001 except against *L. major* promastigotes, for which its activity increased 4-fold. The position 3 monomethylated analogue AS-HK018 and the 3,7-dimethylated AS-HK036 displayed essentially the same activity as AS-HK014, whereas demethylation of the 6-methoxy group (AS-HK034) slightly increased activity against *L. mexicana*. Yet, the 6-mono-methoxy analogue AS-HK048 displayed reduced activity against this species, showing that for this asymmetric curcuminoid series the two rings are not to be considered equal. The di-demethylated analogue AS-HK035 lost all activity against promastigotes of both species while retaining activity against axenic amastigotes. The low activity of AS-HK035 against promastigotes seems attributable to the 2-position hydroxyl group; its removal (AS-HK051 and 057)(Table 3.6) restores anti-promastigote activity, while activity against amastigotes remains essentially unchanged. The above shows clearly that, for enone linker analogues at least, optimisation for activity against promastigotes would not necessarily increase activity against amastigotes, and *vice versa*.

A number of position 3 and/or 7 alkyl ethers and acetates were generated to explore the effect of such substitutions on the enone linker curcuminoids. Addition of cyanomethyl to position 7 appeared only to decrease the activity against amastigotes (AS-HK092), whereas further addition of cyanomethyl to position 3 reversed this and somewhat increased activity to promastigotes (AS-HK093). Substitutions with pentyl ether on positions 3 and/or 7 (AS-HK094-095), or acetylation of these positions (AS-HK096-097), equally failed to improve anti-leishmanial activity, as did the introduction of an 1,2-ethanediol ether on position 3 (AS-HK098). Indeed, even the pentylpyridinium substitutions on position 3 (AS-HK128) or on both positions 3 and 7 (AS-HK127) were unsuccessful in increasing activity against *L. mexicana* amastigotes, although they increased activity against the promastigotes of this species.

In this series, the most successful substitution was found to be a 5-bromopentyl ether on position 3 (AS-HK118), although the same substitution on positions 3 and

7 was much less active, especially against promastigotes (AS-HK117). These final observations highlight the main observations concerning the enone linker series, that a different relationship exists for activity against promastigotes and amastigotes; that the substitutions that increased activity with a conjugated linker (di-ketone or isoxazole) did not increase activity with this linker; and that on the whole substitutions on positions 3 and 7 were unsuccessful. The latter point is powerfully illustrated when considering that the only compound without substitutions on either position (AS-HK057) displayed very nearly the best activity against amastigotes. Especially substitutions on position 7 would seem to be detrimental to anti-leishmanial activity, and the larger groups contributed to worse activity than a hydroxyl group at this position.

Finally, analogue AS-HK053, which had a slightly different enone linker, conjugated with one aromatic ring, displayed an EC_{50} value higher than 100 μM . The introduction of methyl at position 4 for carbon in the linker chain, to create a branched chain linker otherwise identical to AS-HK036, resulting in AS-HK037, reduced the activity against *Leishmania* species.



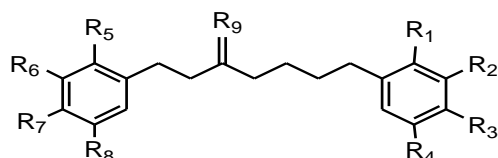
Compound	EC_{50} (μM) of <i>L. major</i> promastigote	EC_{50} (μM) of <i>L. mexicana</i> promastigote	EC_{50} (μM) of <i>L. mexicana</i> amastigote
 AS-HK014	8.9 ± 0.8	34 ± 1	17 ± 2
 AS-HK037	38 ± 3	66 ± 0.1	72
 AS-HK053	86 ± 20	>100	>100

AS-HK	R ₁	R ₂	R ₃	R ₄	R ₅	R ₆	R ₇	R ₈	EC ₅₀ (μM) of <i>L. major</i> promastigote	EC ₅₀ (μM) of <i>L. mexicana</i> promastigote	EC ₅₀ (μM) of <i>L. mexicana</i> amastigote
018	H	O-CH ₃	O-CH ₃	H	H	O-CH ₃	OH	H	13 ± 1	38 ± 1	28 ± 6
034	H	O-CH ₃	OH	H	H	OH	OH	H	10 ± 2	19 ± 6	7.4 ± 1
035	H	OH	OH	H	H	OH	OH	H	>100	>100	17 ± 5
036	H	O-CH ₃	O-CH ₃	H	H	O-CH ₃	O-CH ₃	H	12 ± 1	42 ± 1	28 ± 8
048	H	H	OH	H	H	O-CH ₃	OH	H	15 ± 2	85 ± 30	23 ± 4
051	H	H	OH	H	H	H	OH	H	9.9 ± 1	46 ± 3	21 ± 8
057	H	H	H	H	H	H	H	H	8.9 ± 2	30 ± 0.1	12 ± 2
092	H	O-CH ₃	OH	H	H	O-CH ₃	O-CH ₂ CN	H	14 ± 0.7	25 ± 0.1	50 ± 30
093	H	O-CH ₃	O-CH ₂ CN	H	H	O-CH ₃	O-CH ₂ CN	H	4.5 ± 0.7	12 ± 0.5	25 ± 4
094	H	O-CH ₃	O-C ₅ H ₁₁	H	H	O-CH ₃	O-C ₅ H ₁₁	H	6.6 ± 1.0	51 ± 0.8	53 ± 8
095	H	O-CH ₃	OH	H	H	O-CH ₃	O-C ₅ H ₁₁	H	4.0 ± 1.3	27 ± 0.8	19 ± 4
096	H	O-CH ₃	O-C(O)-CH ₃	H	H	O-CH ₃	O-C(O)-CH ₃	H	7.8 ± 1.0	31 ± 0.8	35 ± 1
097	H	O-CH ₃	O-C(O)-CH ₃	H	H	O-CH ₃	OH	H	7.5 ± 0.8	33 ± 0.8	29 ± 0.8
098	H	O-CH ₃	O-C ₂ H ₄ O H	H	H	O-CH ₃	OH	H	15 ± 0.1	38 ± 4	41 ± 4
117	H	O-CH ₃	OC ₅ H ₁₀ Br	H	H	O-CH ₃	OC ₅ H ₁₀ Br	H	18±2	>100	9.3±2.4
118	H	O-CH ₃	OC ₅ H ₁₀ Br	H	H	O-CH ₃	OH	H	5±0.6	15.3±1.6	5±0.8
127	H	O-CH ₃	OC ₁₀ H ₁₅ N	H	H	O-CH ₃	OC ₁₀ H ₁₅ N	H	9±1.4	5.5±0.4	26.4±6.7
128	H	O-CH ₃	OC ₁₀ H ₁₅ N	H	H	O-CH ₃	OH	H	10 ± 1.3	18 ± 3	14.8±0.8

Table 3.6. The activity of mono keto curcumin analogues

The contribution of the olefinic group of the AS-HK014 linker to its antileishmanial activity was further investigated using a series of mono-keto analogues in a saturated C₇ linker (Table 3.7). The dihydro analogue of AS-HK014, AS-HK038, exhibited decreased activity against *Leishmania*. Likewise, a loss of activity was noted in the saturated keto compound AS-HK049 and in analogue AS-HK050, in which the keto group in AS-HK014 was reduced to a hydroxyl group. On the other hand, replacing the keto group in AS-HK038 with a hydroxyl imine (=N-OH) as in compound AS-HK010 or with a methoxyl imine (=N-O-CH₃) as in compound AS-HK013, did not have a clear effect on the anti-

leishmanial activity, given the already low activity of compound 38. In addition, the introduction or removal of hydroxyl or methoxyl substitutes on one or both of the rings of AS-HK038, as in analogues AS-HK011, AS-HK50, AS-HK052, AS-HK058 and AS-HK061, did also not result in any remarkable change in antileishmanial activity.



Compound	EC ₅₀ (μM) of <i>L. major</i> promastigote	EC ₅₀ (μM) of <i>L. Mexicana</i> promastigote	EC ₅₀ (μM) of <i>L. Mexicana</i> amastigote
 AS-HK013	36 ± 1	>100	35 ± 8
 AS-HK 010	82 ± 5	99 ± 1	32.2
 AS-HK050	50 ± 4	82 ± 20	64 ± 20

AS-HK	R ₁	R ₂	R ₃	R ₄	R ₅	R ₆	R ₇	R ₈	EC ₅₀ (μM) of <i>L. major</i> promastigote	EC ₅₀ (μM) of <i>L. mexicana</i> promastigote	EC ₅₀ (μM) of <i>L. mexicana</i> amastigote
011	H	H	OH	H	H	H	OH	H	>100	>100	67
038	H	O-CH ₃	OH	H	H	O-CH ₃	OH	H	37 ± 3	>100	>50
049	H	O-CH ₃	OH	H	H	H	OH	H	55 ± 3	>100	>100
052	H	H	H	H	H	H	OH	H	97 ± 1	>100	>100
058	H	H	H	H	H	H	H	H	92 ± 20	>100	>100
061	H	H	H	H	H	H	H	H	83 ± 4	41 ± 3	>100

Table 3.7. The EC₅₀ values of different curcumin analogues after introduction and reduction some chemical groups.

Replacing the keto group in compound AS-HK014 with a hydroxylimine (=N-OH) group, as in analogue AS-HK039, led to decreased activity by 2 to 9-fold against the *Leishmania* species tested (Table 3.8). Similarly, AS-HK040, which has methoxyimine (N-O-CH₃) in place of the keto group, showed also less activity than AS-HK014 (up to 4-fold), particularly against *L. major* promastigotes. Overall, the substitution of keto groups for imines has tended to not improve anti-leishmanial activity, and in some cases reduced it.

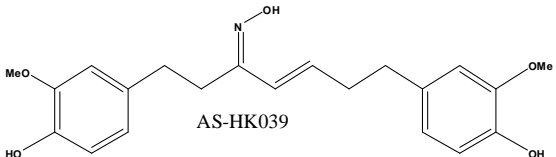
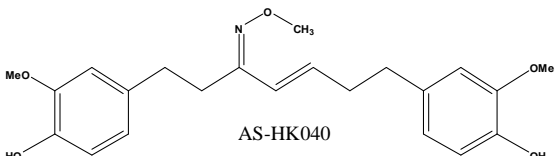
Compound	EC ₅₀ (μM) of <i>L. major</i> promastigote	EC ₅₀ (μM) of <i>L. Mexicana</i> promastigote	EC ₅₀ (μM) of <i>L. Mexicana</i> amastigote
 AS-HK039	76 ± 9	>100	43 ± 20
 AS-HK040	40 ± 2	64 ± 4	23 ± 7

Table 3.8. . Anti-leishmanial activity of imine analogues of AS-HK014.

Next, the importance of the location of the double bond was investigated, with a shift from C₄-C₅ to C₁-C₂. Although there is no exact C₄-C₅ equivalent for AS-HK053 (Table 3.9), the results strongly suggest that this position, conjugated with the aromatic bonds, is unfavourable to anti-leishmanial activity despite the linker remaining unbend (Chem3D Ultra; Fig. 3.3) and the overall structure being perhaps more stable than with a C₄-C₅ double bond.

A further change in double bond location was to position C₆-C₇ of the linker chain, creating AS-HK059, the equivalent of the C₄-C₅ olefinic analogue AS-HK057 (Table 3.6), but with at least 10-fold less anti-leishmanial activity. With this olefinic position, the linker shape is in fact slightly bend (Fig. 3.3), affecting the orientation of the aromatic rings. Once again substitution of the keto group of AS-HK059 to hydroxylamine (AS-HK060) or methoxyimine (AS-HK062) failed to improve activity.

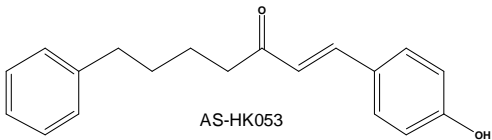
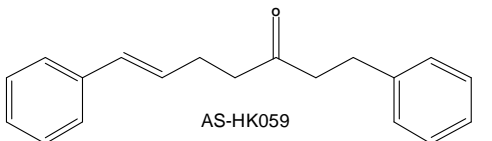
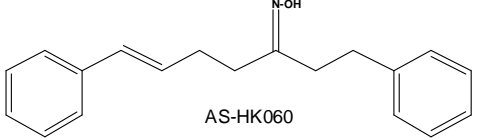
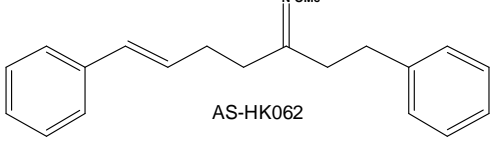
Compound	EC ₅₀ (μM) of <i>L. major</i> promastigote	EC ₅₀ (μM) of <i>L. Mexicana</i> promastigote	EC ₅₀ (μM) of <i>L. mexicana</i> amastigote
 AS-HK053	86 ± 20	>100	>100
 AS-HK059	76 ± 20	>100	>100
 AS-HK060	71 ± 6	74 ± 20	>50
 AS-HK062	69 ± 20	>100	>100

Table 3.9. Anti-leishmanial activity of AS-HK014 analogue with a different olefinic position.

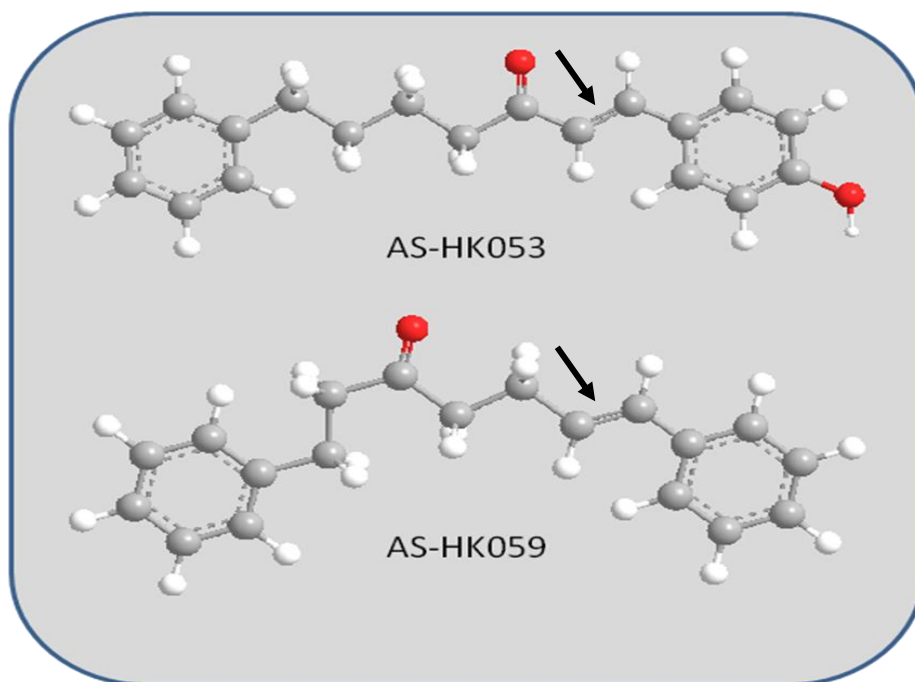
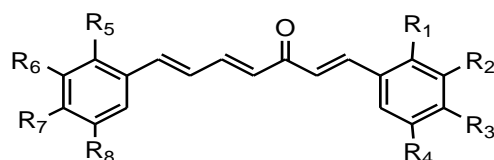


Figure 3.3. 3D structure of compounds 53 and 59, modelled with Chem3D Ultra (CambridgeSoft), (arrows indicate double bonds).

A further series of olefinic linker modifications constituted the inclusion of three double bonds, at positions C₁-C₂, C₃-C₄ and C₆-C₇, giving a highly rigid linear linker with a fully conjugated π -electron system that includes both aromatic rings. Indeed the dispersed π -electron system is the main difference with compounds such as AS-HK053 (Table 3.9 and Fig. 3.3). However, the dienone and trienone linker series presented in Table 3.10 was generally much more effective than the mono-enone series, especially against amastigotes. Out of the 4 dienone, three (compounds 15, 16 and 55) had a straight linker, whereas AS-HK056 had a slightly bent linker like AS-HK059 (Fig. 3.3). While AS-HK056 did indeed display the worst activity (of this series) to *L. major* promastigotes ($42 \pm 2 \mu\text{M}$), its activity against *L. mexicana* amastigotes was surprisingly good ($6.8 \pm 1.2 \mu\text{M}$), although this could be because the rings were almost completely unsubstituted and their orientation was therefore less critical. The activity of AS-HK015, with a C₄-C₅ + C₆-C₇ dienone linker (Table 3.10), was the least promising in the dienone series and a direct comparison with AS-HK016 (same ring substitutions) affords the clear conclusion that a C₁-C₂ + C₄-C₅ dienone displays superior antileishmanial activity. Indeed, a direct comparison with AS-HK014 also shows that the C₆-C₇ double bond was at best neutral, but probably slightly detrimental with respect to anti-leishmanial activity. Furthermore, the trienone compound AS-HK017 exhibited a small decrease in anti-leishmanial activity compared with AS-HK016. The hydroxyl and methoxy substitutions on the ring appear to be far more important for activity against promastigotes than against amastigotes (compare AS-HK016 and AS-HK 055).

A substantial series of trienone analogues was next evaluated for antileishmanial activity (Table 3.10). These included analogues with substitutions on positions 1, 4, 5 and 8 that were previously unexplored. The entire trienone series displayed low micromolar activity against *L. mexicana* amastigotes, showing definitively (a) that different optimisation occurs for promastigotes and amastigotes and (b) that small ring substitutions such hydroxyl, methoxy and chloride are of at most marginal importance for activity against axenic amastigotes. Even the introduction of a nitro group on position 2 (AS-HK131) had no effect on activity against amastigotes, although it increased activity against promastigotes of both species 3-4-fold (compare AS-HK139). Substitutions of methoxy or chloro on position 1 had little effect on activity against promastigotes either (compare AS-

HK139 with AS-HK138 and AS-HK130). Indeed, it is hard to distil a clear trend explaining the substantial variation in anti-promastigote activity from the data in Table 3.10, with EC_{50} values ranging from 3.7 to $>100 \mu\text{M}$. It is hoped that a QSAR approach based on ComFA and ComSIA 3D computer modelling software will be able to give more definitive insights.



Compound	EC_{50} (μM) of <i>L. major</i> promastigote	EC_{50} (μM) of <i>L. mexicana</i> promastigote	EC_{50} (μM) of <i>L. mexicana</i> amastigote
 AS-HK015	30 ± 2	48 ± 1	22 ± 7
 AS-HK016	2.7 ± 0.7	14 ± 2	4.6 ± 0.7
 AS-HK055	13 ± 1	>100	4.0 ± 0.7
 AS-HK056	42 ± 2	46 ± 2	6.8 ± 1.2

AS-HK	R ₁	R ₂	R ₃	R ₄	R ₅	R ₆	R ₇	R ₈	EC ₅₀ (μM) of <i>L. major</i> promastigote	EC ₅₀ (μM) of <i>L. Mexicana</i> promastigote	EC ₅₀ (μM) of <i>L. Mexicana</i> amastigote
017	H	O-CH ₃	OH	H	H	O-CH ₃	OH	H	7.4 ± 0.1	21 ± 2	4.8 ± 1.0
130	O-CH ₃	H	O-CH ₃	H	O-CH ₃	H	H	O-CH ₃	38.3±5	53±11	6.4 ± 1.8
131	H	NO ₂	H	H	O-CH ₃	H	H	O-CH ₃	5.8±0.6	7.2±0.7	4.7 ± 0.6
132	H	OH	O-CH ₃	H	O-CH ₃	H	H	O-CH ₃	11.7±1.2	11.7±2	3.9 ± 1.0
133	O-CH ₃	H	O-CH ₃	H	H	H	Cl	H	>100	>100	5.9 ± 2.0
134	H	H	Cl	H	H	H	Cl	H	36.5±2.5	49.2±5	5.1 ± 0.8
135	O-CH ₃	H	H	O-CH ₃	O-CH ₃	H	H	O-CH ₃	19.2±4.3	22.8±4.4	5.4 ± 1.7
136	H	H	O-CH ₃	H	O-CH ₃	H	H	O-CH ₃	45.1±2.7	57.5±6.7	4.2 ± 1.1
137	H	OH	H	H	O-CH ₃	H	H	O-CH ₃	7.5±0.2	9.2±1	6.7 ± 1.9
138	Cl	H	H	H	O-CH ₃	H	H	O-CH ₃	16.2±1.3	32.4±11	4.4 ± 0.5
139	H	H	H	H	O-CH ₃	H	H	O-CH ₃	20.6±3.5	25.3±4.8	5.0 ± 0.5
140	H	OH	O-CH ₃	H	H	H	Cl	H	13.7±2.4	21.2±0.7	4.9 ± 1.0
141	H	OH	O-CH ₃	H	H	OH	H	H	8.3±0.5	9.5±1.8	4.6 ± 1.1
142	H	H	O-CH ₃	H	H	H	O-CH ₃	H	>100	97.9±6.5	2.8 ± 0.6
143	H	OH	H	H	H	H	O-CH ₃	H	14.9±0.4	16.6±3.2	2.8 ± 0.2
144	H	OH	H	H	H	H	Cl	H	14.1±3	17.6±3.3	3.2 ± 1.3
145	OH	O-CH ₃	H	H	H	O-CH ₃	O-CH ₃	H	3.7±0.01	6.3±1.3	4.9 ± 1.0
146	H	OH	O-CH ₃	H	H	O-CH ₃	O-CH ₃	H	7.5±0.2	9.2±2.5	3.1 ± 0.7
147	H	H	OH	H	H	O-CH ₃	O-CH ₃	H	15±0.1	21.4±4.3	4.9 ± 0.8
148	H	H	OH	H	H	H	O-CH ₃	H	31.7±0.8	37.2±3.8	5.1 ± 0.6
149	H	OH	O-CH ₃	H	O-CH ₃	H	O-CH ₃	H	12.2±1.1	10.8±0.8	2.5 ± 0.3

150	O-CH ₃	H	O-CH ₃	H	O-CH ₃	H	O-CH ₃	H	50.7±12.3	42.7±2.4	5.3 ± 1.4
151	H	H	H	H	H	H	H	H	30.1±1.3	39.1±3.6	4.8 ± 1.2
152	H	H	OH	H	H	H	H	H	25.6±3.4	23.8±1.8	4.7 ± 0.5
153	H	H	O-CH ₃	H	H	H	H	H	>100	75.8±5.6	5.7 ± 1.2
154	H	OH	H	H	H	H	H	H	10.7±1.8	14.2±2.6	1.3 ± 0.3
157	OH	O-CH ₃	H	H	H	H	H	H	10.6±0.5	16±2.5	4.7 ± 1.7
158	O-CH ₃	H	H	O-CH ₃	H	H	H	H	34±4	31±1.5	3.1 ± 1.3
pentamidine									5.1 ± 1.1	3.1 ± 0.7	4.3 ± 0.8

Table 3.10. The effect of the dienone and trienone curcumin compounds

Conclusions

Several conclusions may be drawn from this structure activity analysis of 158 curcumin analogues:

- There was no change in the activity for compounds which have methoxy substitutions, whereas the mono-*O*-demethylated and di-*O*-demethylated compounds exhibited increased activity.
- Adding one or two pentyl pyridinium (C₁₀H₁₅N) groups to positions 3 and/or 7 of curcumin leads to an increased antileishmanial activity.
- Replacing the diketo groups (C=O) with an isoxazole group generally improved the activity of curcumin analogues.
- Introduction of further double bonds to the C₇ linkers generally increases activity, especially against amastigotes.
- Reduction of one of the diketo groups to a monoketo group increases activity, particularly against promastigotes.
- Removing ring all substitutions in curcumin compounds reduces activity.
- Changing the locations of the double bond locations does not affect activity against *Leishmania* species.
- The trienone analogues displayed potently increased activity against *Leishmania* amastigotes.

3.3 Multi-drug resistant strains of *T. b. brucei* are not cross-resistant with curcumin analogues

Resistant strains can be used as a model to investigate cross-resistance between existing treatments and potential new trypanocides. Any new trypanocidal drugs to be developed, whether for human or veterinary use, should at a minimum not be cross-resistant with the current diamidine and arsenic-based drugs. It is exactly because of high levels of resistance to these classes of drugs that the development of new drugs has become such a priority. We therefore tested whether curcumin-based trypanocides would be effective against well-characterised laboratory strains resistant to diamidines and melaminophenyl arsenicals.

In this study, all experiments were performed at least three times for each compound and each experiment included two positive controls, pentamidine, diminazene; drug-free incubations were used as negative controls. Fluorescence intensity was analysed using GraphPad Prism 5 software and the data was plotted to a sigmoid curve by non-linear regression, in order to determine the EC₅₀ values (Effective Concentration that inhibits 50% of maximal growth).

One hundred and fifty-eight synthesized curcumin analogues were tested on three strains of trypanosomes: wild type strain (s427-WT), TbAT1 knock out (KO) and TbAT1-B48 - listed in decreasing sensitivity to diminazene, pentamidine and cymelarsan (Matovu *et al.*, 2003; Bridges *et al.*, 2007). The tests on curcumin compounds AS-HK001-098 were conducted by my colleague Hasan Ibrahim (Ibrahim, 2009) and some of the results were subsequently published (Changtam *et al.*, 2010a). Results from the Alamar blue assays with compounds AS-HK100-158 are presented here. Figure 3.4 shows typical results, of one such assay, with all three strains performed in parallel and only the EC₅₀ values for the diamidine controls shifting to higher resistance levels in TbAT1-KO and B48 (Table 3.11). There was no significant difference in the EC₅₀ values of the 59 curcumin analogues for the three strains of *T. b. brucei* (Table 3.11). This was consistent with the earlier findings with compounds AS-HK001-098.

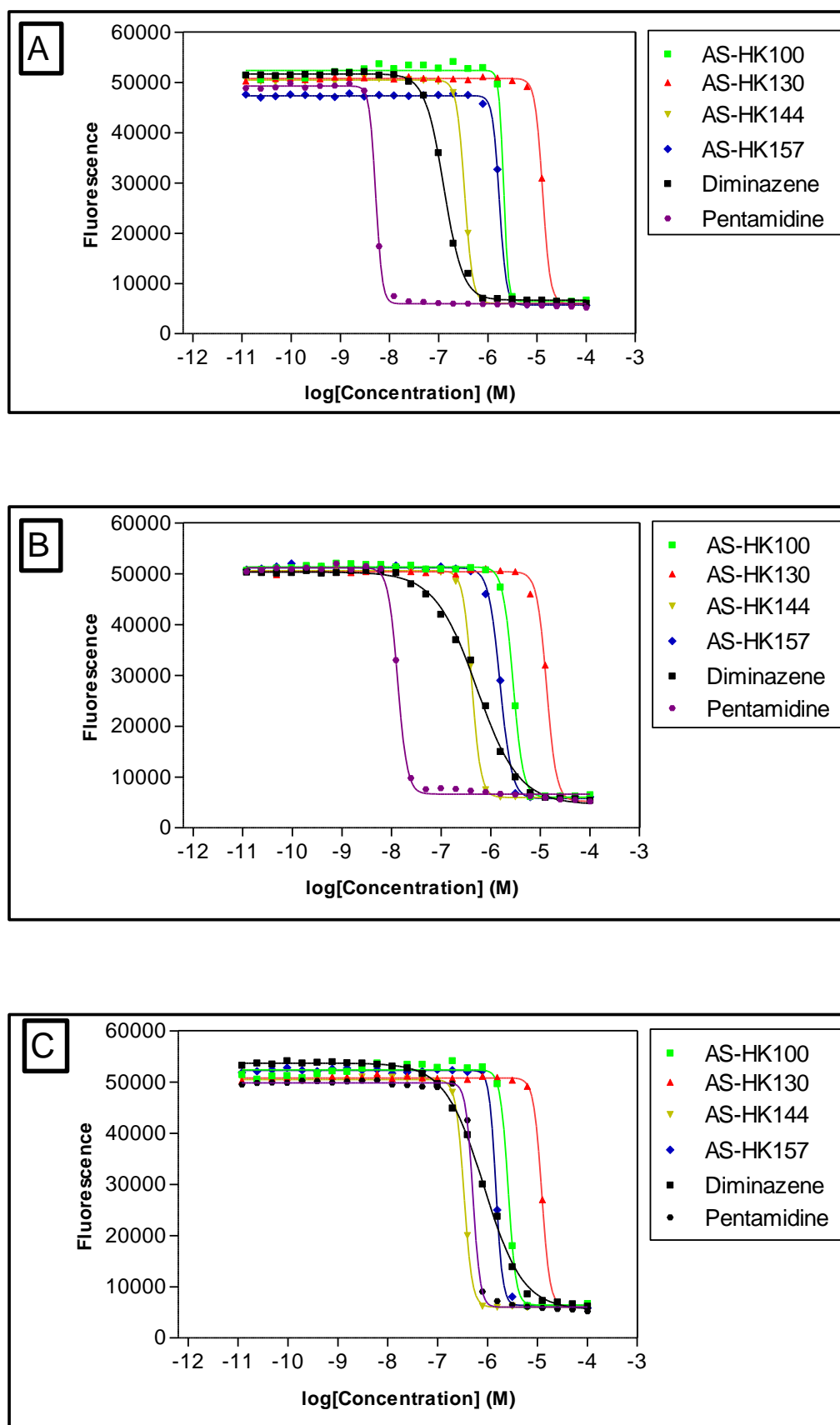


Figure 3.4. The effect of some curcumin compounds on bloodstream forms of three *T. b. brucei* strains, Tb427-WT (A), TbAT1-KO (B) and B48 (C) by using Alamar blue assay. Diminazene and pentamidine were used as positive controls.

Compound	<i>T. b. b.</i> (WT) $\mu\text{M} \pm \text{SEM}$	<i>T. b. b.</i> (KO) $\mu\text{M} \pm \text{SEM}$	<i>T. b. b.</i> (B48) $\mu\text{M} \pm \text{SEM}$
AS-HK 100	2.1 \pm 0.28	3.16 \pm 0.45	2.82 \pm 0.34
AS-HK 101	0.12 \pm 0.02	0.66 \pm 0.18	0.45 \pm 0.08
AS-HK 102	2.56 \pm 0.5	4.25 \pm 1.15	2.97 \pm 1.01
AS-HK 103	1.09 \pm 0.22	1.03 \pm 0.25	0.86 \pm 0.09
AS-HK 104	1 \pm 0.15	0.88 \pm 0.04	1.09 \pm 0.07
AS-HK 105	1.96 \pm 0.31	1.95 \pm .068	1.63 \pm 0.25
AS-HK 106	2.25 \pm 0.21	1.72 \pm 0.13	2 \pm 0.2
AS-HK 107	1.43 \pm 0.11	1.23 \pm 0.07	1.34 \pm 0.11
AS-HK 108	4.01 \pm 1.37	3.09 \pm 0.6	3 \pm 0.96
AS-HK 109	3.08 \pm 1.06	3.87 \pm 1.34	2.56 \pm 0.92
AS-HK 111	4.6 \pm 1.36	3.97 \pm 1.24	3.95 \pm 1.52
AS-HK 112	5.44 \pm 1.7	4.19 \pm 1.19	4.66 \pm 1.82
AS-HK 113	5.97 \pm 1.17	6.25 \pm 0.92	6.23 \pm 1.47
AS-HK 115	2.07 \pm 0.02	2.95 \pm 0.44	2.89 \pm 0.16
AS-HK 116	13.06 \pm 2.89	12.2 \pm 2.91	8.82 \pm 2.37
AS-HK 117	1.15 \pm 0.13	0.79 \pm 0.17	1.61 \pm 0.45
AS-HK 118	0.51 \pm 0.14	0.1 \pm 0.03	0.45 \pm 0.24
AS-HK 119	0.07 \pm 0.024	0.15 \pm 0.05	0.1 \pm 0.04
AS-HK 120	0.018 \pm 0.01	0.05 \pm 0.02	0.04 \pm 0.02
AS-HK 122	0.064 \pm 0.018	0.06 \pm 0.001	0.08 \pm 0.01
AS-HK 123	0.042 \pm 0.018	0.08 \pm 0.03	0.03 \pm 0.01
AS-HK 124	0.033 \pm 0.007	0.06 \pm 0.02	0.04 \pm 0.006
AS-HK 125	0.031 \pm 0.004	0.07 \pm 0.02	0.06 \pm 0.01
AS-HK 126	0.015 \pm 0.003	0.05 \pm 0.01	0.03 \pm 0.007
AS-HK 127	0.35 \pm 0.05	0.65 \pm 0.1	0.57 \pm 0.06
AS-HK 128	1.24 \pm 0.23	1 \pm 0.15	1.04 \pm 0.12
AS-HK 129	47.75 \pm 4.8	70.1 \pm 8	86.5 \pm 23.7
AS-HK 130	15.09 \pm 1.43	13.13 \pm 1.07	12.6 \pm 1.5
AS-HK 131	0.99 \pm 0.15	1 \pm 0.07	0.87 \pm 0.08
AS-HK 132	1.05 \pm 0.04	0.93 \pm 0.02	0.86 \pm 0.07
AS-HK 133	34.97 \pm 3	32.42 \pm 4.1	21.56 \pm 3.2
AS-HK 134	12.45 \pm 0.76	12.74 \pm 1.15	10.3 \pm 1.04
AS-HK 135	4.73 \pm 0.42	4.46 \pm 0.3	3.60 \pm 0.15
AS-HK 136	3.76 \pm 0.17	4.06 \pm 0.16	3.65 \pm 0.1
AS-HK 137	0.62 \pm 0.03	0.55 \pm 0.02	0.58 \pm 0.08
AS-HK 138	3.3 \pm 0.34	2.5 \pm 0.17	2.19 \pm 0.24
AS-HK 139	3.04 \pm 0.15	2.48 \pm 0.27	2.25 \pm 0.12
AS-HK 140	2.33 \pm 0.23	1.83 \pm 0.15	1.57 \pm 0.14
AS-HK 141	0.54 \pm 0.07	0.45 \pm 0.02	0.37 \pm 0.04
AS-HK 142	4.86 \pm 0.82	4.33 \pm 0.43	4.02 \pm 0.29
AS-HK 143	0.58 \pm 0.01	0.71 \pm 0.06	0.72 \pm 0.07
AS-HK 144	0.34 \pm 0.05	0.44 \pm 0.01	0.41 \pm 0.05
AS-HK 145	0.37 \pm 0.03	0.40 \pm 0.05	0.3 \pm 0.02

AS-HK 146	0.69 ± 0.06	0.49 ± 0.05	0.47 ± 0.06
AS-HK 147	1.08 ± 0.07	1.13 ± 0.09	0.93 ± 0.04
AS-HK 148	1.95 ± 0.09	1.79 ± 0.06	1.83 ± 0.16
AS-HK 149	1.89 ± 0.36	1.21 ± 0.06	1.41 ± 0.23
AS-HK 150	12.62 ± 0.1	10.87 ± 0.5	11.8 ± 0.9
AS-HK 151	1.09 ± 0.02	1.02 ± 0.02	1.38 ± 0.18
AS-HK 152	2.01 ± 0.07	1.71 ± 0.13	1.65 ± 0.18
AS-HK 153	3.67 ± 0.14	2.8 ± 0.14	3.24 ± 0.35
AS-HK 154	0.40 ± 0.01	0.45 ± 0.01	0.43 ± 0.03
AS-HK 155	0.73 ± 0.14	0.62 ± 0.06	0.67 ± 0.07
AS-HK 156	3.28 ± 0.21	3.32 ± 0.26	3.06 ± 0.31
AS-HK 157	1.58 ± 0.05	1.47 ± 0.1	1.41 ± 0.21
AS-HK 158	6.25 ± 0.06	6.26 ± 0.31	5.61 ± 0.08
Diminazene	0.12 ± 0.01	0.54 ± 0.086	0.73 ± 0.2
Pentamidine	0.004 ± 0.001	0.01 ± 0.005	0.41 ± 0.02

Table 3.11. Average EC₅₀ values for curcumin compounds against *T. b. brucei* wild type, TbAT1- knockout and B48 blood stream form plus standard errors. All data are the average of at least 3 independent experiments.

3.4 Structural determinants of curcumin analogues important for antileishmanial activity – comparison with *T. b. brucei*

The structural determinants for activity of curcumin analogues against *T. b. brucei* are similar to those found to be important for antileishmanial activity. The first similarity is that the mono-*O*-demethylated analogue AS-HK033 showed increased effectiveness against both the *Leishmania* species and *T. b. brucei* when comparing the original compound, AS-HK001, and the *O*-demethylated analogue, AS-HK073. The second similarity is that the addition of one or two pentyl pyridinium (C₁₀H₁₅N) groups leads to an increase of activity in both the *Leishmania* species and *T. b. brucei*, as it is found in compounds AS-HK119, 122, 123, 124, 125 and 126. Additionally, the activity was greater when replacing the diketo group with an isoxazole ring as found in compounds AS-HK125 and 126. Furthermore, the omission of one of the keto groups, resulting in a enone linker such as in compound AS-HK014, resulted in a slight increase in the activity against parasites, although this was much more pronounced in *T. b. brucei* (Changtam *et al.*, 2010a). Moreover, adding one pentyl bromide (OC₅H₁₀Br) as in

AS-HK118 led to the improvement of activity against both *Leishmania* species as well as *T. b. brucei*. Finally, when compared with the original compound AS-HK001, more than half of the trienone analogues increased their activity against all parasites that were tested in this study. It is thus clear that some of the main structural motifs highlighted in the current study ensure broad activity against kinetoplastid parasites and should be investigated for further anti-infective activity. However, it is vital to first assess, at this point, whether the general anti-kinetoplastid activity is merely a reflection of a general cellular toxicity that would disqualify the compounds from further therapeutic development.

3.5 Selectivity of curcuminoids: therapeutic index relative to Human Embryonic Kidney cells

Compound	<i>T. brucei</i> WT s427	<i>L. mexicana</i> amastigotes	HEK cells	Therapeutic index Trypanosoma	Therapeutic index Leishmania
	EC ₅₀ (μM)	EC ₅₀ (μM)	EC ₅₀ (μM)		
AS-HK 100	2.14 ± 0.28	9.2 ± 1.9	47.8 ± 3	22.3	5.2
AS-HK 101	0.12 ± 0.02	2.0 ± 0.3	40 ± 9.1	333	20
AS-HK 102	2.56 ± 0.5	17.3 ± 1.7	195 ± 44	76	11.2
AS-HK 103	1.09 ± 0.22	5.5 ± 1.2	59.4 ± 15.7	54.5	10.8
AS-HK 104	1.00 ± 0.15	6.7 ± 1.4	61.3 ± 14.7	61	9.1
AS-HK 105	1.96 ± 0.31	11.6 ± 2.4	229.5 ± 44.2	117	20
AS-HK 106	2.25 ± 0.21	11.7 ± 2.1	> 400	> 177	> 35
AS-HK 107	1.43 ± 0.11	5.3 ± 0.5	> 400	> 280	> 75.5
AS-HK 108	4.01 ± 1.37	2.5 ± 0.3	> 400	> 100	> 160
AS-HK 109	3.08 ± 1.06	3.9 ± 0.5	59.5 ± 19	19.3	15.25
AS-HK 111	4.60 ± 1.36	5.1 ± 0.6	70 ± 15.6	15.2	13.7
AS-HK 112	5.44 ± 1.7	10.4 ± 1.6	186.5 ± 50.6	34.3	18
AS-HK 113	5.97 ± 1.17	3.3 ± 0.4	> 400	> 67	> 121
AS-HK 115	2.07 ± 0.02	2.0 ± 0.2	> 400	> 193	> 200
AS-HK 116	13.06 ± 2.9	5.6 ± 0.8	> 400	> 30.6	> 71.4
AS-HK 117	1.15 ± 0.13	9.3 ± 2.4	34 ± 3.4	29.5	3.6
AS-HK 118	0.51 ± 0.14	5.0 ± 0.8	17.1 ± 0.6	33.5	3.4
AS-HK 119	0.07 ± 0.02	9.5 ± 0.9	43.5 ± 3.1	621	4.6
AS-HK 120	0.02 ± 0.01	16.8 ± 4.5	> 400	> 20000	> 32.8
AS-HK 122	0.06 ± 0.018	6.5 ± 1.8	63 ± 1	562	5.5
AS-HK 123	0.042 ± 0.01	7.4 ± 2	46.7 ± 1	1112	6.3
AS-HK 124	0.03 ± 0.007	15.6 ± 4.2	56 ± 0.5	1697	3.6
AS-HK 125	0.03 ± 0.004	10.0 ± 2.5	38.8 ± 3.6	1251	3.9

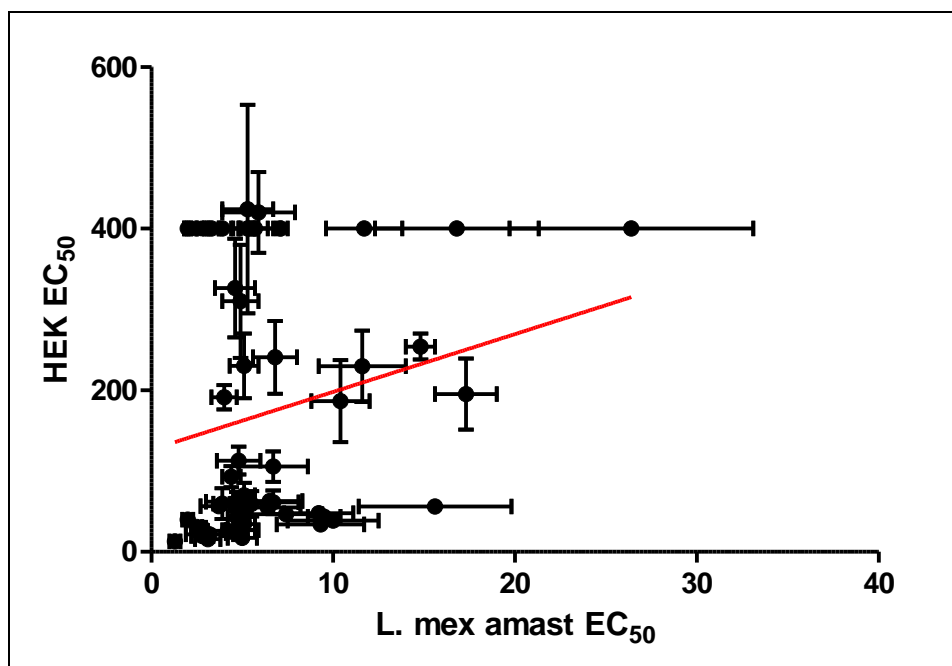
AS-HK 126	0.01 ± 0.003	3.7 ± 1	56.4 ± 4.1	3760	15.2
AS-HK 127	0.35 ± 0.01	26.4 ± 6.7	> 400	> 1142	> 15
AS-HK 128	1.24 ± 0.23	14.8 ± 0.8	254 ± 16	205	17
AS-HK 129	47.75 ± 4.86	7.1 ± 0.4	> 400	> 8.3	> 56.3
AS-HK 130	15 ± 1.43	4.9 ± 1.0	310 ± 70	20.5	63
AS-HK 131	0.99 ± 0.15	6.4 ± 1.8	55 ± 6	55.5	8
AS-HK 132	1.05 ± 0.04	4.7 ± 0.6	23 ± 3	22	5
AS-HK 133	34.9 ± 1	3.9 ± 1.0	>400	>11.5	>103
AS-HK 134	12.4 ± 0.76	5.9 ± 2.0	420 ± 50	34.8	71
AS-HK 135	4.73 ± 0.42	5.1 ± 0.8	230 ± 40	48.6	45
AS-HK 136	3.76 ± 0.17	5.4 ± 1.7	> 400	> 106	> 74
AS-HK 137	0.62 ± 0.03	4.2 ± 1.1	26.1 ± 3.4	42	6
AS-HK 138	3.3 ± 0.34	6.7 ± 1.9	105.5 ± 18.9	32	16
AS-HK 139	3.04 ± 0.15	4.4 ± 0.5	92.8 ± 13.1	30.5	21
AS-HK 140	2.33 ± 0.7	5.0 ± 0.5	50.6 ± 4.5	21.8	10
AS-HK 141	0.54 ± 0.07	4.9 ± 1.0	26.6 ± 2.4	49	5
AS-HK 142	4.86 ± 0.82	4.6 ± 1.1	326.4 ± 60.9	67.2	71
AS-HK 143	0.58 ± 0.01	2.8 ± 0.6	19.6 ± 2.6	33.8	7
AS-HK 144	0.34 ± 0.05	2.8 ± 0.2	29.8 ± 6.2	87.6	11
AS-HK 145	0.37 ± 0.03	3.2 ± 1.3	21.6 ± 2.5	58.4	6
AS-HK 146	0.69 ± 0.06	3.1 ± 0.7	15.8 ± 1.8	22.9	5
AS-HK 147	1.08 ± 0.07	4.9 ± 0.8	27.1 ± 3.1	25	5
AS-HK 148	1.95 ± 0.09	5.1 ± 0.6	34.3 ± 6.6	17.6	7
AS-HK 149	1.89 ± 0.36	2.5 ± 0.3	30.9 ± 4.0	16.4	12
AS-HK 150	12.62 ± 0.1	5.3 ± 1.4	423.9 ± 129.0	33.5	80
AS-HK 151	1.09 ± 0.02	4.8 ± 1.2	112.9 ± 17.3	103.6	24
AS-HK 152	2.01 ± 0.07	4.7 ± 0.5	43.0 ± 4.3	21.4	9
AS-HK 153	3.67 ± 0.14	5.7 ± 1.2	> 400	> 108	> 70
AS-HK 154	0.40 ± 0.01	1.3 ± 0.3	12.9 ± 2.8	32.3	10
AS-HK 155	0.73 ± 0.14	4.0 ± 0.7	191.1 ± 15.1	261.8	48
AS-HK 156	3.28 ± 0.21	6.8 ± 1.2	240.6 ± 44.9	73.4	35
AS-HK 157	1.58 ± 0.05	4.7 ± 1.7	62.2 ± 11.7	39.4	13
AS-HK 158	6.25 ± 0.06	3.1 ± 1.3	> 400	> 64	> 129
PAO			2.6 ± 0.1		

Table 3.12. : Average EC50 values for curcumin compounds against *T. b. brucei* wild type blood stream form, *L. mexicana* amastigotes plus standard errors. Also shown are the average EC50 values with Human Embryonic Kidney (HEK) cells and standard errors, plus the Selectivity Index (EC50 of HEK cells / EC50 of parasites). PAO (Phenyl Arsine Oxide) as a positive control for HEK cells.

Curcuminoids compounds (AS-HK100-158) were tested by Alamar blue for their effects on human embryonic kidney (HEK) cells in order to determine whether the antiprotozoal activity is the result of general toxicity or is more specifically antiprotozoal (Table 3.12). Toxicity assays for HEK cells showed that the

curcumin compounds that have an effect on *L. mexicana* amastigotes and *T. b. brucei* have a much lower activity on HEK cell growth and viability. Therapeutic index rates (EC_{50} of HEK cells / EC_{50} of parasites) for *Trypanosoma* and *Leishmania* are shown in table 3.12. The highest of therapeutic index values were > 20000, 3760, 1697 and 1697-fold for wild-type *T. brucei* with AS-HK120, AS-HK126 and AS-HK124 respectively. These were all pentylpyridinium analogues, which all displayed mid - to low nanomolar activity against the trypanosomes. The best therapeutic indices with respect to *L. mexicana* amastigotes were >200, >160 and >129-fold for AS-HK115, AS-HK 108 and AS-HK 158 respectively. Compounds 115 and 158 contain rigidly linear C_7 linkers with 3 double bonds, either partly integrated in an isoxazole ring or trienone motif, respectively; AS-HK108 is a direct analogue of curcumin, with bromopentyl ether substitutions on positions 3 and 7. It is worth mentioning that in many cases, the higher limit of the therapeutic index could not be obtained as the highest concentration tested in our HEK cell screen was 400 μ M and a significant percentage of compounds had no growth retarding effects on the human cell line at that concentration. While the results presented here are highly encouraging, it is acknowledged that far more pharmacological and toxicological tests must be performed to develop this series of curcuminoids into genuine lead compounds for anti-parasitic drug development.

At the same time, there is no steady line correlation between the activity of these compounds on amastigotes and HEK cells, as shown in Figure 3.5. Therefore, it is possible to optimise for activity against amastigotes without increasing toxicity to HEK cells at the same time.



3.5. Correlation between EC₅₀ values against axenic *L. Mexicana* amastigotes and cultured HEK cells. Trend line was calculated by linear regression yielding a correlation coefficient of 0.05; the slope was not significantly different from zero (runs test) and thus there is no significant correlation between the two data sets. In some cases the value 400 was entered as the EC₅₀ value for HEK cells could not be determined and 400 μ M was the highest concentration used in the assay.

3.6 Discussion

158 curcumin analogues were tested against *L. major* promastigotes, *L. mexicana* promastigotes and *L. mexicana* amastigotes. Alamar blue assays were used to obtain the EC₅₀ for curcumin analogues in at least three independent determinations for studying the structure-activity relationship (SAR) of curcumin analogues as compounds against *Leishmania* species. A number of curcumin compounds have activities similar or better than current clinical drugs such as pentamidine (Ibrahim *et al.*, 2011). Curcumin compounds AS-HK119 and AS-HK122, containing one or two pentyl pyridinium (C₁₀H₁₅N) groups, displayed at least the same antileishmanial activity as pentamidine in all *Leishmania* species tested. The replacement of the diketo motif with an isoxazole ring as in compounds AS-HK125 and 126 resulted in similar activity. Most importantly perhaps the trienone motif produced a series with consistently high activity against amastigotes, allowing the selection of some members of the series that, like AS-HK158, display low toxicity to the human cell line. In all 18 out of 158 curcumin compounds exhibited the same or higher activity than pentamidine against *L. mexicana* amastigotes.

Curcumin analogues were also tested against *Trypanosoma brucei brucei* in order to obtain EC₅₀ values. 59 out of 158 curcumin compounds (AS-HK100-158) are reported in this study because the first compounds already were studied by my colleague Hasan Ibrahim. As it is essential for any new compound considered for development to be active against resistant strains comparisons of the activity of curcumin analogues against different strains of *Trypanosoma brucei brucei* (WT, KO and B48) were made. The results show that there is no significant cross-resistance between the entire class of curcumin compounds and the diamidine or melaminophenyl arsenical classes of trypanocides. As diamidine and arsenical resistance in these strains has been linked to loss of the P2 transporter and the HAPT transporter (Bridges *et al.*, 2007; Matovu *et al.*, 2003), it is concluded that uptake of curcumoids is not dependent on the expression of these transporters.

The cytotoxicity of curcumin analogues towards HEK cells showed substantial differences, and this screen will be only a first filter to narrow down compounds

from the substantial library for further testing. However, all of these compounds show lower toxicity towards HEK cells than to *Trypanosoma brucei brucei* and *Leishmania* species. The calculated therapeutic index value for *T. b. brucei* exceeded 100-fold for 19 out of 59 curcumin compounds; 5 out of 59 of those compounds displayed a therapeutic index >100 for *L. mexicana* amastigotes. This finding is completely consistent with the data published by Changtam and his colleagues (2010) who reported that the curcumin analogues have lower toxicity to human cells than to kinetoplastid parasites.

One of the more significant findings to emerge from this study is that there are some curcumin analogues were very active against the parasites in this study, such as, mono-*O*-demethylated, *O*-demethylated, pentyl pyridinium, isoxazole, monoketo and pentyl bromide analogues.

Curcumin has been reported effective against parasites in many studies. For example, the EC₅₀ value for *L. major* promastigotes was 37.6 µM (Koide *et al.*, 2002), which is very close to the EC₅₀ in this study 33 µM. The Curcuminoids AS-HK001, AS-HK002 and AS-HK003 have been tested on *L. major* promastigotes and *P. falciparum* and the IC₅₀ values were between 3 and 21 µM (Rasmussen *et al.*, 2000). In addition, previous studies have reported that curcumin analogues AS-HK001, AS-HK004, AS-HK025 and AS-HK073 are effective against *P. falciparum* with IC₅₀ ranges between 2.3 and 8.5 µM (Mishra *et al.*, 2008). AS-HK073 thus has a similar activity against *Plasmodium* (Mishra *et al.*, 2008) and *Leishmania* species, IC₅₀ of 7.8, 2.8, 18 and 10 µM of IC₅₀ for *P. falciparum*, *L. major* promastigotes, *L. mexicana* promastigotes and *L. mexicana* amastigotes, respectively.

The antimycobacterial activity of some curcumin compounds has also been investigated. Curcumin compounds, such as AS-HK001, AS-HK043 and AS-HK046, were tested against *Mycobacterium tuberculosis* and the activities for compounds 43 and 46 were higher than for curcumin itself (Changtam *et al.*, 2010b). Moreover, Changtam and his colleagues discovered that the isoxazole analogues are the most active compound series against these bacteria, which correlates with the results of the present study, which show that the isoxazole analogues have very clear activity against *Leishmania* spp. Recently, curcumin has been reported to be also effective against *Trypanosoma cruzi*; it caused

reduced parasitemia in infected mice and killed the parasites *in vitro* (Nagajyothi *et al.*, 2012).

Finally, the Alamar Blue method is a widely-used tool for primary screening of compound libraries on numerous cell types, including protozoa (Raz *et al.*, 1997; Fumarola *et al.*, 2004; Al-Salabi & de Koning, 2005). However, it is essential that hit compounds identified in such a screen are followed on by more informative techniques. For instance, screening axenic *Leishmania* amastigotes using the Alamar Blue assay can eliminate from consideration a high percentage of compounds screened. The remainder can then be screened using the far more predictive parasite burden assays with intra-macrophage amastigotes to further narrow down the number of hits by eliminating those that do not adequately penetrate the macrophage and the phagolysosome, or are too toxic to the macrophages. This will then yield a final set of hit compounds to be tested in an animal model of leishmaniasis.

4 Chapter four: Investigation into the mechanism of the trypanocidal activity of curcumin analogues bearing the enone motif

4.1 Introduction

An overview of the results in Chapter 3 (Changtam *et al.*, 2010;Ibrahim, 2009) shows that there are strong trypanocidal effects for some curcumin analogues. For instance, curcumin AS-HK014 has a strong effect on trypanosome and a low toxicity activity on human embryonic kidney cells (T293), which means this compound holds great promise in the future. Therefore, its mechanism of action must be elucidated in order to initiate structure activity relationship studies and rational lead compound optimisation.

An earlier work by my colleague Hasan Ibrahim showed that, in bloodstream trypanosomes, curcumin and its analogues have no effect on normal cell cycle progression and mitochondrial membrane potential, do not cause DNA fragmentation, and do not increase the levels of reactive oxygen species in trypanosomes. However, one curcumin compound (AS-HK014) rapidly decreased the glutathione content in the hepatocytes of rat (Ibrahim, 2009).

In this study, further tests on the mechanism of action of curcumin are conducted. In particular, the fast action of enone curcumins was suggestive of a rapid change in the cells, possibly mediated by changes to the plasma membrane permeability or effects on levels of second messengers such as cAMP or intracellular calcium. The possibility of a plasma membrane event was further confirmed by the observation of Hasan Ibrahim that the enone curcumins but not the di-ketone curcumins induced rapid plasma membrane permeabilisation in *T. brucei brucei* (Ibrahim, 2009).

Induction of *T. b. brucei*-resistant cell lines could help in the understanding of the mechanism of action of drug (Bridges *et al.*, 2007;Barrett *et al.*, 1995). Two resistant cell lines were established, for AS-HK001 (curcumin) and AS-HK014, respectively, in order to study the effect of curcumin compounds on these cell lines and to compare the effect with parental cell line. The concentrations were increased gradually depending on the cells' viability. Several studies that focused on resistant cell lines were used to understand the mechanism of action of drug, including the metabolomic assessment of curcumin and AS-HK014 on *T. b. brucei*, which pointed to changes in thiol content. This prompted an

investigation of expression levels of glutathione synthetase (GS) and γ -glutamylcysteine synthetase (GGS), as well as sequence analysis of GS and γ -glutamylcysteine synthetase genes in wild-type and resistant trypanosomes clones.

4.2 Effect of curcuminoids on intracellular cAMP levels in trypanosomes

The intracellular cAMP level was investigated by my colleague Dr. Neils Quashie who worked in Dr. Harry De Koning's laboratory. cAMP was assessed using an enzyme-linked immunosorbant assay (ELISA) kit. The trypanosomes were incubated with two enone curcumin compounds (AS-HK014 and AS-HK096) at 500 nM for 15 min in order to determine their effect on intracellular cAMP levels.

The results show that curcumin compounds 14 and 96 had no significant effect on the cAMP levels compare with Drug free (negative control), whereas the positive control (CpdA at 1 μ M) has a very clear effect on the cAMP levels (figure 4.1). CpdA is an inhibitor of *T. brucei* phosphodiesterase B1 and B2 and increases cellular cAMP levels (de Koning *et al.*, 2012).

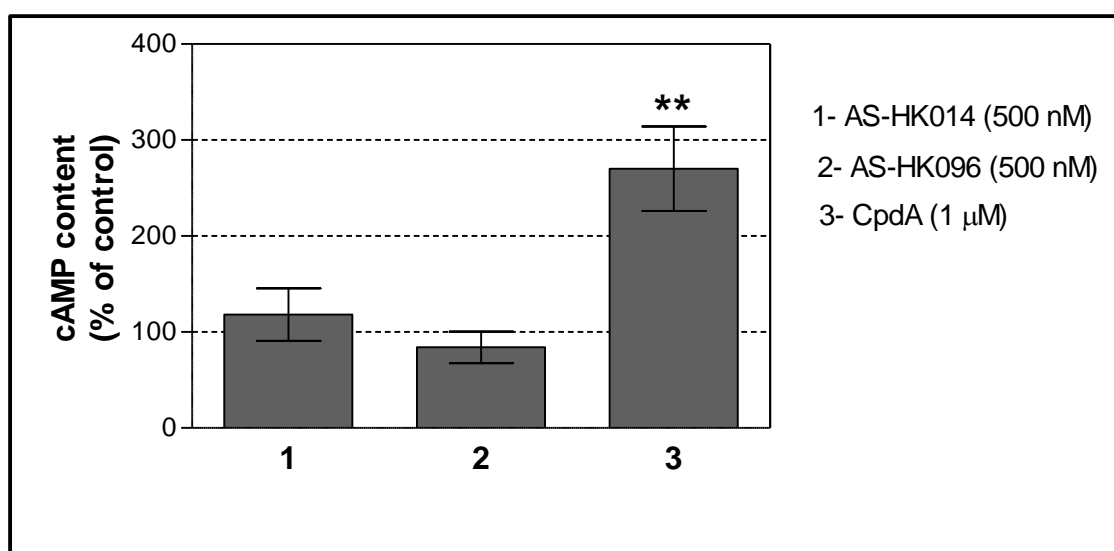


Figure 4.1. Average intracellular cAMP in bloodstream-form *T. b. brucei* incubated at different concentrations for 15 min. cAMP was measured with the use of ELISA kit. The density of the cells was 5×10^6 cell/mL. All results were obtained by Dr. Neils Quashie. The experiment was performed on three separate occasions, and the data shown are the average \pm SEM of these three experiments. The data expressed as % difference of cAMP content from the control (drug free), P-values calculated using the unpaired Student's t-test (** $P < 0.01$).

4.3 Modulation of plasma membrane potential and intracellular calcium by curcuminoids

Differences in the extracellular and intracellular concentration of ions result in the plasma membrane potential V_m . All eukaryotic cells maintain such a potential, which plays a central role in transport mechanisms and signal transduction. Any change in this potential leads to changes in the cellular concentration of ions and consequently to loss of homeostasis and eventual loss of viability. Therefore, a study on the effect of curcumin compounds on V_m and intracellular calcium levels (Ca^{2+}) was conducted.

4.3.1 Effect of curcumin compounds on membrane potential

A set of curcumin compounds with different concentrations was tested on trypanosomes to monitor *in vitro* plasma membrane potential. This potential was determined using the fluorescent dye bis-(1,3 dibutylbarbituric acid)trimethine oxonol (Invitrogen). The negative control was an assay buffer that contained 1% ethanol, and the positive control consisted of 10 μ M gramicidin. As shown in Figure 4.2, none of the curcumin compounds had an effect on membrane potential over 10 min after the addition of the compounds, even at concentrations up to 20-fold their Ec_{50} values. In contrast, gramicidin had a very clear depolarising effect on membrane potential, resulting in a strong increase in fluorescence.

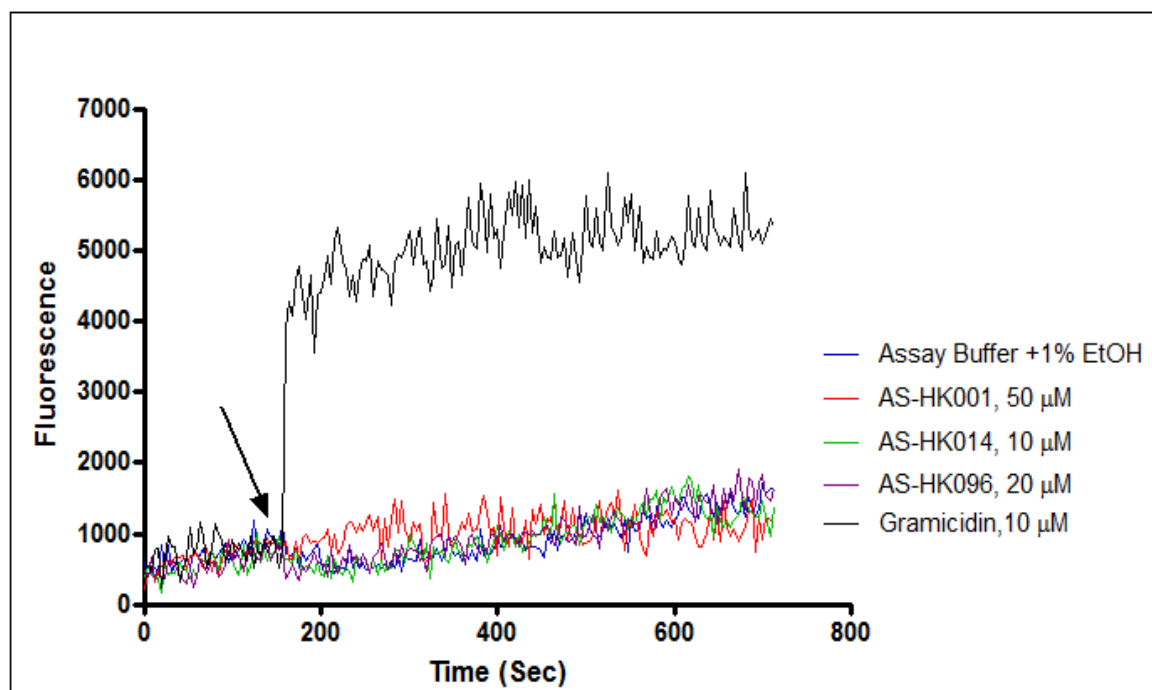


Figure 4.2. Effect of curcumin compounds on the fluorescence of bisoxonol in bloodstream-form *T. b. brucei*. Cells (1×10^7 /mL) were pre-incubated in an assay buffer containing $0.1 \mu\text{M}$ of bisoxonol at room temperature. The fluorescence was read for 160 sec before different compounds (at the final concentration presented in the figure) were added to the cells (arrow), and the fluorescence was recorded for an additional 10 min. Separate traces were recorded in the absence of cells and were subtracted from those presented in the figure.

4.3.2 Effect of curcumin compounds on intracellular calcium level

Intracellular Ca^{2+} was measured with the use of the Screen Quest™ Fluo-8 Calcium Kit (ABD Bioquest). Fluo-8 can cross the cell membrane to bind with intracellular calcium, and this binding causes Fluo-8 to fluoresce. The effect of some curcumin compounds on intracellular Ca^{2+} was determined; calcium ionophore A23187 was used as the positive control ($10 \mu\text{M}$). Figure (4.3) shows that three curcumin analogues, namely, AS-HK001 ($50 \mu\text{M}$), AS-HK014 ($10 \mu\text{M}$) and AS-HK096 ($20 \mu\text{M}$), had no effect on intracellular calcium levels.

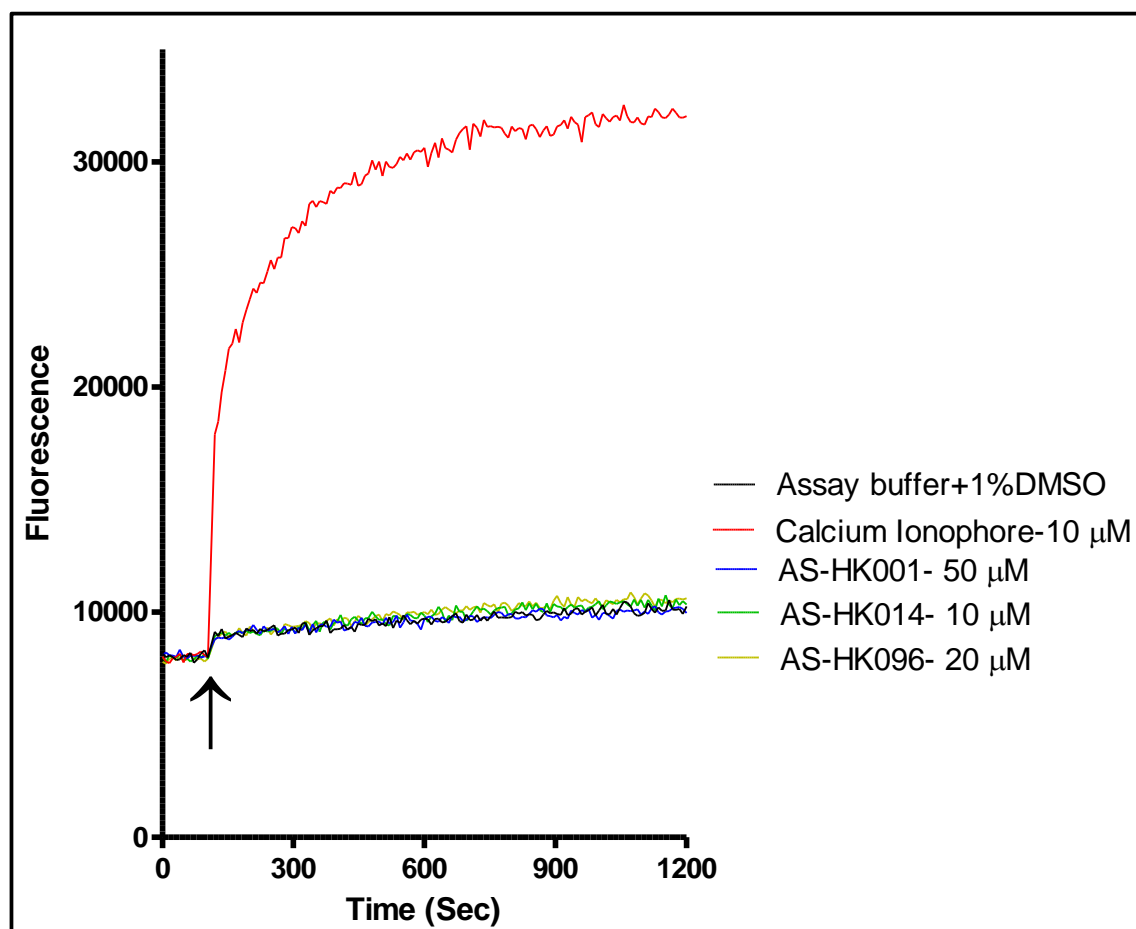


Figure 4.3. Effect of curcumin compounds on the intracellular calcium level in bloodstream-form *T. b. brucei*. Parasites (4×10^6 /mL) were loaded with Fluo-8 dye, and the fluorescence intensity was measured. The fluorescence was read for 120 sec before addition of the curcumin compound or calcium ionophore (at the final concentration presented in the figure) was added to the cells (see arrow), and the fluorescence was recorded for an additional 18 min. Separate traces were recorded in the absence of cells and were subtracted from those presented in the figure, in order to compensate for any innate fluorescence of the compounds or buffer components.

4.4 Extracellular L-glutathione affects the trypanocidal activity AS-HK001 and AS-HK014

As mentioned in the Introduction, earlier observations show that AS-HK014 but not AS-HK001 rapidly depletes glutathione in primary cell suspensions of fresh murine hepatocytes. Therefore, additional experiments on the relationship of glutathione with curcumin activity were conducted. The Alamar blue test was used to determine the EC_{50} of curcumin compounds with different

concentrations of L- Glutathione in the medium (0, 10, 100, 1000 μM). The experiment was exactly the same as the standard Alamar blue experiment, except for the different L-Glutathione content of the medium.

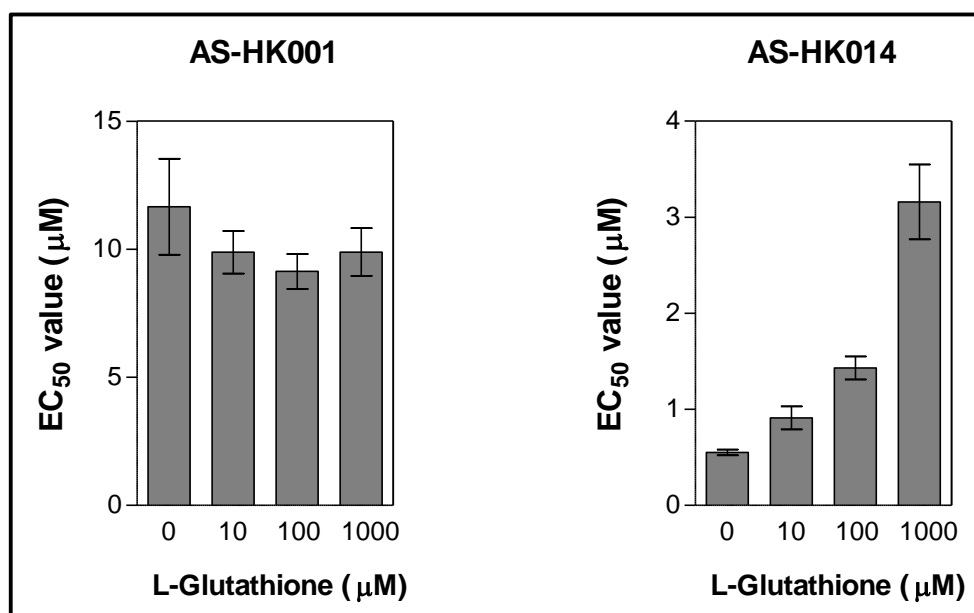
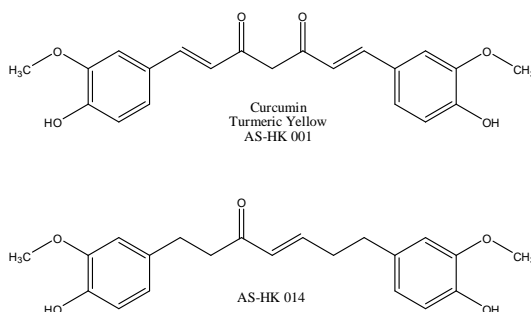


Figure 4.4. EC_{50} values for AS-HK001 and AS-HK014 in the presence of various concentrations of glutathione, as determined by Alamar blue assay on s427 WT *T. b. brucei*. The experiment was performed on three separate occasions, and the data shown are the average \pm SEM of these three experiments.

Indeed, co-incubation of AS-HK014 with different concentrations of L-glutathione led to a gradual decrease in the activity of the drug with an increase in the concentration of L-glutathione. By contrast, the activity of curcumin (AS-HK001) did not show any change when it was co-incubated with different concentrations of L-glutathione (Figure 4.4).

4.5 Induction of *T. b. brucei* cell lines resistant to AS-HK014 and to curcumin

Two resistant cell lines were established for AS-HK001 (curcumin) and AS-HK014, and in the experiment; the initial media concentrations were 5 and 0.25 μM for AS-HK001 and AS-HK 014, respectively. The concentration was slowly increased over many passages until the maximum concentration at which the cells did not grow anymore was reached. After 11 months, the concentration of AS-HK001 reached only 8 μM indicating an inability of *T. brucei* to meaningfully adapt to curcumin, but for AS-HK014, the concentration reached 4.5 μM (Figure 4.5). In addition, the results obtained from Alamar blue showed that there is no significant difference in EC_{50} between the AS-HK001-exposed clonal line and the 'wild-type' cells of *T. b. brucei* (s427-WT), as shown in Figure 4.6 A. By contrast, there were significant differences between the AS-HK014-adapted line (designated TA014) and the parental cells of *T. b. brucei* (s427-WT). The EC_{50} values, which were determined using the Alamar Blue assay, were more than six-fold higher for TA014 ($3.1 \mu\text{M} \pm 0.12$) than for the parental cells, which displayed an EC_{50} value of $0.53 \mu\text{M} \pm 0.05$ as shown in Figure 4.6 B. In vitro growth rates of WT 427 and TA014 trypanosomes were identical (Figure 4.7).

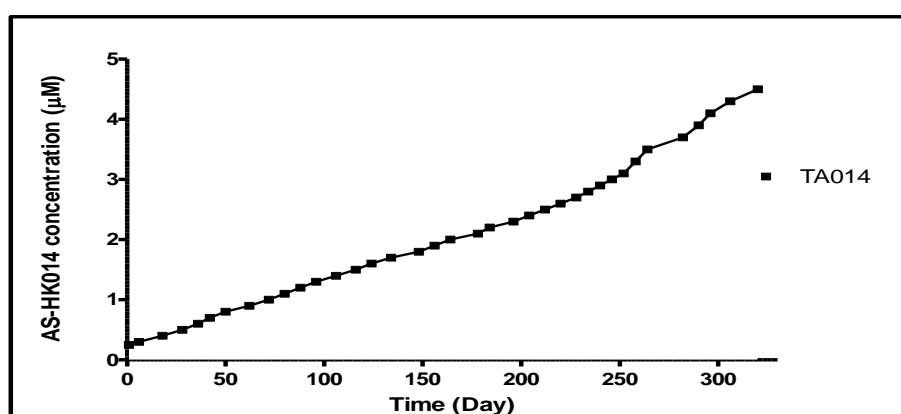


Figure 4.5. Creation of the TA014 cell line. The drug concentration steadily increased for a period of about 11 months.

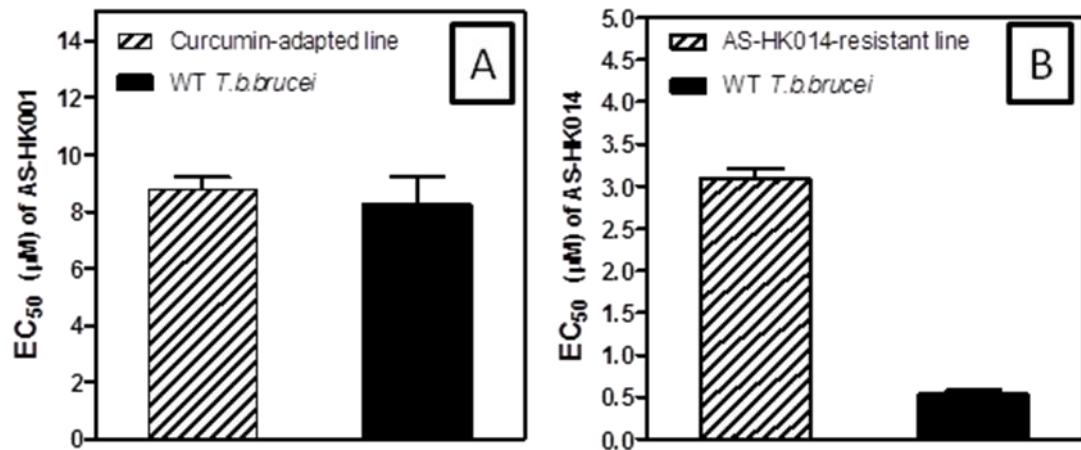


Figure 4.6. Average EC₅₀ values of the clonal lines that were long-term exposed to AS-HK001 (A) or AS-HK014 (B) compared with wild-type *T. b. brucei* bloodstream forms, determined using the Alamar blue assay. The experiment was performed on three separate occasions, and the data shown are the average \pm SEM of these three experiments.

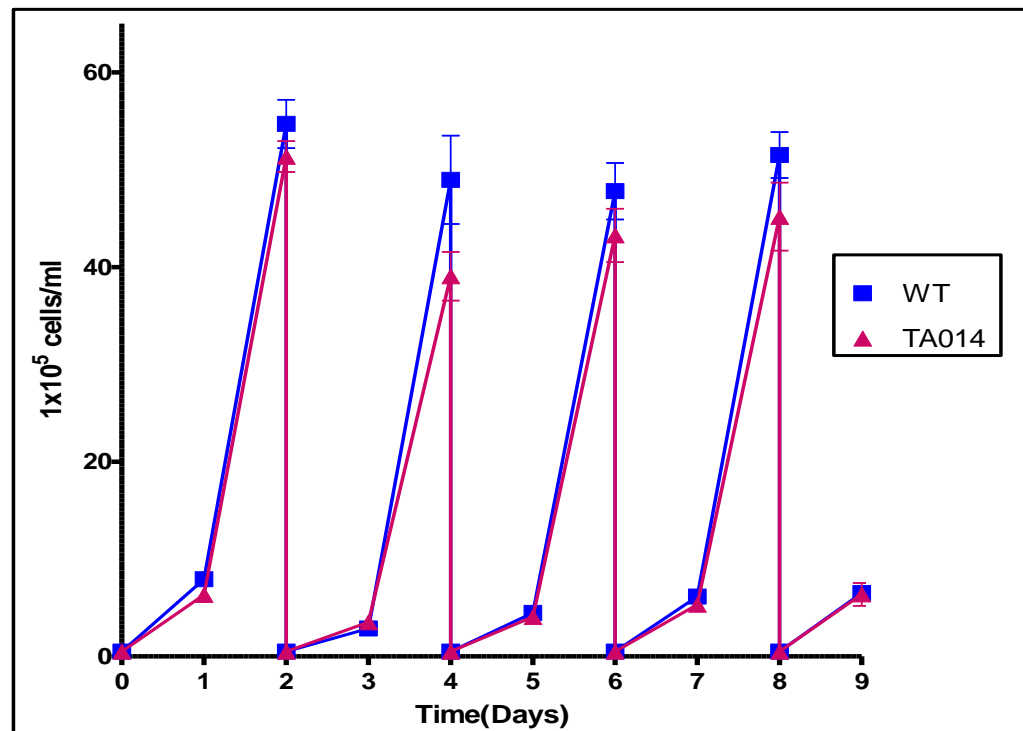


Figure 4.7. Growth rates of WT 427 and TA014 trypanosomes. The cells were seeded at 5×10^4 cells/ml in fresh HMI-9 + 10% FCS. Data represents three independent experiments of growth for 9 days involving 4 passages at 5×10^4 cells/ml.

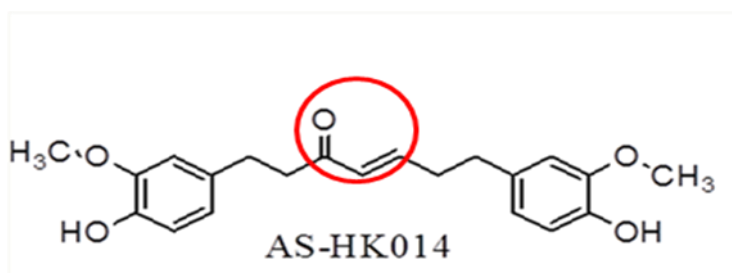
4.6 Assessment of cross-resistance between *T. b. brucei*-WT and TA014 cell lines

Alamar Blue EC₅₀ values were obtained for the Tb427-WT and TA014 resistance lines. The purpose was to examine the level of resistance of the TA014 cell line

obtained through induction of TA014 to some curcumin analogues, and to study cross-resistance to current clinical trypanocides.

The TA014 cell line shows significant resistance to some curcumin analogues. As mentioned previously, the EC_{50} value for AS-HK014 was $0.53 \pm 0.05 \mu\text{M}$ and $3.1 \pm 0.12 \mu\text{M}$ for the Tb427-WT and TA014 cell lines, respectively, with a resistance factor of 5.8-fold ($P < 0.001$) (Table 4.1). The compound AS-HK093 showed an EC_{50} value that increased from $0.56 \pm 0.02 \mu\text{M}$ to $1.45 \pm 0.04 \mu\text{M}$ in the TA014 line ($P < 0.001$), which represents a 2.6-fold increase; AS-HK097 and AS-HK096 demonstrated about 2.5-fold resistance ($P < 0.001$ for both); AS-HK018 also showed a 2.3-fold increase in resistance from $1.79 \pm 0.08 \mu\text{M}$ to $4.19 \pm 0.39 \mu\text{M}$ in EC_{50} in the TA014 line ($P < 0.01$).

No significant cross-resistance was demonstrated by the resistance line TA014 to any of the trypanocide chemotherapies used in the present study. Furthermore, for other curcumin compounds, there was also no significant cross-resistance (Table 4.1). Indeed, this very clear indicator that significant cross-resistance was only for curcumin analogues with a mono-enone linker as mention below.



Compound	Tb427-WT EC ₅₀ (μM)	TA014 EC ₅₀ (μM)	Resistance Factor	P-values (different from Tb427-WT)
AS-HK001	8.24 ± 0.97	8.78 ± 0.43	1.06	NS
AS-HK014	0.53 ± 0.05	3.1 ± 0.12	5.85	P < 0.001
AS-HK015	15.07 ± 0.49	16.3 ± 0.9	1.08	NS
AS-HK016	0.65 ± 0.02	0.53 ± 0.04	0.81	NS
AS-HK017	1.34 ± 0.05	1.3 ± 0.02	0.97	NS
AS-HK018	1.79 ± 0.08	4.19 ± 0.39	2.34	P < 0.01
AS-HK028	1.15 ± 0.07	1.08 ± 0.02	0.94	NS
AS-HK033	3.19 ± 0.02	2.94 ± 0.22	0.92	NS
AS-HK034	7.24 ± 0.4	8.82 ± 0.94	1.2	NS
AS-HK073	1.45 ± 0.11	1.59 ± 0.1	1.1	NS
AS-HK085	5.24 ± 0.27	4.72 ± 0.35	0.9	NS
AS-HK093	0.562 ± 0.02	1.45 ± 0.04	2.6	P < 0.001
AS-HK096	1.48 ± 0.06	3.74 ± 0.02	2.5	P < 0.001
AS-HK097	1.29 ± 0.01	3.34 ± 0.06	2.6	P < 0.001
AS-HK118	2.57 ± 0.11	2.54 ± 0.03	1	NS
AS-HK131	1.67 ± 0.09	1.54 ± 0.08	0.92	NS
Diminazene	0.13 ± 0.03	0.15 ± 0.04	1.15	NS
Pentamidine	0.005 ± 0.001	0.003 ± 0.001	0.6	NS
Eflornithine	39.5 ± 3.76	43.17 ± 3.64	1.1	NS
Nifurtimox	9.27 ± 1.09	7.21 ± 1.38	0.78	NS
Suramin	0.025 ± 0.005	0.036 ± 0.006	1.44	NS

Table 4.1. Average EC₅₀ values of some curcumin compounds and trypanocides as determined by Alamar Blue assay in bloodstream-form Tb427-WT and TA014. Also shown is the resistance factor which is the ratio EC₅₀ TA014 / EC₅₀ WT. The values are averages ± SEM of three independent experiments, and statistical significance was calculated with the use of paired student's t-test (NS= not significant).

4.7 Resistance profile of the ASHK014-adapted line TA014 and effect of L-glutathione on resistance

As mentioned in Section 4.4, Alamar Blue test was again used to determine the EC₅₀ of AS-HK014 compounds with different concentrations of L- Glutathione in the medium for the s427 WT *T. b. brucei* and TA014 resistance lines.

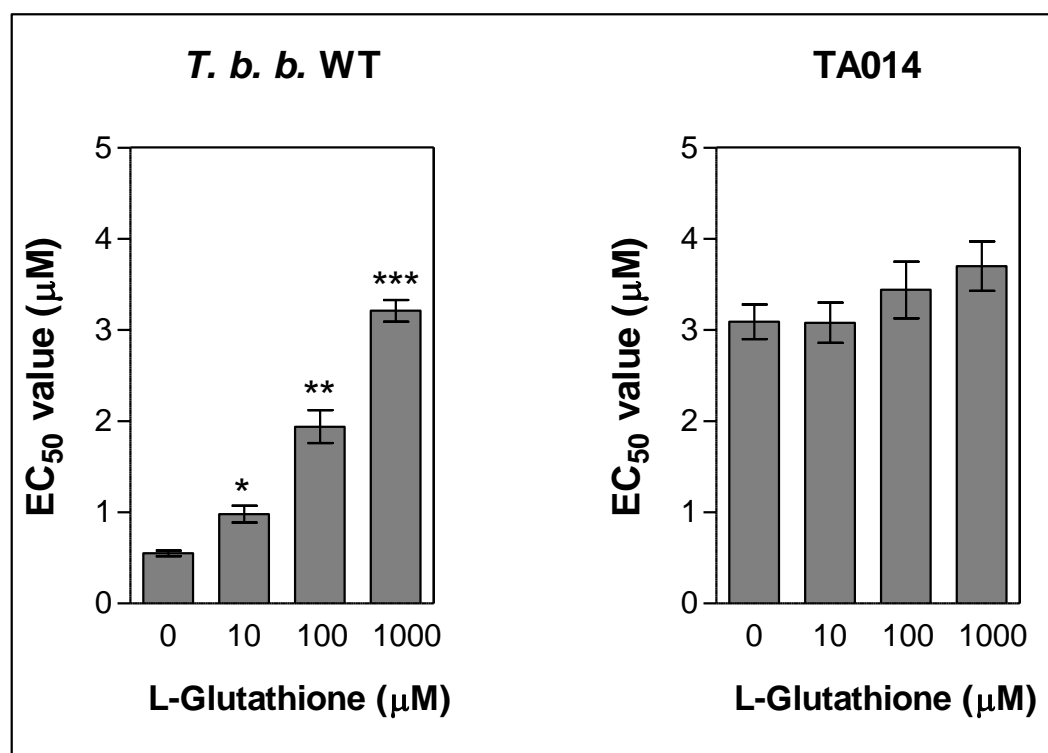


Figure 4.8. EC₅₀ values for curcumin AS-HK014 with various concentrations of glutathione, as determined by Alamar Blue assay for the s427 WT *T. b. brucei* and TA014 resistance lines. The experiment was performed on three separate occasions, and the data shown are the average \pm SEM of these three experiments. P-values are significant different with control (0 μ M of L-glutathione), * $P < 0.05$, ** $P < 0.01$, *** $P < 0.001$.

The results in Figure 4.8 show that although there was a clear effect of L-glutathione on the EC₅₀ of *T. b. brucei* -WT, the same was not the case on the EC₅₀ of the TA014 resistance line. Indeed, the EC₅₀ increased with an increase in the L-Glutathione concentration for *T. b. brucei* -WT from $0.55 \pm 0.03 \mu$ M at 0 μ M of L-Glutathione to $3.21 \pm 0.12 \mu$ M at 1000 μ M of L-Glutathione ($P < 0.001$). In contrast, the EC₅₀ was not significantly different with different concentrations of L-glutathione for the TA014 line, indicating that the residual effect of AS-HK014 in the resistant line might not be due to the same glutathione-sensitive mechanism.

4.8 AS-HK014 makes a chemical adduct with glutathione

To determine whether curcumin AS-HK014 reacts with glutathione to form an adduct, Apichart Suksamrarn (Department of Chemistry, Ramkhamhaeng University, Thailand) conducted the reaction in his laboratory. Added to the

phosphate buffer (1.5 mL, pH 7.4), which contained 130 mg (0.42 mmol) of glutathione, was 130 mg (0.37 mmol) of AS-HK014 in 3 mL ethanol. The reaction was stirred at ambient temperature (30 °C - 32 °C), and the reaction was observed by thin layer chromatography. The plate was developed using an anisaldehyde reagent, followed by heating on a hot plate in order to visualise spots. The adduct 2 (Figure 4.9) was detected in the 15 min sample.

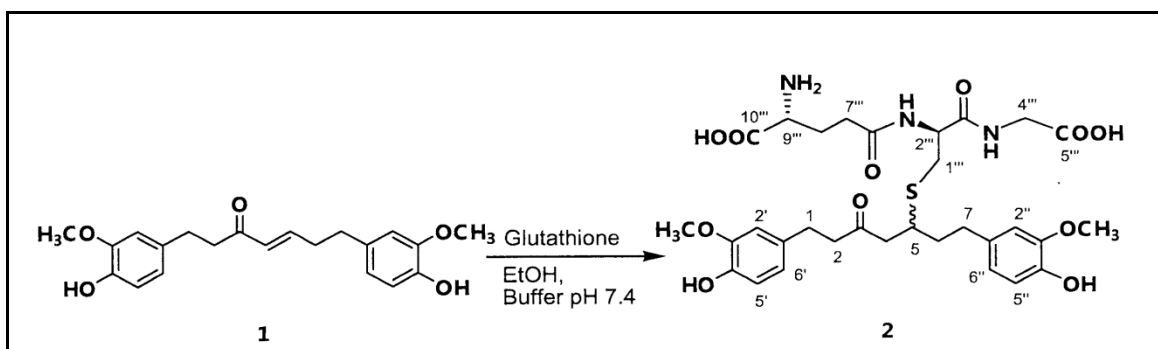


Figure 4.9. Chemical reaction between curcumin AS-HK014 and glutathione (performed by Apichart Suksamrarn). 1: AS-HK014 and 2: adduct.

4.9 Metabolomic assessment of ASHK014 action on *T. b. brucei*

The initial experiments with glutathione presented in this chapter show that that glutathione may play an important role in the mode of action of curcumin AS-HK014. Therefore, glutathione and trypanothione metabolism was examined further to determine the effect of AS-HK014 on *T. b. brucei* -WT and TA014 resistance lines.

4.9.1 Experimental design

A fairly extensive investigation of how fast these compounds act on cell proliferation and cell survival is necessary to design and interpret experiments on their mode of action. Measurements of cellular parameters must be taken at appropriate time points after incubation with appropriate concentrations of compounds. First, as mentioned previously, the EC_{50} values for both cell lines are about 0.5 and 3 μM for *T. b. brucei*-WT and resistance line TA014,

respectively. Second, the growth curve was determined at different concentrations of AS-HK014 (0, 0.5 and 1 μM) for both strains.

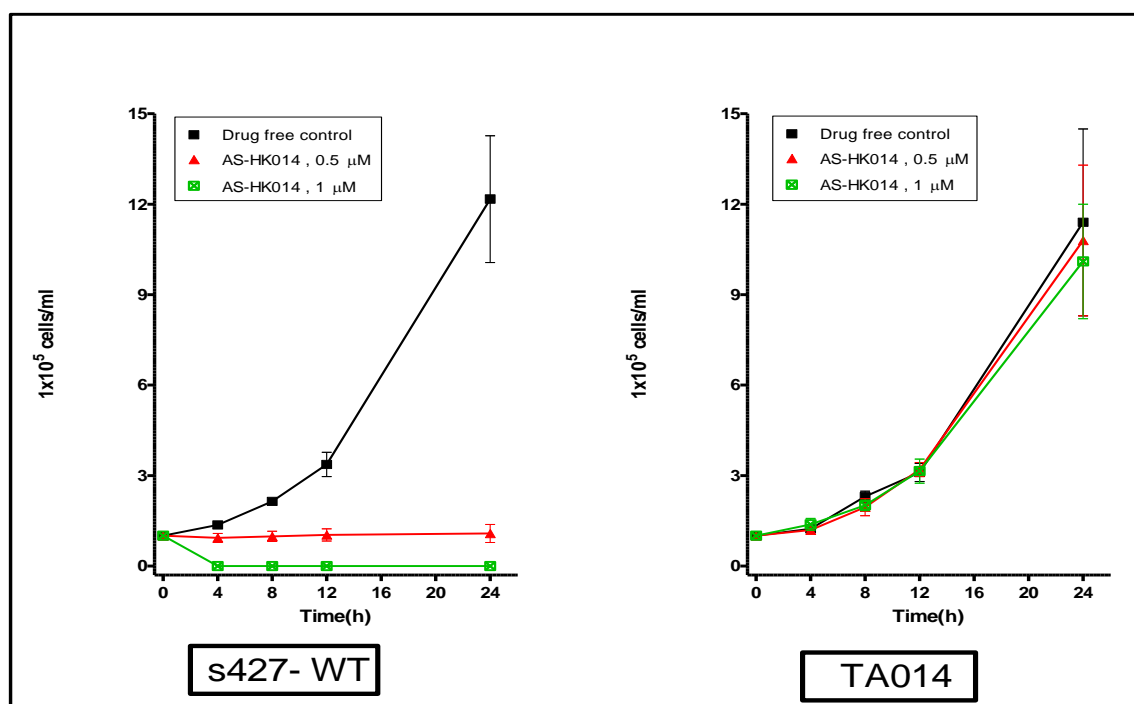


Figure 4.10. Effect of different concentrations of AS-HK014 on the growth curve of bloodstream form *T. brucei brucei* WT and TA014 resistance lines. The results shown are the average of three independent determinations; error bars depict standard errors.

Cell density was adjusted to the desired concentration (which was 1×10^5 cells/mL in this experiment). The cell count was taken in triplicate at 0, 4, 8, 12 and 24 h for each concentration. From Figure 4.10, the AS-HK014 compound clearly showed an effect on the cell survival of *T. b. brucei*-WT at 0.5 μM , and the growth curve was steady for 24 h, whereas no growth was observed at 1 μM after 4 h. For the TA014 resistance line, there was no effect for AS-HK014 at 0.5 and 1 μM at 24 h, and there was no significant difference between these concentrations and the drug-free control.

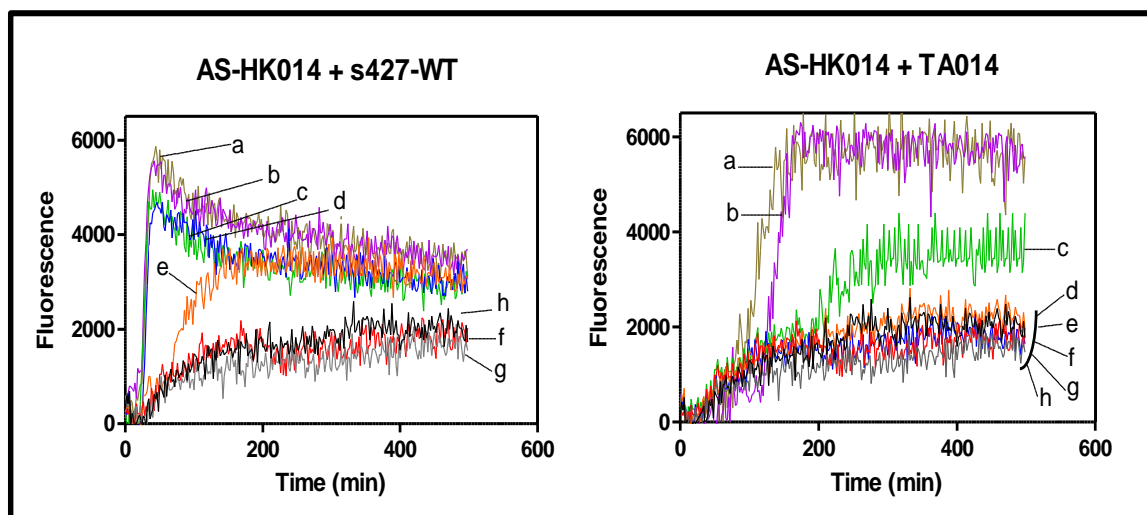


Figure 4.11. Dose response curve of the AS-HK014 compound for bloodstream-form *T. b. brucei* and TA014 resistance line. The different concentrations were incubated with and without parasites in HMI-9 medium which has 10% FCS at 37 °C with 5% CO₂. The drug was tested at 50 µM (a), 25 µM (b), 6.25 µM (c), 1.56 µM (d), 0.78 µM (e), 0.39 µM (f), 0.19 µM (g) and drug free (h) conditions. Propidium iodide was added at 9 µM, and the fluorescence was measurement over 8 h at 544 nm excitation and 620 nm emission. Separate traces were recorded in the absence of cells and were subtracted from those presented in the figures.

Finally, monitoring the speed of action of the test compound on trypanosomes in real time is important. Cells become fluorescent as propidium iodide enters the cells and binds to nucleic acids. This binding occurs only upon breach of the plasma membrane, i.e. loss of cellular integrity. AS-HK014 rapidly killed WT trypanosomes at concentrations >1.56 µM (approximately 30 min). At 0.78 µM the cells started to die after 60 min. By contrast, for the TA014 strain, the compound killed the cells after 2 h at concentrations > 25 µM (Figure 4.11).

Consequently, according to previous results on cellular parameters, 0.75 µM of the AS-H014 compounds was selected for further mechanism of action studies in both cell lines at an incubation time of 30 min.

4.9.2 Metabolism of curcumin AS-HK014 in trypanosome: possible reactions with glutathione

This section utilises untargeted metabolomics to assess the impact of AS-HK014 treatment on trypanosomes. In untargeted metabolomics there is no a priori assumption on a mechanism of action and the entire metabolome is analysed to

the limit of the technology. We directly compared metabolic changes between WT and TA014 of trypanosomes. It was immediately obvious from a global overview of most-changed metabolites that AS-HK014 impacted particularly on intracellular thiol levels (Figure 4.12), with trypanothione content down by >99% and glutathione and S-glutathionyl-L-cysteine levels reduced by >90% in AS-HK014-treated WT cells. In the subsequent metabolomic analyses described below the cellular levels of the relevant thiols (cysteine, glutathione and trypanothione) were determined by a modification of the monobromobimane method (Fahey & Newton, 1983; Fairlamb *et al.*, 1987). This method can derivatise intracellular sulfhydryls, to prevent their oxidation and allow detection of both oxidised and reduced forms of intracellular thiols.

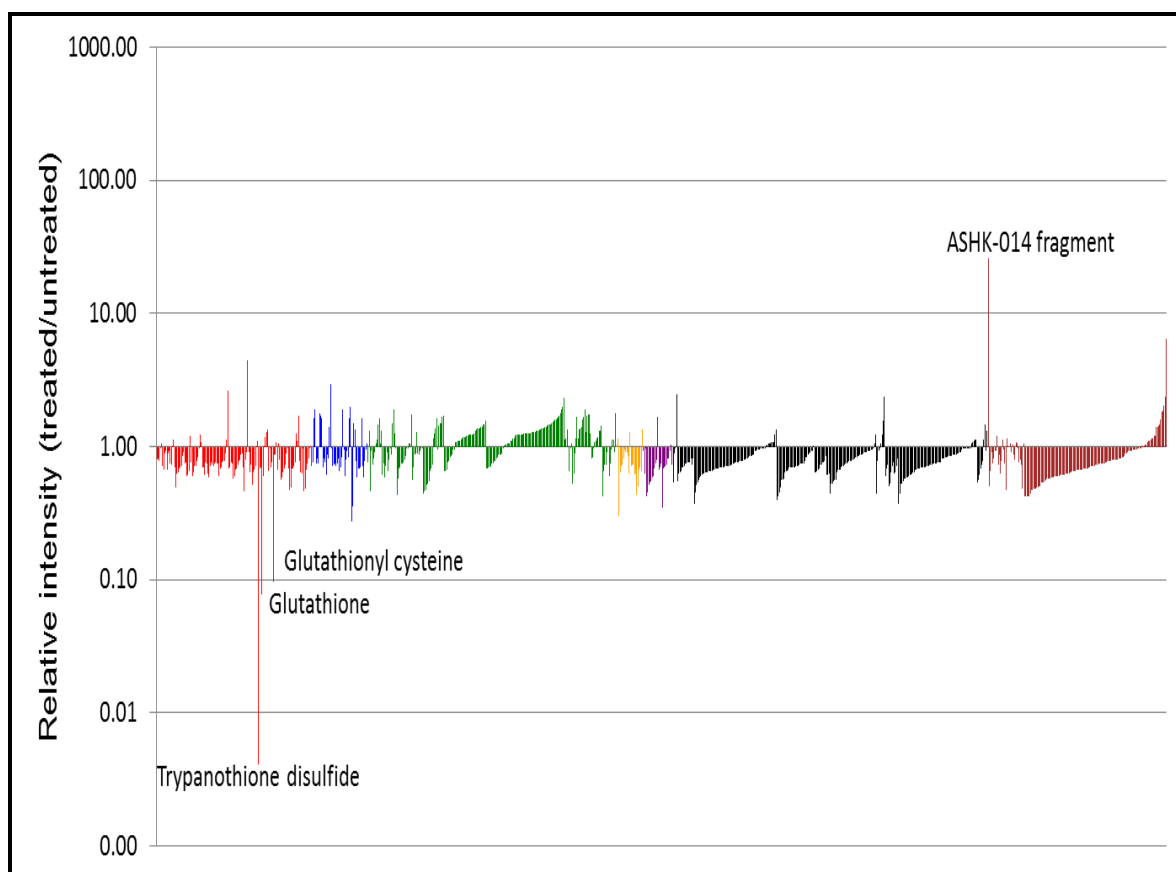


Figure 4.12. Relative abundance of 915 putative metabolites from cells treated with ASHK-014 relative to untreated cells. Untargeted metabolomics was conducted with LC-MS, metabolite abundance is measured by raw peak height and putative identification was based on accurate mass. Metabolites are grouped by metabolic pathways where red = amino acid metabolism, blue = carbohydrate metabolism, green = lipid metabolism, orange = metabolism of cofactors and vitamins, purple = nucleotide metabolism, black = peptides and brown = unknown pathways.

The relevant pathway (depicted in Fig 4.13) starts with the biosynthesis of glutathione from three amino acids: cysteine, glutamate and glycine. Two molecules of glutathione are then coupled consecutively to spermidine to form trypanothione, the main trypanosomal thiol.

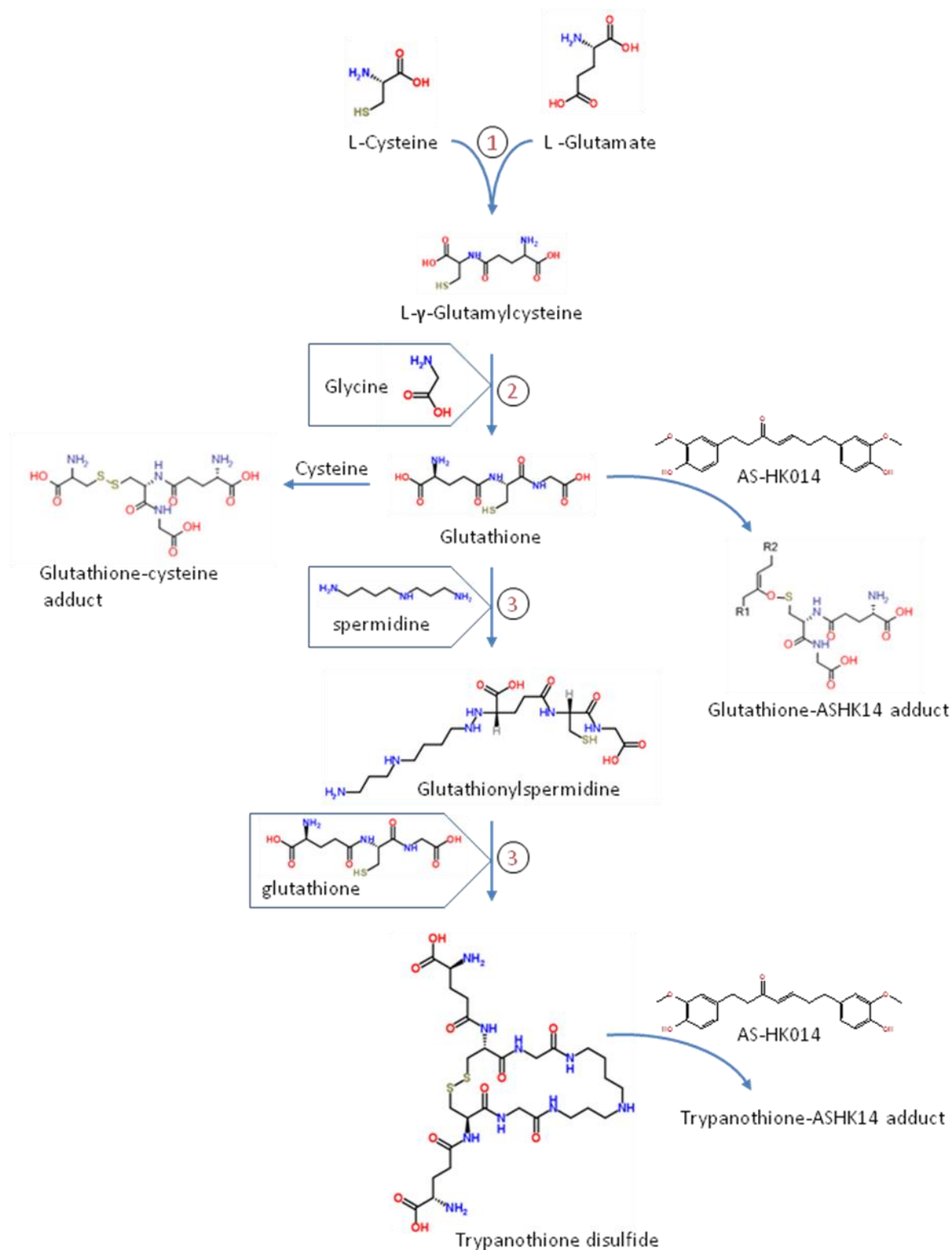


Figure 4.13. Trypanothione pathway. 1- Gamma glutamylcysteine synthetase, 2- Glutathione synthetase, 3- Trypanothione synthetase

In WT trypanosomes, treatment with just 0.75 μM of AS-HK014 for 30 min led to very clear reductions in thiol levels (Figure 4.14). Trypanothione levels, both in reduced form (detected as di-monobromobimane adduct (di-mBBr)) and as disulfide, were dramatically reduced under these conditions (to $12 \pm 3\%$ ($P < 0.01$) and $6 \pm 2\%$ ($P < 0.001$), respectively). Similar reductions in glutathione mBBr ($P < 0.01$), S-glutathionyl-L-cysteine ($P < 0.02$) and glutathionylspermidine mBBr ($P < 0.01$) were also observed, opening the strong possibility that biosynthesis of trypanothione was inhibited due to a depletion of glutathione. Further upstream, there was a slight but significant ($P < 0.05$) reduction in levels of L-cysteine mBBr and of glycine, but there was no change in glutamate levels (Figure 4.14). All three of these amino acids are present at high levels in the HMI-9 culture medium so any changes might be difficult to unearth with the conditions used. In addition, the pathway leading up to spermidine (Figure 4.15) was analysed. There was no change in spermidine levels upon treatment with AS-HK014, nor in any of the metabolites of its biosynthesis pathway: ornithine, S-adenosyl methionine and putrescine (Figure 4.14). Furthermore, there was no significant change in the level of 5'-methylthioadenosine (data not shown), the reaction product after the aminopropyl donation by S-AdoMet in the synthesis of spermidine.

The above shows that the only metabolomic perturbations upon incubation with AS-HK014 were the dramatically reduced levels of thiols, whereas the constituent metabolites in their biosynthetic pathways displayed at most very minor changes. This contrasts with treatment of the same trypanosome strain with the inhibitor of ornithyl decarboxylase, eflornithine, which resulted in rapid changes in intracellular levels of putrescine, ornithine (and both of their acetylated forms) and 5'-thioadenosine metabolites (Vincent *et al.*, 2012).

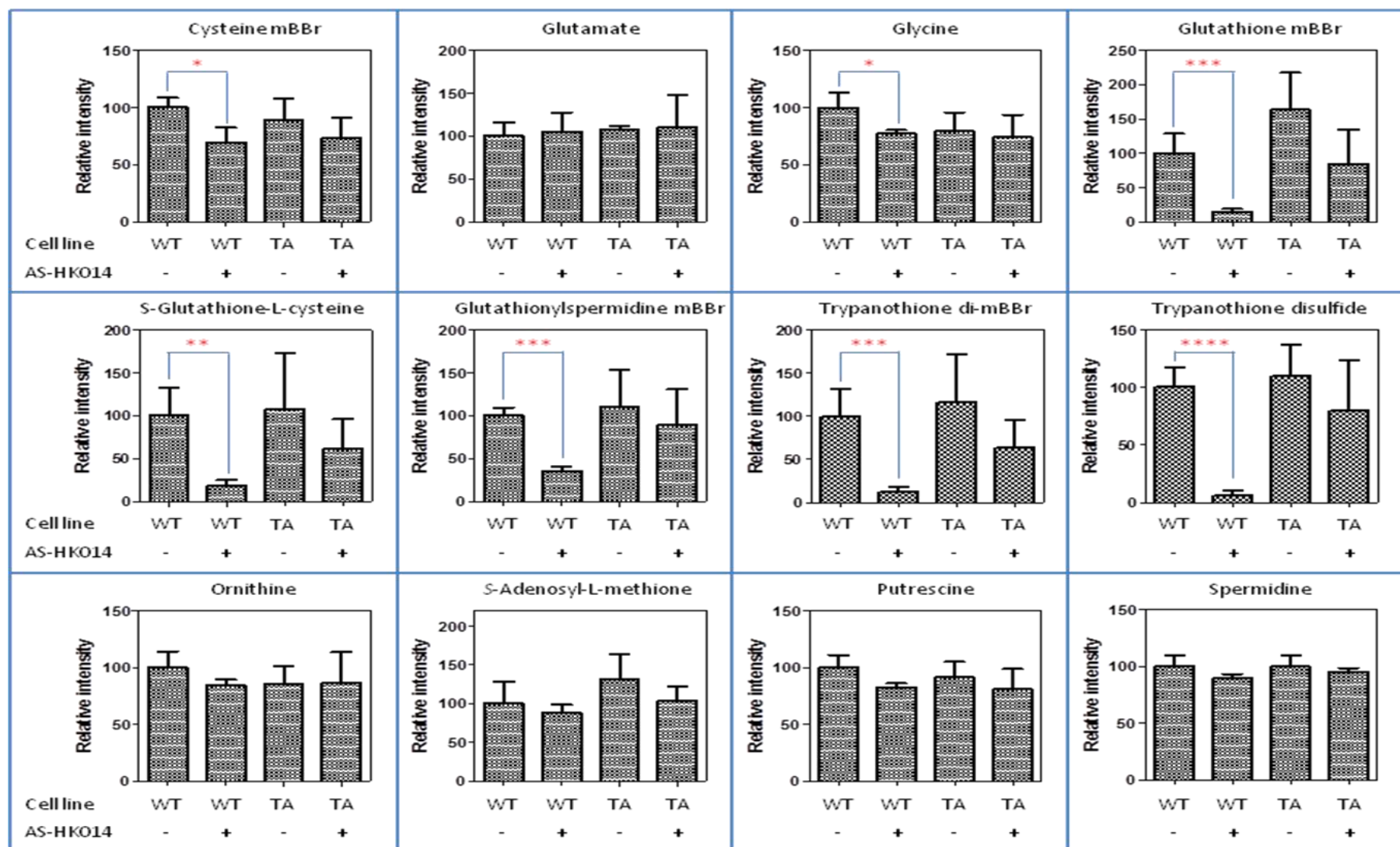


Figure 4.14. Metabolomic analysis of the AS-HK014 compound in the *T. b. brucei*-WT and TA014 resistance line cell extracts. For each cell sample, 25 mL of cell culture (2×10^6 cells/mL) was incubated for 30 min at 37 °C with and without AS-HK014 (0.75 μ M) for both strains. * $P < 0.05$, ** $P < 0.02$, *** $P < 0.01$, **** $P < 0.001$.

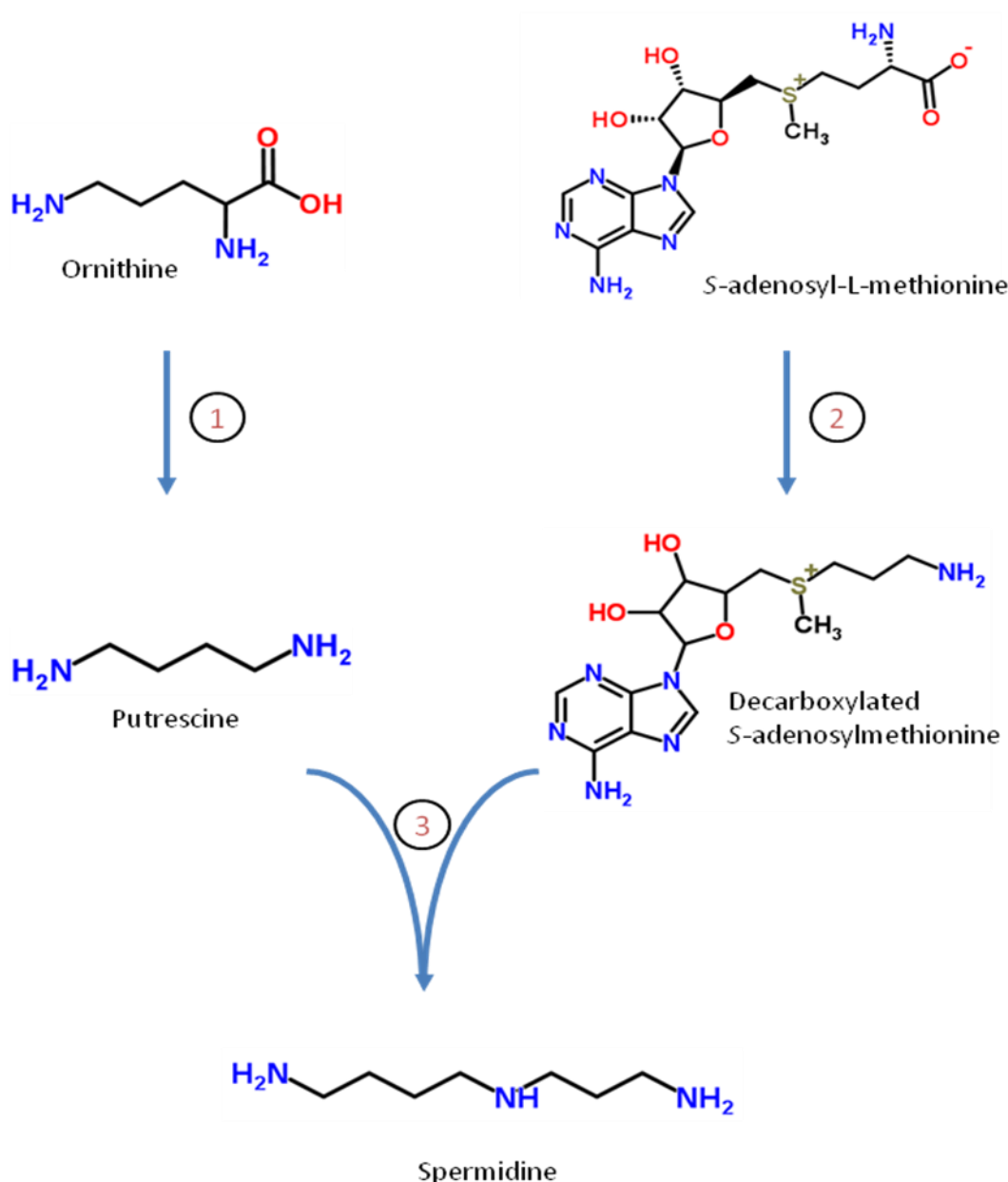


Figure 4.15. Spermidine pathway, 1- Ornithine decarboxylase, 2- S-adenosylmethionine decarboxylase, 3- Spermidine synthase.

One explanation for the rapid depletion of thiols would be the reaction with AS-HK014 to form a stable adduct. This type of mechanism has been proposed for melarsoprol which forms the trypanothione adduct MelT (Fairlamb *et al.*, 1989), which in turn inhibits trypanothione reductase (Cunningham *et al.*, 1994). MelT can be exported from the cells by ABC transporters (Shahi *et al.*, 2002), although, unlike ASHK-014, melarsoprol treatment does not significantly decrease cellular trypanothione concentration (Fairlamb *et al.*, 1992), presumably because it is used at a much lower concentration than AS-HK014.

Stable adducts were indeed found in AS-HK014-exposed trypanosomes, both with trypanothione and glutathione (Figure 4.16). However, the adducts were observed not only in cells exposed to AS-HK014 for the 'standard' 30 min at 37 °C, but also when AS-HK014 was added after 30 min drug-free incubation, after the cells had been rapidly cooled to 4 °C in a dry-ice/ethanol bath; these cells were then immediately processed for metabolite extraction (quenched cells). Indeed, the levels of adduct were almost identical in the incubated and in the quenched cells, showing clearly that the AS-HK014 reaction with thiols is a rapid chemical reaction with free thiols, rather than an enzymatic reaction.

Thus, we conclude that AS-HK014 undergoes a rapid chemical reaction with reactive intracellular thiols, particularly glutathione and trypanothione, effectively depleting these essential thiols and leading to cell death. It is possible that the compound furthermore reacts with additional thiols, perhaps in proteins, leading to irreversible inhibition of the function of these proteins. As curcuminoids are most likely able to efficiently diffuse into the cells (AS-HK014 has a cLogP of 3.84; ChemDraw Pro 10.0, CambridgeSoft), it is highly likely that uptake is driven by the reaction and continues until thiol content is effectively depleted. It might thus be expected that the ASHK-014 adducts would accumulate to a very high level. To the contrary, adduct levels were not greater than those obtained from unexposed, quenched cells (Figure 4.16), which did not exhibit significant thiol depletion (data not shown). This suggests that the adducts may undergo metabolic degradation, or be released from the cell through ABC transporters, much like the trypanothione-melarsoprol adduct MeIT. The metabolomics data does not provide any direct evidence for either pathway, as no novel metabolite signals were specifically enriched in cells exposed to drug for 30 minutes, and no adduct peaks were detected in the spent medium. However, it is possible that the latter metabolites fall below the limit of detection after dilution in the extracellular medium. As an alternative to thiol depletion directly by chemical reaction with AS-HK014, the depletion could be explained by inhibition of glutathione synthesis, but it is unlikely that this mechanism would cause such a dramatic effect on the total thiol pool within 30 minutes.

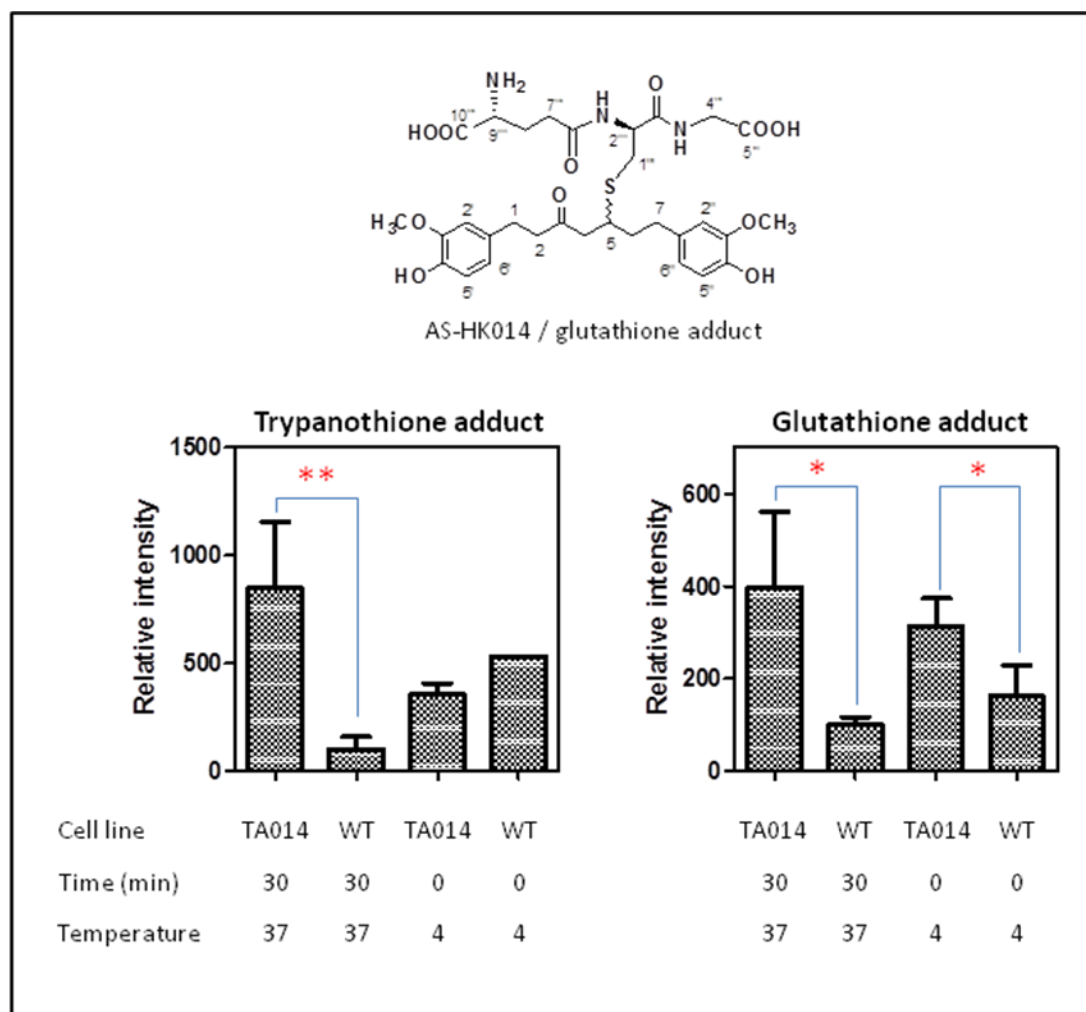


Figure 4.16. Adduct levels of Trypanothione and Glutathione, *P<0.05, **P<0.02

The entire metabolomic analysis was performed in parallel with the AS-HK014-resistant line TA014 as well. The same trend on thiol levels as in WT *T. b. brucei* was apparent (Figure 4.14), but none of the reductions in thiol concentrations reached significance under the assay conditions of 0.75 μ M for 30 minutes - consistent with the lack of impact that this concentration has on the TA014 cells. More interesting was that the levels of thiols, polyamines, relevant amino acids and 5'-thioadenosine metabolites were all statistically identical in unexposed WT, unexposed TA014 and AS-HK014 exposed TA014 cells (Figure 4.14). This shows that the resistance adaptation was not the result of significantly higher cellular levels of trypanothione and/or glutathione. Nor was AS-HK014 prevented from entering the cells (loss of import transporter or expression of export transporter), as AS-HK014 (detected intact or as a $C_{10}H_{10}O_2$ MS-generated fragment) levels were equivalent in both wild-type and resistant cells (Figure 4.17). Furthermore, much higher levels of glutathione ($P<0.05$) and trypanothione ($P<0.02$) adducts were found in AS-HK014 exposed TA014 cells than in WT trypanosomes (Figure 4.16), possibly reflecting the higher thiol levels

present in the exposed TA014 cells. This observation provides strong confirmation that it is not the adduct that is deleterious to the cells and is consistent with the diffusion model of AS-HK014 uptake. Yet, in the resistant cells, the thiol depletion is minimal, indicating an increased synthetic capacity that allows the cells to maintain their glutathione and trypanothione levels in the presence of the drug.

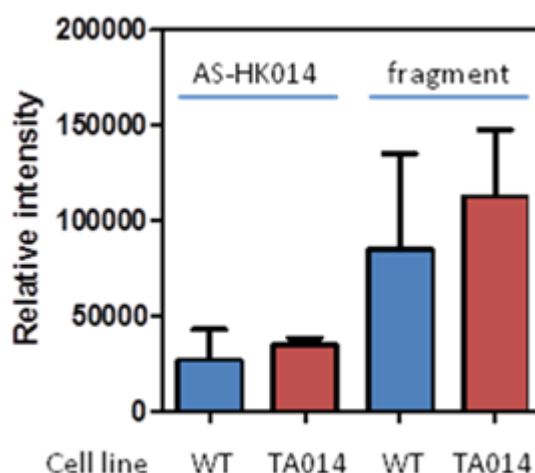


Figure 4.17. Levels of AS-HK014 in WT s427 and TA014 trypanosomes as determined in a metabolomic experiment performed without mBBR treatment. Incubation was with 0.75 μ M AS-HK014 for 30 minutes at 37 °C. Data shown are the average of triplicate determinations within a single experiment. Error bars are Standard Errors. There were no significant differences between the cell lines ($P>0.05$). Experiments analysed after extraction in the presence of mBBR showed essentially similar results but with much lower relative intensities (not shown).

4.10 Analysis of the protein expression levels of glutathione synthetase and γ -glutamylcysteine synthetase in wild-type and TA014 trypanosomes

The metabolomic analysis to determine the effect of AS-HK014 on two strains of trypanosomes as described in Section 4.9.2 showed a clear difference in glutathione and trypanothione levels between the strains and presented a possible explanation for this difference. Two enzymes are involved in glutathione synthesis: γ -glutamylcysteine synthetase (γ -GCS) and glutathione synthetase (GS). Therefore, western blotting was used to analyse the protein expression of these two enzymes. Primary antibody (either with rabbit polyclonal anti-gamma GCS antibody or with rabbit polyclonal anti-GS; both

antibodies were obtained from Professor Margaret Phillips, University of Texas Southwestern Medical Center) was used to measure the protein expression level. For both strains, 1×10^6 cells/mL were treated with $0.75 \mu\text{M}$ of AS-HK014 for 30 min, with untreated cells incubated in parallel serving as controls, and their extracts were used to run the gel and subsequent western blot. The results showed that there was no difference between the treated and the untreated cells, and the level of expression was almost the same in both strains for both enzymes (Figure 4.18).

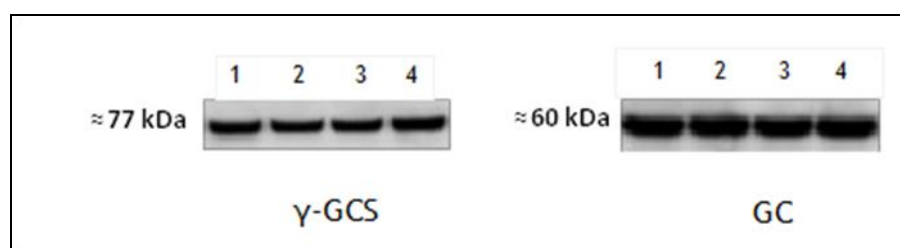


Figure 4.18. Western blot of the *T. b. brucei*-WT and TA014 resistance lines at 1×10^6 cells/mL. The cells were incubated for 30 min in the presence or absence of $0.75 \mu\text{M}$ of AS-HK014 and. Two antibodies were used for both strains: $\gamma\text{-GCS}$ and GS. (1) *T. b. b.* WT, drug free, (2) *T. b. b.* WT + AS-HK014, (3) TA014, drug free, (4) TA014 + AS-HK014.

4.11 Identification of Tb427.10.12370 and Tb427.07.4000 genes

As mentioned previously, two genes are involved in glutathione synthesis: Tb427.10.12370 ($\gamma\text{-GCS}$) and Tb427.07.4000 (GS). Although the protein level of $\gamma\text{-GCS}$ and GS was shown not to be different in WT and TA014 trypanosomes (Section 4.10) the possibility of functional mutations in the coding regions of the genes also needed to be explored as an explanation for the difference in AS0HK014 sensitivity. The amplification and cloning of these genes from WT and TA014 strains, and their sequence analysis, is reported in this section.

4.11.1 Polymerase chain reaction

Polymerase chain reaction (PCR) was used to verify the presence of both genes in trypanosome wild-type and resistance lines. Forward and reverse PCR primers were designed, and Go Taq polymerase was used as described in Chapter 2. PCR products were run on 1% agarose gel to observe the PCR products (Figure 4.19). Bands of the expected size were amplified from both strains.

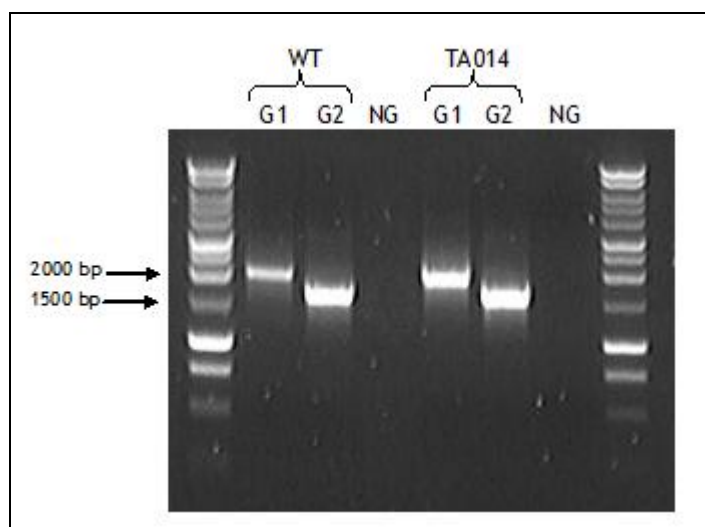


Figure 4.19. PCR amplification of G1 (γ -GCS) and G2 (GS) for both strains of bloodstream-form *T. b. b.* WT and TA014 resistance line, NG: negative control which consists of all PCR components except genomic DNA.

4.11.2 Sequence analysis

As mentioned in Chapter 2, several steps must be performed before sending the plasmid DNA of multiple bacterial colonies for sequencing, namely, PCR, extraction of gel, A-overhang of PCR product, ligation into the pGEM-TEasy Vector, transformation of competent *Escherichia coli* and purification of plasmid DNA from individual *E. coli* colonies. For the analysis of the γ -GCS and GS ORFs, band of the correct size, from three independent PCR reactions, were extracted from their gels, cloned in to pGEM-TEasy and amplified in *E. coli*. For each gene, nine colonies were sent for sequencing. The data received from Eurofins was analysed using CLC Genomics Workbench 4.8 software to form the full open reading frame (ORF) for both genes in both strains.

The sequencing for γ -GCS from the wild-type and TA014 strains (see Appendix F & E) were not very different from each other, with the differences found in TA014 following the treatments found also in the wild-type strain. One notable difference was that at base-pair 187 of the ORF the base was Adenine in four out of nine colonies in both cell lines, and Guanine in the other five colonies.

For GC, also there were only two notable changes. First, at base-pair 1568 of the ORF, seven out of nine colonies in the TA014 had a Cytosine while the other two have Adenine, whereas only one out of nine colonies had Cytosine in the wild-type. Second, at the same at base-pair 931, four out nine colonies in the TA014 had Cytosine and the others Adenine, while only one had Cytosine in the wild-type.

4.1 Discussion

The potential mechanism of action of curcumin analogues is explored in this study. As mentioned in the Introduction (Section 4.1), curcumin analogues are used against *T. b. brucei* bloodstream form (Changtam, 2010), some of which have potent antiparasitic activity and low toxicity, such as AS-HK014 (mono-enone linker). An early study by my colleague Hasan Ibrahim (Ibrahim, 2009) investigated the mechanism of action of curcumin compounds and did not confirm specific effects: for example, there was no effect on cell cycle, mitochondrial membrane potential or levels of reactive oxygen species for the *T. b. brucei* bloodstream form.

Curcumin analogues have rapid effects on parasite cells, so cellular parameters were investigated to elucidate the mechanism of action of curcumin compounds on *T. b. brucei* bloodstream form. We found no effects on signal transduction (intracellular calcium, cAMP, membrane potential) for curcumin compound or AS-HK014.

On the other hand, in early work also by Ibrahim, toxicological and pharmacological results on glutathione (GSH) content in rat hepatocytes treated with different curcumin compounds showed no significant effect of curcumin and its close analogue AS-HK009, whereas there was a significantly reduced GSH content when treated with the enone AS-HK014. This result indicates that AS-HK014 leads to a depletion of GSH. Furthermore, it was observed that co-incubation of curcumin and AS-HK014 compounds with different concentrations of L-glutathione led to decreased activity of AS-HK014 (Figure 4.4), while no change in the activity of curcumin compound was observed. It was shown that AS-HK014 but not curcumin reacts with glutathione to form an adduct in a chemical, non-enzymatic reaction.

As part of the effort to understand the mechanism of action, trypanosome cultures were long-term exposed to increasing concentrations of curcumin or AS-HK014 in order to induce resistance. After 11 months of exposure, a resistant line was obtained for AS-HK014, but not for curcumin (Figure 4.6). In view of the chemical structure for both compounds, the di-keto linker of curcumin (AS-

HK001) is fairly unreactive, making the compound quite stable in a biological environment. In contrast, the mono-enone linker of AS-HK014 is much more reactive, and indeed was shown to be instrumental in forming the adduct with glutathione, making it highly likely that this group is responsible for the much higher activity of this compound, compared to curcumin, and by a different mechanism of action from that of AS-HK001. For the purpose of this thesis, resistance is used as a statistically significant reduction *in vitro* susceptibility to the drug under investigation. However, a more useful definition would be that resistance is the lack of effect of a clinical dosage of treatment on the pathogen *in vivo*, due to genetic adaptations by the pathogen.

The study of cross-resistance for TA014 resistance lines with different curcumin analogues and trypanosomiasis chemotherapies appeared to show that although the TA014 line did not display cross-resistance with different trypanosomiasis chemotherapies such as pentamidine, suramin and nifurtimox, there was a significant loss of sensitivity for some curcumin compounds. Specifically, there was cross-resistance for curcumin analogues with a mono-enone linker such as AS-HK018, AS-HK093, AS-HK096 and AS-HK097 (Table 4.1). Certainly, this seems to show that the TA014 resistance line is resistant to the mono-enone moiety, and also confirm that this linker has responsibility for drug activity. Additionally, repeat testing for the activity of AS-HK014 on wild-type and TA014 resistance line cells with the inclusion of glutathione in the growth medium led, as mentioned, to a drop of EC_{50} of AS-HK014 in wild-type cells, but glutathione caused no significant change in AS-HK014 sensitivity for resistant line TA014 (Figure 4.8).

These data led to the testing of the effect of the AS-HK014 compound on the metabolome of wild-type and resistant cell lines. Parasites incubated with 0.75 μ M for 30 minutes contained a much-reduced level of glutathione, trypanothione and trypanothione disulfide for the wild-type (7, 9 and 17-fold respectively) but no significant changes in thiol levels were observed in resistant cells. That appears to support our hypothesis that AS-HK014 reacts with glutathione to form an adduct and cause depletion of GSH. This situation is reminiscent of the report by Yarlett et al (Yarlett *et al.*, 1991), which describes how arsenicals rapidly deplete *Trypanosoma brucei rhodesiense* of trypanothione, but not in resistant lines during 30 minutes of incubation time. This result was confirmed (Section

4.8) when curcumin AS-HK014 was found to produce a chemical adduct with glutathione, both as a controlled reaction in ethanol, or under standard culture conditions and in the presence of WT *T. b. brucei*. Moreover, it has been reported that glutathione can form adducts with a number of other compounds (Kang *et al.*, 2007; Naylor *et al.*, 1988; Stock *et al.*, 1986).

To study the adaptation change which led to resistance, analysis of protein expression and sequence analysis was performed for Tb427 WT and resistant lines to identify any change in the activity of the two genes (γ -GCS and GS). Analysis of glutathione synthetase (GS) and γ -glutamylcysteine synthetase (γ GCS) protein levels by Western blot showed no change in resistant trypanosomes, in the presence or absence of drug challenge. Neither were mutations found in the GS and γ GCS open reading frames. This is consistent with the absence of any significant changes in thiols or glutathione biosynthesis metabolites between unchallenged WT and TA014 trypanosome cultures.

The nature of reduced AS-HK014 susceptibility in TA014 was clearly linked to the prevention of thiol depletion, as the same 30 minute exposure had only minor effects (not significant) on cellular thiol levels. However, no detectable increase in γ -GCS or GS expression was detected using Western blotting, nor were any potentially activating mutations found in these enzymes, and no increases were found in steady state levels of relevant metabolites in TA014 cells. This seems to rule out any significant increase in trypanothione production as the resistance mechanism. Furthermore, the same level of a fragment of AS-HK014 was detected in the metabolome of WT and TA014 strains, giving no indication of reduced uptake. Nor have we found clear evidence of segregation of AS-HK014 in the resistant cells, as the level of AS-HK014 adduct with trypanothione and with glutathione was 8.5 and 4-fold higher in resistant cells, probably reflecting the high thiol levels in these cells as compared to similarly exposed WT cells. It therefore remains unclear by which mechanism the TA014 trypanosomes prevent the rapid depletion of thiols.

It can be concluded that AS-HK014 forms an adduct with glutathione and trypanothione which leads AS-HK014 to rapid depletion of trypanothione in trypanosomes, and that this does not happen in resistant *T. brucei*. The rapid death of trypanosomes exposed to AS-HK014 correlates with thiol depletion,

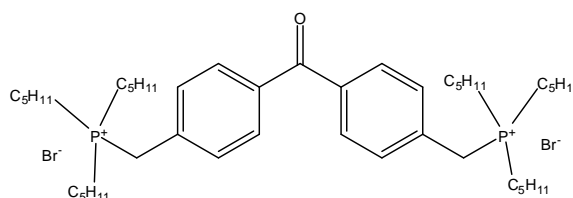
which is a different mechanism of action from that of the parent compound curcumin.

5 CHAPTER Five: Phosphonium salts compounds as novel trypanocidel agents

5.1 Introduction

In 1979, Kinnamon (Kinnamon *et al.*, 1979) reported the potent antitrypanosomal activity of benzyltriphenylphosphonium salts against *T. brucei*, and mentioned that a few of these compounds were usable in the murine model of *T. b. rhodesiense* infection. Despite this major discovery, for the past 30 years, further evaluation of the phosphonium salts with regard to their antiprotozoal properties has been discontinued both due to lack of experience and scarcity of information and guidance on this topic.

Recently, the salt derivatives of benzophenone-derived bisphosphonium have been synthesised, which has reopened the research on phosphonium salts having anti parasitic properties. The benzophenone-derived bisphosphonium salt derivatives produced a strong antileishmanial activity *in vitro* (Luque-Ortega *et al.*, 2010). The most potent activity against *Leishmania* spp was found to be exhibited by 4,4'-bis((tri-n-pentylphosphonium) methyl) benzophenonedibromide). This compound inhibited complex II of the mitochondrial respiratory chain.



As some of the anti-leishmanial compounds also displayed promising trypanocidal activity (Dardonville & Brun, 2004) 60 new variable phosphonium derivatives were prepared in order to systematically examine the structure-activity relationship for *Trypanosoma* spp. This investigation included variations in (a) linker type, (b) linker length, (c) number of cations, (d) nature of the counterion, and (e) nature of the phosphonium groups substituents R_1 , R_2 , R_3 (Chart 1).

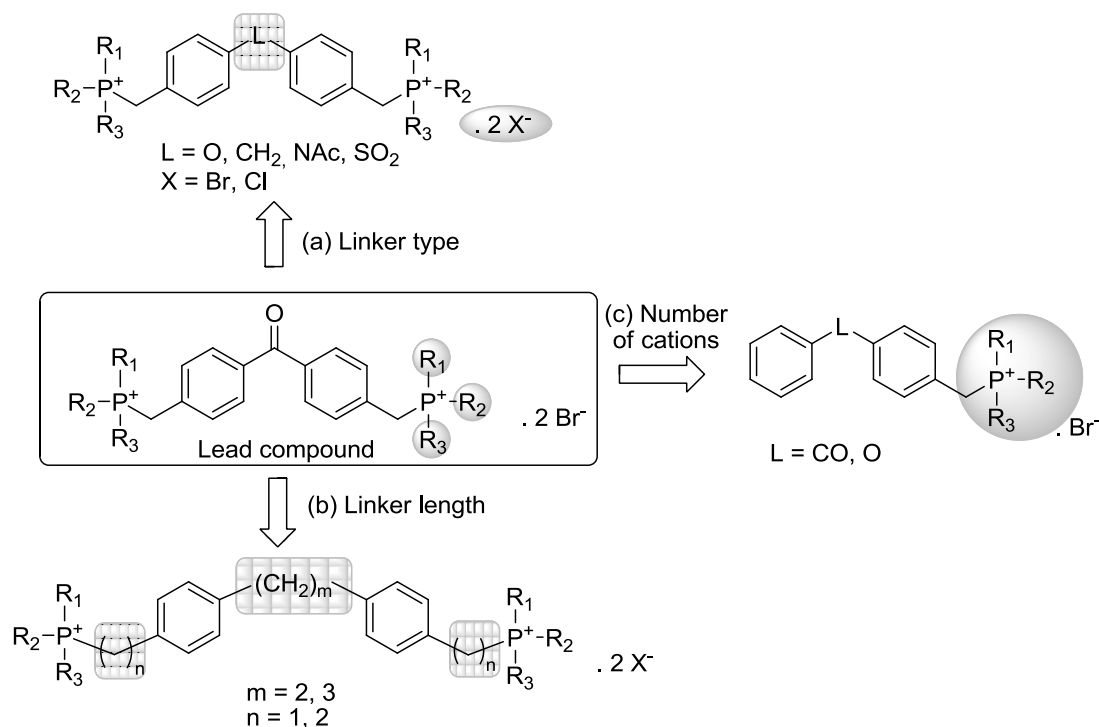


Figure 5.1. General structure of benzophenone-derived bisphosphonium salt derivatives with antileishmanial and antitrypanosomal activity (Luque-Ortega *et al.*, 2010) and the new series being studied (Chart reproduced from Taladriz *et al.*, 2012).

The following parameters were obtained for these compounds: (1) EC_{50} value against *T. b. brucei*; (2) assessment of cross-resistance with current trypanocides; (3) toxicity to human cells; (4) dynamics of trypanosomal action (trypanocidal or trypanostatic); (5) speed of the effects on trypanosomal proliferation and viability; and (6) minimum time of exposure. Finally, an analysis of the structure activity relationship (SAR) was performed.

Much of the content of this chapter has already been published as (Taladriz *et al.*, 2012).

5.2 Assessment of the activity of phosphonium compounds on wild-type and multi-drug resistant trypanosome lines; determination of in vitro therapeutic index

The antiparasitic effects of phosphonium analogues were investigated using the *in vitro* Alamar blue viability assay. In addition, resistant strains were used as a model to investigate the cross-resistance between the existing treatments and potential new trypanocides. Any new trypanocidal drugs to be developed, whether for human or veterinary use, should at a minimum not be cross-resistant with the current diamidine and arsenic-based drugs. The toxic effect of phosphonium compounds on HEK cells was evaluated using Alamar blue to determine the level of toxicity to human cells.

5.2.1 In vitro activity on *T. b. brucei* bloodstream form

83 compounds were obtained from Dr Christophe Dardonville (Instituto de Química Médica, Madrid, Spain) and tested for their effect on the *Trypanosoma brucei brucei* bloodstream form using the Alamar blue method (Raz *et al.*, 1997). All experiments were performed at least three times for each compound, including two positive controls, pentamidine and diminazene, plus drug-free incubations as negative controls in each experiment. Fluorescence intensity was plotted to a sigmoid curve equation using GraphPad Prism 4 software to plot the data and to determine the EC₅₀ values.

The Alamar Blue results demonstrated a strong trypanocidal activity of the phosphonium compounds against the wild-type s427 bloodstream forms, and the majority of these compounds displayed an EC₅₀ of less than 1 µM. In addition, 19 of 83 compounds displayed EC₅₀ values <100 nM. Among the bisphosphonium compounds the most potent activity was displayed by AH117 and EFp127, with EC₅₀ values of 24 and 29 nM, respectively. However, some monophosphonium compounds displayed even higher levels of activity, with AT31 and AT33 displaying EC₅₀ values of 11 and 15 nM, respectively. Moreover, 22 compounds

were more active than the standard veterinary drug diminazene, showing that this class of compounds has highly promising anti-protozoal activity (Table 5.1).

Compound	WT-s427 EC ₅₀ (μM)	TbAT1-KO EC ₅₀ (μM)	Resistance Factor -KO	TbAT1-B48 EC ₅₀ (μM)	Resistance Factor -B48	HEK cells EC ₅₀ (μM)	Selectivity Index
CD38	0.204±0.005	0.17±0.01	0.83	0.18±0.01	0.87	68.7±4.9	336
CDIV20	0.24±0.07	0.36±0.07	1.51	0.38±0.06	1.59	>300	>1250
CDIV22	>100	>100	ND	>100	ND	ND	ND
CDIV23	19.7±4.1	27.15±3.8	1.38	31.3±4.1	1.6	ND	ND
CDIV24	20.5±5.2	33.4±6.2	1.63	38.8±6.4	1.9	ND	ND
CDIV25	2.62±0.7	8.34±3.08	3.18	6.30±1.4	2.4	>300	>114.5
CDIV26	8.6±2.14	17.75±2.03	2.07	15.17±3.7	1.7	>300	>34.9
CDIV27	0.70±0.24	1.43±0.41	2.03	1.33±0.26	1.9	>300	>428.5
CDIV28	1.53±0.38	2.08±0.63	1.36	2.05±0.38	1.34	>300	>196
CDIV29	19.17±7.17	28.77±5.62	1.50	24.55±4.8	1.3	ND	ND
CDIV31	>100	>100	ND	>100	ND	ND	ND
CDIV33	0.14±0.03	0.23±0.05	1.63	0.25±0.04	1.8	>300	>2142
CDIV34	0.97±0.27	2.10±0.54	2.16	1.76±0.3	1.8	>300	>309
CDIV35	0.48±0.11	1.32±0.46	2.73	1.63±0.46	3.4	>300	>625
CDIV48	0.042±0.002	0.06±0.001	1.44	0.045±0.001	1	26.7±1.52	637
CDIV49	36.9±1.2	33.8±1.2	0.92	21.7±1.2	0.6	ND	ND
CDIV50	0.20±0.01	0.24±0.03	1.22	0.22±0.02	1.13	213.2±8.6	1065
CDIV52	0.18±0.002	0.18±0.01	1.01	0.18±0.00	1	272±33	1511
CDIV53	0.24±0.03	0.26±0.04	1.11	0.29±0.03	1.25	>300	>1250
CDIV57	0.33±0.10	0.52±0.03	1.57	0.32±0.09	0.96	273.03±34.7	827
AHI04	7.22±0.15	6.5±0.4	0.9	6.15±0.9	0.85	>300	>41

AHI05	5.45±1.09	4.6±0.8	0.84	3.84±1.2	0.7	>300	>55
AHI07	0.59±0.06	0.8±0.10	1.35	1.06±0.34	1.8	>300	>508
AHI08	0.7±0.03	0.88±0.10	1.26	0.88±0.06	1.26	>300	>430
AHI09	0.082±0.01	0.08±0.00	0.94	0.064±0.01	0.77	239.4±8.62	>2900
AHI10	0.24±0.04	0.19±0.03	0.80	0.18±0.02	0.75	>300	>1250
AHI15	0.037±0.004	0.045±0.005	1.21	0.04±0.002	1.1	21.87±0.87	590
AHI16	0.033±0.006	0.033±0.005	1	0.04±0.002	1.2	18.09±2.6	550
AHI17	0.024±0.005	0.025±0.004	1.04	0.02±0.001	0.87	85.2±6.62	3550
AHI18	0.08±0.002	0.08±0.003	1.0	0.074±0.001	0.9	231.57±14	2900
AHI19	0.16±0.011	0.14±0.01	0.88	0.13±0.002	0.8	112.7±15	710
AHI20	0.135±0.017	0.17±0.04	1.26	0.14±0.014	1	161.5±17.4	1200
AHI21	0.056±0.011	0.057±0.008	1.01	0.045±0.004	0.8	140.1±6	2500
AHI22	0.080±0.004	0.074±0.003	0.92	0.066±0.002	0.8	203±13.5	2530
AHI30	0.23±0.014	0.25±0.002	1.11	0.27±0.008	1.2	>300	>1310
AHI40	16.65±0.5	13.57±2.22	0.81	13.3±1.55	0.8	ND	ND
AHI43	0.322±0.012	0.30±0.009	0.94	0.3±0.009	0.9	>300	>930
EFpl1	0.29±0.06	0.41±0.01	1.4	0.31±0.04	1.1	>300	>1040
EFpl2	1.08±0.21	1.37±0.02	1.26	1.08±0.19	1	63.18±7.66	58.5
EFpl3	0.856±0.30	2.10±0.03	2.47	1.16±0.22	1.35	>300	>350
EFpl4	0.35±0.12	0.52±0.02	1.5	0.27±0.07	0.8	172.27±6.9	493
EFI11	0.128±0.03	0.16±0.01	1.25	0.09±0.028	0.7	131.27±16.94	1025
EFpl6	0.286±0.06	0.32±0.02	1.14	0.207±0.074	0.7	106.65±16.05	372
EFpl7	0.106±0.04	0.18±0.01	1.7	0.093±0.041	0.9	141±9.33	1330
EFpl8	0.916±0.18	1.02±0.02	1.13	1.26±0.3	1.3	>300	>327

EFpl10	0.197±0.07	0.34±0.00	1.8	0.19±0.068	1	91.47±4.57	464.3
EFpl27	0.029 ± 0.005	0.049 ± 0.007	1.7	0.053 ± 0.003	1.8	25.8 ± 1.7	897
EFpl28	0.15 ± 0.06	0.15 ± 0.02	1.0	0.15 ± 0.06	1.0	32.4 ± 2.4	213
EFpl32	1.27 ±0.33	1.37 ± 0.11	1.1	1.09 ± 0.38	0.9	>300	>230
EFpl33	2.59 ± 0.64	2.62 ± 0.16	1.0	1.8 ± 0.58	0.5	>300	>110
CRMI46	0.038 ± 0.001	0.05 ± 0,01	1.3	0.035±0.003	0.9	16.55±0.74	435
VHI1	5.05 ± 1.84	8.51 ± 1.98	1.7	2.73 ± 0.76	0.5	>300	>60
VHI13	0.077 ± 0.022	0.043 ± 0.009	0.6	0.048 ± 0.007	0.6	5.6 ± 0.2	73
VHI14	0.125 ± 0.027	0.094 ± 0.023	0.8	0.089 ± 0.017	0.7	12.8 ± 0.9	103
VHI19	0.100 ± 0.034	0.066 ± 0.005	0.7	0.062 ±0.004	0.6	12.7 ± 0.5	127
VHI20	0.058 ± 0.026	0.030 ± 0.008	0.5	0.045 ± 0.018	0.8	23.3 ± 0.4	404
VHI22	0.094 ± 0.023	0.065 ± 0.002	0.7	0.073 ± 0.025	0.8	24 ± 1.2	254
AT1	21.5 ± 0.3	18.5 ± 0.4	0.9	19.3 ± 0.2	0.9	>300	>14
AT2	36.5 ± 3.5	34.9 ± 0.2	1.0	36.6 ± 0.6	1.0	>300	>8
AT6	0.373 ± 0.003	0.40 ± 0.01	1.1	0.43 ± 0.08	1.1	>300	>800
AT7	0.44 ± 0.04	0.40 ± 0.03	0.9	0.43 ± 0.09	1.0	>300	>680
AT8	0.14 ± 0.02	0.14 ± 0.01	1.0	0.13 ± 0.02	0.9	72.6 ± 7.1	524
AT9	2.68 ± 0.05	3.79 ± 0.09	1.4	2.74 ± 0.02	1.0	>300	>110
AT11	>100	>100	ND	>100	ND	>300	ND
AT15	0.25± 0.03	0.28 ± 0.01	1.1	0.3 ± 0.01	1.2	233 ± 31	914
AT16	0.33 ± 0.02	0.33 ± 0.01	1.0	0.33 ± 0.01	1.0	>300	>900
AT17	0.057 ± 0.013	0.043 ± 0.004	0.7	0.088 ± 0.024	1.5	45.4 ± 12.4	792
AT19	23.2 ± 3.1	9.9 ± 1.9	0.4	6.68 ± 1.65	0.3	>300	>10
AT20	>100	>100	ND	>100	ND	>300	ND

AT37	0.23 ± 0.06	0.37 ± 0.09	1.6	0.28 ± 0.04	1.2	77.1 ± 8.6	338
AT38	0.24 ± 0.06	0.32 ± 0.05	1.3	0.28 ± 0.05	1.2	174 ± 23	723
AT05	0.04±0.002	0.03±0.01	0.75	0.02±0.001	0.5	>300	>7500
AT10	0.023 ± 0.001	0.024 ± 0.002	1.0	0.023 ± 0.001	1.0	>300	>12500
AT21	0.064 ± 0.004	0.012 ± 0.002	0.2	0.011 ± 0.003	0.2	32.5 ± 3.6	505
AT33	0.015 ± 0.002	0.013 ± 0.0006	0.8	0.010 ± 0.001	0.7	17.6 ± 1.2	1145
AT22	0.17 ± 0.05	0.15 ± 0.03	0.8	0.11 ± 0.03	0.7	48.2 ± 2.4	281
AT34	0.028 ± 0.002	0.021 ± 0.002	0.8	0.017 ± 0.0003	0.6	24.5 ± 2.3	876
AT27	5.9 ± 0.7	6.1 ± 0.9	1.0	6.28 ± 0.85	1.1	>300	>50
AT28	0.15 ± 0.03	0.15 ± 0.02	1.0	0.10 ± 0.01	0.7	76.8 ± 2.0	504
AT29	>100	>100	ND	>100	ND	>300	ND
AT30	0.21 ± 0.05	0.22± 0.06	1.1	0.15 ± 0.03	0.7	63.2 ± 4.4	306
AT31	0.011 ± 0.004	0.008 ± 0.003	0.7	0.022 ± 0.011	1.9	13.4 ± 0.3	1198
AT39	42.7 ± 6.2	46.6 ± 2.3	1.1	45.8 ± 12.8	1.1	>300	>7
Diminazene	0.12±0.05	0.54±0.086	4.5	0.736±0.2	6.13	ND	ND
Pentamidine	0.004±0.001	0.01±0.00	2.5	0.55±0.054	137	ND	ND
PAO	ND	ND	ND	ND	ND	8.65±1.35	ND

Table 5.1. Average EC₅₀ values for phosphonium compounds against *T. b. brucei* wild type, TbAT1- knockout, and B48 bloodstream form plus standard errors. In addition, it shows the resistance factor for the KO and B48 strains. Also shown are the average EC₅₀ values with Human Embryonic Kidney (HEK) cells and standard errors, plus the Selectivity Index (EC₅₀ of HEK cells / EC₅₀ of *T. b. b.*-WT). Diminazene and Pentamidine are the positive controls against parasites, and phenylarsine oxide (PAO) is used as a positive control of HEK cells. The averages of EC₅₀ values ± SEM of three independent experiments are shown. Highlighted cells indicate monophosphonium compounds; others are bisphosphonium compounds. ND = not determined.

5.2.2 Assessment of cross-resistance

Resistant strains can be used as a model to investigate cross-resistance between existing treatments and potential new trypanocides. Any new trypanocidal drugs to be developed, whether for human or veterinary use, should at a minimum not be cross-resistant with the current diamidine and arsenic-based drugs. It is exactly because of high levels of resistance to these classes of drugs that the development of new drugs has become such a priority. Therefore, we investigated whether phosphonium-based trypanocides would be effective against well-characterised laboratory strains resistant to diamidines and melaminophenyl arsenicals.

Eighty three phosphonium analogues were tested on three strains of trypanosomes: wild type strain (s427-WT), TbAT1 knockout (KO), and TbAT1-B48 –listed in decreasing sensitivity to diminazene, pentamidine, and cymelarsan (Matovu *et al.*, 2003; Bridges *et al.*, 2007). EC₅₀ values were found to be statistically identical for the s427, TbAT1-KO, and B48 strains in all cases (Student *t*-test; *P*>0.05), indicating that the phosphonium cations are not cross-resistant with the crucial diamidine and melaminophenyl arsenical classes of trypanocides (Table 5.1).

5.2.3 Cytotoxic activity of phosphonium compounds on Human Embryonic Kidney (HEK) cells and Therapeutic index values

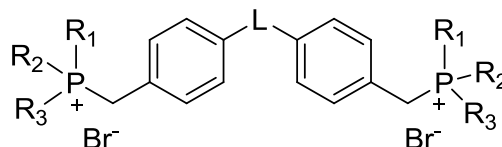
The toxic effect of phosphonium compounds on HEK cells was assessed using the Alamar blue assay, as explained in Chapter 3, at a maximum concentration of 300 µM of the phosphonium compounds. Toxicity assays for HEK cells showed that the phosphonium compounds that have an effect on *T. b. brucei* have a much lower activity on HEK cell growth and viability. Therapeutic index rates (EC₅₀ of HEK cells / EC₅₀ of *T. b. brucei*) are shown in Table 5.1. The highest therapeutic index (TI) values were >12500, 7000, 3567, and 2930-fold with AT10, AT5, AHI17, and AHI9, respectively. In addition, 60 of 83 phosphonium compounds displayed a TI >200.

5.3 Analysis of structural determinants of phosphonium analogues contributing to trypanocidal activity

The antiparasitic effects of phosphonium analogues were investigated using the *in vitro* Alamar blue viability assay to determine the EC₅₀ values. In addition, the structure-activity relationship (SAR) of phosphonium analogues as compounds against the *Trypanosoma brucei brucei* bloodstream form was analysed.

Phosphonium analogues were divided into five groups according to type of substituents.

The activity of bisphosphonium salts having aliphatic and phenyl substituents was different; compounds with three short alkyl substituents (Me, Et, or Pr) on the phosphonium cations were weakly active against trypanosome (EC₅₀ ≥ 20 μM) (Table 5.2, compounds 1-6). The activity was improved with the increase in chain length (*n*-octyl ≈ *n*-hexyl > *c*-hexyl ≈ *n*-pentyl > *n*-Bu > *i*-Bu) and 8 of 11 compounds had an EC₅₀ less than 500 nM (Table 5.2, compounds 7-17). Replacement of one short alkyl substituent (e.g. methyl, ethyl) with phenyl rings (R₁, R₂ = alkyl; R₃ = Ph) increased the activity against *Trypanosoma brucei brucei* (Table 5.2, compounds 19-24); further replacement of such short aliphatic groups with phenyl (R₁ = alkyl (R₂, R₃ = Ph)) continued to increase the activity, with EC₅₀ < 1 μM (Table 5.2, compounds 26-31).

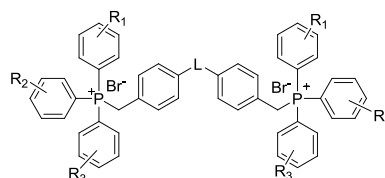


No	Compound	L	R ₁	R ₂	R ₃	WT-s427 EC ₅₀ (μM)
1	CDIV31	CO	Me	Me	Me	>100
2	CDIV22	CO	Et	Et	Et	>100
3	AT 1	CH ₂	Et	Et	Et	21.5 ± 0.3
4	AT 2	O	Et	Et	Et	36.5 ± 3.5
5	CDIV23	CO	<i>n</i> -Pr	<i>n</i> -Pr	<i>n</i> -Pr	19.73 ± 4.11
6	CDIV24	CO	ⁱ Pr	ⁱ Pr	ⁱ Pr	20.55 ± 5.19
7	CDIV35	CO	<i>n</i> -Bu	<i>n</i> -Bu	<i>n</i> -Bu	0.48 ± 0.11
8	CDIV25	CO	ⁱ Bu	ⁱ Bu	ⁱ Bu	2.62 ± 0.69
9	AHI08	CH ₂	ⁱ Bu	ⁱ Bu	ⁱ Bu	0.70 ± 0.03
10	AHI07	O	ⁱ Bu	ⁱ Bu	ⁱ Bu	0.59 ± 0.06
11	AHI40	SO ₂	ⁱ Bu	ⁱ Bu	ⁱ Bu	16.7 ± 0.5
12	CD38	CO	<i>n</i> -pentyl	<i>n</i> -pentyl	<i>n</i> -pentyl	0.20 ± 0.03
13	CRMI46	CO	<i>n</i> -hex	<i>n</i> -hex	<i>n</i> -hex	0.038 ± 0.001
14	AHI16	CH ₂	<i>n</i> -hex	<i>n</i> -hex	<i>n</i> -hex	0.03 ± 0.006
15	AHI15	O	<i>n</i> -hex	<i>n</i> -hex	<i>n</i> -hex	0.037 ± 0.004
16	CDIV33	CO	<i>c</i> -hex	<i>c</i> -hex	<i>c</i> -hex	0.14 ± 0.03
17	CDIV48	CO	<i>n</i> -octyl	<i>n</i> -octyl	<i>n</i> -octyl	0.042 ± 0.002
18	CDIV29	CO	Me	Me	Ph	19.17 ± 7.17
19	AHI05	CH ₂	Me	Me	Ph	5.45 ± 1.09
20	AHI04	O	Me	Me	Ph	7.22 ± 0.16
21	EFpl 33	(CH ₂) ₂	Me	Me	Ph	2.59 ± 0.64
22	EFpl 32	(CH ₂) ₃	Me	Me	Ph	1.27 ± 0.33
23	CDIV26	CO	Et	Et	Ph	8.59 ± 2.16
24	CDIV53	CO	<i>c</i> -hex	<i>c</i> -hex	Ph	0.24 ± 0.03
25	CDIV28	CO	Me	Ph	Ph	1.53 ± 0.38
26	CDIV34	CO	Et	Ph	Ph	0.97 ± 0.27
27	AT 6	CH ₂	<i>n</i> -Pr	Ph	Ph	0.37 ± 0.003
28	AT 15	O	<i>n</i> -Pr	Ph	Ph	0.25 ± 0.03
29	AT 7	CH ₂	ⁱ Pr	Ph	Ph	0.44 ± 0.04
30	AT 16	O	ⁱ Pr	Ph	Ph	0.33 ± 0.02
31	Efpl 1	CO	<i>c</i> -hex	Ph	Ph	0.30 ± 0.03

Table 5.2. Antitrypanosomal activity of bisphosphonium salts having aliphatic and phenyl substituents. The averages of EC₅₀ values ± SEM of three independent experiments are shown; *c*-hex, cyclohexane; ⁱBu, isobutyl; ⁱPr, isopropyl.

The effect of phosphonium compounds on WT-s427 when including substituents on the aromatic ring was investigated. The results are shown in Table 5.3. It appeared that the activity was superior to the small aliphatic substituents, but similar to aliphatic chains of C_n ≥ 5. All compounds had an EC₅₀ < 1 μM. In this

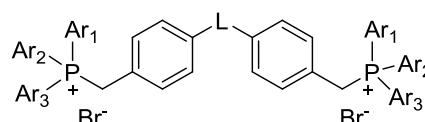
series the best activity was displayed by AHI17, which has 4-methylphenyl substituents on all 6 positions, with an EC_{50} value of 24 ± 5 nM. The substituent pattern for the phenyl ring, in order of increasing activity, was 4-Me > 3-Me > H and 2-OMe > 4-OMe > 4-Cl \approx 4-F > 4-CF₃. This seems to confirm a pattern seen with the aliphatic substituents that activity correlates with increased shielding of the phosphonium cations and increased hydrophobic surface area.



No	Compound	L	R ₁	R ₂	R ₃	WT-s427 EC ₅₀ (μM)
1	CDIV20	CO	H	H	H	0.24 ± 0.07
2	CDIV50	CO	H	H	2-Me	0.20 ± 0.01
3	CDIV52	CO	H	H	4-Me	0.180 ± 0.002
4	AHI10	CH ₂	H	H	4-Me	0.24 ± 0.04
5	AHI09	O	H	H	4-Me	0.082 ± 0.014
6	Efpl 2	CO	4-Cl	4-Cl	4-Cl	0.94 ± 0.14
7	Efpl 3	CO	4-F	4-F	4-F	0.85 ± 0.17
8	Efpl 4	CO	4-OMe	4-OMe	4-OMe	0.32 ± 0.07
9	Efpl 6	CO	2-OMe	2-OMe	H	0.24 ± 0.04
10	Efpl 11	CO	2-OMe	2-OMe	2-OMe	0.11 ± 0.02
11	AHI22	CH ₂	2-OMe	2-OMe	2-OMe	0.080 ± 0.004
12	AHI21	O	2-OMe	2-OMe	2-OMe	0.056 ± 0.011
13	VHI1	CO	4-CF ₃	4-CF ₃	4-CF ₃	5.05 ± 1.84
14	AT37	CH ₂	4-CF ₃	4-CF ₃	4-CF ₃	0.23 ± 0.06
15	AT38	O	4-CF ₃	4-CF ₃	4-CF ₃	0.24 ± 0.06
16	Efpl 7	CO	4-Me	4-Me	4-Me	0.11 ± 0.02
17	VHI 22	CO	4-Me	4-Me	4-Me	0.094 ± 0.023
18	AHI18	CH ₂	4-Me	4-Me	4-Me	0.080 ± 0.002
19	EFpl 28	(CH ₂) ₂	4-Me	4-Me	4-Me	0.15 ± 0.06
20	VHI20	(CH ₂) ₂	4-Me	4-Me	4-Me	0.058 ± 0.026
21	EFpl 27	(CH ₂) ₃	4-Me	4-Me	4-Me	0.029 ± 0.005
22	VHI19	(CH ₂) ₃	4-Me	4-Me	4-Me	0.100 ± 0.034
23	AHI17	O	4-Me	4-Me	4-Me	0.024 ± 0.005
24	AHI30	SO ₂	4-Me	4-Me	4-Me	0.23 ± 0.01
25	AHI43	NAc	4-Me	4-Me	4-Me	0.32 ± 0.01
26	AT 8	CH ₂	3-Me	3-Me	3-Me	0.14 ± 0.02
27	AT 17	O	3-Me	3-Me	3-Me	0.057 ± 0.013

Table 5.3. Antitrypanosomal activity of bisphosphonium salts having substituted phenyl substituents. The averages of EC_{50} values \pm SEM of three independent experiments are shown.

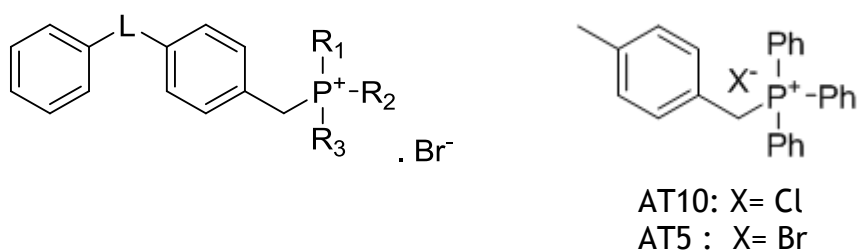
Next, the activity was evaluated for bisphosphonium salts that have aryl groups or heterocycle substituents. Replacement of the phenyl substituents of the phosphonium cation by 2-thienyl groups (Table 5.4, compounds 1-2) or 1-naphthyl substituents (Table 5.4, compounds 10-12) maintained the activity. In contrast, the introduction of an oxygenated (2-furanyl) and thus more polar heterocycle led to a decreased EC_{50} by 150-fold; also, the introduction of an amino (2-pyridyl) heterocycle decreased the EC_{50} by 3-fold (Table 5.4, compounds 3-4). Similarly, the replacement of one phenyl substituent by a more polar phenylsulphonate or pentafluorophenyl ring abolished the trypanocidal activity (Table 5.4, compounds 6-9). All these observations reinforce the notion that maximum trypanocidal activity correlates directly with increased hydrophobicity and that the introduction of either hydrogen bond donors or acceptors is deleterious to activity.



No	Compound	L	Ar ₁	Ar ₂	Ar ₃	WT-s427 EC ₅₀ (μM)
1	CDIV20	CO	Ph	Ph	Ph	0.24 ± 0.07
2	CDIV57	CO	2-thienyl	2-thienyl	2-thienyl	0.33 ± 0.06
3	CDIV49	CO	2-furanyl	2-furanyl	2-furanyl	36.9 ± 1.2
4	CDIV27	CO	Ph	Ph	2-pyridyl	0.70 ± 0.24
5	EFpl 8	CO	Bn	Ph	Ph	0.81 ± 0.12
6	AT 9	CH ₂	Ph	Ph	C ₆ F ₅	2.68 ± 0.05
7	AT 19	O	Ph	Ph	C ₆ F ₅	23.2 ± 3.1
8	AT 11	CH ₂	Ph	Ph	3-(SO ₃ Na)Ph	>100
9	AT 20	O	Ph	Ph	3-(SO ₃ Na)Ph	>100
10	EFpl 10	CO	1-naphthyl	1-naphthyl	1-naphthyl	0.18 ± 0.04
11	AHI20	CH ₂	1-naphthyl	1-naphthyl	1-naphthyl	0.14 ± 0.02
12	AHI19	O	1-naphthyl	1-naphthyl	1-naphthyl	0.16 ± 0.01

Table 5.4. Antitrypanosomal activity of bisphosphonium salts having aryl groups or heterocycle substituents. The averages of EC_{50} values ± SEM of three independent experiments are shown.

The more surprising correlation is with the removal of one of the phosphonium cations to create monophosphonium salts. The trypanocidal activity was generally higher for the mono-phosphonium than for the corresponding bisphosphonium compound (Table 5.5). Specifically, slightly lower EC₅₀ values were observed for AT21, AT33, AT34, AT28, and AT31 compared with their bisphosphonium salt compound (VHI22, AHI17, AT17, CDIV52, and CRMI46, respectively). The SAR of substituents was identical to that observed for the bisphosphonium compounds. Interestingly, the replacement of the carbonyl group by an ether linker further increased the activity between 6 and 4-fold against WT-s427 (compare AT21 with AT33 and AT22 with AT34), yielding compounds with low nanomolar activity.



No	Compound	L	R ₁	R ₂	R ₃	WT-s427 EC ₅₀ (μM)
1	AT10 (Cl)					0.023 ± 0.001
2	AT5 (Br)					0.043 ± 0.001
3	AT21	CO	4-Me-Ph	4-Me-Ph	4-Me-Ph	0.064 ± 0.004
4	AT33	O	4-Me-Ph	4-Me-Ph	4-Me-Ph	0.015 ± 0.002
5	AT22	CO	3-Me-Ph	3-Me-Ph	3-Me-Ph	0.17 ± 0.05
6	AT34	O	3-Me-Ph	3-Me-Ph	3-Me-Ph	0.028 ± 0.002
7	AT27	CO	ⁱ Bu	ⁱ Bu	ⁱ Bu	5.9 ± 0.7
8	AT28	CO	4-Me-Ph	Ph	Ph	0.15 ± 0.03
9	AT29	CO	Et	Et	Et	>100
10	AT30	CO	2-MeO-Ph	2-MeO-Ph	2-MeO-Ph	0.21 ± 0.05
11	AT31	CO	<i>n</i> -hex	<i>n</i> -hex	<i>n</i> -hex	0.011 ± 0.004
12	AT39	CO	Me	Me	Ph	42.7 ± 6.2

Table 5.5. Antitrypanosomal activity of monophosphonium salts. The averages of EC₅₀ values ± SEM of three independent experiments are shown.

5.4 Effect of test compounds on trypanosome proliferation after limited exposure

Two bisphosphonium compounds (AHI15 and AHI16) were selected for determining the inhibition of trypanosome proliferation after exposure of a limited duration. Trypanosomes need only to be incubated briefly with some drugs, like the diamidines, even though cell death does not occur for hours after the exposure has ceased. In other words, their early effects are irreversible and cells will not recover. Clearly this is important in the evaluation of potential trypanocides, with major implications for any dosage regimen.

First, cells were incubated in the continuous presence of three concentrations for each compound (0.05, 0.25, and 1 μM) as well as without drugs (control) to choose the best concentration for inhibiting growth during 48 h using microscopic cell counts every 4 h. The results (Figure 5.2) show that the concentration of 0.25 μM was the most active concentration that did not lead to extensive cell death during the incubation.

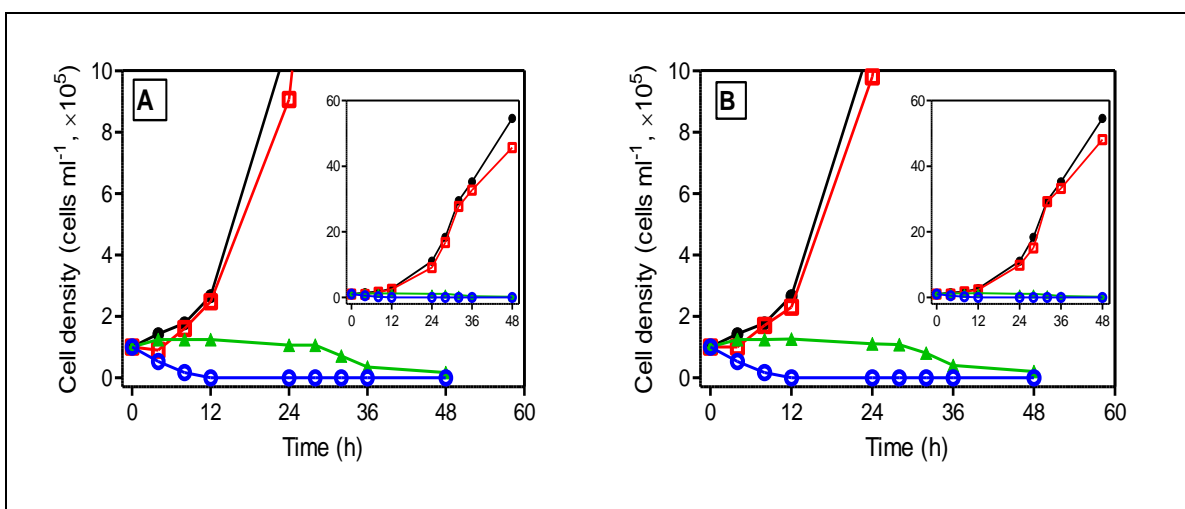


Figure 5.2. 1 Effect of bisphosphonium compounds AHI15 (A) and AHI16 (B) on the growth curve of the *T. b. b.* bloodstream form with different concentrations: (●) drug free, (□) 0.05 μM , (▲) 0.25 μM , and (○) 1 μM . Cells were set up at 10^5 cells/ml. Microscopic cell counts were performed in triplicate using a haemocytometer.

In the next experiment, the cell density was adjusted to 1×10^5 cells/ml and the bloodstream form s427 trypanosomes were exposed for two durations (0.5 and 4 h) to the compounds. At the predetermined time, the culture was transferred to

centrifuge tubes, spun at $1100 \times g$ for 10 min, and washed twice in fresh medium or continued with fresh medium has $0.25 \mu\text{M}$ for both compounds. The cell count was taken in triplicate at four time points (0, 4, 8, and 12 h/day) for each concentration of compounds for 48 h.

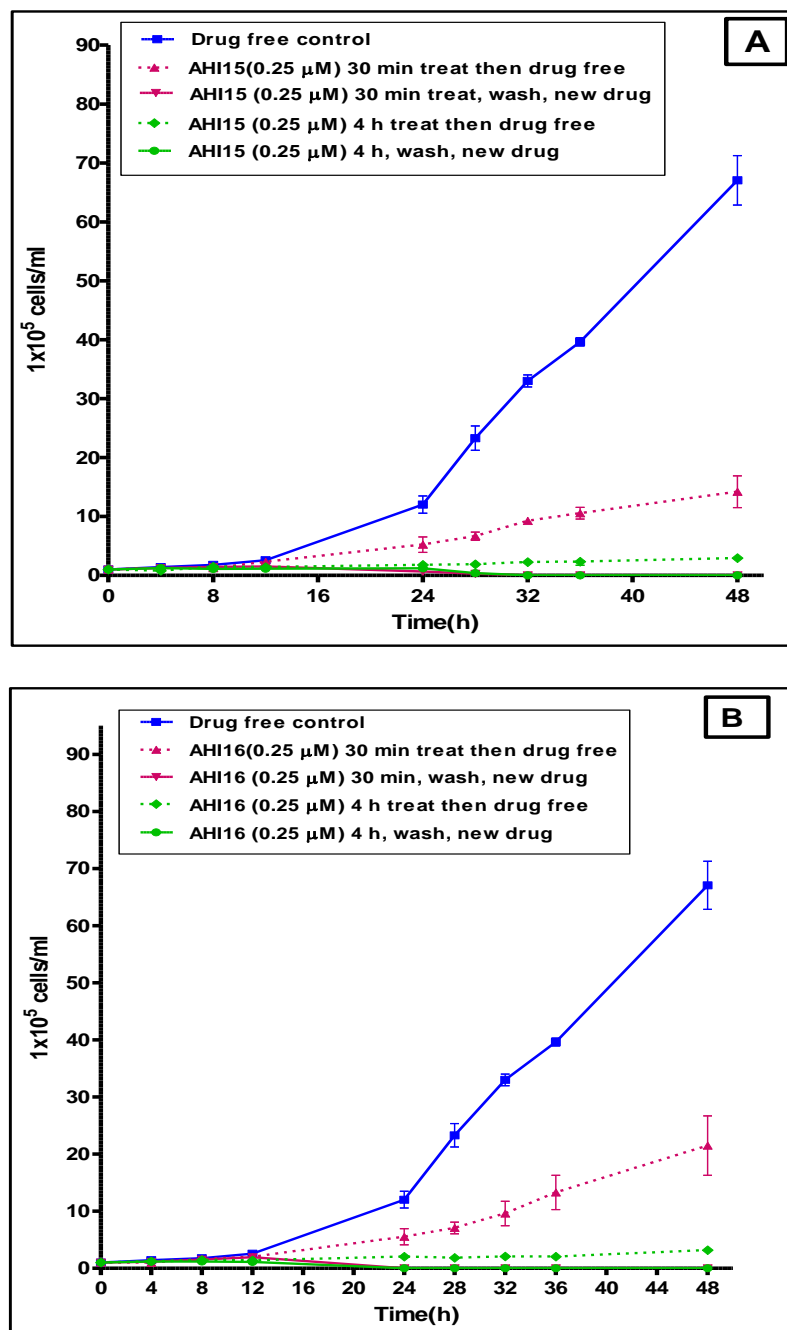


Figure 5.3. Effect of bisphosphonium compounds AHI15 (A) and AHI16 (B) on Tb427 wild type bloodstream form trypanosome proliferation. Growth inhibition by $0.25 \mu\text{M}$ for both compounds was determined by centrifugation ($1100 \times g$) after either 30 min or 4 h (as mentioned in the figure) and replacement with drug-free fresh medium or fresh medium with $0.25 \mu\text{M}$ of compounds or control culture (drug free) was used. Cultures were seeded at 10^5 cells/ml. Microscopic cell counts were performed in triplicate using a haemocytometer. The results shown are the average of three independent experiments; error bars depict standard errors.

Although trypanosomes died slowly on incubation with phosphonium compounds, only a relatively short exposure time was required. Figure 5.3 shows that the removal of these compounds after a mere 30 min of incubation allowed for only limited resumption of growth, reaching a maximum density of $14.2 \pm 2.7 \times 10^5$ cells/ml at 48 h and 20% of the drug-free control for AHI15, and $21.5 \pm 5.2 \times 10^5$ cells/ml at 48h and 30% of the drug-free control for AHI16. Removal of drugs after 4 h did not lead to any resumption of growth at all, and the trypanosome population either remained stable or, for some compounds, slowly dwindled over the following 36 h (Fig. 5.2; Taladriz et al., 2012). Continuous exposure to the drug resulted in sterilisation of the culture after approximately 30 h.

5.5 Monitoring the speed of action of test compound on Trypanosomes by using propidium iodide

The purpose is to monitor the speed of action of the test compounds on trypanosomes in real time. Cells become fluorescent as PI enters the cell and binds to nucleic acids. This occurs only upon breach of the plasma membrane (i.e., loss of cellular integrity). Serial dilutions of bisphosphonium compounds were used to study the effect of the CD38 compound on the cell viability for three strains of trypanosomes (WT, KO, and B48) during 8 h.

Figure 5.4 indicates that CD38 only affected cellular viability during 8 h at concentrations >15-fold its EC_{50} and there was no significant difference among the three strains of trypanosomes. Similar observation were made for several bisphosphonium compounds (Taladriz *et al.*, 2012).

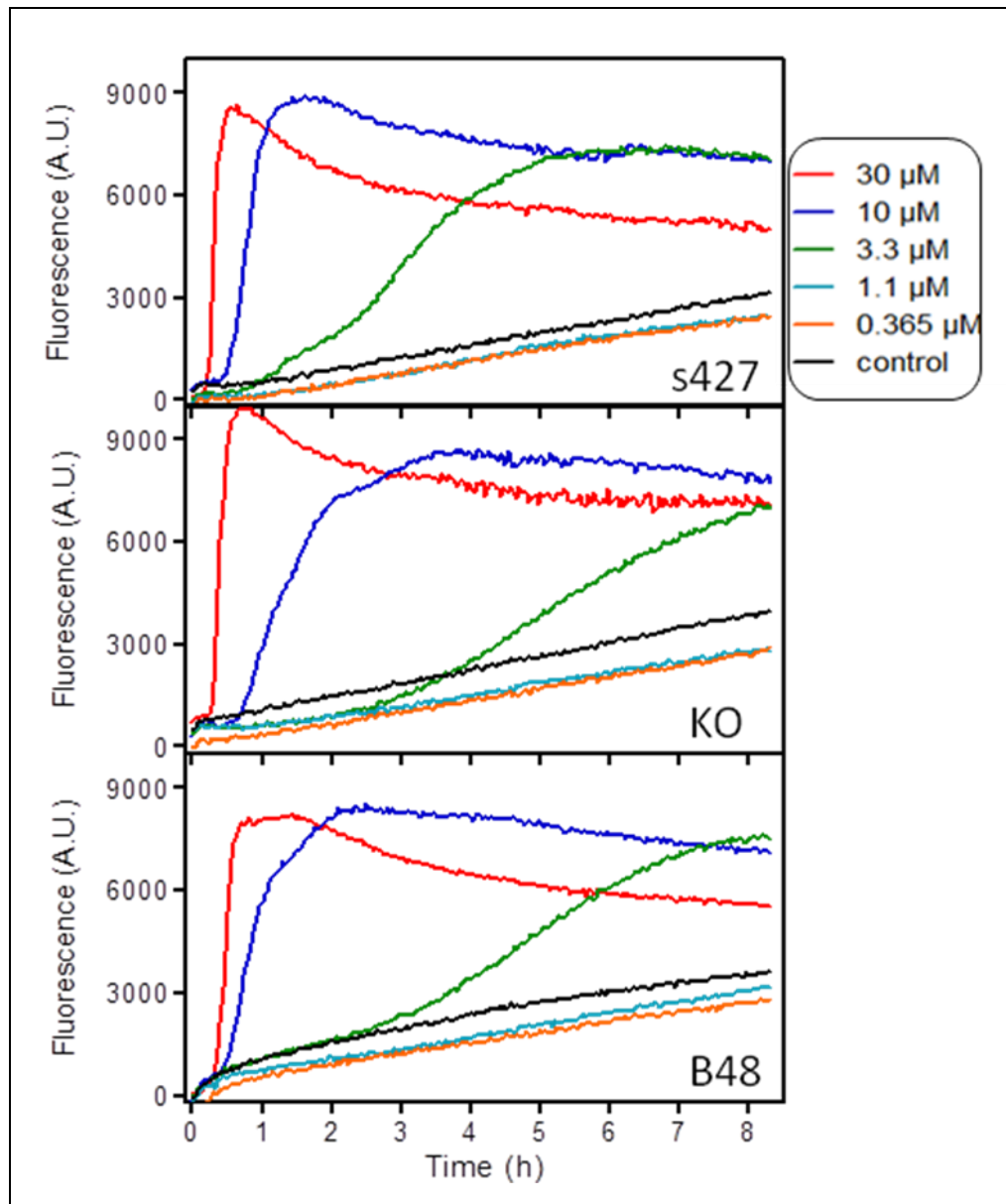


Figure 5.4. Dose response curve of the CD38 compound for the bloodstream form of various strains of *T. b. brucei*. The different concentrations were incubated with and without parasites in HMI-9 medium, which has 10% FCS at 37 °C with 5% CO₂. Propidium iodide at 9 μM was added, and the fluorescence was measured over 8 h at 544 nm excitation and 620 nm emission. Separate traces were recorded in the absence of cells and were subtracted from those presented in the figures.

5.6 Discussion

The heavily substituted phosphonium salts that are here shown to have potent anti-protozoal activity are lipophilic cations bearing a greatly delocalized and shielded charge. Therefore, they have the advantage of being able to diffuse through biological membranes, with the membrane potential providing a driving force for accumulation. Thus, phosphonium compounds are known to accumulate not only in the *Leishmania* mitochondria (Luque-Ortega et al., 2010), but also in mammalian mitochondria (Murphy, 2008;Porteous *et al.*, 2010;Smith & Murphy, 2010). Thus, the various benzophenone-derived bisphosphonium salts present in *Leishmania* accumulated in the parasite's mitochondria as a result of the strong inside-negative mitochondrial membrane potential (Luque-Ortega et al., 2010). It is reasonable to hypothesise that a similar mitochondrial targeting underlies their trypanocidal activity and this will be investigated in chapter six.

The SAR of the compounds under study here for their effects against African trypanosomes shared considerable similarity with the SAR against *Leishmania*. For example, for compounds with homoalkyl groups, optimum activity was observed with 5- to 8-carbons, independently of the linker (Tables 5.2 and 5.5). Similarly, the addition of two phenyl groups (with their alkyl substituents) provided it with a submicromolar activity. However, the addition of one phenyl group with two short alkyl substituents (Me, Et) provided a micromolar EC₅₀. These observations are clearly supported by the CoMFA models that show that a minimum bulk around the phosphonium cations is favourable to the activity, but this volume is also limited in size (Taladriz *et al.*, 2012).

Clearly, the SAR findings are entirely consistent with increased membrane penetration being the determining factor for anti-protozoal activity for both bisphosphonium and mono-phosphonium salts. This is achieved by increased shielding of the positively charged phosphorous atom(s) and distribution of the charge over aromatic substituents. These cations are thus eminently capable of diffusing across biological membranes independent of drug *T. b. brucei* transporters such as P2, HAPT1, and LAPT1. This explains the absence of cross-resistance with diamidine and arsenical drugs, which has been shown to be correlated with the loss of these transporters (de Koning, 2008).

Although various bisphosphonium compounds have the ability to dose-dependent inhibit the HAPT1 and LAPT1 transporters (Taladriz *et al.*, 2012), with IC₅₀ values of 5.2 and 2.2 μ M for compound CD38. However, these compounds are likely too big to be a substrate (as opposed to an inhibitor) of such transporters because their molecular weights ranged from 800 to 1300, compared with 340 for pentamidine. In contrast, di-cationic diamidines do require transporters including HAPT1 and LAPT1 to cross membranes (de Koning, 2001;Teka *et al.*, 2011). Yet, cationic compounds such as the symmetrical choline-derived experimental trypanocides with long aliphatic linkers that we recently described compounds (Ibrahim *et al.*, 2011) were also not dependent on transporters, for the same reasons as the bisphosphonium compounds described here. The observation that substituents such as furan, pyridine, and phenylsulphonate, which can form H-bonds display low antitrypanosomal activity, as their diffusion rates across plasma and mitochondrial membranes.

An important aspect of the SAR analysis presented here is that mono-phosphonium compounds are at least as active as the equivalent bis-phosphonium compounds with the same substituents, despite the fact that molecules with the higher charge (bisphosphonium) would be expected to have a higher mitochondrial accumulation rate than mono-cations. Consistent with the redundancy of the second phosphonium group was that the introduction of increasingly flexible linkers, such as ethylene instead of methylene linkers, had very little effect on trypanocidal activity. The equivalence or superiority of the mono-phosphonium compounds is of considerable value considering that the smaller mono-cations are likely to have a better pharmacokinetic behaviour *in vivo*.

In the paper presented by Kinnamon (Kinnamon *et al.*, 1979) it was observed that the chloride salt monophosphonium compound AT10 showed a 100% curative activity (53 mg/kg sc) against *T. b. rhodesiense* infection in a murine model; the bromide analogue AT5 was reported to be less efficient *in vivo* compared to its chloride counterpart. The invitro screening reported here is in agreement with that report as AT10 displayed excellent activity against *T. b. brucei* and *T. b. rhodesiense*.

The excellent *in vitro* trypanocidal activities and high *in vitro* selectivity indices obtained for this set of phosphonium compounds, indicates that this class may have therapeutic potential. The compounds also have the ability to irreversibly inhibit trypanosome growth, which eventually leads to the extinction of a specific population after minimum exposure time. This situation is similar to the diamidine trypanocides, which also require only a short exposure time to inhibit population growth, and ultimately kill the trypanosomes in 1-2 days (Ward *et al.*, 2011). This observation supports keeping the dose of the drug low, and suggests that a single dose can suffice just like a single dose of the diamidine diminazene aceturate is sufficient for the routine treatment for animal trypanosomiasis (Delespaulx & de Koning, 2007). In addition, the association of lipophilicity with membrane penetration ability will cause a more efficient penetration into the central nervous system, which is very important for cure of the cerebral stage of trypanosomiasis (Rodgers, 2009), as well as oral availability. However, a note of caution must be that preclinical development of this class may have to further optimise specificity as a potential concern is that the compounds will also accumulate in mammalian mitochondria. With selection of the most potent trypanocides, allowing for minimal dosages, it may be possible to overcome this hurdle.

In conclusion, the *in vitro* screening of 83 phosphonium compounds against African trypanosomes allowed the discovery of some trypanocidal compounds that have nanomolar activities and much lower toxicity against HEK cells. The structure activity relationship demonstrated that large substituents around phosphonium cations (i.e., any 5 to 8 homoalkyl chains of C₅ - C₈ length, or phenyl rings) are essential for optimised activity, while the exact nature of the linkers have less effect on the activity - at least for bisphosphonium salts as the diphenyl ether linker seemed to be more clearly preferred in the case of monophosphonium compounds.

Phosphonium compounds displayed a similar structure activity relationship against *T. brucei* and *Leishmania*. This observation strongly suggests a similar mechanism of action against the two parasite species, and indicates that this class may have broad anti-protozoal activity. This is the topic of Chapter 6, which focuses on the mode of action of bisphosphonium compounds in the *T. b. brucei* bloodstream form.

Importantly, the screening reported here confirmed that the new compounds were not cross-resistant with existing diamidines and arsenical trypanocides, such as pentamidine and melarsoprol, currently in clinical use – an essential condition for any new preclinical candidate.

6 CHAPTER Six: Investigation into the mode of action of Bisphosphonium compounds in *T. b. brucei* bloodstream form

6.1 Introduction

This chapter investigates the effect of selected bisphosphonium compounds *in vitro* on bloodstream-form *Trypanosoma brucei brucei* to attempt to understand the mode of action. Many cellular parameters were determined in an unbiased investigation of the trypanocidal activity of this class of compounds, including their effects on the mitochondrial membrane potential, intracellular calcium levels, cellular ATP level, the cell cycle, as well as an assessment of the morphology of cells exposed to bisphosphonium analogues.

A recent paper described promising anti-leishmanial activity of bisphosphonium compounds. It was also found that these agents act on the *Leishmania* mitochondria, specifically by inhibition of Complex II formation, which leads to the alteration of cell shape. Specifically, it caused cellular swelling, decreased levels of ATP, as well as a reduction of the mitochondrial membrane potential and the O₂ consumption rate (Luque-Ortega *et al.*, 2010). It has also been reported that the bisphosphonium compound, 4,4'-bis[(tri-*n*-pentylphosphonium)methyl] benzophenone dibromide displays *in vitro* activity against *T. brucei* (Dardonville & Brun, 2004). However, we have not assumed that the trypanocidal mode of action is, identical to the reported antileishmanial activity, as bloodstream trypanosomes, in contrast to procyclic forms, are not believed to express Complex II (Acestor *et al.*, 2011; Chaudhuri *et al.*, 2006).

Cellular parameters are important as the first stage of studying the mode of action. As a first step, *T. brucei* growth curves in the presence of various concentrations of active compound were made in order to determine suitable combinations of concentration and incubation time for the study of cellular effects. The effects of bisphosphonium compounds on the life cycle of *T. brucei* were studied using flow cytometry for DNA content, and by fluorescent microscopy with the DNA stain 4', 6'-diamidino-2-phenylindole hydrochloride (DAPI), allowing the evaluation of the effects these compounds have on cell division. These tests were used to assess the distribution of DNA with respect to time. With the flow cytometry, the DNA content of fixed cells stained with propidium iodide is evaluated. However, this method gives no information about

the (number of) kinetoplasts, whereas the microscopic assessment with DAPI accurately reveals the number of nuclei and kinetoplasts per cell, and may additionally reveal morphological changes to the DNA-containing organelles.

Light microscopy was performed in order to study the effects of the bisphosphonium compounds on the overall morphology of the parasite. Bright field, differential interference contrast (DIC), transmission electron microscopy (TEM), and scanning electron microscopy (SEM), were all employed to study the cellular changes occurring in the cell and DNA of the organism as a result of exposure to bisphosphonium compounds.

Finally, to investigate whether exposure to these compounds led to programmed cell death (PCD), also known as apoptosis, two tests were performed. Firstly, cells were treated with the protein synthesis inhibitor cycloheximide (CHX), followed by treatment with bisphosphonium compounds. The inhibition of protein synthesis would have inhibited any PCD. Secondly, as it is known that PCD leads to DNA fragmentation or DNA breaks, a TUNEL assay was used to detect DNA fragmentation in trypanosomes after they were treated with bisphosphonium compounds.

6.2 Effect of test compounds on trypanosome growth

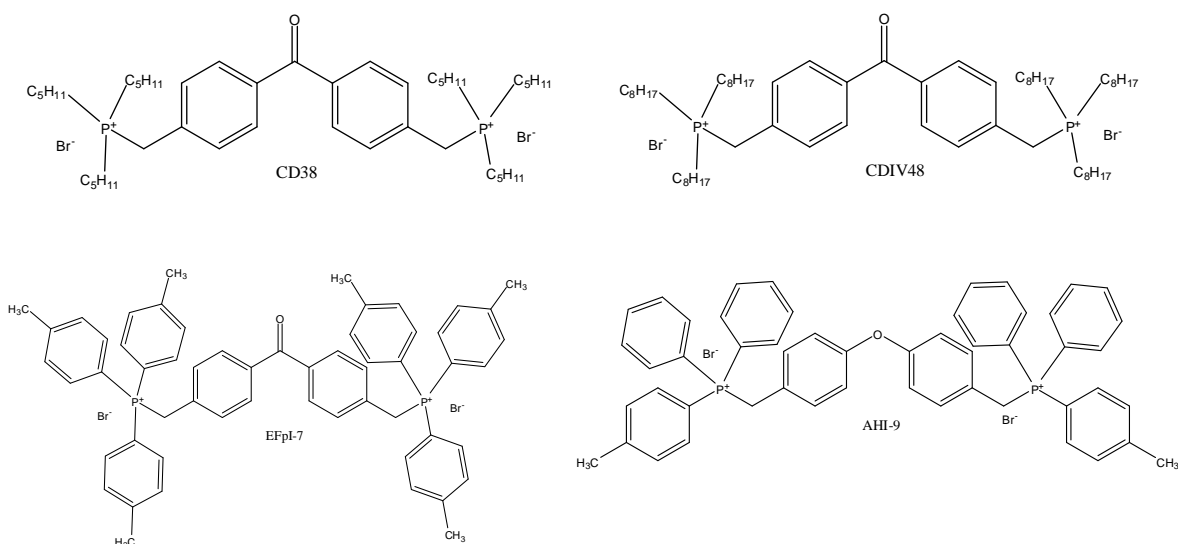
A set of bisphosphonium compounds were tested on trypanosomes at different concentrations (0, 0.1, 0.3, and 1 μM), in order to monitor *in-vitro* cell growth, using microscopic cell counts. Wild-type *T. b. brucei* were taken from cultures at the late logarithmic phase of growth, and cell density was calculated using a haemocytometer. Cell density was adjusted to the desired concentration, which was 1×10^5 cells/ml in this experiment, and diluted with fresh HMI9 medium and 10% FCS. The cell count was taken in triplicate at four time points (0, 4, 8, and 12 h/day) for each concentration of the compounds, for 96 h.

Untreated and treated cells were seeded for up to 96 h with selected bisphosphonium compounds, which were CD38, CDIV48, EFpI7 and AHI9, and three different concentrations of each compound were used. There were no

dramatic effects on the growth rates for these compounds at 0.1 μM , while the growth was inhibited at 0.3 μM after 24h for all compounds except CD38. At 1 μM , the compounds killed the trypanosome population, so no live parasites were detected after 24 - 28 hours (figure 6.1).

CD38 had no effect at 0.1 μM due to the fact that this concentration was less than EC_{50} (0.20 μM). There was a slight inhibition at 0.3 μM , which is slightly more than EC_{50} , whereas at 1 μM , the growth was inhibited after 12 h. CDIV48 did inhibit growth at 0.1 μM , consistent with the concentration being 2.5-fold its EC_{50} value of 42 nM. In contrast, there was only a minor effect at this concentration for EFpI7 and AHI9 due to the fact that this concentration is almost equal to their respective EC_{50} values (110 and 82 nM, respectively). These observations are consistent with the results presented in Chapter Five, which indicated that phosphonium compounds have no immediately effect on the growth of cells (Section 5.5) and that they need more than 8 h to affect cellular viability at a concentration >15-fold of EC_{50} .

These growth curves allow us to choose between the various concentrations of different bisphosphonium compounds in order to study the mode of action. These are CD38, CDIV48, EFpI7, and AHI9 at 0.7, 0.5, 0.5, and 0.7 μM , respectively.



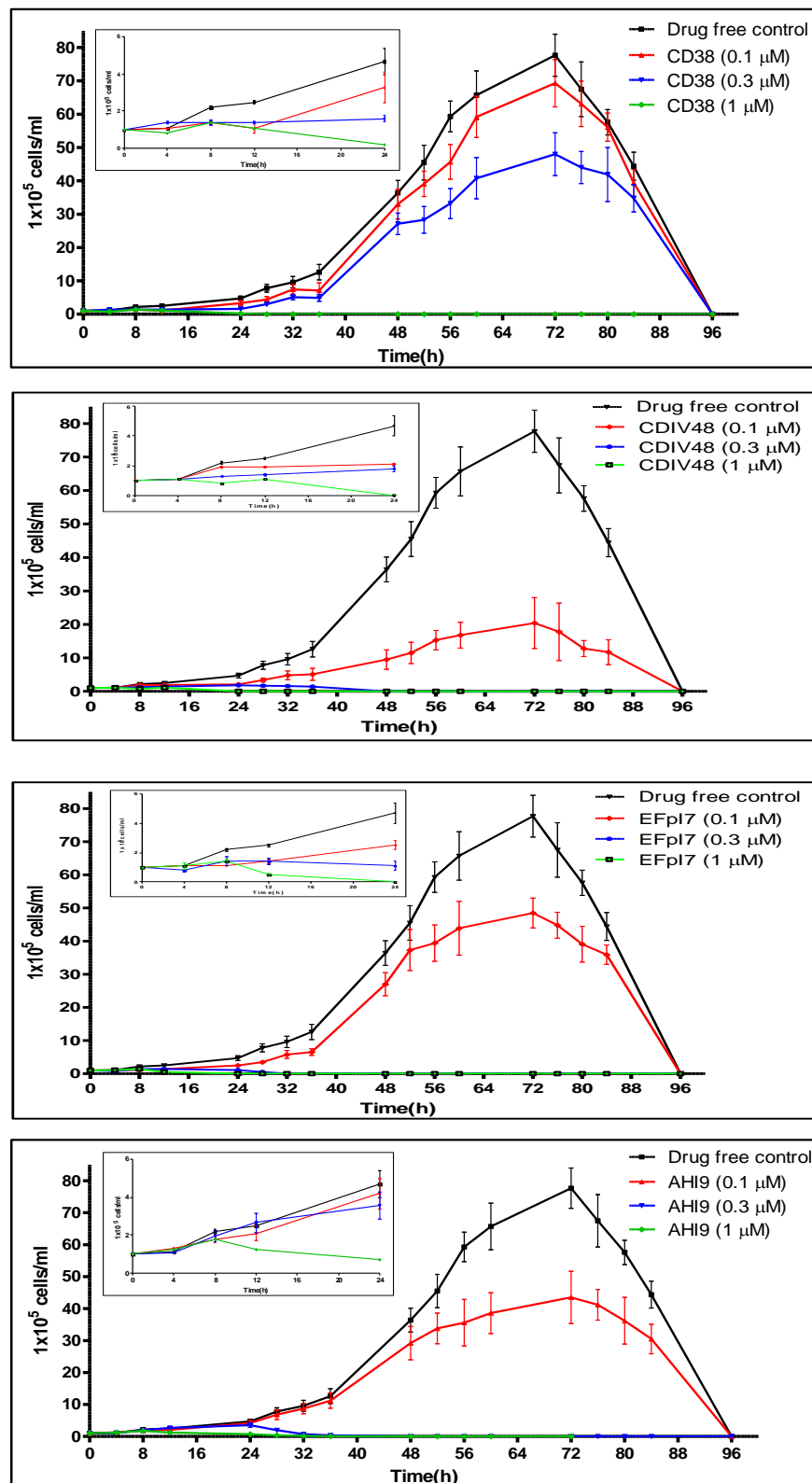


Figure 6.1. Effect of different concentrations of four bisphosphonium compounds on the growth of bloodstream form *T. brucei brucei* WT over 96 h. Cell cultures were seeded at 10^5 cells/ml. Inset shows the same data, but only for 24 h. Microscopic cell counts were performed in triplicate using a haemocytometer. The results shown are the average of three independent determinations; error bars depict standard errors.

6.3 Bisphosphonium compounds strongly affect mitochondrial membrane potential (Ψ_m)

As mentioned in the introduction, bisphosphonium compounds have a strong effect on the mitochondrial membrane potential (Ψ_m) of the parasite *Leishmania* (Luque-Ortega *et al.*, 2010). Accordingly, we investigated whether these compounds affect mitochondrial function in African Trypanosomes.

The mitochondrial membrane potential of treated and untreated cells were assessed by using Tetramethylrhodamine ethyl ester (TMRE) (Denninger *et al.*, 2007a). The cell density was adjusted to 1×10^6 cells/ml with and without test compounds for the duration of the experiment. One millilitre of sample was transferred into microfuge tubes at each time point and spun at 2500 rpm for 10 min at 4 °C and was then resuspended in 1 ml PBS containing 25 nM TMRE. Cells were then incubated at 37 °C for 30 min in the presence or absence of test compounds; valinomycin (100 nM) and troglitazone (10 μ M) were used as controls because they are known to induce mitochondrial membrane depolarisation and hyperpolarisation, respectively (Ibrahim *et al.*, 2011). All samples were analysed via flow cytometry by using a FL2-height detector and CellQuest software. Values are given as the percentage of cells with fluorescence above 100 arbitrary units (AU), which was set at about 50% for the controls (untreated cells). A shift to higher fluorescence indicates an increase of Ψ_m (hyperpolarisation), whereas a shift to lower fluorescence indicates a decrease of Ψ_m (depolarization) (Denninger *et al.*, 2007b).

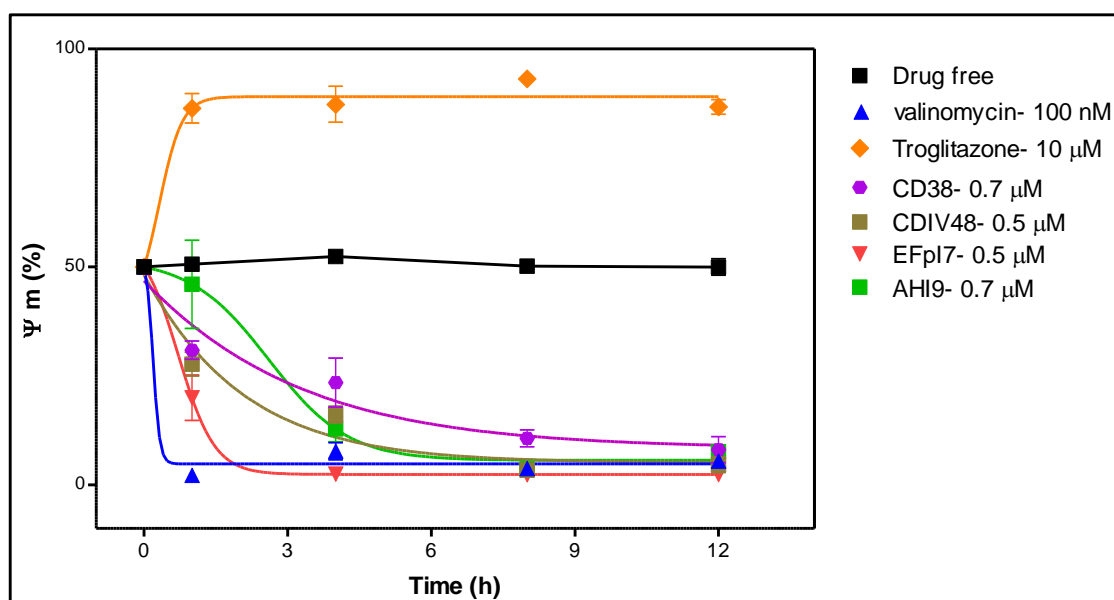


Figure 6.2. Effect of Bisphosphonium compounds on mitochondrial membrane potential (Ψ_m) as measured by flow cytometric analysis of bloodstream-form *T. b. b.* incubated with 25 nM tetra-methylrhodamine (TMRE). The results shown are the average of three independent determinations; error bars depict standard errors.

Results are presented in histograms of TMRE fluorescence (Appendix C). The results summary, shown in Figure 6.2, shows the Ψ_m at 0, 1, 4, 8 and 12 h. As expected, no change in Ψ_m for untreated cells appeared during 12 h, valinomycin induced a rapid and profound depolarisation of the mitochondrial membrane, and troglitazone caused a clear hyperpolarisation. There were clear effects on Ψ_m with CD38, CDIV48, and EFpI7, and at 1 h, the Ψ_m was already reduced, which continued until 12 h. In contrast, the Ψ_m appeared to be without change after 1 h of incubation with compound AHI9, after which it sharply decreased after 4 h. These results indicate that bisphosphonium cause depolarisation of mitochondrial membrane potential.

6.4 Effects of bisphosphonium compounds on ATP levels in *T. b. brucei*

As it was found in the above that the bisphosphonium compounds led to the depolarisation of mitochondrial membrane potential and it has been established

that the oligomycin-sensitive ATP synthase is accountable for maintaining the mitochondrial membrane potential in bloodstream form *Trypanosoma brucei brucei* (Brown *et al.*, 2006), we tested these compounds, at the same concentrations as above, for their effects on ATP levels.

ATP was measured by using an ATP determination kit (Invitrogen), which has D-Luciferin and Luciferase (firefly recombinant), as mentioned in Chapter Two (Section 2.14). A time course that was used to determine the ATP levels at 1, 4, 8, and 12 hours in *Trypanosoma brucei brucei*. During this time, the cells were grown in HMI-9 medium + 10% FCS in vented flasks with and without test compounds. Oligomycin (2 µg/ml) was used as positive control. The luminescence was recorded for each sample after subtracting the background luminescence. A standard curve was prepared using different concentrations of ATP standard solution (0, 10, 50, 100, 500 and 1000 nM) in order to calculate the ATP concentration of the samples from the standard (Figure 6.3).

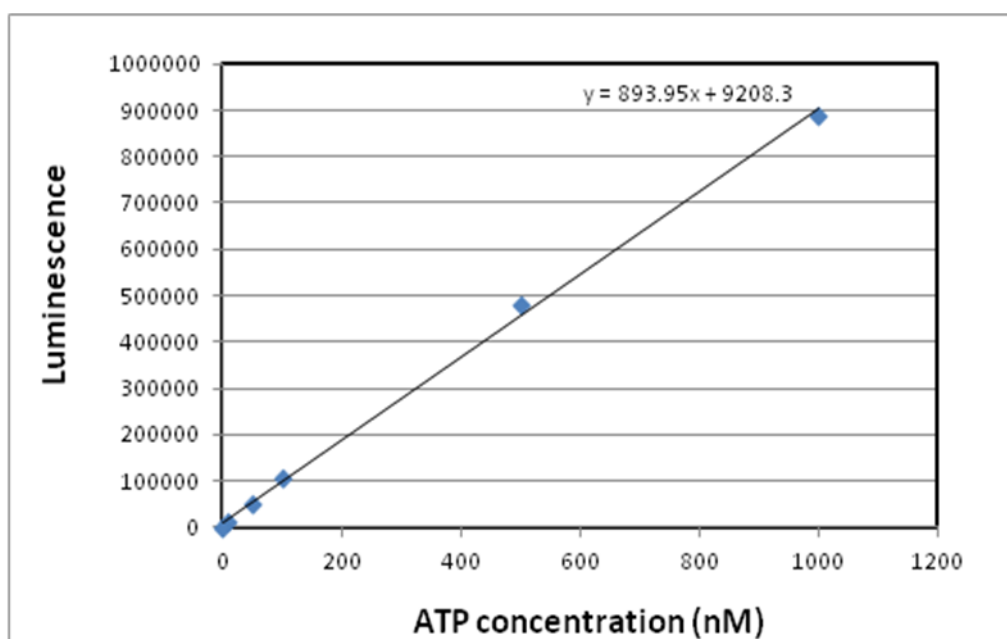


Figure 6.3. ATP standard curve. A standard curve was generated by serial dilutions of ATP to 0, 10, 50, 100, 500, and 1000 nM. 10 µl of the solution was added to the wells of a 96-well plate, which contained 90 µl of standard reaction solution. Luminescence was read by using a luminometer.

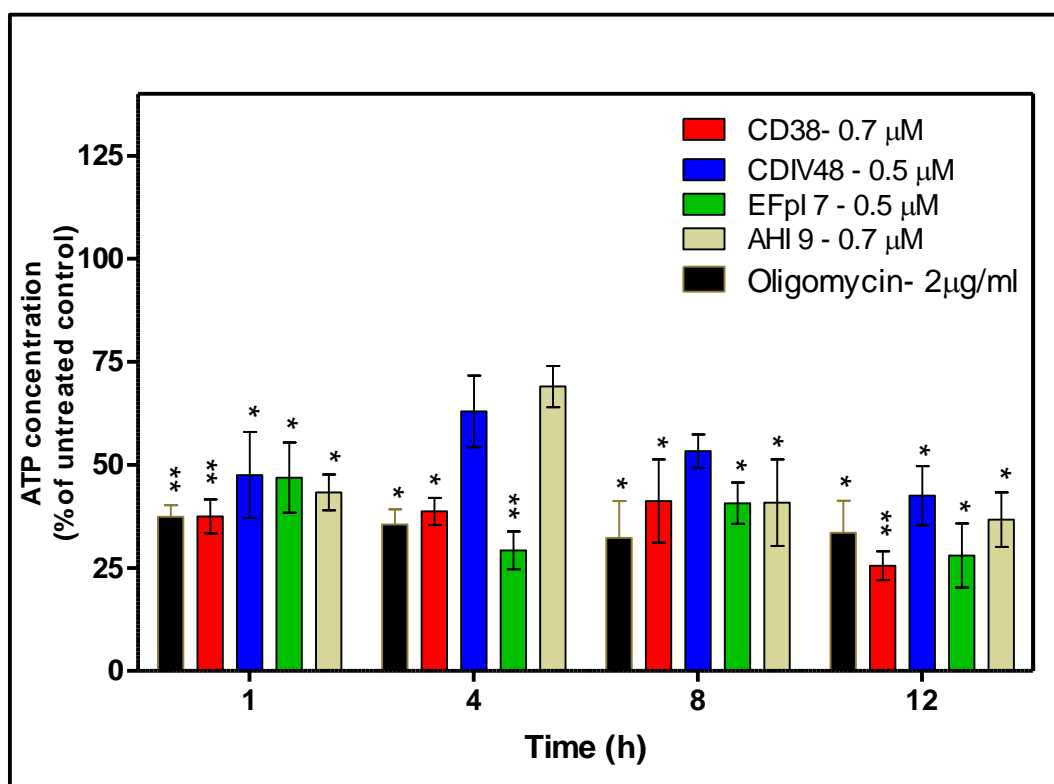


Figure 6.4. ATP concentration was measured using the ATP Determination Kit (Invitrogen) as described in section 2.12. 1×10^6 cells/ml of untreated and treated *T. b. brucei* bloodstream forms were incubated with different of bisphosphonium compounds and with oligomycin for up to 12 hrs. ATP concentrations were calculated from the standard curve and presented in this graph as the percent of untreated control. Results are the average of four independent determinations and error bars are SEM. P-values were calculated using the unpaired Student's t-test (* $P < 0.05$, ** $P < 0.01$).

The results showed the effects of the bisphosphonium compounds CD38, CDIV48, EFpI7, and AHI9 (at 0.7, 0.5, 0.5, and 0.7 μ M, respectively) on intracellular ATP levels of *T. b. brucei* (figure 6.4). It is very clear that all these compounds inhibited ATP levels after one hour by more than 50%. This decline tended to continue with the progress of time, and at 12 h, the ATP levels were at about 30% for most of the compounds. Interestingly, there is a correlation between depolarisation of mitochondrial membrane potential and the reduction in intracellular ATP levels. However, the question is which of these actions will happen first. However, it is quite difficult to answer this from the data presented because these compounds affected both Ψ_m and ATP levels as early as 1 h.

6.5 Effects of bisphosphonium compounds on intracellular calcium levels

The mitochondria have a large ability to sequester Ca^{2+} , and it was found in the above that there was depolarization of the mitochondrial membrane potential when they were treated with bisphosphonium compounds, so it could be speculated that this would lead to the release of Ca^{2+} from the mitochondria. Consequently, the effects of bisphosphonium compounds on intracellular calcium levels were examined. Intracellular Ca^{2+} was measured using the Screen Quest™ Fluo-8 Calcium Kit produced by ABD Bioquest. First of all, as mentioned in Chapter Two (Section 2.8), Ca^{2+} was determined during a 15 min exposure of the cells to 20 μM of different of bisphosphonium compounds. However, there was no calcium response over this period, although the positive control, 10 μM of the calcium ionophore A23187, caused a sharp and immediate increase in Ca^{2+} (data not shown). Therefore, a time course was used to determine Ca^{2+} level over a much longer period, i.e. at 0, 4, 8, and 12 h. During this time, the trypanosomes were grown in HMI-9 medium + 10% FCS in vented flasks with and without test compounds, as mentioned in the materials and methods section in Chapter 2 (section 2.8).

Figure 6.5 shows the effects of the bisphosphonium compounds CD38, CDIV48, EFpI7, and AHI9 (at 0.7, 0.5, 0.5, and 0.7 μM , respectively) on intracellular calcium levels; cells that were not exposed to any drug, but treated exactly the same with 1% DMSO instead, were used as a negative control. The results were expressed as a percentage of fluorescence for the non-treated control, the zero time point was taken immediately after the addition of the test compound. None of the compounds displayed a clear effect on Ca^{2+} levels at 4 h. However, Ca^{2+} levels were raised after 8 h for all compounds and this was still evident at 12 h.

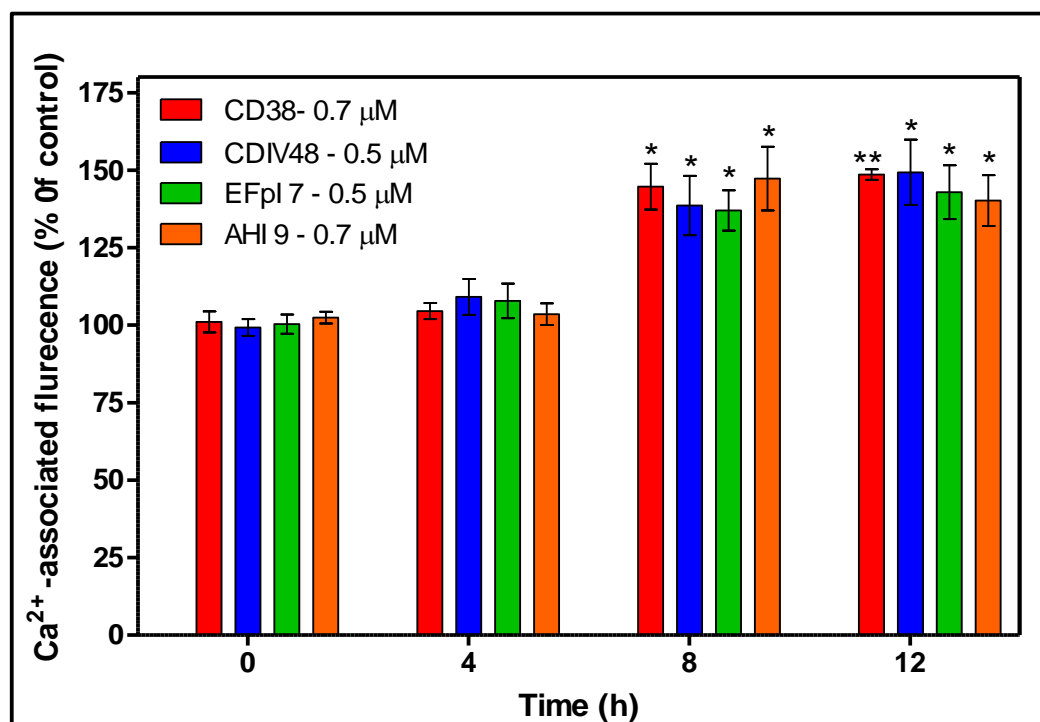


Figure 6.5. Effect of Bisphosphonium compounds on intracellular calcium levels of WT s427 bloodstream-form *T. brucei brucei* at 0, 4, 8, and 12 h. Parasites were loaded with Fluo-8 fluorescent indicator after 0, 4, 8, or 12 h of incubation with Bisphosphonium compounds. Data are presented as percentages of the non-treated control, for which calcium-associated fluorescence was measured in parallel cultures at the same time points. Results are the average of three independent determinations, and error bars are standard errors. * $P < 0.05$, ** $P < 0.01$ (Paired Student's t-test).

Interestingly, these results perfectly mirror the effects of the same compounds on Ψ_m , but they are delayed by several hours. Apparently, the slow rise in intracellular calcium is preceded by damage to the mitochondria. While it is not possible to prove cause and effect at this point, the data are suggestive of a leakage of calcium from dysfunctional mitochondria and are consistent with the mitochondria being the primary target of the cationic bisphosphonium compounds.

6.6 Cell cycle analysis in bisphosphonium-exposed cells

In order to establish whether bisphosphonium compounds have any effect on the cell cycle of trypanosomes, the DNA content was measured over 36 h. Flow cytometry was used as described (Hammarton *et al.*, 2003). The cell density was adjusted to 1×10^6 cells/ml with and without test compounds for the duration of the experiment. As described in Section 2.7, each sample was fixed in 1 ml of 70% methanol and 30% PBS and left at 4 °C overnight. After storage, the samples

were washed twice with 1 ml of PBS and subsequently resuspended in 1 ml of PBS containing propidium iodide and RNase A (both at 10 $\mu\text{g/ml}$) and incubated at 37 °C for 45 minutes while being protected from light. Samples were analysed by Becton Dickinson FACSCalibur using the FL2-Area detector and CellQuest software.

The results appeared to indicate that there was no effect on the *T. b. brucei* cell cycle by any of the bisphosphonium salts tested, as shown in Figure 6.6. There was no immediately obvious difference between the drug-free control and the test compounds, although the growth curve was reduced over the incubation time. Consequently, the ModFit programme was used to analyse the flow cytometry.

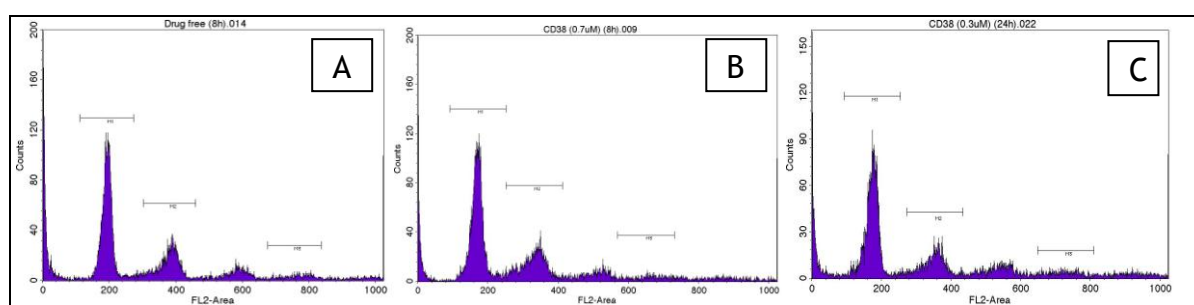


Figure 6.6. An example for flow cytometry analysis of the DNA content of bloodstream-form wild type *T. b. b.*, which was incubated for 8 and 24 h. (A) Drug free, 8h (B) CD38 (0.7 μM), 8h (C) CD38 (0.7 μM), 24h.

ModFit LT software (Verity Software House) helps to analyse the flow cytometry data by modelling the histogram peaks in order to find the percentages of the population at each cell cycle phase (G1: all cells have one kinetoplast and one nucleus; G2: all cells have two kinetoplast and two nucleus; S: DNA synthesis). Four bisphosphonium compounds (CD38, CDIV48, EFpI7, and AHI9 at 0.7, 0.5, 0.5, and 0.7 μM , respectively), including a drug-free control, were tested in order to study their effect on the cell cycle of wild type Tb427 over 36 h.

The results obtained from the analysis of the cell cycle by using ModFit software are presented in Appendix and the summary results are presented in Figure 6.8. It can be seen from the data in Figure 6.7 that there was a clear reduction of the cells in the S phase. This was observed for all compounds tested after 8 h of incubation, whereas as expected, there was no change in the S phase for the drug-free control when it maintained a normal growth rate. The percentages of

S phase decreased by more than 50% at 12 h for all compounds, except CDIV48, which displayed a 30% decrease of S phase at 12 h. This decrease continued over the incubation period, and S phase was decreased by about 80% of its original rate over 24 h of incubation for all test compounds. In contrast the percentage of cells in the G1 rate was increased by more than 10% at 12 h for all compounds.

The most striking result to emerge from the data is the strong relationship between the S phase and the growth curve, as is shown in Figure 6.8. The reduced S phase coincides with an inhibition of growth. Apparently the observed inhibition of DNA synthesis led to a cessation of growth and finally to the complete inhibition of the growth of the cells.

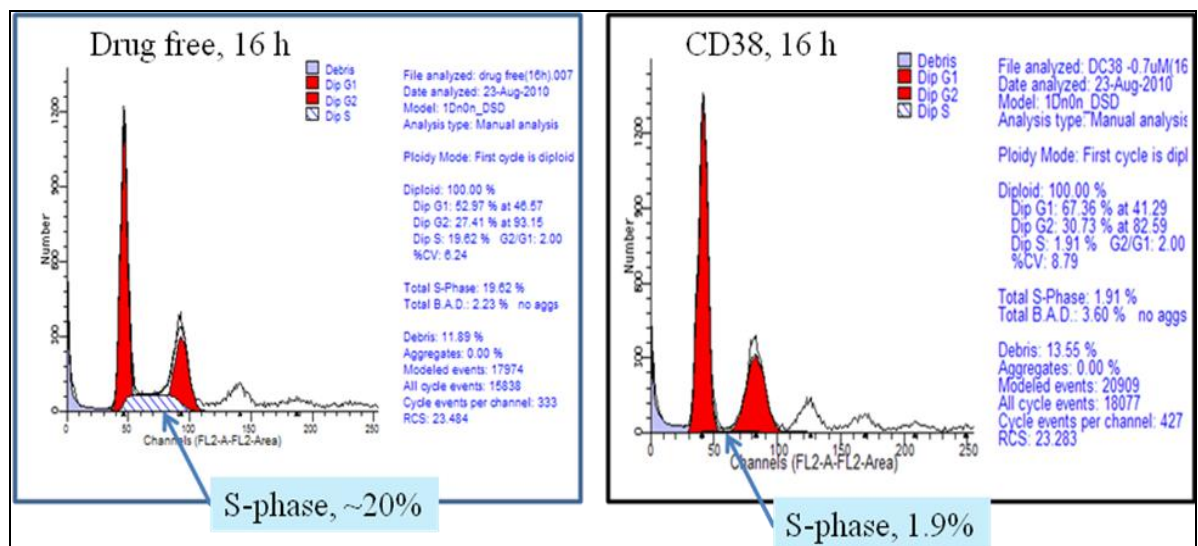


Figure 6.7. An example of flow cytometry analysis of DNA content by Modfit LT software for two samples, drug-free and CD38 (0.7 μ M), which were incubated for 16 hrs.

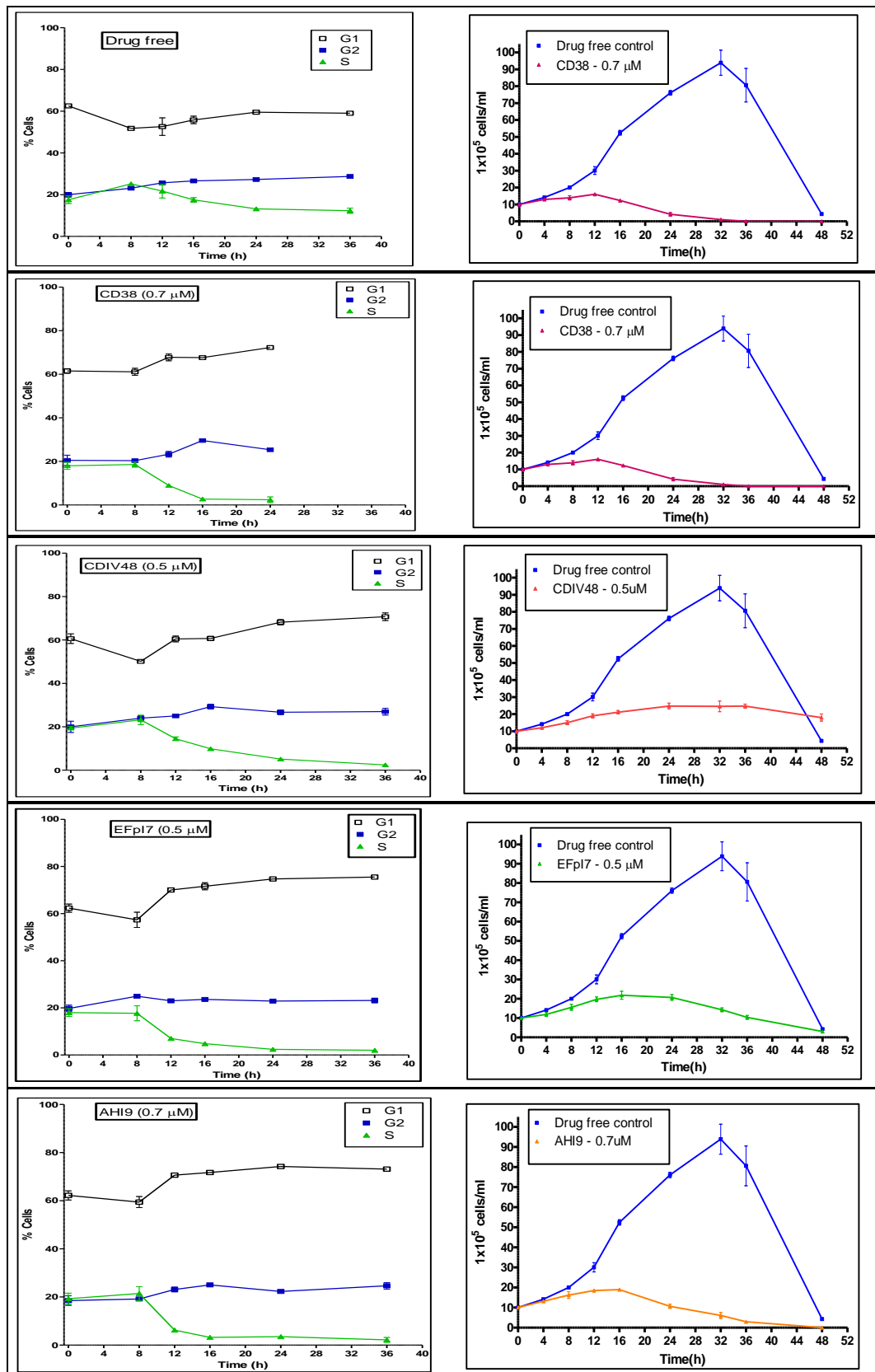


Figure 6.8. FACS analysis of DNA content of BSF *T. b. b.* for untreated and treated cells with bisphosphonium compounds. The percentages of cells in the G1, G2 and S phases were determined by using ModFit LT software and plotted on the left-hand side of each panel. In addition, the growth curve for each test compound was presented on the right-hand side of each panel, which was measured by using microscopic cell counts performed in triplicate using a haemocytometer. The results shown are the average of three independent determinations; error bars depict standard errors.

6.7 Analysis of the effect of bisphosphonium compounds on DNA configuration using fluorescence microscopy

The previous section showed that DNA synthesis was inhibited after 12 h of incubation, which was led to a clear reduction in S phase cells, and a block of cell division at that time. However, the flow cytometry gives no information as to whether both nuclear and kinetoplast division is affected. In order to examine cell cycle progression in detail and confirm that cell division will be inhibited by exposure to those compounds, fluorescent microscopy (DAPI stain) was carried out.

DNA configuration from nuclei and kinetoplasts were assessed using the dye 4,6-diamidino-2-phenylindole (DAPI), which fluoresces when bound with DNA. Five hundred cells were recorded for each sample, scoring for the presence of DNA in nuclei and kinetoplasts. Cells were scored into the following these groups: 1N1K (one nucleus and one kinetoplast), 1N2K (one nucleus and two kinetoplasts, 2N2K-E (two nuclei and two kinetoplasts, but no clear furrow towards cell division), and 2N2K-L (two nuclei and two kinetoplasts and the cells were almost completely divided into two daughter cells). Two samples were used in this experiment, a drug free control and CD38 (0.7 μ M). The initial cell density for both the treated and untreated samples was 5×10^5 cell/ml. Once again a time course was used in this experiment, and the treated and untreated cells were examined at 0, 8, 16, and 24 h, and the percentage of population was determined by observing the improvement of the cell cycle.

The results are shown in Figure 6.9. As was expected, there was no difference between the drug free controls and cells treated with CD38 at 0 h of incubation for all cell cycle stages. However, the percentages of cells in 1N2K that were incubated with CD38 was significant decreased from 10% to 4% ($P < 0.001$) after 8 h of incubation and continued to decrease to 2% after 16 h of incubation. In addition, after 24 h of incubation with CD38, no cells in 1N2K were measured. This clearly shows that the block was effective at the earliest part of cell division, i.e. the division of the kinetoplast, as well as inhibiting nuclear DNA synthesis (section 6.6). The percentages of cells in 2N2K-E decreased gradually

over the time incubation for the treated cells. It went from 7.7% at 0 h to 3% at 8h and continued to decrease to 1% at 16 h, which was significantly different from the drug free control ($P<0.01$). Furthermore, the percentages of the population in 2N2K-L was slightly increased at 8 h of incubation for treated cells, but it had reduced at 16 h, and at 24 h, there was a significant difference as compared with control cells ($P<0.001$). Apparently, those cells that had entered cell division were able to complete this cycle. This conclusion is consistent with the observation that the percentage of cells in 1N1K was maintained at its original level for both the untreated and treated cells until 8 h of incubation but increased slightly at 16 h and significantly at 24 h, with 96% of cells in this cell cycle stage as compared with 82% for untreated cells ($P<0.05$). It is very clear that cells treated with CD38 cannot re-enter the cell cycle, due to inhibited DNA synthesis, explaining that after 24 h of incubation the majority of the population was in stage 1N1K, whereas at the same time there was dramatic decline in the other stages of the cell cycle.

This result confirms the results of previous experiments (DNA content) that found that bisphosphonium compounds led to the inhibition the growth because DNA synthesis was inhibited.

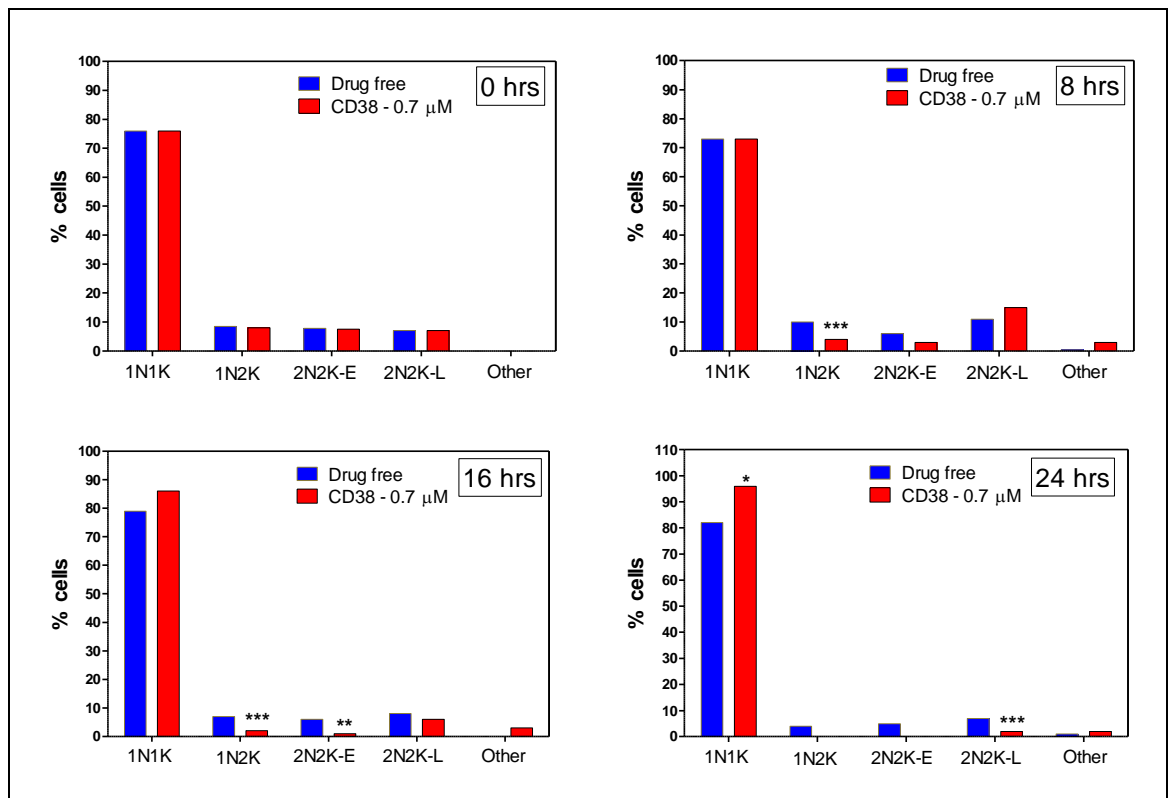


Figure 6.9. Percentage of wild type Tb427 populations in each stage of the cell cycle, with and without incubation with CD38 (0.7 μ M) over 24 h. For each culture, about 500 cells were counted and scored in terms of nuclei and kinetoplasts. N = nuclei, K = kinetoplasts, E = early stage of division, L = late stage of division. (* $P < 0.05$, ** $P < 0.01$, *** $P < 0.001$) which indicate a significant difference from the drug free control. P-values were calculated by using the Chi-squared statistical test.

6.8 Microscopical investigation of cellular morphology after treatment with selected bisphosphonium analogues

The previous results indicated that bisphosphonium compounds had a strong effect on bloodstream-form *T. b. brucei*, so it is important to study the trypanosomes' exterior morphology after exposure to these compounds. Giemsa staining and life cell microscopic images were produced to study the cellular morphology

6.8.1 Using Giemsa staining

When cultures of *T. b. brucei* that were treated with bisphosphonium compound, followed by Giemsa staining, were observed under a light microscope some atypical cells were observed. Some of the cells were swollen, in a characteristic manner i.e. they had posterior swelling and some had swelling in the middle of the cells. Many other cells appeared to be completely broken up (Figure 6.10).

The drug concentration was increased to 1 μM , as initially imaging was done at 0.7 μM CD38, 0.5 μM CDIV48, 0.5 μM EFpI7 and 0.7 μM AHI9 treated cells and the results showed that very few cells were affected by the presence of drug and showed the effects. So to observe a more noticeable swelling in the cell the drug stress on the cells was increased so that they may give a higher response to the drug and obvious swelling could be noted by increasing the concentration of the drug.

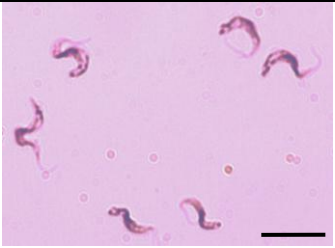
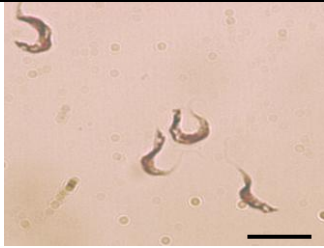

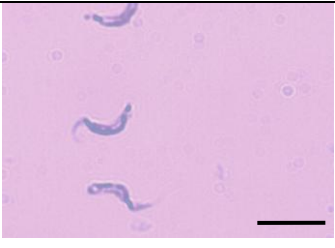
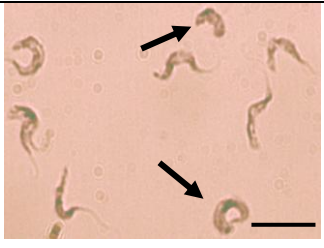
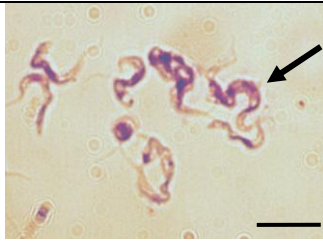



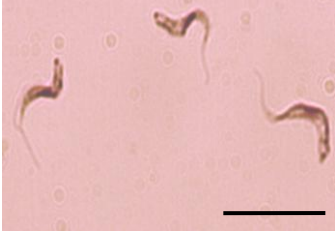





Drug	0 hrs	12 hrs	24 hrs
Drug free			
CD38 1 µM			
CDIV48 1 µM			
EFpl 7 1 µM			
AHI9 1 µM			

Figure 6.10. shows the cells under bright field light microscopy with the visualisation of BSF *T. b. b.* stained with Giemsa stain. Cells were incubated with 1 µM CD38, CDIV48, EFpl7, and AHI9, in addition to a drug free culture, at 0, 12, and 24 h. It can be seen that the samples from 12 and 24 hours of incubation showed swelling at the posterior–central parts, indicated with an arrow in the figure (scale bar = 50 µM).

6.8.2 Life cells images

Using the above method, images were taken of unstained cells. The images thus captured can show the swelling present in the cells. Cells incubated with test

compound for 12 or 24 h showed swelling of the posterior and central regions as shown with the help of arrows (Figure 6.11).

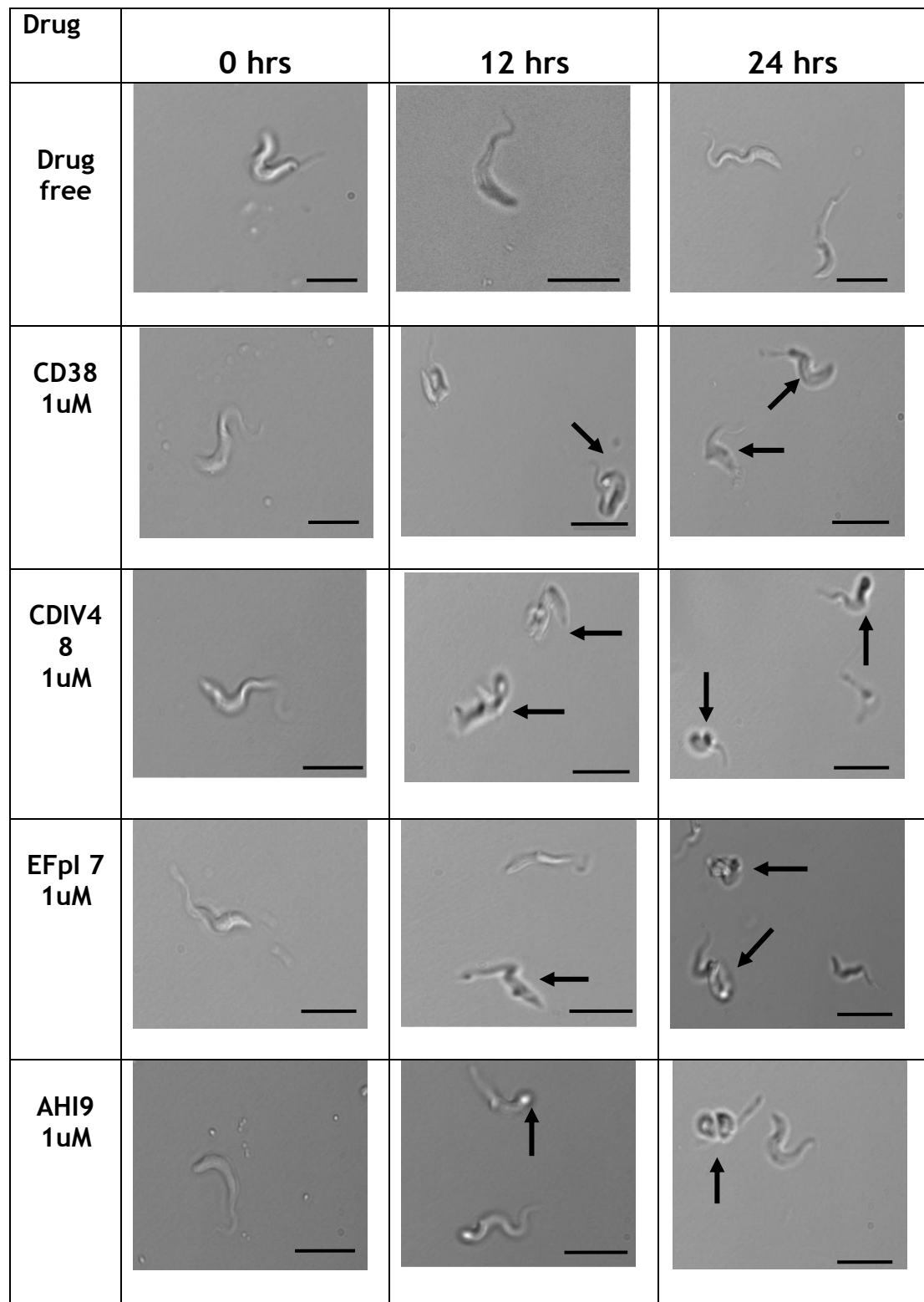


Figure 6.11. shows the images of live WT-s427 trypanosome cell samples. Samples were taken at 0, 12 and 24 h of incubation and were treated with 1 μ M CD38, CDIV48, EFpI7, and AHI9, in addition to a drug free control, and were observed under DIC microscopy. Arrows indicate swelling and abnormal cells. Scale bar = 25 μ M.

6.9 Electron microscopy of trypanosomes exposed to bisphosphonium compounds (TEM and SEM)

According to the results that were obtained from the microscopic investigation of cellular morphology after treatment with selected bisphosphonium analogues, there is clear proof that these compounds had an effect on the morphology of the treated cells. Consequently, Transmission Electron Microscopy (TEM) and Scanning Electron Microscopy (SEM) were used to study the effects of these compounds on the cellular structure of the cells.

6.9.1 Transmission electron microscopy (TEM)

The study focused on the organelles that are considered as to be the major ones affected by trypanocides: the mitochondria, glycosomes, microtubule distribution, the nucleus, the flagellum, and the flagellar pocket. These were studied in detail under transmission electron microscopy (TEM). Parasites were treated with 1 μM of CD38 over 20 h or left untreated (control).

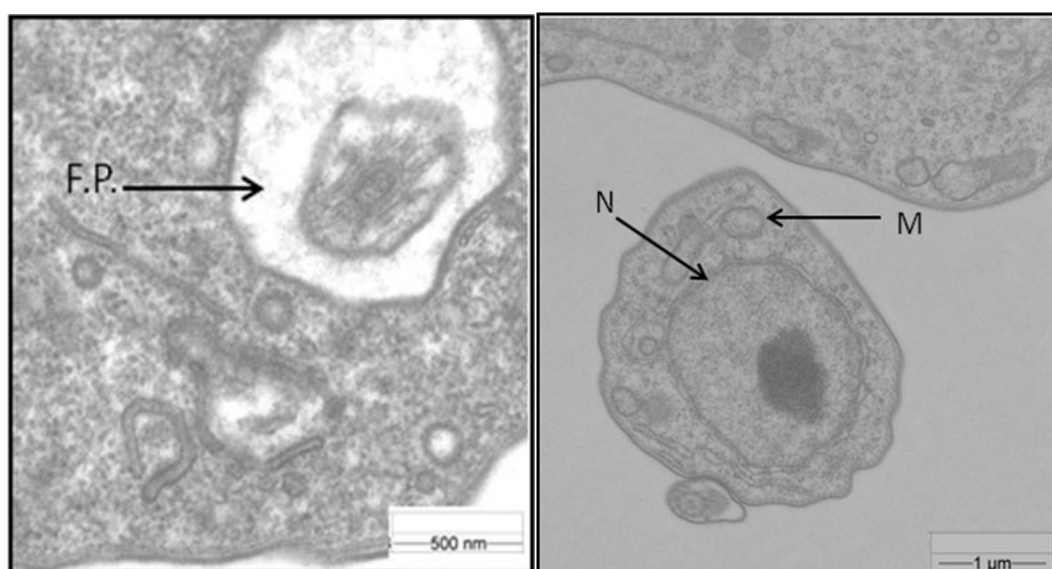


Figure 6.12. Transmission electron micrograph of an untreated bloodstream-form Tb427 wild type trypanosome. Control images taken at 0 h. (F.P.) = the flagellar pocket, (N) = the nucleus, and (M) = the mitochondrion. Magnification of 5000x.

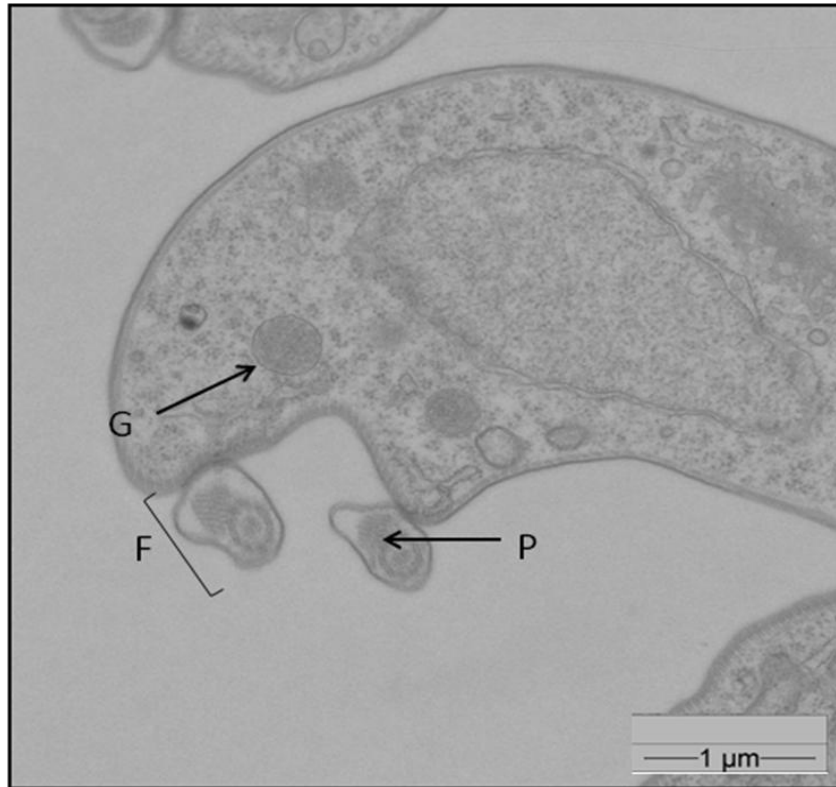


Figure 6.13. Transmission electron micrograph of a wild type bloodstream-form Tb427 trypanosome. Control images taken at 0 h . (F) = the flagellum, (P) = the paraflagellar rod, and (G) = glycosome. Magnification of 5000x.

Samples taken at 0, 12, 16, and 20 h showed the effect of the drug, and they were observed to be more bloated and rounded than those in the 0-hour incubation control sample (Figure 6.12 and 6.13). Those that were drug treated had thin cytoplasm; the cell was seen to be patchy and had an irregular appearance under the microscope.

The mitochondrion is one of the organelles that show the earliest signs that pathology has taken place. Abnormality in the mitochondrion can be observed at the 12 h and 16 h time points. The contents of the mitochondrion become very electron dense as they start to condense, whereas kinetoplasts appear to be unaffected at even this stage (Figure 6.14).

When the culture is observed after 12 hours, pathology can be noticed around the flagellar pocket, but is not that obvious (Figure 6.15).

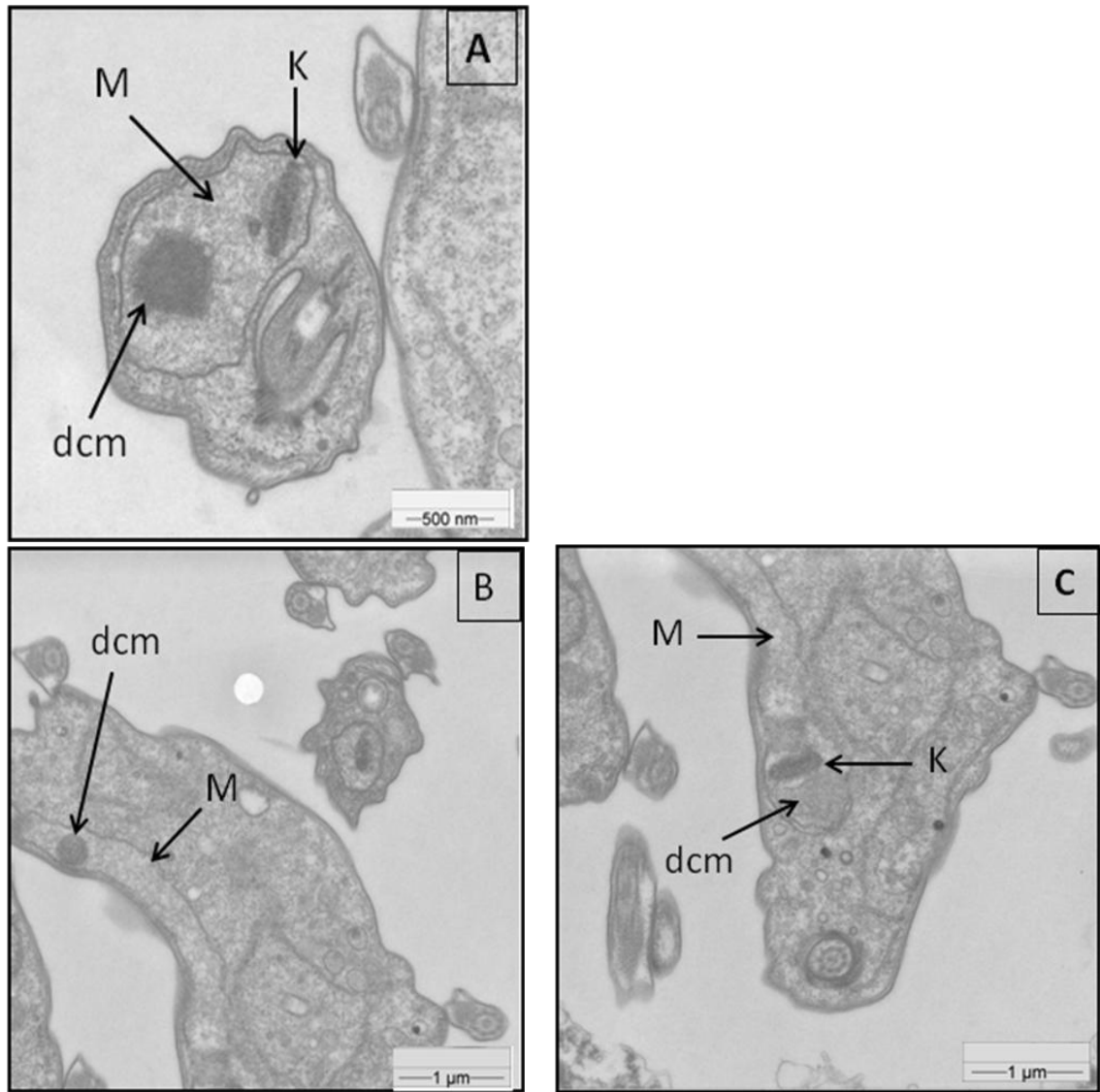


Figure 6.14. Transmission electron micrograph of a wild type bloodstream-form Tb427 Trypanosome. Cells treated with 1 μ M CD38 and incubated for 12 hrs (image A) and 16 hrs (image B and C). (M) = the mitochondrion, (K) = the kinetoplast, and (dcm) = distinct condensation of material. It can be shown that the matrix is patchy and uneven for M at 12 h with dcm, but there is no change in K. Images B and C are of different areas of the same cell. dcm is present in image B, whereas in image C, it has just started to form, and K is still not changed. Magnification of 8000x for image A and 5000x for images B and C.

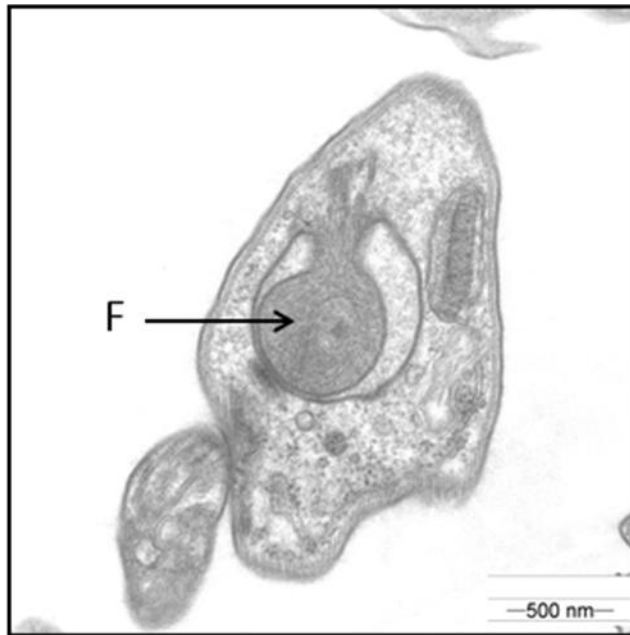


Figure 6.15. Transmission electron micrograph of an untreated bloodstream-form Tb427 Trypanosome. Cells were treated with 1 μ M CD38 and incubated for 12 h. (F) = the flagellum, which is swelling. Magnification of 5000x.

It was observed that microtubules grew in the cytoplasm of the affected cell and that they were not seen in the region where they normally occur. This was noted in the treated cells taken after 16 h, as shown in (Figure 6.16).

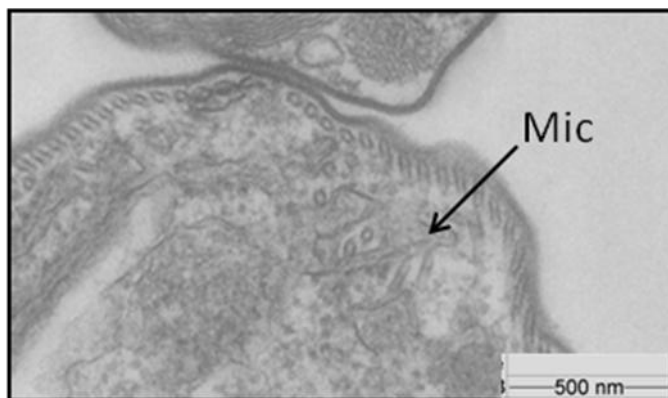


Figure 6.16. Transmission electron micrograph of a wild type bloodstream-form Tb427 trypanosome. Cells were treated with 1 μ M CD38 and incubated for 16 h. (Mic) = the microtubules, which are abnormal. Magnification of 5000x.

Another organelle that is affected is the glycosome. Glycosomes from the control and treatment group were compared and it was seen that the

glycosomes from the treatment group had their content distributed and appeared irregular after 12 and 16 h (Figure 6.17).

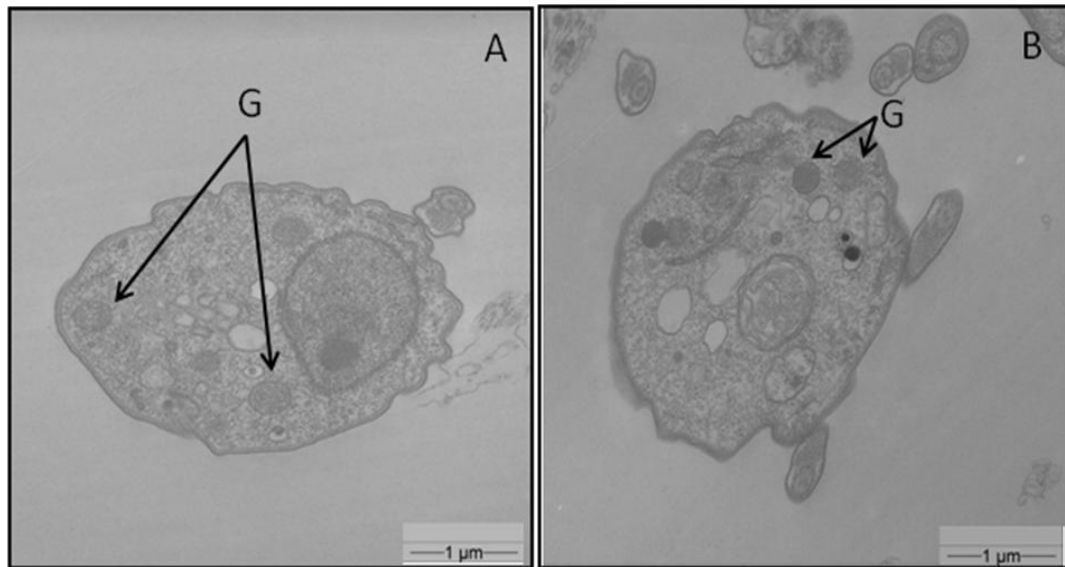


Figure 6.17. Transmission electron micrograph of a wild type bloodstream-form Tb427 trypanosome. Cells were treated with 1 μ M of CD38 and incubated for 16 h (image A) and 20 h (image B). (G) = glycosome. In both images, all glycosomes are disrupted, and more incubation time led to the reduced density of glycosomes and increased patchiness, as shown in image B. Magnification of 5000x.

It was observed in the cells taken at 20 h that the drug can also affect the nucleus of the cell. Under the microscope, it was seen that in the control group, the nucleus had round, visible boundary with a nucleolus present in it, whereas in the affected cell, the boundary of the nucleus appeared irregular, no nucleolus was visible, and the chromatin material of the nucleus was seen to be dispersed in the nucleus (Figure 6.18).

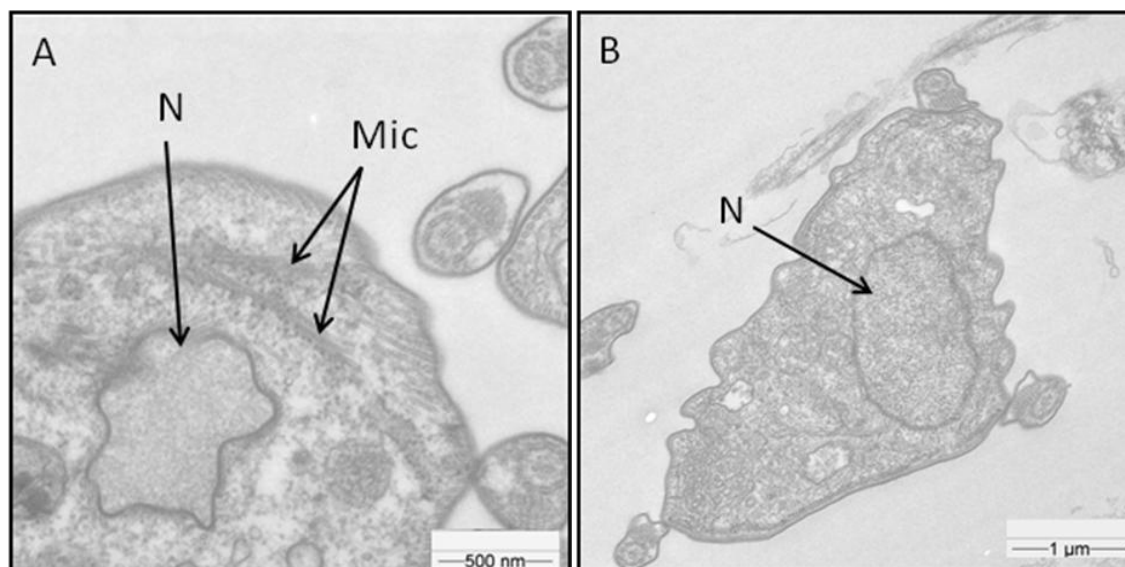


Figure 6.18. Transmission electron micrograph of a wild type bloodstream-form Tb427 trypanosome. Cells were treated with 1 μ M CD38 and incubated for 16 h (image A) and 20 h (image B). (N) = the nucleus, (Mic) = the microtubules. The nucleus became flaccid and the nucleolus is absent at 16 h, whereas at 20 h, the genetic material is dispersed and the nucleolus is as well. Magnification of 10000x for image A and 5000x for image B.

6.9.2 Scanning electron microscopy (SEM)

Bloodstream-form *T. b. brucei* was incubated with 1 μ M CD38 and its morphology was studied by using scanning electron microscopy (SEM) to observe the changes in the shapes of the cells. Trypanosomes were incubated with or without the test compound for 20 h.

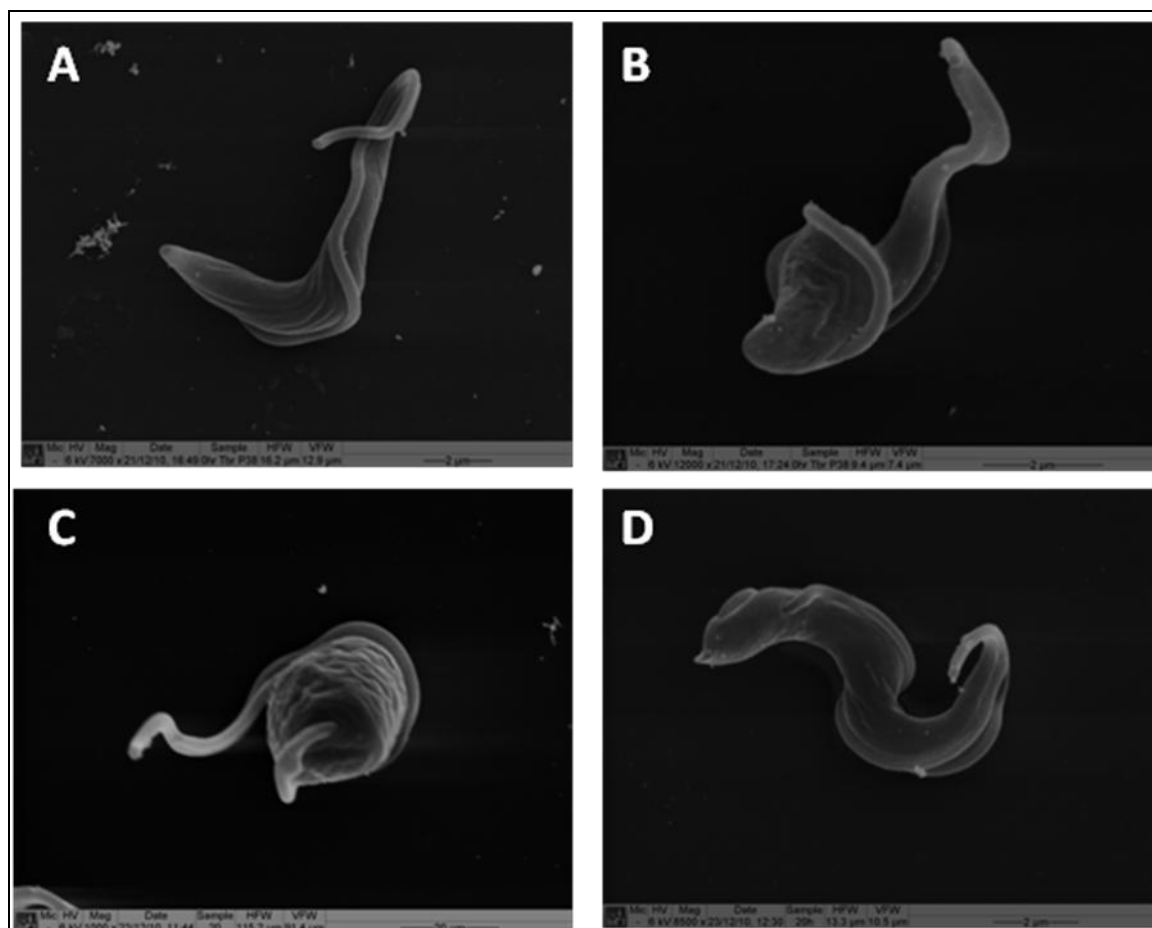


Figure 6.19. Scanning electron microscopy of bloodstream-form *T. b. brucei* that were incubated for 20 h. A: Drug free; B, C and D incubated for 20 h with 1 μ M CD38.

Figure (6.19 A) shows the control SEM of the normal structure of the trypanosomes that were incubated without the test compound for 20 h. Figure (6.19 B) shows that exposure of parasites with 1 μ M of CD38 for 20 h resulted in clear distortions in general structure. In addition, Figure (6.19 C) demonstrates that there was a disorganisation of the structure of the cell surface, which led to the swelling of the cells. Figure (6.19 D) shows that the posterior of the trypanosome was concave as compared with normal cells.

6.10 Bisphosphonium-induced cell death in trypanosomes does not require protein synthesis

It is confirmed by the results presented in this thesis that bisphosphonium compounds have a strong effect on trypanosomes and can kill them at even sub-

micromolar amounts. Apoptosis or Programmed Cell Death (PCD) is reported to occur in African trypanosomes, and this is a process that requires protein synthesis (Duszenko *et al.*, 2006). Therefore, to examine whether bisphosphonium compounds-induced cell death depends on protein synthesis or not, cells were pretreated with cycloheximide (CHX), an inhibition of protein synthesis, and then treated with different concentrations of bisphosphonium compounds to observe cell growth over 24 h. Control cultures were left untreated.

The cell density of bloodstream-form *T. b. brucei* was adjusted to 5×10^5 cells/ml, and the cells were divided into two groups. One of them was treated with 10 µg/ml of CHX, and the second was left without CHX, but with the same concentration of DMSO (less than 1%). Then, the cells were incubated in normal culture conditions for 1 h. Both cultures were subsequently aliquoted into different flasks and treated with bisphosphonium compounds (CD38 and EFpI7) at 0, 1, and 3 µM. The cell count was performed by using light microscopy and a haemocytometer at 0, 4, 8, 12, and 24 h.

Treatment of trypanosomes with CHX displayed growth arrest even in the absence of bisphosphonium compounds, due to their inability to produce the required proteins; this shows that the CHX treatment was effective. More interestingly, the results in Figure 6.20 show that after treatment with different concentrations of CD38 and EFpI7 the growth curves with and without CHX pretreatment were identical over 24 h. This appears to confirm that bisphosphonium-induced cell death in trypanosomes does not require protein synthesis and does not support the hypothesis that bisphosphonium compounds lead to programmed cell death for trypanosomes.

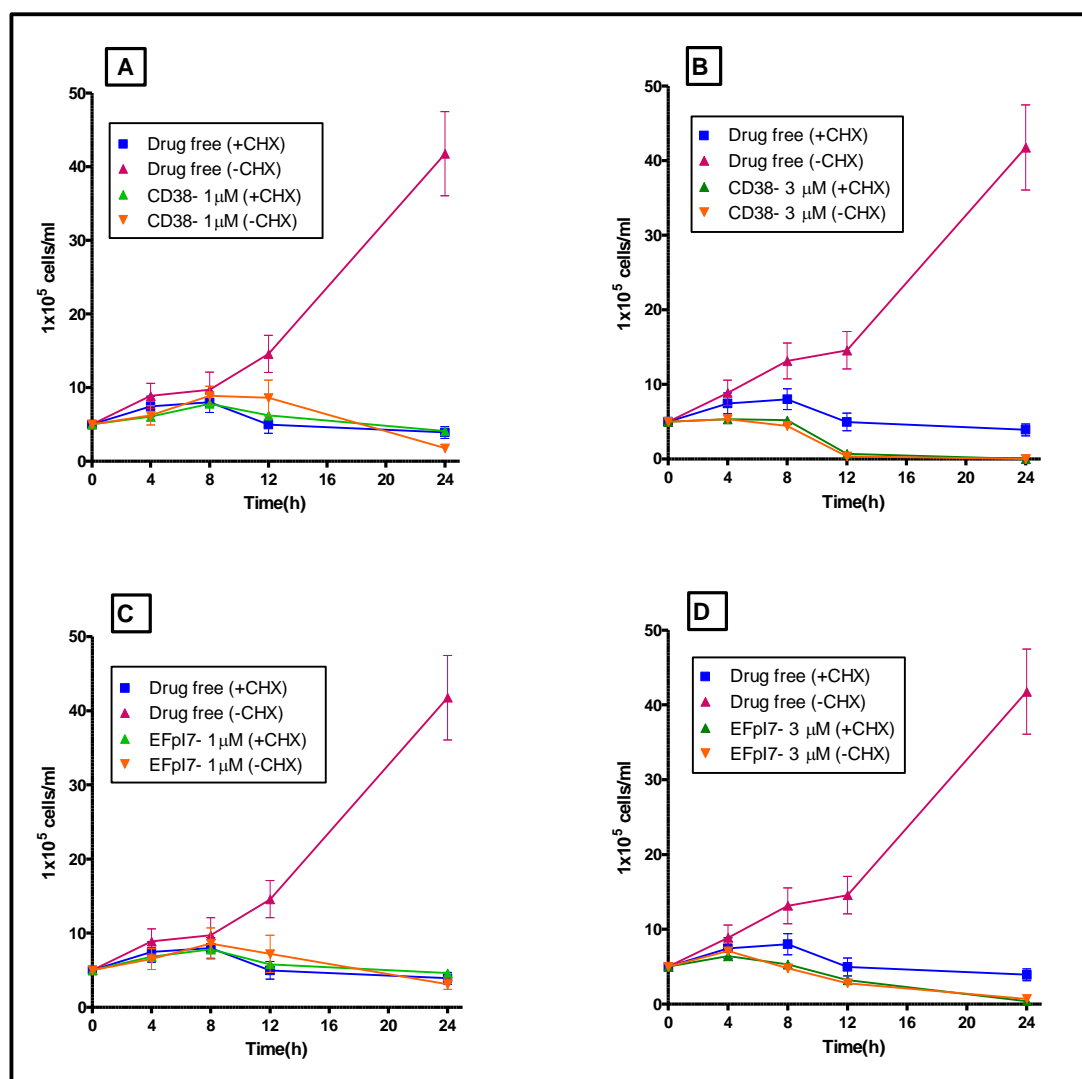


Figure 6.20. Effect of different concentrations of bisphosphonium compounds on the growth curve of bloodstream-form *T. brucei brucei* WT over 24 hrs. Cells were seeded at 5×10^5 cells/ml and treated with and 10 μ g/ml of cycloheximide or not (+CHX, -CHX) for one hour and then treated with different concentrations of chemicals as follows: A: drug free and 1 μ M of CD38, B: drug free and 3 μ M of CD38, C: drug free and 1 μ M of EFpI7, D: drug free and 3 μ M of EFpI7. Microscopic cell counts were performed in triplicate using a haemocytometer. The results shown are the average of triplicate determinations, each triplicate taken from a separate sample but within the same experiment; error bars depict standard errors.

To confirm that CHX led to the inhibition of protein synthesis, the concentration of CHX used in this experiment was identical to the one used in the experiments involving cell counting (above). First we performed a cell culturing step up to a density of 5×10^6 cells/ml and the culture was dispensed into two separate flasks, followed by the addition of cycloheximide (10 μ g/ml) into one of them. In the other flask, no CHX was added, but 1% DMSO was added instead (CHX solvent) and served as the control. Both flasks were kept in incubators at 37°C

and 5% CO₂ for 1 h. The addition of a radioactive isotope was performed in each flask, employing 25 µCi of [³H] lysine, and they were kept in incubation for 3 h. As mentioned in Chapter Two (Section 2.16.1), the labelling of the protein pool in *T. b. brucei* was determined by measuring the amount of incorporation of [³H] lysine in the trypanosome populations in both flasks.

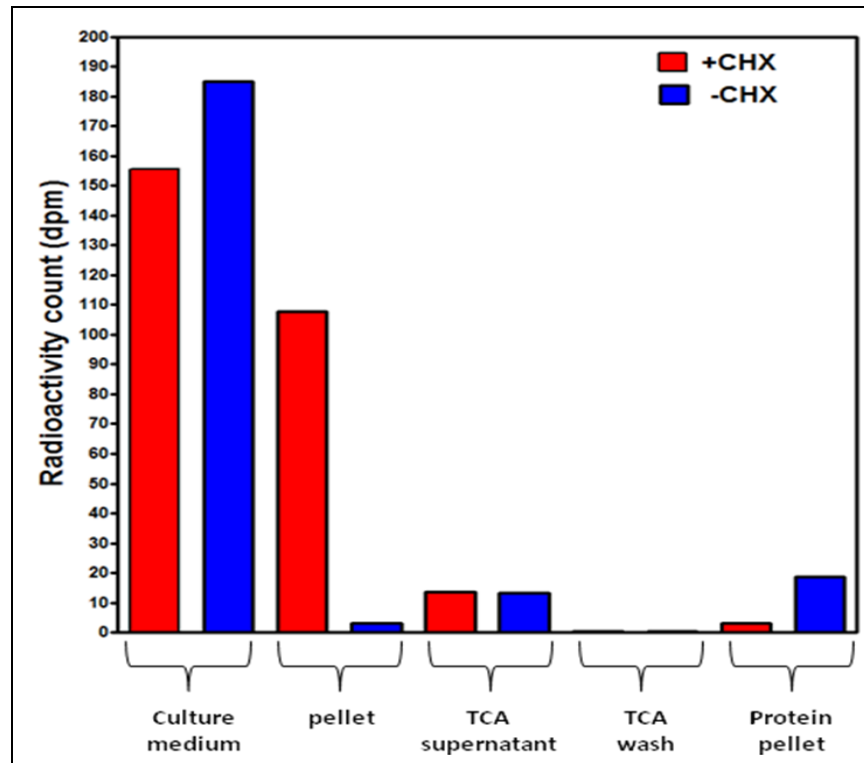


Figure 6.21. The graph shows the radioactivity count of a 10 ml culture of bloodstream-form *T. b. b.* at 5×10^6 cells/ml, which were incubated with (+CHX) and without (-CHX) 10 µg/ml cycloheximide for 1 h, following incubation with 25 µCi of [³H] lysine for 3 hrs. As mentioned before, the measurement of the radioactivity was performed at different stages. 1- Culture medium after first spin (100 µl), 2- pellet of cells after added 1% SDS for lysing the cells, 3- trichloro acetic acid (TCA) supernatant, 4- the second TCA supernatant for washing, 5- protein pellet.

From Figure 6.21, the radioactivity count for both samples, with and without CHX, in different stages can be seen. However, the main result in this graph is that the amount of [³H] lysine in the protein pellet for the culture that was treated with CHX is six-fold less than that of the sample which was untreated with CHX, which confirmed the fact that the CHX led to the inhibition of protein synthesis.

6.11 TUNEL assay

Programmed cell death or apoptosis is also associated with DNA fragmentation. Therefore, a TUNEL assay was used to detect DNA fragmentation after exposure to different compounds. Two bisphosphonium compounds, CD38 (0.7 μM) and EFpI7 (0.5 μM), were used in this experiment, and a positive control was used, which was phleomycin (2 $\mu\text{g/ml}$) (Sleigh, 1976). In addition, a negative control was drug free. The cells were treated for 24 h, and the results show that there was significant difference between the drug free cultures and the cells treated with CD38 or EFpI7 (Figure 6.22). Phleomycin also displayed a strong effect on the cell population but, at the concentrations used, the bisphosphonium compounds appeared to induce an even more pronounced DNA fragmentation after 24 h (Figure 6.23).

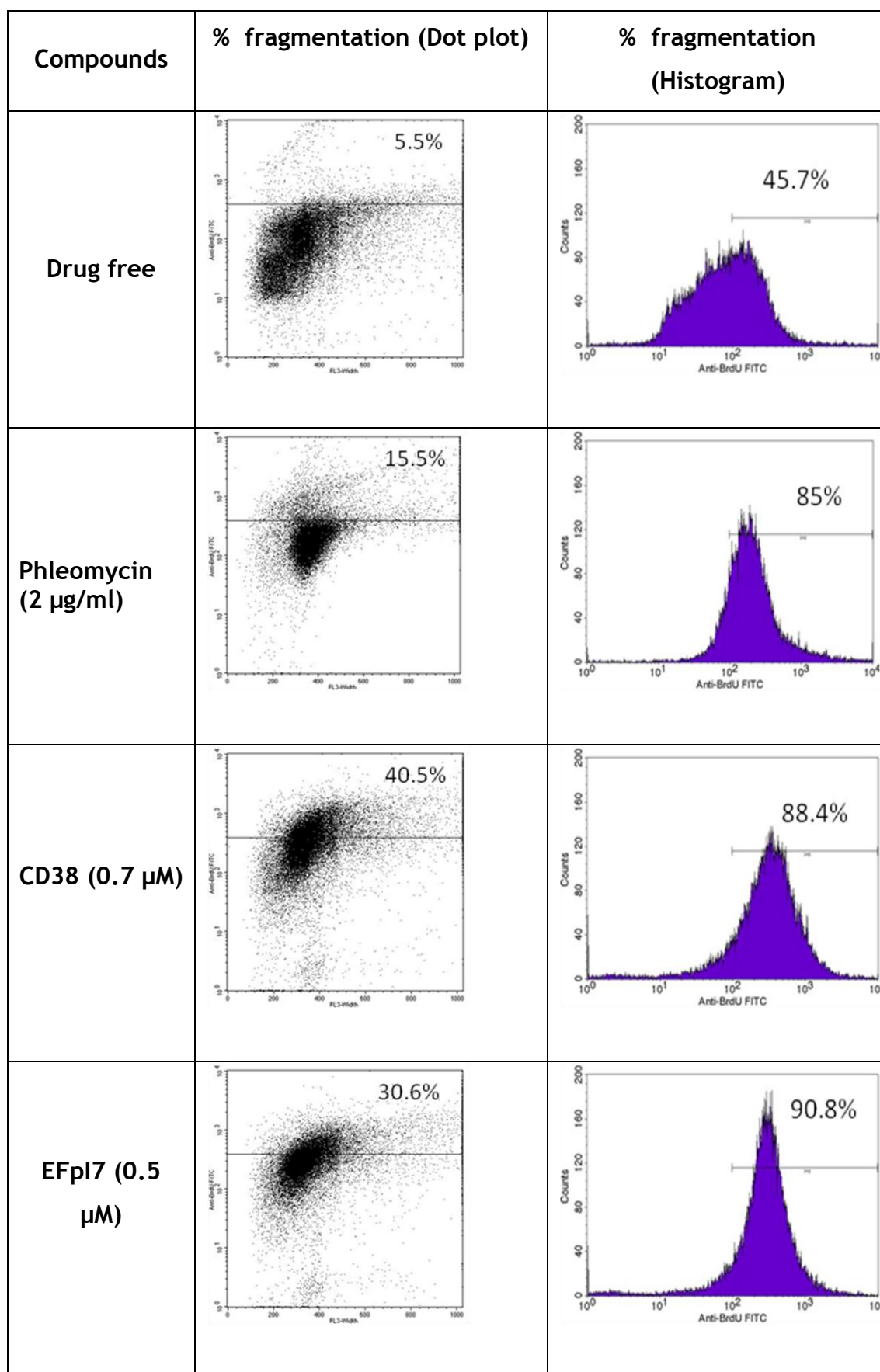


Figure 6.22. TUNEL assay of apoptotic cells of bloodstream-form *T. b. b.* that were treated with different compounds or left untreated and incubated for 24 h. Cellular DNA was stained with PI while DNA strand breaks were labelled with Br-dUTP followed by FITC-conjugated Br-dU antibody.

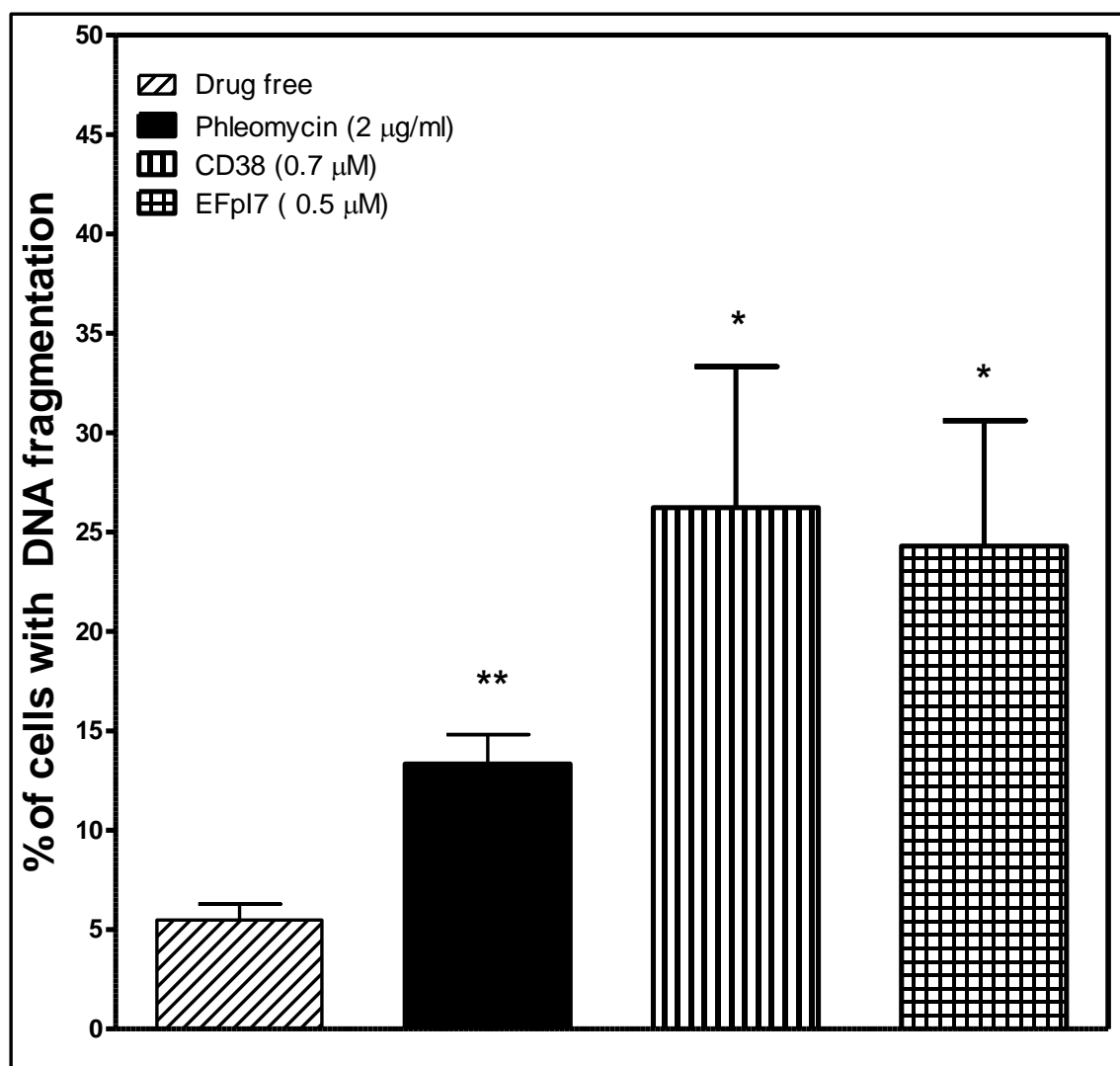


Figure 6.23. . TUNEL assay of DNA fragmentation cells of bloodstream-form *T. b. b.* that were treated with different compounds or left untreated and incubated for 24 h. Cellular DNA was stained with PI while DNA strand breaks were labelled with Br-dUTP followed by FITC-conjugated Br-dU antibody. Results are the average of three independent determinations and error bars are Standard errors for Dot plot figures. The data are expressed as % difference of cells with significant DNA fragmentation. P-values calculated using the unpaired Student's t-test (* $P < 0.05$, ** $P < 0.01$) compared with drug free control.

6.12 Discussion

A study of the mode of action of bisphosphonium compounds in wild type bloodstream-form *T. b. brucei* was performed in this chapter. As mentioned before, bisphosphonium compounds have a strong effect on the mitochondria of Leishmania (Luque-Ortega *et al.*, 2010), which led to the inhibition of complex II of the respiratory chain, leading in turn to several other changes, such as decreased levels of ATP and reduced mitochondrial membrane potential. Therefore, our hypothesis here is that the target of the bisphosphonium compounds in bloodstream-form *T. b. brucei* could be the mitochondria.

A number of techniques were used and developed to assess the effects of these compounds on trypanosome growth, mitochondria membrane potential, intracellular calcium level, ATP level, DNA content, DNA configuration and cell morphology after treatment with test the compounds. In addition, that these compounds induce apoptosis in trypanosomes was investigated.

An assessment of trypanosome growth shows that bisphosphonium compounds have a slow effect at concentrations close to EC_{50} , whereas the effect was increasingly rapid at higher concentrations. For example, at concentrations $\leq EC_{50}$ of CD38, there was little effect on growth, while at $5 \times EC_{50}$ ($1 \mu M$), all cells were killed after 24 h. The slow effect of bisphosphonium compounds has already been confirmed by various experiments, such as real-time viability monitoring (Taladriz *et al.*, 2012). On the other hand, these results assisted us in choosing the best concentrations and incubation time combinations for studying the mode of action. Indeed, the concentration that has a strong inhibitory effect on cells, but does not yet kill the cells is preferred because it helps in tracking the early changes in the cells over the period of the test.

Monitoring the mitochondrial membrane potential (Ψ_m) with TMRE flow cytometry shows that cells treated with bisphosphonium compounds led to the depolarisation of Ψ_m . With the exception of AHI9, all compounds decreased Ψ_m after 1 h of incubation time, and at 4 h all compounds showed a depolarisation of Ψ_m , which continued until the end of the time course at 12 h. In addition, there was the inhibition of intracellular ATP levels when cells were treated with

these compounds after 1 h as well, which may be good evidence that the effect on Ψ_m led to inhibited ATP levels because the loss of MMP caused the dysfunction of the mitochondria, which led to inhibition of ATP synthesis. The mitochondria were unable to recover as Ψ_m and ATP levels remained reduced throughout the 12 hours of the experiment.

It is difficult to decide which one of these actions happens first, ATP inhibition or Ψ_m depolarisation. However, both actions depend on one another. Due to bisphosphonium compounds' effect on Ψ_m , which led to the dysfunction of the mitochondria, Ca^{2+} was released (or leaked) from the mitochondria into the cytosol, and intracellular calcium levels started to increase after 8 h of incubation. This result is similar to the effect choline-derived compounds displayed on Ψ_m and Ca^{2+} level when the depolarisation of MMP led to increased Ca^{2+} level (Ibrahim *et al.*, 2011).

The initial findings from this study show that treated cells experienced stress, expressed clearly in reduced Ψ_m and ATP levels. Another effect of bisphosphonium compounds was on cell cycle, and their cell cycle arrest of trypanosomes, apparently preventing entry into S phase. In other words, DNA synthesis was inhibited and the cell cycle could not be completed. As a result cells accumulated in the G1 phase, which was significantly increased after 8 h, showing that cells in cell division were able to complete this and re-enter G1.

This was confirmed by fluorescence microscopy. Staining trypanosomes exposed to CD38 (0.7 μM) with DAPI and scoring the DNA configuration appears to show that after 8 h of incubation with CD38 DNA synthesis was inhibited even before kinetoplast division and that, consequently, the number of cells that had 1N2K decreased gradually with increasing treatment cells. At the same time, the number of cells that had 1N1K gradually increased, and the cell cycle progression blocked.

The microscopic investigation of the morphology of cells that were treated with selected bisphosphonium compounds was applied. Giemsa staining and life cell images were used first, and the results show that these compounds have a slow effect on cell morphology, which was very clear after 12 h of exposure. For all the compounds that were used, the cells had damage and swelling, but light

microscopy did not provide the resolution necessary to determine which organelles caused these, so transmission electron microscopy (TEM) and scanning electron microscopy (SEM) were used to observe changes in the cells. When seen under TEM, it was observed that the material in the cell was condensed. This condensation of the contents of the cell may be due to the destruction of the organelles or due to the accumulation of the drug compound within the organelles, which is a significant mode of action for diamidines (Mathis *et al.*, 2006).

One explanation for the swelling observed in the light microscopy pictures would be an effect on the flagellar pocket. We know that the flagellar pocket plays an important role in protein trafficking (Field & Carrington, 2009). When endocytosis or exocytosis is inhibited this area becomes affected first, usually appearing grossly enlarged as a result. There are two possible reasons for this, one being that it is the only site at which all the endocytosis takes place, so it is the nearest region to become affected. The other reason is that because this area of the cell is important in protein trafficking, an inhibition of vesicular traffic results in a damaging accumulation of material at that site, and a dearth of essential proteins in some organelles. However, the TEM images do not support this explanation, as flagellar pockets appeared normal after treatment and there was no gross build-up of vesicular matter in its vicinity, nor were any abnormalities of the flagellum itself observed.

Instead the bisphosphonium compounds appeared to affect other organelles, such as the mitochondria, nucleus, glycosomes, and microtubules. It was not possible to determine with certainty the sequence by which these organelles were affected, but at 12 h the most striking observation was probably the appearance of condensed, electron-dense material in the mitochondria. This is consistent with the decrease of Ψ_m and ATP levels as early events after exposure, as well as the known mitochondrial targeting of phosphonium compounds in *Leishmania* (Luque-Ortega *et al.*, 2010) and human cells (Jiang *et al.*, 2009). In addition to the mitochondrial effects, bisphosphonium compounds clearly affected the nuclei, showing loss of shape and nucleolus; this is probably the cause for the specific cell cycle arrest in G1 phase. After 24 h the TUNEL assay indicated the presence of double strand breaks in DNA, although the DNA content assays showed that after 24 h the total content of nuclear DNA was not

strongly affected, i.e. the evidence suggests the presence of breaks rather than wholesale degradation of DNA.

The TUNEL result and mitochondrial damage could be taken as evidence for apoptosis or programmed cell death (PCD). Certainly, DNA fractionation is commonly taken to be part of the apoptotic process in mammalian cells and has equally been proposed to be a PCD indicator in protozoa; the slow release of mitochondrial calcium stores after mitochondrial damage also fits this model (van Zandbergen *et al.*, 2010). However, PCD is also believed to have an absolute requirement for protein synthesis and the prediction would be that inhibition of protein synthesis by pre-incubation with CHX would prevent bisphosphonium-induced lysis. In fact, this was not observed and we provisionally conclude that the cell death observed is not the result of apoptosis, at least not in the classical sense, where proteases are expressed in order to digest the cellular content, leading to cell death.

7 Chapter Seven: General Discussion

Despite the strenuous efforts of some organisation including as Medecins-sans-Frontiers, DNDi, the Bill & Melinda Gates Foundation and the Consortium for Parasitic Drug Development, as well as the efforts generated by the Millennium Goals, the burden of human and veterinary parasitic disease is still unacceptably high, especially in less developed countries. Among the most neglected tropical parasitic diseases, Human African trypanosomiasis (HAT) and leishmaniasis are infections that are caused by species of protozoa called *Trypanosoma* and *Leishmania* species, respectively. Many efforts are being made to control these diseases, including the use of chemotherapy. However, there are many problems associated with the few available drugs, including drug toxicity, resistance, a lack of guaranteed supply and high cost. Toxicity of some antiparasitic drugs has become a concern and has led doctors to urge precautions before use. For example, melarsoprol, which was used for treatment of the second stage of African trypanosomiasis, is toxic and causes a 5% death rate for patients who use it (Burri, 2010). In addition, side effects consist of nausea, vomiting and encephalopathy (Garcia, 2007; Jannin & Cattand, 2004; Legros *et al.*, 2002). The other issue is resistance to current antiparasitic agents. For instance, resistance to eflornitine (Vincent *et al.*, 2010) and melarsoprol (Delespaulx & de Koning, 2007; Legros *et al.*, 1999) for late stage HAT, and pentavalent antimonials for leishmaniasis (Sundar *et al.*, 2008) have been reported, further limiting treatment options. A further serious problem is the cost of the drugs, which has led to increased problems with therapy, especially in the poor countries where the diseases are concentrated. For example, the average cost to treat a second-stage *T. b. gambiense* HAT patient rose from €28 to €336 (Simarro *et al.*, 2012) from 2002 to 2010. As a result, for the reasons above and because of the limitations of existing drugs, development of new drugs is urgently needed for the most neglected diseases, such as trypanosomiasis and leishmaniasis.

Development of new anti-trypanosomiasis/leishmaniasis drugs should aim at an affordable cost, which would lead to an overall reduction in treatment costs. Solutions with an appropriate cost/benefit balance could well include natural products, but the search for new antiparasitics should by no means be limited to this strategy alone. However, the impetus to make new compounds from natural products is considerable (Newman & Cragg, 2007). Our study examined two types of compounds, which are curcumin and phosphonium-based, as potential

therapeutic lead compounds against *Trypanosoma* and *Leishmania* parasites. Curcumin, a polyphenolic compound obtained from the nutritional spice turmeric, is derived from the rhizome and roots of the plant *Curcuma longa* (Ammon & Wahl, 1991). Curcumin is used as an herb for adding spice, colour and flavour to food and is used as a traditional medicine in India and as such has little or no toxicity, and is cheap. Phosphonium compounds also include natural products (Taladriz *et al.*, 2012).

Methods that are generally used to evaluate drug activity were used in this study to examine the effectiveness of curcumin and phosphonium compounds against trypanosomes and leishmania parasites. A total of 158 curcumin analogues were tested against *Leishmania* species, and many of the analogues appeared to be effective against these parasites. In some cases, they were more active, measured by in vitro EC_{50} , than clinical drugs like pentamidine. Similarly, a majority of phosphonium analogues that were tested in this study (83) displayed strong activity against bloodstream form *Trypanosoma brucei brucei*, and more than 20% of these compounds have EC_{50} values < 100 nM. Resistant strains were also applied in this study as a model to examine cross-resistance between existing treatments and potential new trypanocides, a key issue for any new antiparasitic agent. Two *T. brucei* strains of increasing levels of multi-drug resistance were used and the results with both strains was compared with the activities observed against the sensitive parental strain, obtained in parallel. None of the analogues of curcumin and phosphonium displayed cross-resistance with the diamidine and melaminophenyl arsenical classes, *i.e.* there were no significant differences in EC_{50} values between the three strains for any of the compounds tested. As resistance to these important trypanocides has been linked to the loss of the P2 and HAPT drug transporters (Bridges *et al.*, 2007;Matovu *et al.*, 2003) it follows that these are not involved in the internalisation of curcuminoid and phosphonium compounds.

As mentioned above, it is very important for the development of new antiparasitic drugs that the new compounds must not be toxic to human cells; thus, their effectiveness against parasites should be optimised while toxicity is reduced, leading to increasing selectivity index (SI). Therefore, the toxicity levels for curcumin and phosphonium analogues were determined by testing these compounds on Human Embryonic Kidney (HEK) cells *in vitro* using an

Alamar Blue test. The results show that all of curcumin compounds were lower in toxicity to HEK cells than to bloodstream form *T. b. brucei* and *L. mexicana* amastigotes, consistent with our previously published results (Changtam *et al.*, 2010a). In addition, all phosphonium analogues appeared to have lower toxicity for human cells than to bloodstream form *T. b. brucei*: 60 out of 83 phosphonium compounds displayed an SI >200-fold.(Taladriz *et al.*, 2012).

A Structure Activity Relationship (SAR) is the relationship between the biological activity of a molecule and its structure. Using SAR analysis on a library of compounds will help determine the most important functional groups of the pharmacophore and is an essential tool in the further optimisation of the scaffold. SAR analysis was used in this study and depended on the EC₅₀ that was established by Alamar Blue tests for curcumin and phosphonium analogues. For curcumin compounds, 158 were tested on *Leishmania* spp and *T. b. brucei* and the results of SAR indicated the activity was improved in the following cases. First, mono-*O*-demethylated analogues increased activity against these parasites. Second, the addition of one or two pentyl pyridinium (C₁₀H₁₅N) groups leads to an increase of activity. Third, analogues that have an isoxazole ring show more activity against parasites, which is identical with other literature that has indicated that isoxazole analogues also have activity against *Mycobacterium tuberculosis* (Changtam *et al.*, 2010b). Fourth, pentyl bromide (OC₅H₁₀Br) substitutions at positions R3 led to the improvement of activity. Finally, the trienone analogues showed increased activity against all parasites tested. For phosphonium analogues, 83 of these compounds also were tested against *T. b. brucei*. SAR studies indicated that the EC₅₀ for some compounds were at nanomolar levels due to the bulky substituents around the bisphosphonium cations, while the linkers have less power to determine the activity. In addition, some monophosphonium analogues, such as AT31 and AT33, registered the lowest value of EC₅₀ of all the phosphonium compounds. The fact that phosphonium analogues displayed SAR against *T. b. brucei* and *Leishmania* (Luque-Ortega *et al.*, 2010) and in some cases displayed promising selectivity over human cells, gives hope that they might have broad anti-kinetoplastid activity. The essential next step is a thorough investigation of their in vivo efficacy.

To investigate the mode of action for curcumin compounds, various methods were employed. A preliminary investigation into the cellular actions of some curcuminoids was performed by my colleague Hasan Ibrahim, and he employed several tests including cell cycle progression, mitochondrial membrane potential, DNA fragmentation and production of reactive oxygen species. Although curcuminoids did not affect any of these parameters there was one experiment that could open new doors for understanding their mode of action. AS-HK014 compounds showed a strong and fast depletion of glutathione content in the hepatocytes of rats.

As part of the mode-of-action investigation we determined whether curcuminoids affect the plasma membrane or second messenger systems of trypanosomes, but there was no effect on cellular cAMP levels, plasma membrane potential, or any rapid effect on the intracellular free calcium concentration in bloodstream form *T. b. brucei*. However, addition of different concentrations of L-glutathione to trypanosome cultures led to a dose-dependent decrease of AS-HK014 activity. Evidently, glutathione reacted with the active compound and this appeared to confirm the observation with primary hepatocytes cultures.

A common method to study the mode of action is through an induction of resistance for the drug. So, a new line, resistant for AS-HK014, was generated for that reason. Metabolomic assessment of ASHK014 action on *T. b. brucei* was employed on both sensitive cells (WT) and the resistance line of AS-HK014 (TA014). The results show that for WT, AS-HK014 led to depletion of glutathione and trypanothione during 30 minutes of incubation, relative to the control (untreated cells). Results also showed reduced trypanothione disulfide. However, there was no evidence for an inhibition of trypanothione synthesis, as there was no change to levels of glutamate, ornithine and spermidine, which means that the effect is probably not metabolic but chemical, *i.e.* a direct chemical reaction between AS-HK014 and certain thiols. Strong evidence for this was also provided by the laboratory of Prof. Apichart Suksamrarn, which synthesised the curcuminoid library, and showed that AS-HK014 indeed forms a covalent adduct with glutathione (section 4.8).

On the other hand, it does not explain the resistance mechanism of TA014 cells. First, the protein expression levels of the two key enzymes of trypanothione biosynthesis, γ -GCS and GS, were analysed by western blot, but the result showed no difference in protein level between the cell lines, or for untreated and treated cells. Second, sequence analysis of two genes (γ -GCS and GS) was used to look for any mutation in the resistance line that led to resistance; however, no mutations were found in the γ -GCS and GS open-reading frames.

To gain an insight into the possible resistance mechanism, cross-resistance between *T. b. brucei*-WT and TA014 cell lines for some curcumin analogues and current clinical trypanocides was assessed. Although there was no cross-resistance between WT and TA014 for some curcumin compounds and clinical trypanocides, a clear cross-resistance was detected for curcumin compounds with a mono-enone linker, which confirms that this linker has some responsibility for the drug's activity and the resistance is to the mono-enone moiety and the chemical reaction it makes with thiols. The resistance may be linked to an increased efflux of the curcumin analogue or, more likely, the trypanothione adduct.

The effect of some bisphosphonium analogues on bloodstream form *Trypanosoma brucei brucei* was investigated to identify the target of these compounds. The compounds have been reported as *leishmanicidal* compounds, by causing mitochondrial dysfunction (Luque-Ortega *et al.*, 2010) and indeed these lipophilic cations accumulate in organelles, specifically mitochondria (Ross *et al.*, 2006). We found that all bisphosphonium analogues tested in this study led to a rapid reduction of *T. b. brucei* Ψ_m after as little as 1 hour of incubation and decreased the intracellular ATP level within the same incubation period. These observations are consistent with the mitochondria being the target these compounds. It was also observed that levels of intracellular calcium increased gradually after 8 hrs of incubation with these compounds and we interpret this as possible evidence that the damaged mitochondria are unable to retain the stored Ca^{2+} as their membrane potential dissipates.

Although bisphosphonium analogues act slowly on trypanosomes' viability (Taladriz *et al.*, 2012), their effect on mitochondria and ATP levels was relatively fast; this encouraged us to study their effect on the cell cycle,

reasoning that their effect could be trypanostatic, through deprivation of ATP, long before the treatment killed the trypanosome population outright. This was also visualised using growth curves in the presence of various concentrations of selected bisphosphonium salts. After 8 h of incubation with different compounds the cell cycle defects were becoming apparent because DNA synthesis could not be initiated, leading to a dramatic reduction of cells in S phase. Definitively, some actions, such as reduction in Ψ_m and ATP level, happened well before 8 h, suggesting, but not proving, a causal relationship between the mitochondrial damage and cell cycle arrest. A final observation adding weight to the mitochondrial target hypothesis is the mitochondrial damage observed in TEM images taken after 12 h of exposure to selected bisphosphonium salts.

In a further investigation of the mechanism of action for bisphosphonium analogues, we tested whether these compounds can induce programmed cell death (PCD or apoptosis) in trypanosomes. TUNEL assay was employed for detecting DNA fragmentation, and the results showed an increase in DNA fragmentation after 24 h of incubation with CD38 and EFpl7 compounds. This result, along with the results of Ψ_m , could be taken as evidence that PCD occurs in treated cells. However, the evidence for PCD was inconclusive and would need far more stringent investigation, especially as bisphosphonium-induced cell death appeared to not depend on protein synthesis.

Overall, it can be concluded that curcumin and phosphonium analogues have promising antiparasitic qualities. Unfortunately, initial *in vivo* results for these compounds, determined by Hasan Ibrahim at the University of Glasgow (curcuminoids) and Marcel Kaiser at the Swiss Tropical and Public Health Institute (phosphonium salts), were not encouraging. However, these initial tests were performed with only a few compounds and doses, and with a more systematic approach as well as optimisation of protocols and lead compounds it may yet be possible to develop genuine pre-clinical drugs from these series. For instance, for the curcuminoid scaffold the *in vivo* and mode of action work has so far focussed mostly on the very interesting enone series, but we must conclude that in their present chemical form the enones are too reactive with (host) thiols to have genuine drug-like qualities, despite their undoubted *in vitro* activity. Several other curcuminoids, that were not thiol-reactive, also displayed promising *in vitro* activity and further investigation should now focus on those

analogues. On the other hand, using ADME (Administration, Distribution, Metabolism and Excretion) analysis in order to discover new drug before *in vivo* studies is very useful to shorten the time, reduce the cost and avoid false negatives, i.e. failure of the compound in the *in vivo* model due to inappropriate administration protocols *etc.* Therefore, a proper investigation of ADME issues before testing a lead compound in an animal model can much improve the value of the test.

Appendices

Appendix A: general buffers and solution

1-Assay buffer (pH 7.3)

Components	Quantity per liter
D-Glucose	2.53 g
HEPES	8 g
MOPS	5 g
NaHCO ₃	2 g
KCl	347.5 mg
MgCl ₂ .6H ₂ O	62.5 mg
NaH ₂ PO ₄ .2H ₂ O	913.5 mg
CaCl ₂ . 2H ₂ O	40.7 mg
MgSO ₄ . 7H ₂ O	19.9 mg
NaCl	5.7 g
Store at 4 °C.	

2- 10% SDS

Sodium Dodecyl Sulfate	10 g
ddH ₂ O	500 ml

3- LB medium -Luria Bertani broth- (pH 7)

LB powder (Sigma-Aldrich)	25 g
dH ₂ O	1 L

4- LB agar

Luria Agar (Sigma-Aldrich)	35 g
dH ₂ O	1 L
Autoclaved and agar is liquefied before making agar plates.	

5- 1× TE

1 M Tris.HCl	10 ml
0.5 M EDTA at pH 8.0	2 ml
dd H ₂ O	1 litre

6- NTE buffer

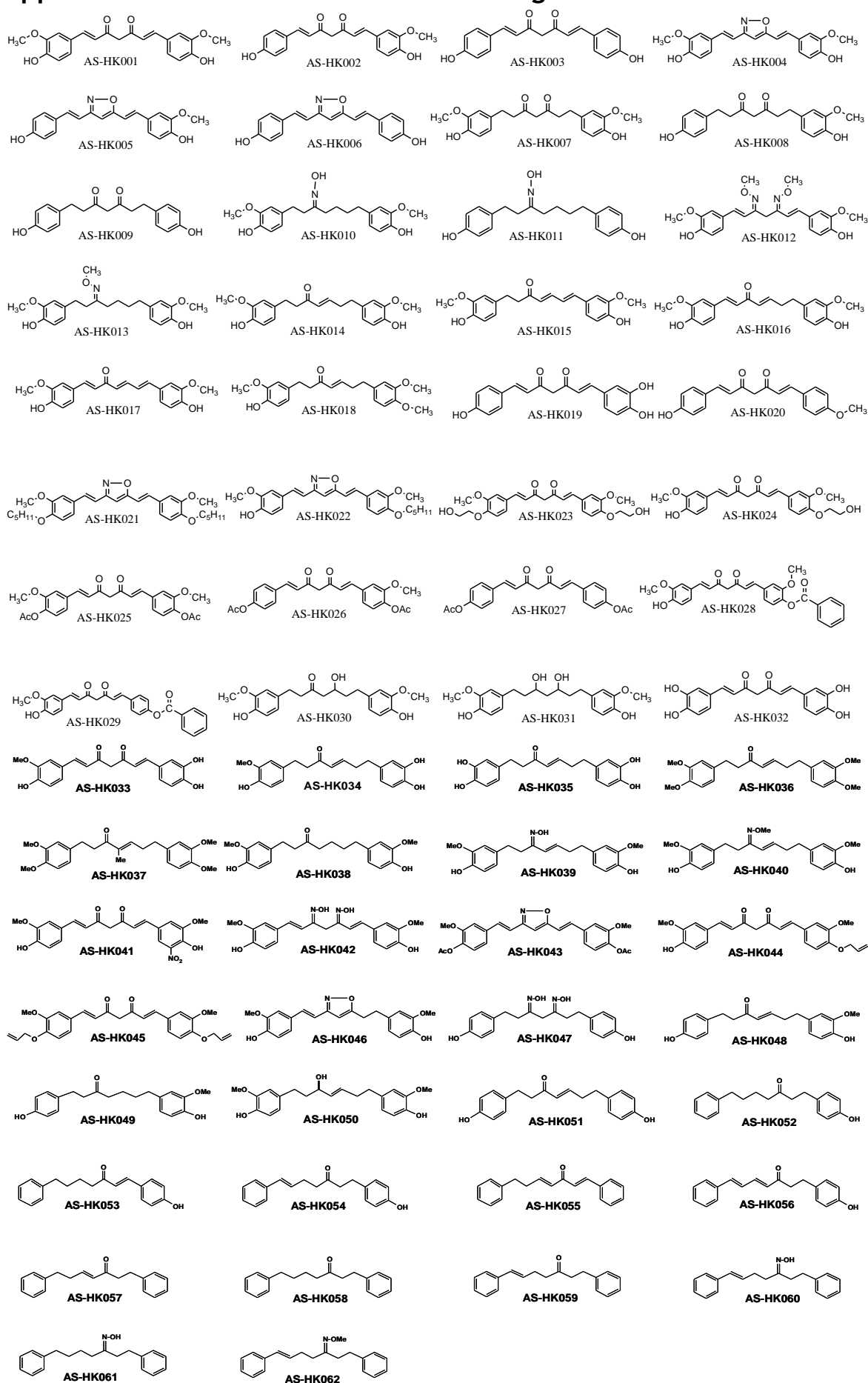
Tris-HCl, pH 8.0	10 mM
NaCl	100 mM
EDTA	5 mM

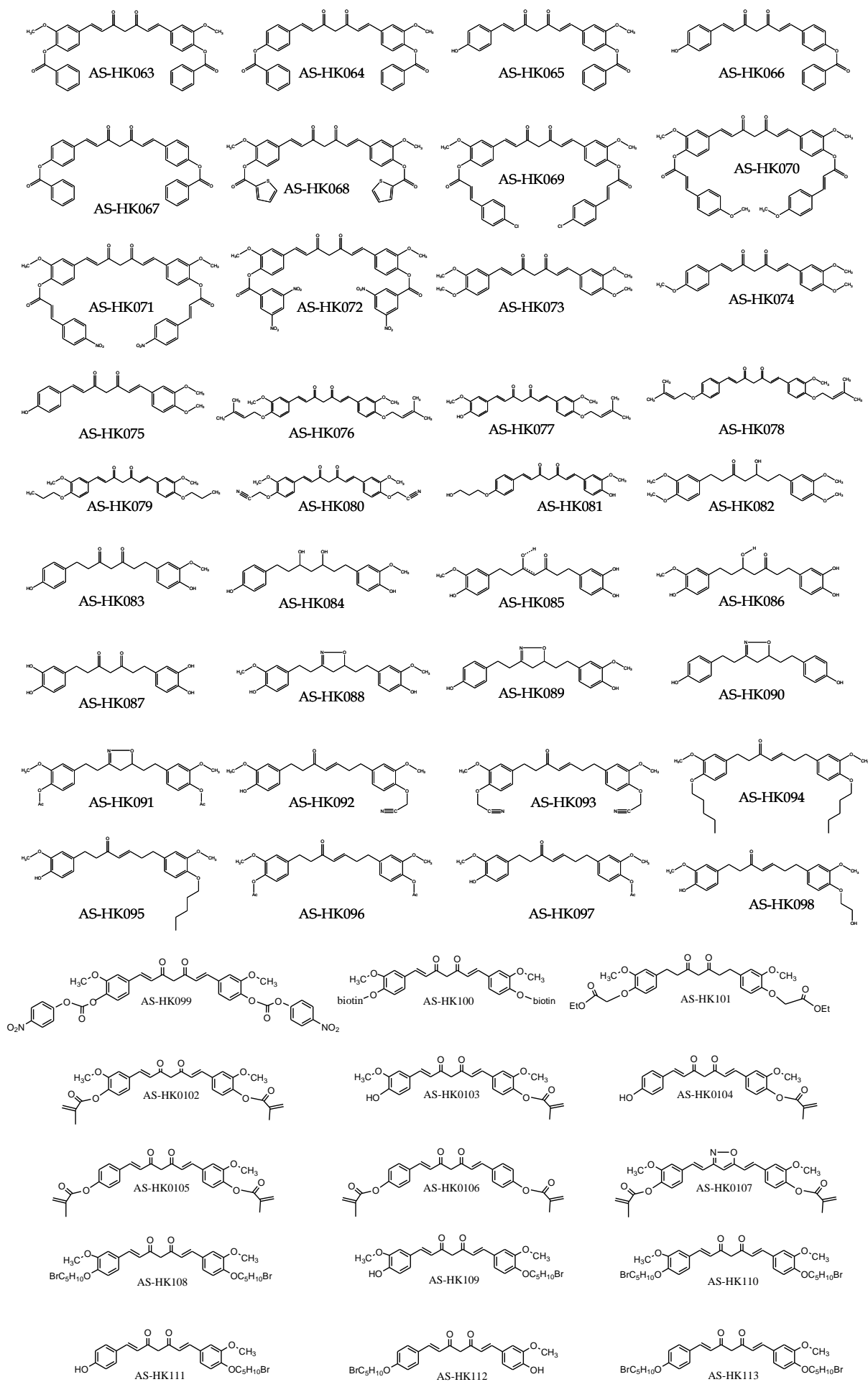
7- SOC medium

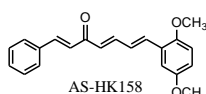
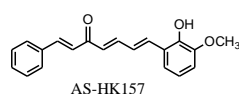
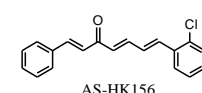
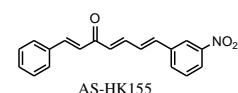
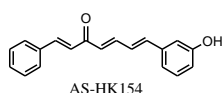
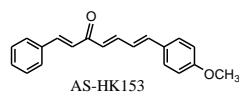
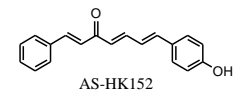
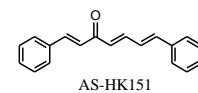
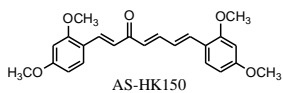
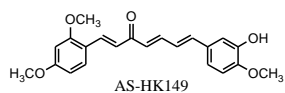
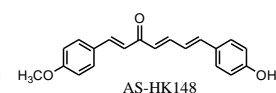
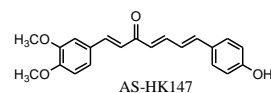
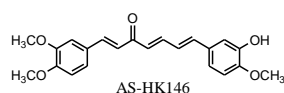
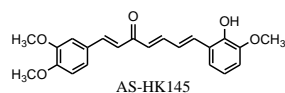
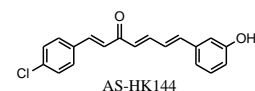
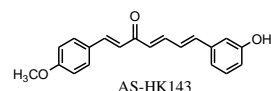
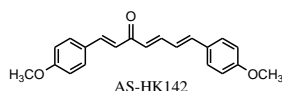
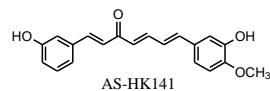
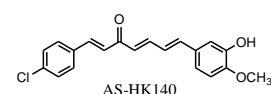
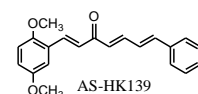
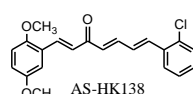
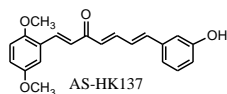
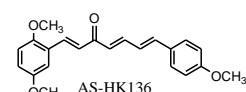
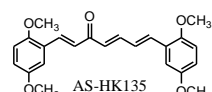
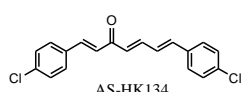
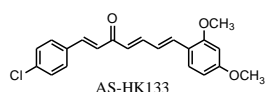
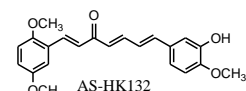
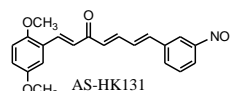
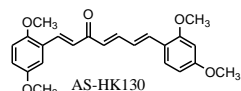
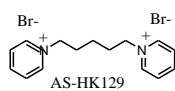
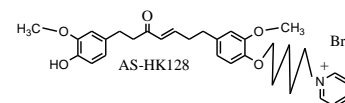
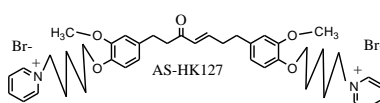
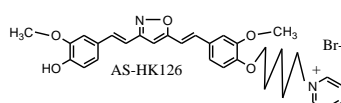
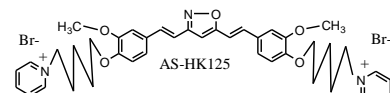
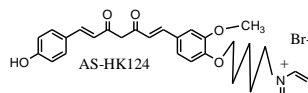
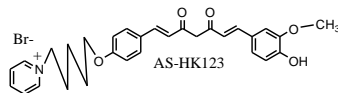
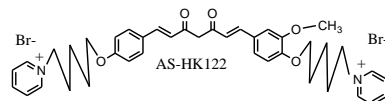
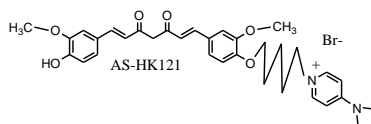
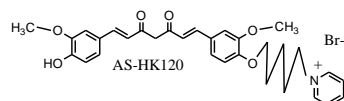
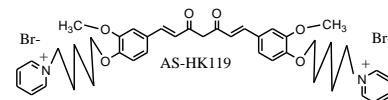
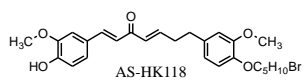
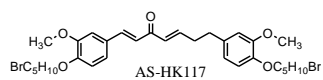
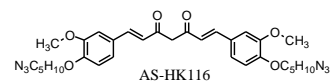
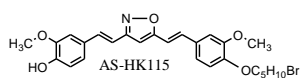
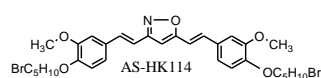
Tryptone	20 g
Yeast extract	5 g
NaCl	0.5 g
250 mM KCl	10 ml
2 M MgCl ₂	5 ml
dd H ₂ O	1 litre

Adjust pH at 7.0 with 5 M NaOH. Autoclave and when cooled down 1 M of sterile glucose 20 ml was added.

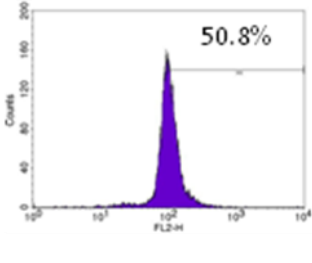
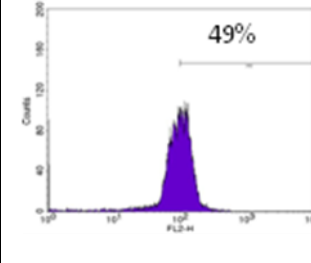
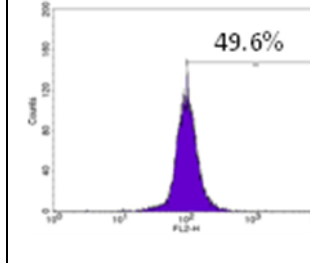
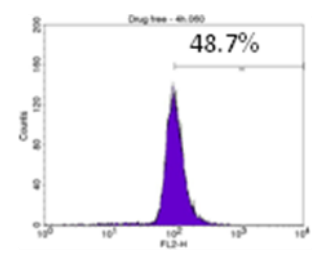
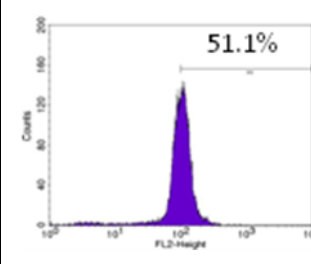
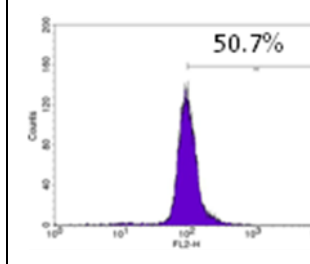
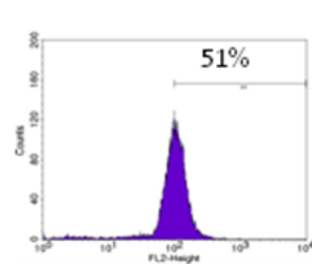
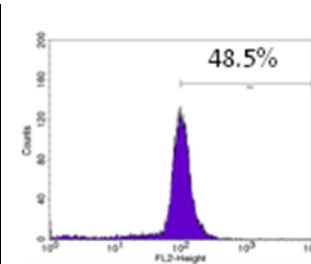
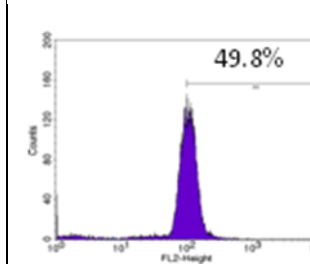
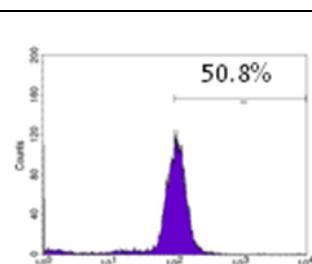
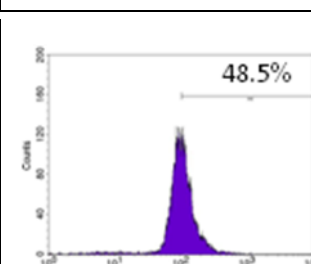
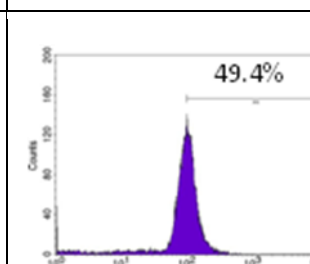
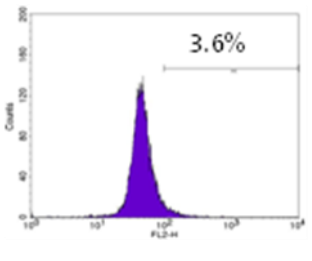
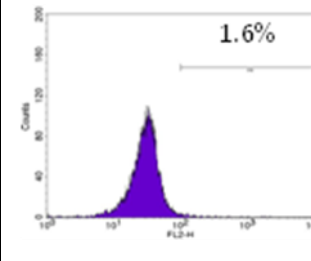
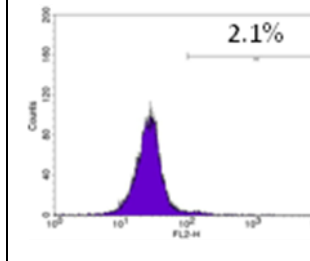
Appendix B: Structures of Curcumin analogues

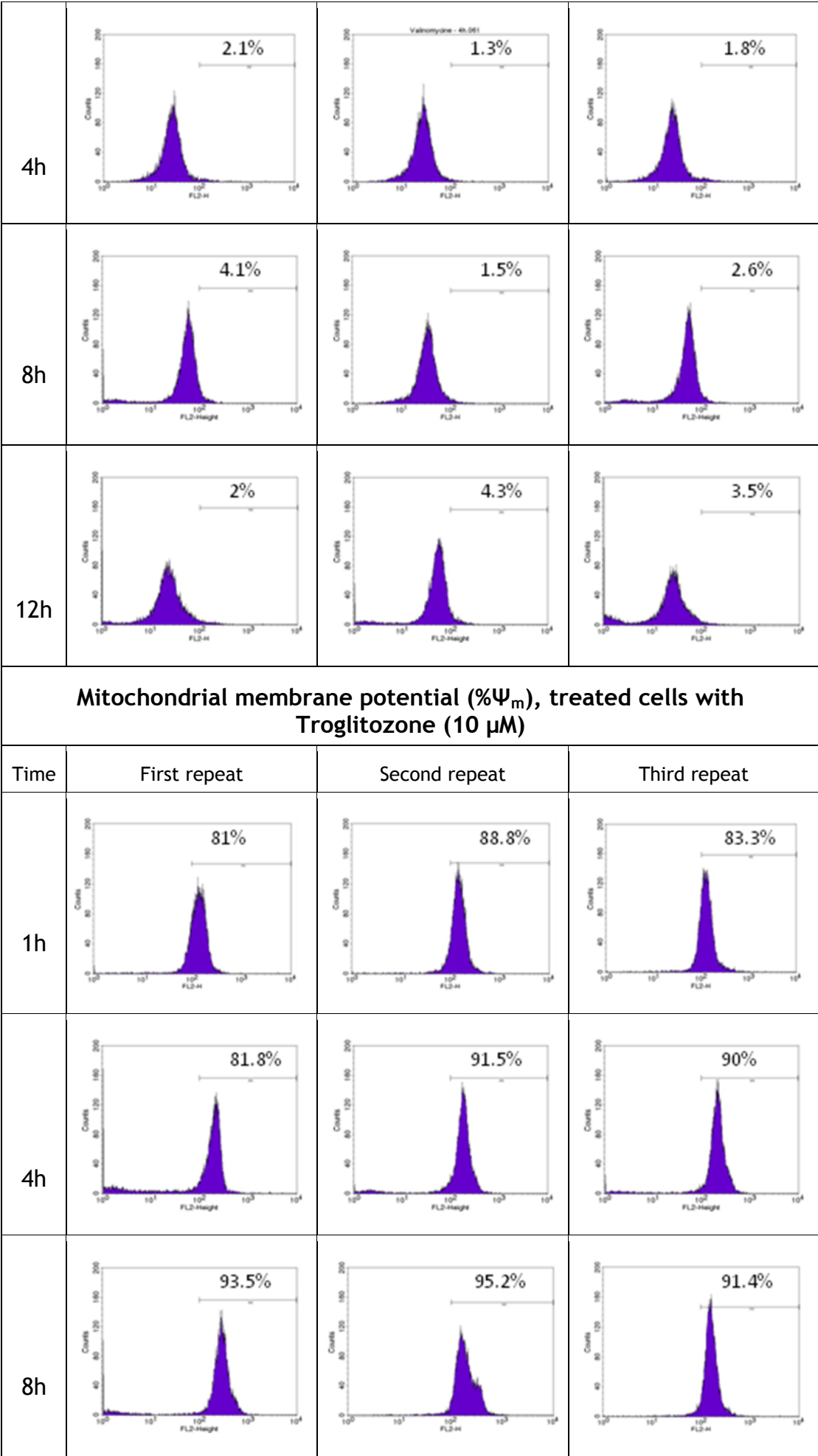


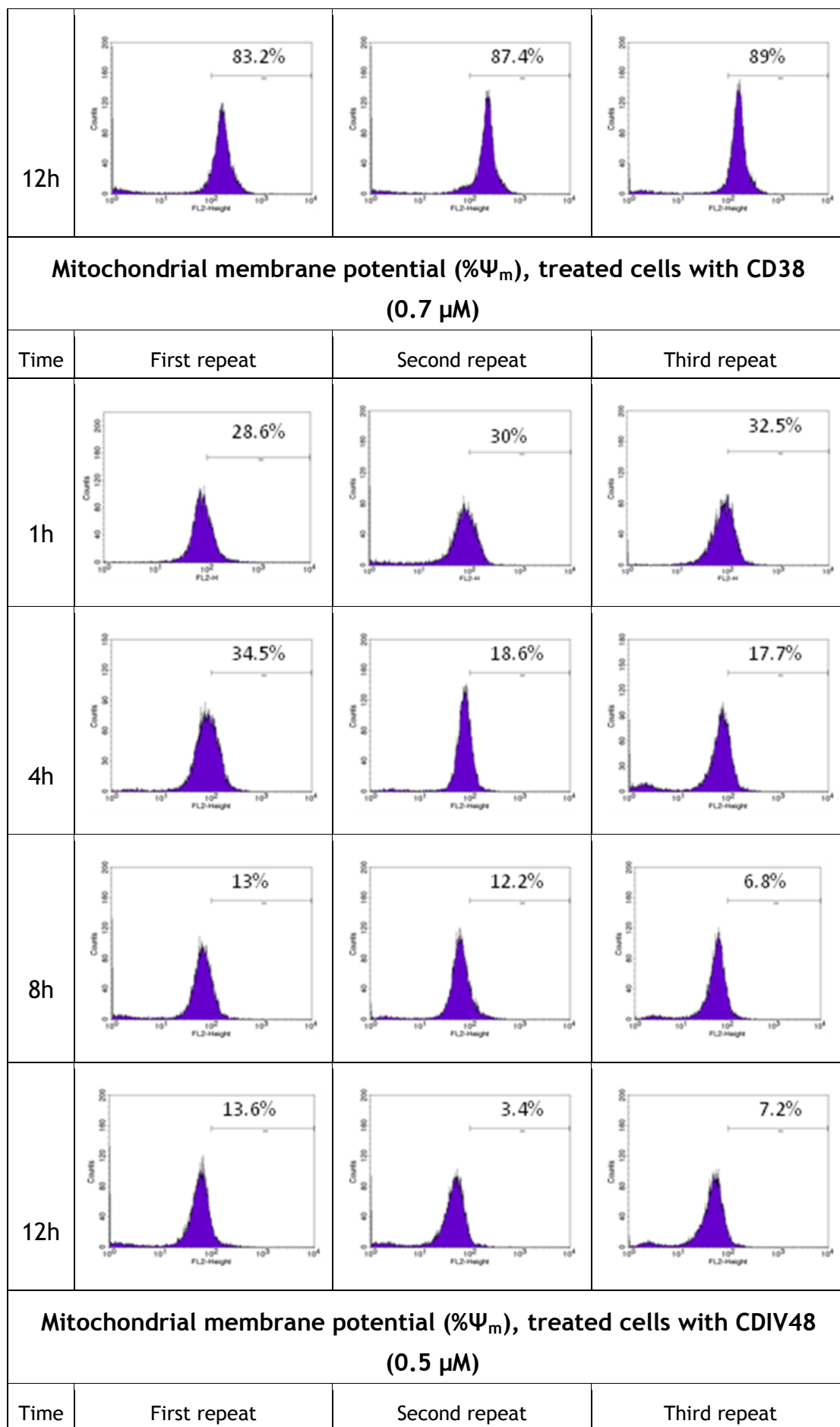


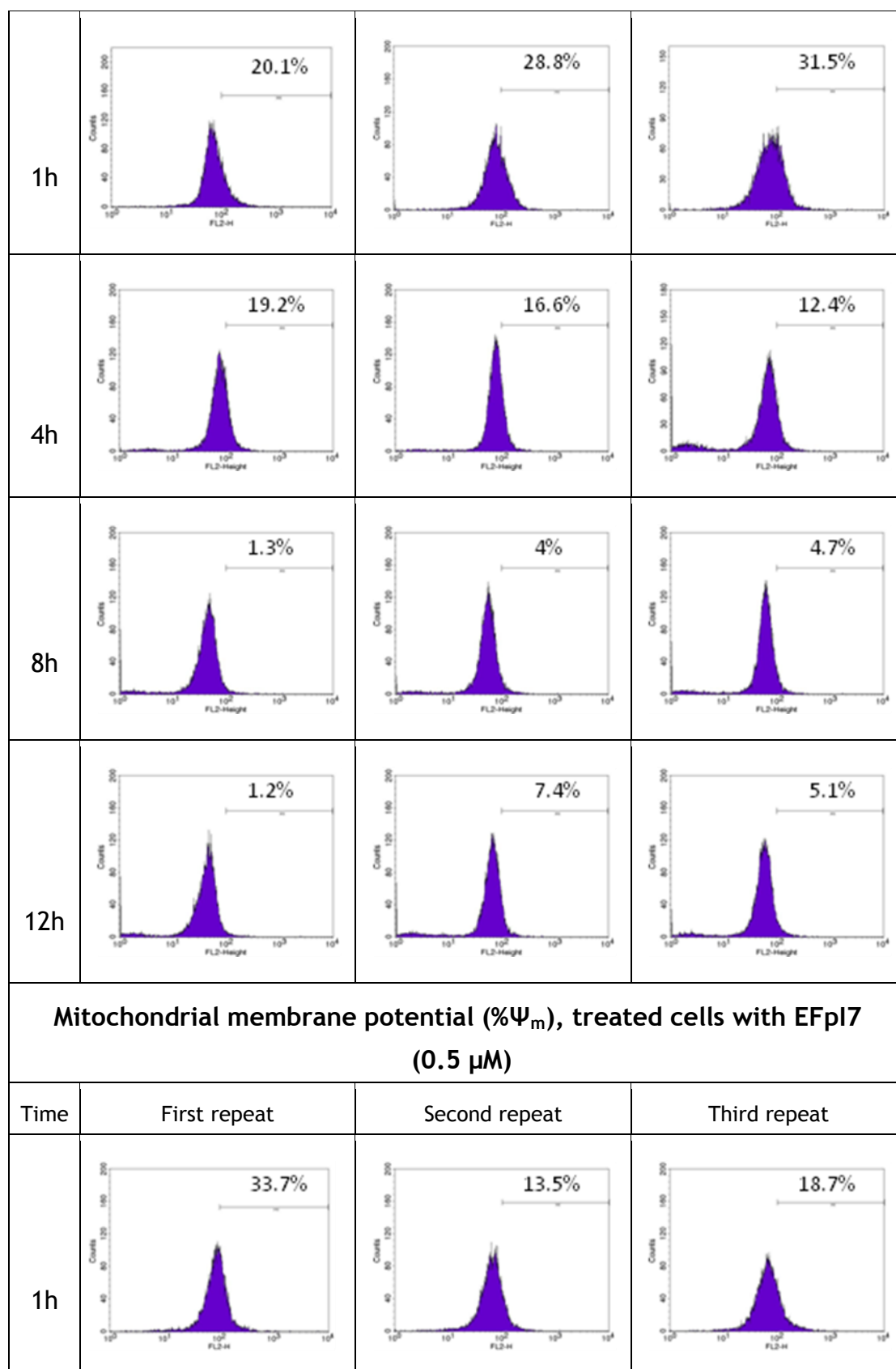


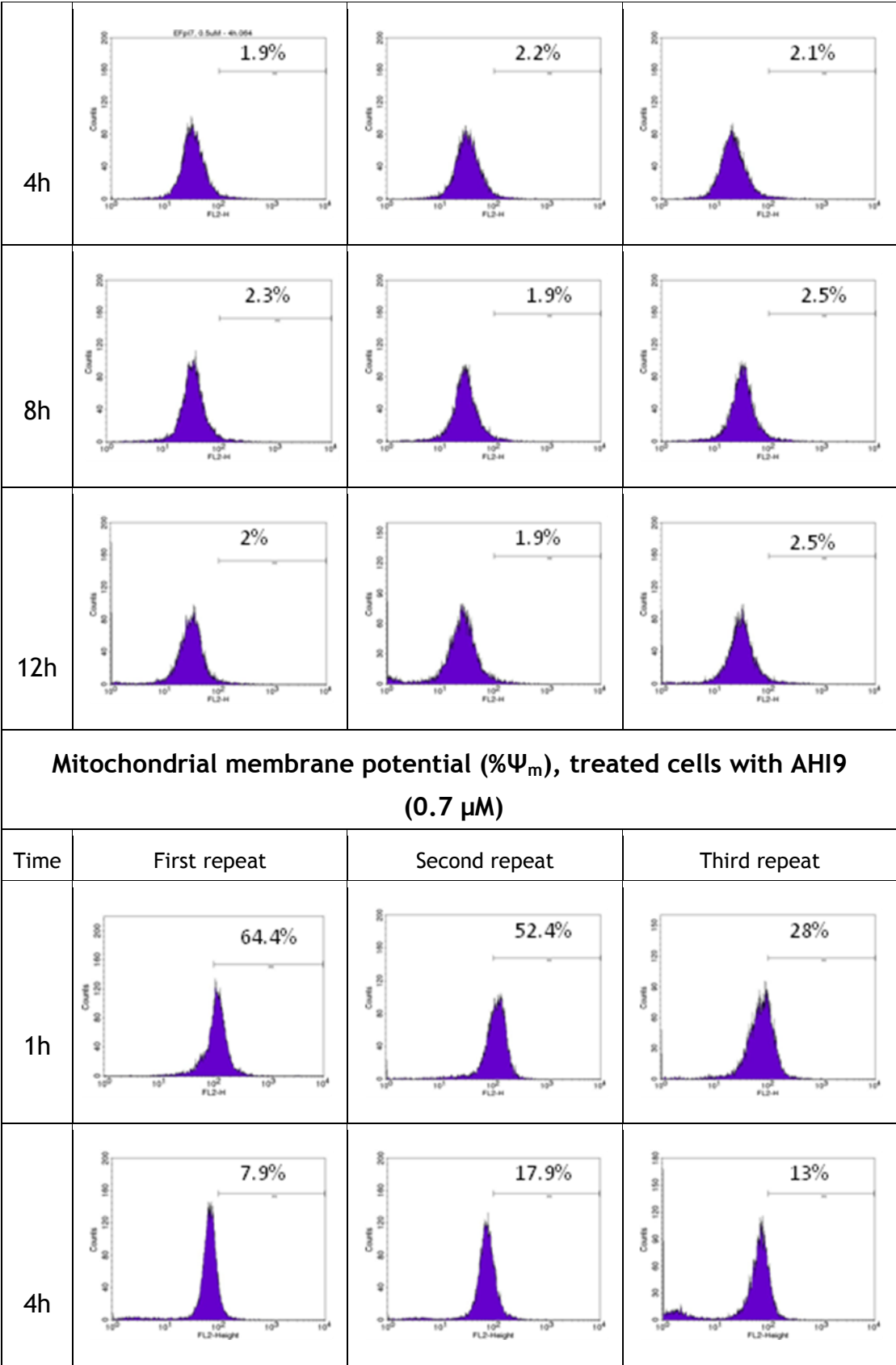
Appendix C: Mitochondrial membrane potential determinations

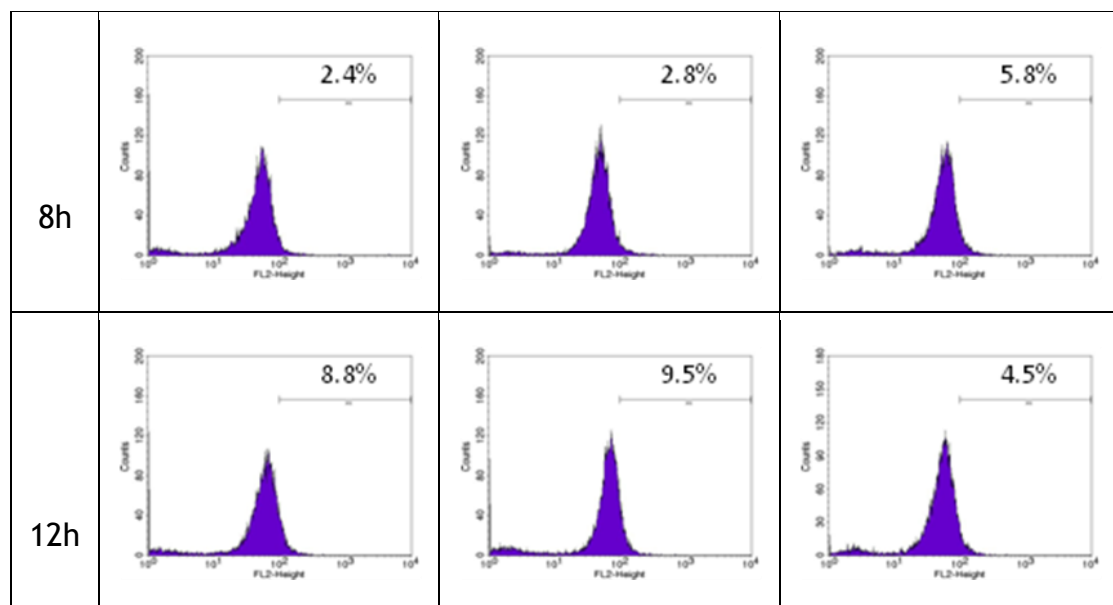
Mitochondrial membrane potential (Ψ_m), untreated cells (drug free)			
Time	First repeat	Second repeat	Third repeat
1h			
4h			
8h			
12h			
Mitochondrial membrane potential (Ψ_m), treated cells with Valinomycin (100 nM)			
Time	First repeat	Second repeat	Third repeat
1h			



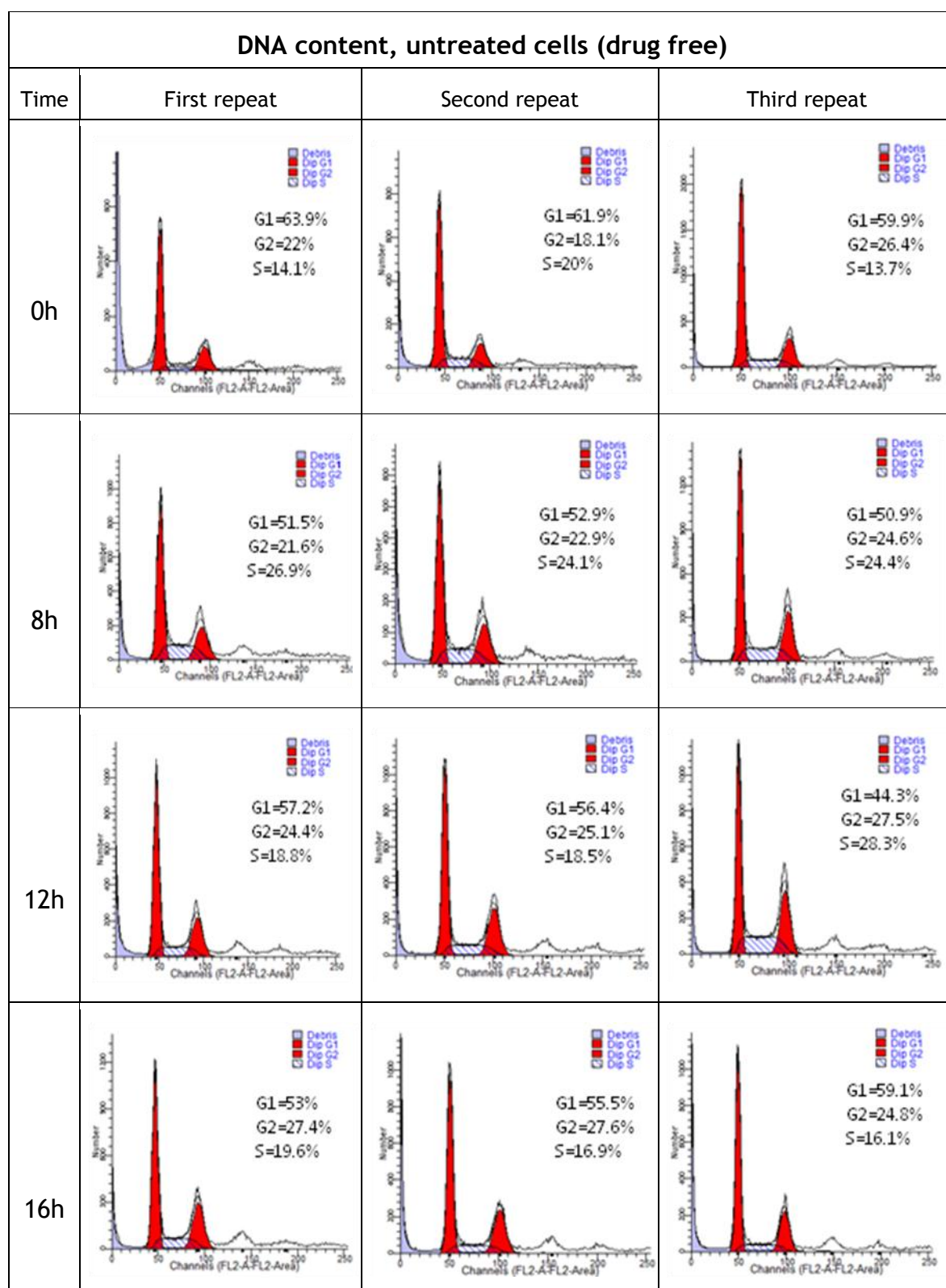


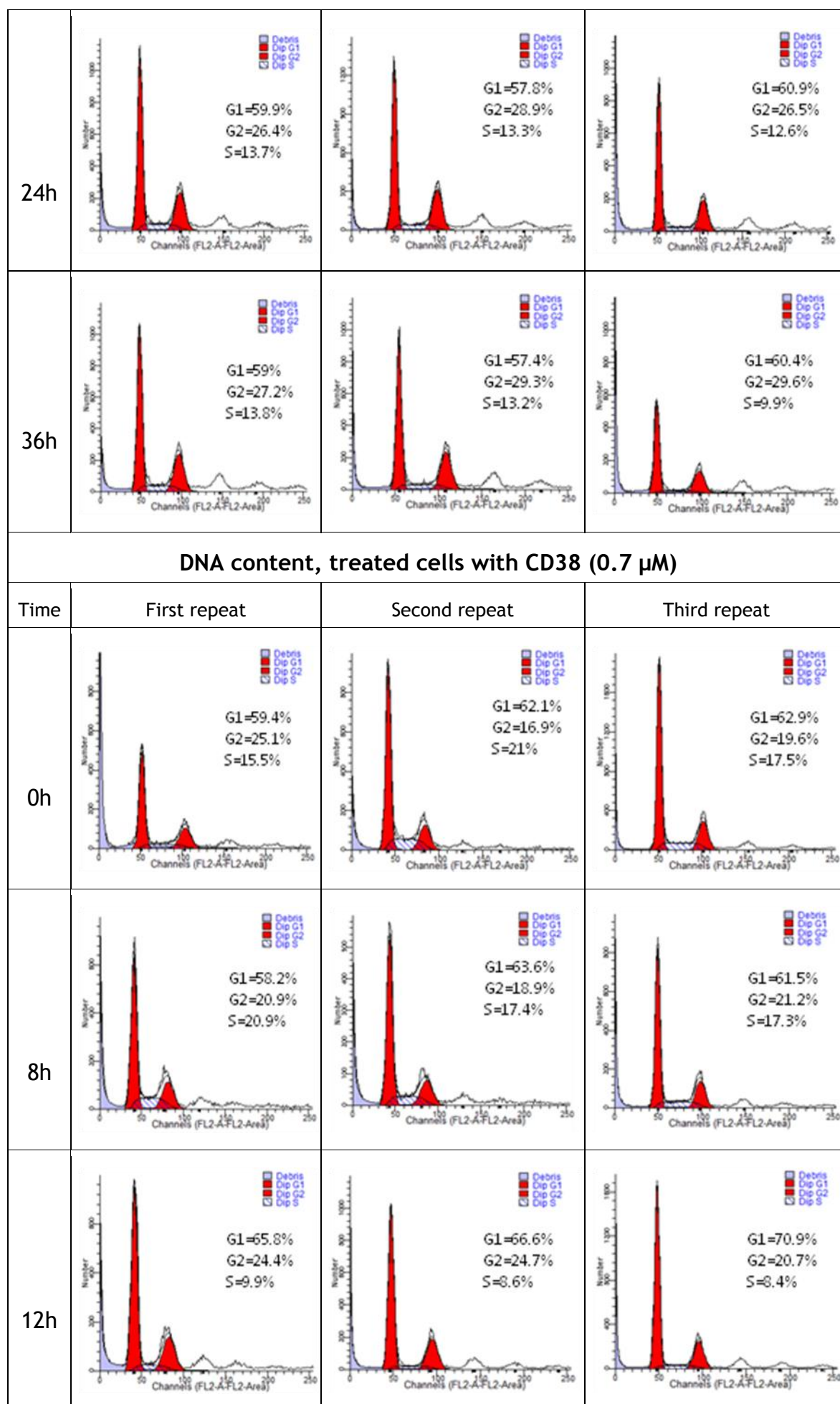


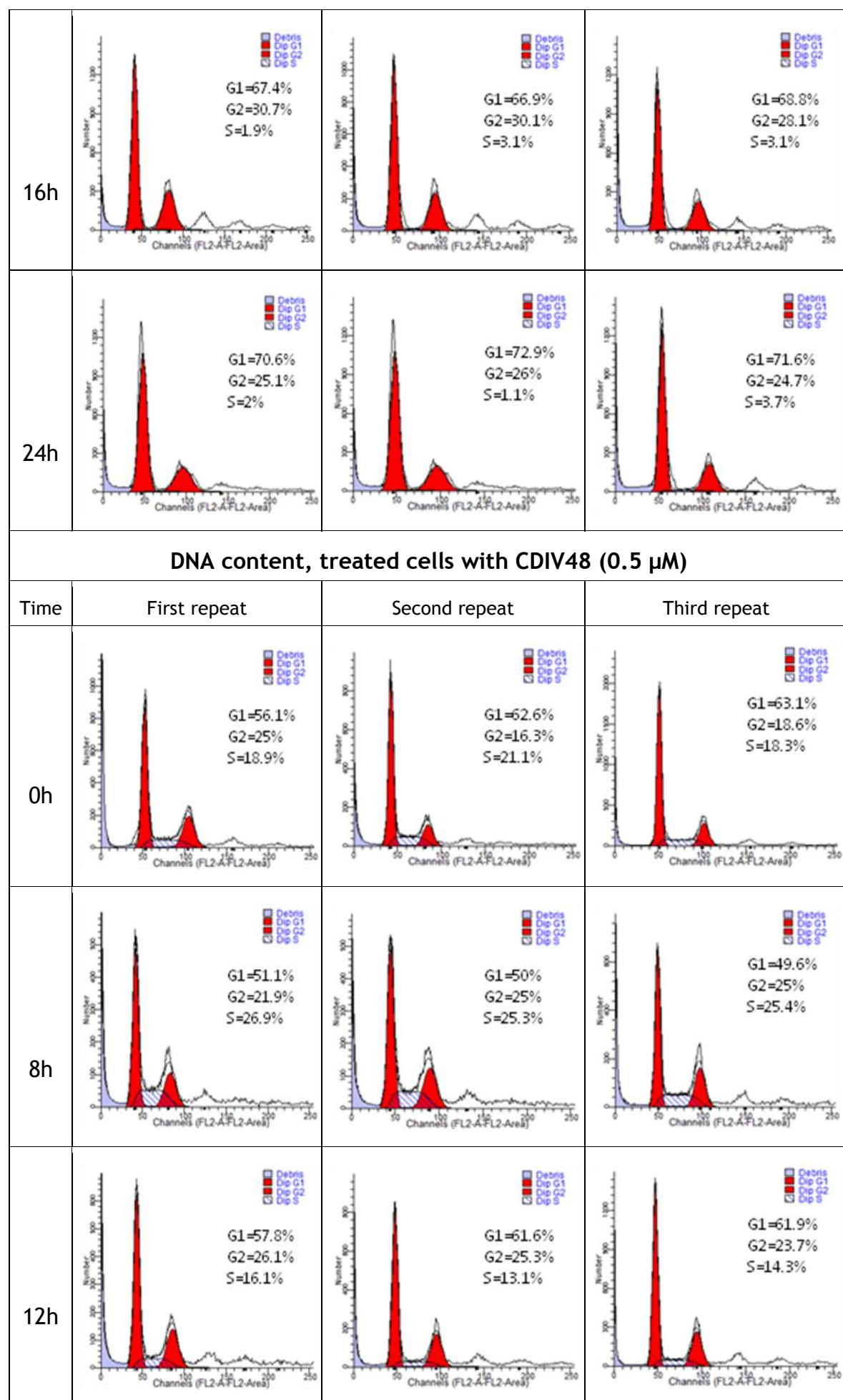


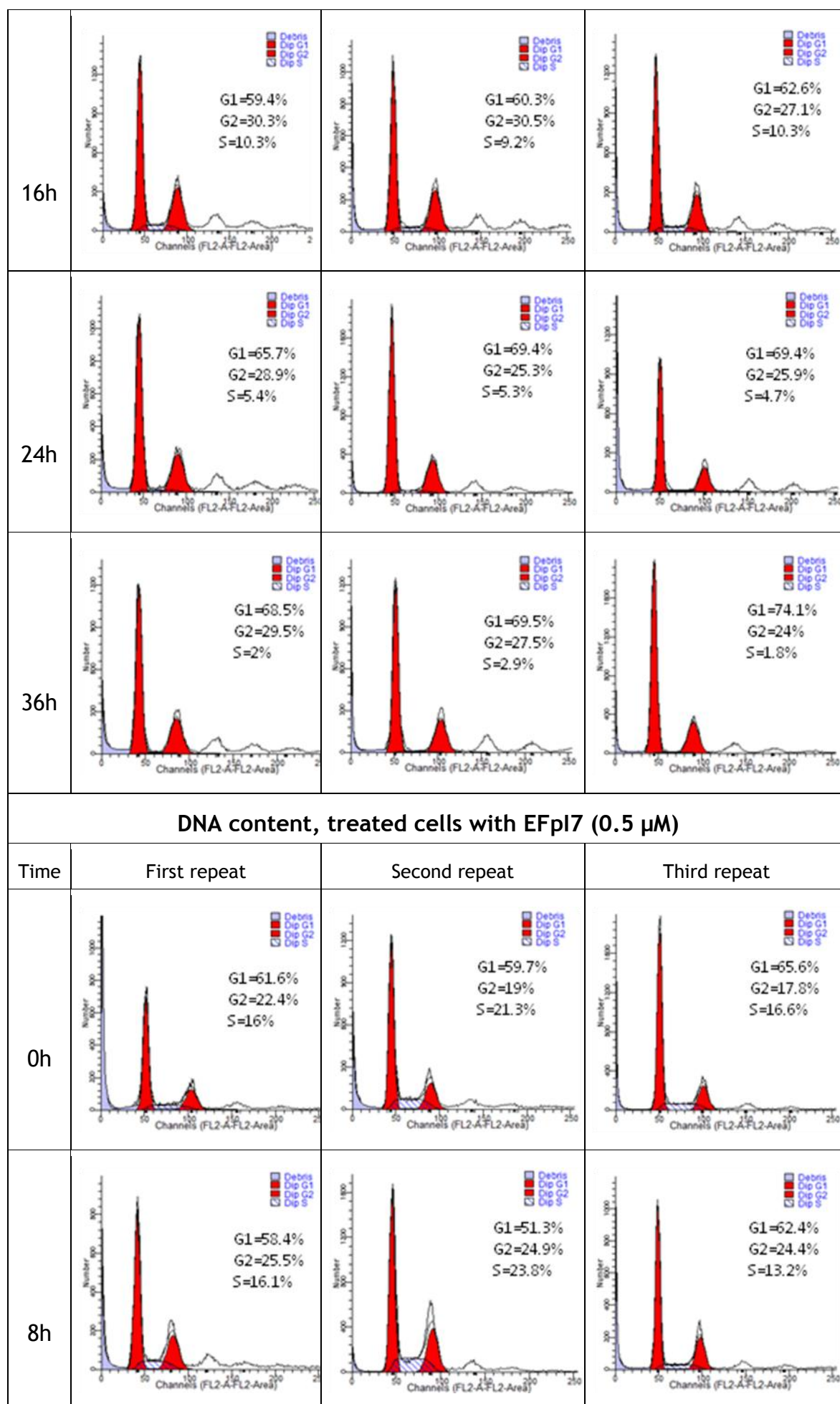


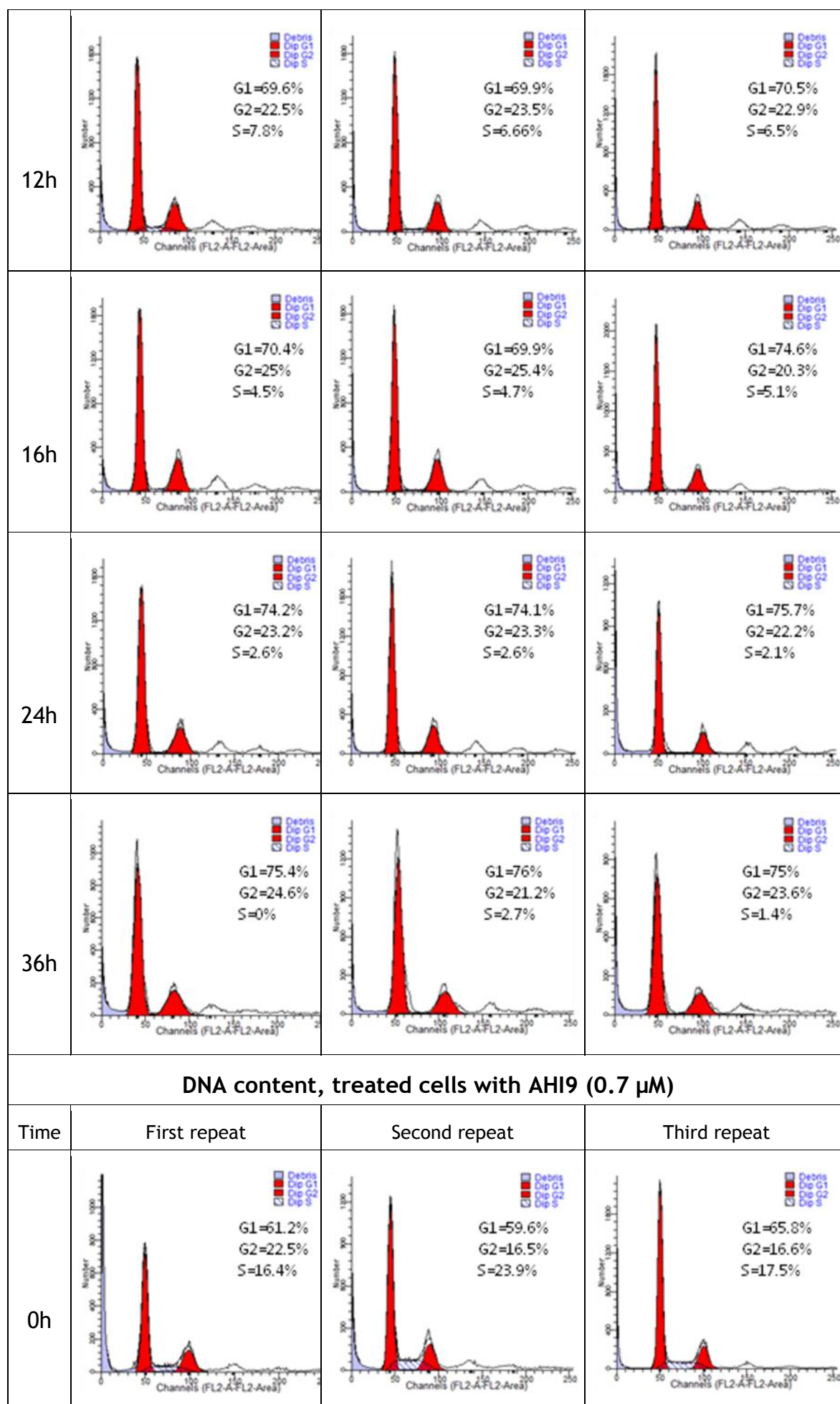
Appendix D: DNA content

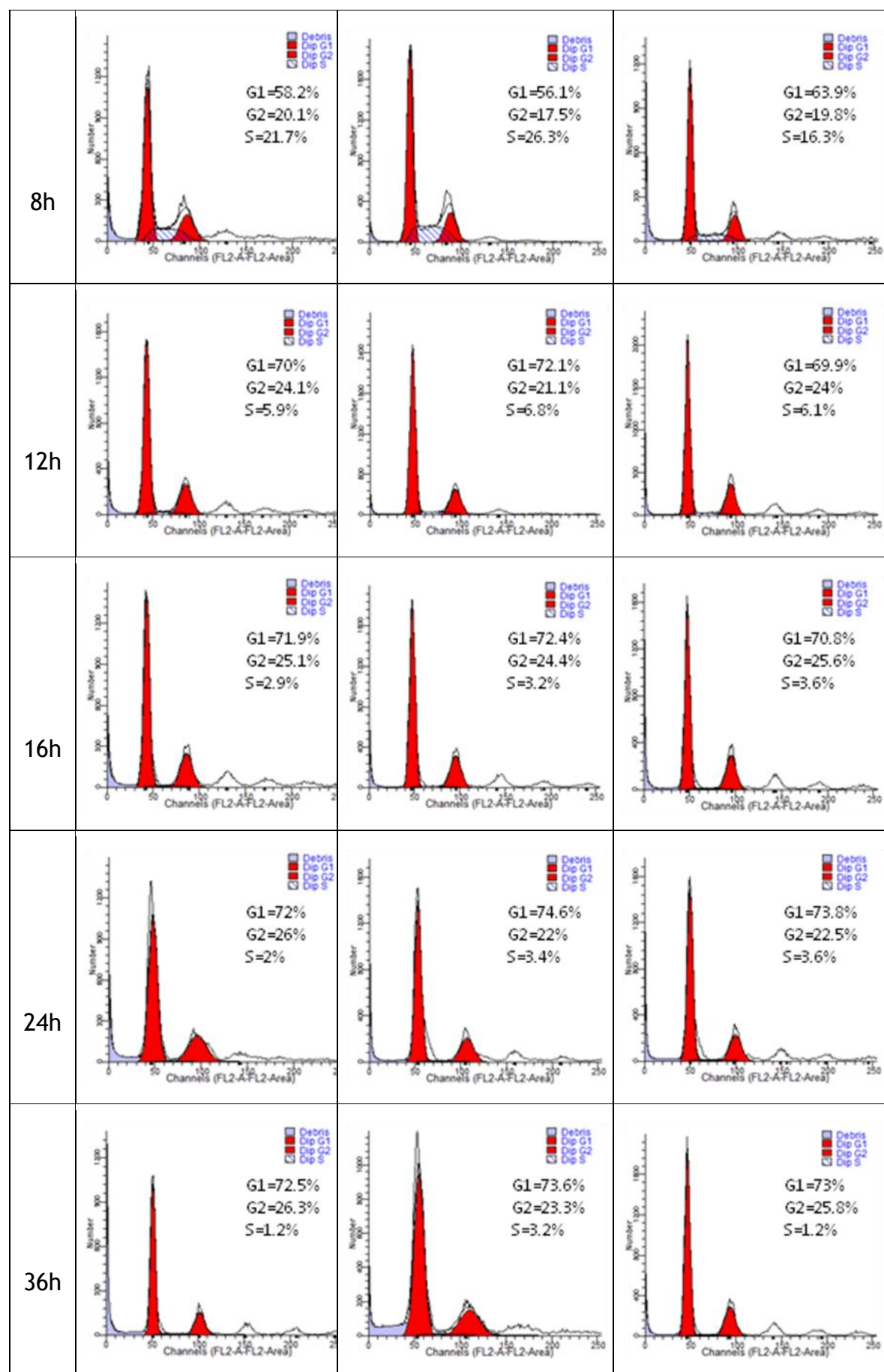




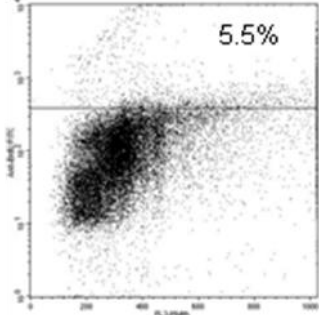
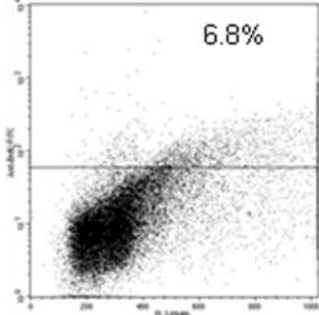
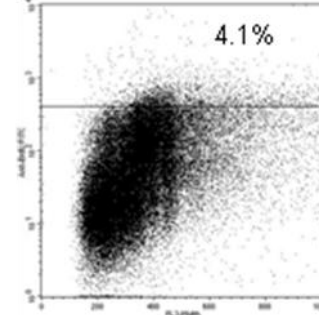
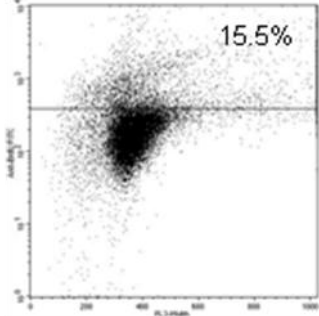
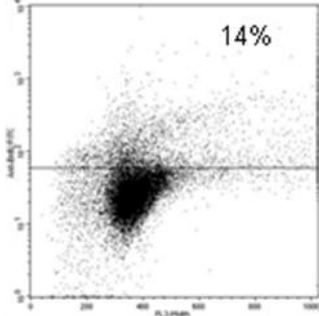
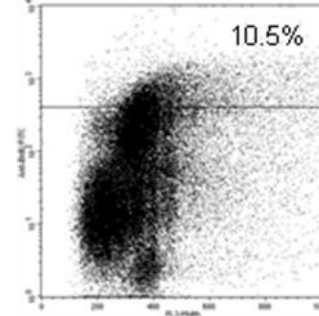
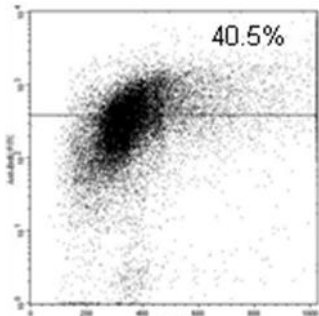
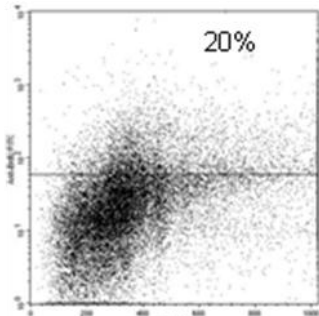
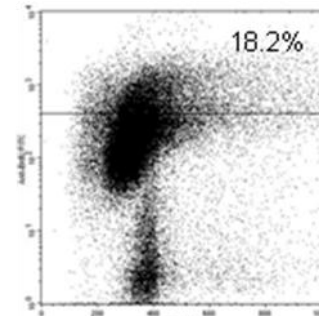
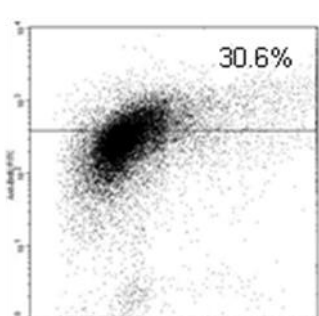
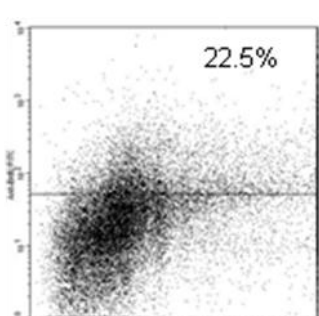
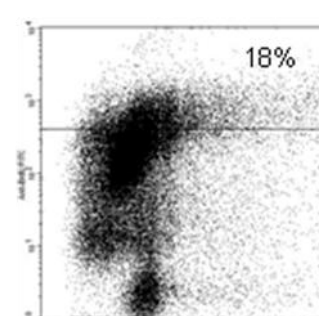


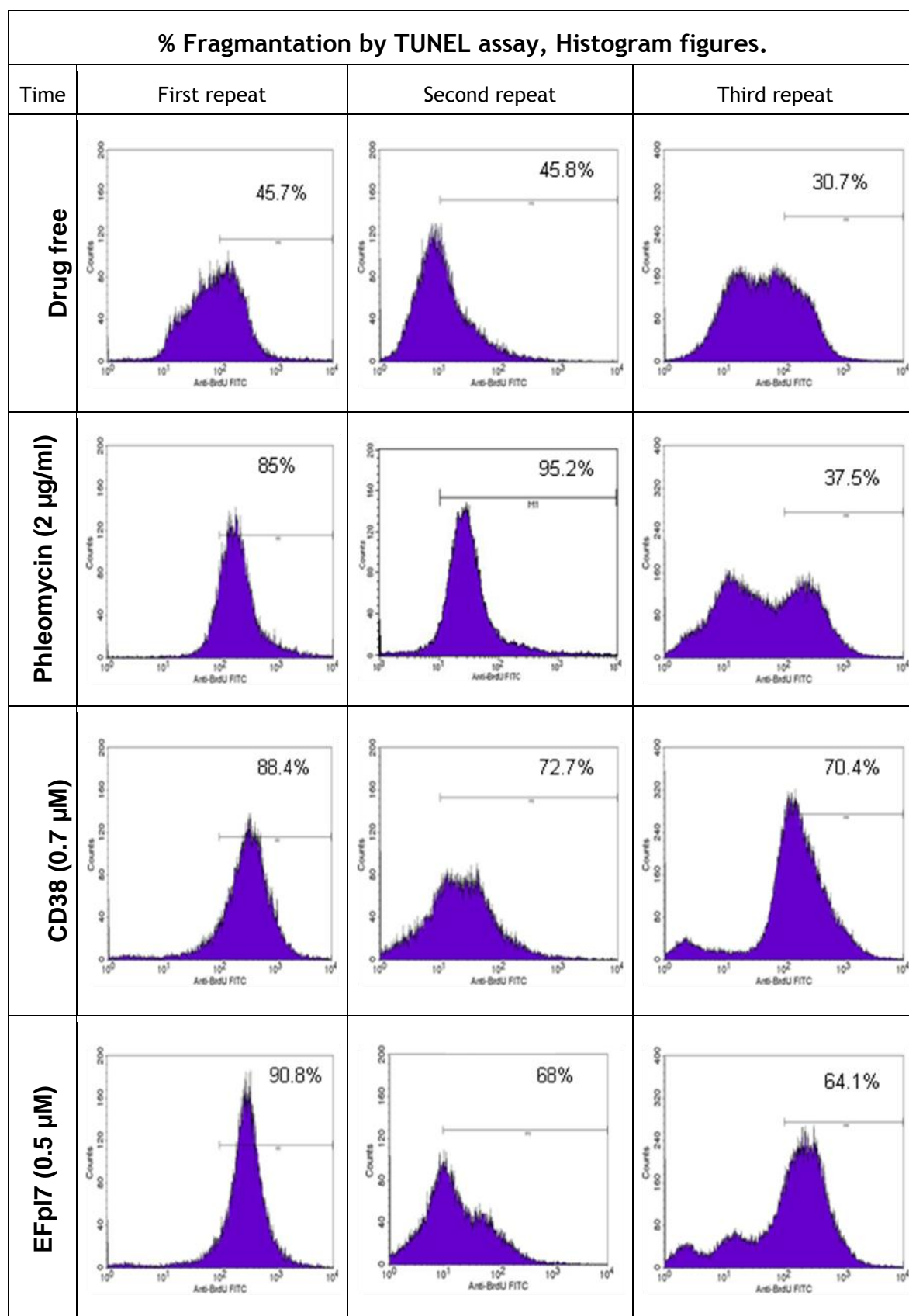






Appendix E: TUNEL assay

% Fragmentation by TUNEL assay, Dot Plot figures.			
Time	First repeat	Second repeat	Third repeat
Drug free			
Phleomycin (2 µg/ml)			
CD38 (0.7 µM)			
EFp17 (0.5 µM)			



[illegible]

[illegible]

[illegible]

[illegible]

	1,060	1,080	1,100	1,120	1,140																											
G1	ACCCCGT	TTCAAAGGGCA	ATTCTCTGCGAGTGGACG	TCGCTGGTTGACGATCACCGCCTCCGT	TGATGACCGCAAGTATGAGGAGGTGCCGCAC																											
Translation +1	T	P	F	Q	K	G	I	L	C	E	S	D	V	R	W	L	T	I	T	A	S	V	D	D	R	K	Y	E	E	V	P	H
Consensus	ACCCCGT	TTCAAAGGGCA	ATTCTCTGCGAGTGGACG	TCGCTGGTTGACGATCACCGCCTCCGT	TGATGACCGCAAGTATGAGGAGGTGCCGCAC																											
Translation +1	T	P	F	Q	K	G	I	L	C	E	S	D	V	R	W	L	T	I	T	A	S	V	D	D	R	K	Y	E	E	V	P	H
WT, G1 #1 old	ACCCCGT	TTCAAAGGGCA	ATTCTCTGCGAGTGGACG	TCGCTGGTTGACGATCACCGCCTCCGT	TGATGACCGCAAGTATGAGGAGGTGCCGCAC																											
Translation +1	T	P	F	Q	K	G	I	L	C	E	S	D	V	R	W	L	T	I	T	A	S	V	D	D	R	K	Y	E	E	V	P	H
WT, G1 #21	ACCCCGT	TTCAAAGGGCA	ATTCTCTGCGAGTGGACG	TCGCTGGTTGACGATCACCGCCTCCGT	TGATGACCGCAAGTATGAGGAGGTGCCGCAC																											
Translation +1	T	P	F	Q	K	G	I	L	C	E	S	D	V	R	W	L	T	I	T	A	S	V	D	D	R	K	Y	E	E	V	P	H
WT, g1_#5	ACCCCGT	TTCAAAGGGCA	ATTCTCTGCGAGTGGACG	TCGCTGGTTGACGATCACCGCCTCCGT	TGATGACCGCAAGTATGAGGAGGTGCCGCAC																											
Translation +1	T	P	F	Q	K	G	I	L	C	E	S	D	V	R	W	L	T	I	T	A	S	V	D	D	R	K	Y	E	E	V	P	H
WT, G1 #25	ACCCCGT	TTCAAAGGGCA	ATTCTCTGCGAGTGGACG	TCGCTGGTTGACGATCACCGCCTCCGT	TGATGACCGCAAGTATGAGGAGGTGCCGCAC																											
Translation +1	T	P	F	Q	K	G	I	L	C	E	S	D	V	R	W	L	T	I	T	A	S	V	D	D	R	K	Y	E	E	V	P	H
WT, G1 #9	ACCCCGT	TTCAAAGGGCA	ATTCTCTGCGAGTGGACG	TCGCTGGTTGACGATCACCGCCTCCGT	TGATGACCGCAAGTATGAGGAGGTGCCGCAC																											
Translation +1	T	P	F	Q	K	G	I	L	C	E	S	D	V	R	W	L	T	I	T	A	S	V	D	D	R	K	Y	E	E	V	P	H
WT G1 #17	ACCCCGT	TTCAAAGGGCA	ATTCTCTGCGAGTGGACG	TCGCTGGTTGACGATCACCGCCTCCGT	TGATGACCGCAAGTATGAGGAGGTGCCGCAC																											
Translation +1	T	P	F	Q	K	G	I	L	C	E	S	D	V	R	W	L	T	I	T	A	S	V	D	D	R	K	Y	E	E	V	P	H
WT, G1 #5 old	ACCCCGT	TTCAAAGGGCA	ATTCTCTGCGAGTGGACG	TCGCTGGTTGACGATCACCGCCTCCGT	TGATGACCGCAAGTATGAGGAGGTGCCGCAC																											
Translation +1	T	P	F	Q	K	G	I	L	C	E	S	D	V	R	W	L	T	I	T	A	S	V	D	D	R	K	Y	E	E	V	P	H
WT Gene1 #13	ACCCCGT	TTCAAAGGGCA	ATTCTCTGCGAGTGGACG	TCGCTGGTTGACGATCACCGCCTCCGT	TGATGACCGCAAGTATGAGGAGGTGCCGCAC																											
Translation +1	T	P	F	Q	K	G	I	L	C	E	S	D	V	R	W	L	T	I	T	A	S	V	D	D	R	K	Y	E	E	V	P	H
WT G1 #1	ACCCCGT	TTCAAAGGGCA	ATTCTCTGCGAGTGGACG	TCGCTGGTTGACGATCACCGCCTCCGT	TGATGACCGCAAGTATGAGGAGGTGCCGCAC																											
Translation +1	T	P	F	Q	K	G	I	L	C	E	S	D	V	R	W	L	T	I	T	A	S	V	D	D	R	K	Y	E	E	V	P	H
TA014, G1 #15	ACCCCGT	TTCAAAGGGCA	ATTCTCTGCGAGTGGACG	TCGCTGGTTGACGATCACCGCCTCCGT	TGATGACCGCAAGTATGAGGAGGTGCCGCAC																											
Translation +1	T	P	F	Q	K	G	I	L	C	E	S	D	V	R	W	L	T	I	T	A	S	V	D	D	R	K	Y	E	E	V	P	H
TA014, G1 #19	ACCCCGT	TTCAAAGGGCA	ATTCTCTGCGAGTGGACG	TCGCTGGTTGACGATCACCGCCTCCGT	TGATGACCGCAAGTATGAGGAGGTGCCGCAC																											
Translation +1	T	P	F	Q	K	G	I	L	C	E	S	D	V	R	W	L	T	I	T	A	S	V	D	D	R	K	Y	E	E	V	P	H
TA014, G1 #23	ACCCCGT	TTCAAAGGGCA	ATTCTCTGCGAGTGGACG	TCGCTGGTTGACGATCACCGCCTCCGT	TGATGACCGCAAGTATGAGGAGGTGCCGCAC																											
Translation +1	T	P	F	Q	K	G	I	L	C	E	S	D	V	R	W	L	T	I	T	A	S	V	D	D	R	K	Y	E	E	V	P	H
TA014, G1 #27	ACCCCGT	TTCAAAGGGCA	ATTCTCTGCGAGTGGACG	TCGCTGGTTGACGATCACCGCCTCCGT	TGATGACCGCAAGTATGAGGAGGTGCCGCAC																											
Translation +1	T	P	F	Q	K	G	I	L	C	E	S	D	V	R	W	L	T	I	T	A	S	V	D	D	R	K	Y	E	E	V	P	H
TA014, G1 #2 old	ACCCCGT	TTCAAAGGGCA	ATTCTCTGCGAGTGGACG	TCGCTGGTTGACGATCACCGCCTCCGT	TGATGACCGCAAGTATGAGGAGGTGCCGCAC																											
Translation +1	T	P	F	Q	K	G	I	L	C	E	S	D	V	R	W	L	T	I	T	A	S	V	D	D	R	K	Y	E	E	V	P	H
TA014, G1 #3	ACCCCGT	TTCAAAGGGCA	ATTCTCTGCGAGTGGACG	TCGCTGGTTGACGATCACCGCCTCCGT	TGATGACCGCAAGTATGAGGAGGTGCCGCAC																											
Translation +1	T	P	F	Q	K	G	I	L	C	E	S	D	V	R	W	L	T	I	T	A	S	V	D	D	R	K	Y	E	E	V	P	H
TA014, G1 #31	ACCCCGT	TTCAAAGGGCA	ATTCTCTGCGAGTGGACG	TCGCTGGTTGACGATCACCGCCTCCGT	TGATGACCGCAAGTATGAGGAGGTGCCGCAC																											
Translation +1	T	P	F	Q	K	G	I	L	C	E	S	D	V	R	W	L	T	I	T	A	S	V	D	D	R	K	Y	E	E	V	P	H
TA014, G1 #6 old	ACCCCGT	TTCAAAGGGCA	ATTCTCTGCGAGTGGACG	TCGCTGGTTGACGATCACCGCCTCCGT	TGATGACCGCAAGTATGAGGAGGTGCCGCAC																											
Translation +1	T	P	F	Q	K	G	I	L	C	E	S	D	V	R	W	L	T	I	T	A	S	V	D	D	R	K	Y	E	E	V	P	H
TA014, G1 #7	ACCCCGT	TTCAAAGGGCA	ATTCTCTGCGAGTGGACG	TCGCTGGTTGACGATCACCGCCTCCGT	TGATGACCGCAAGTATGAGGAGGTGCCGCAC																											
Translation +1	T	P	F	Q	K	G	I	L	C	E	S	D	V	R	W	L	T	I	T	A	S	V	D	D	R	K	Y	E	E	V	P	H

[illegible]

[illegible]

[illegible]

[illegible]

	2,020	2,040
G1	AGTAAAGACAA	CGCGAAGGGTGA
Translation +1	S K R Q R E G	*
Consensus	AGTAAAGACAA	CGCGAAGGGTGA
Translation +1	S K R Q R E G	*
WT, G1 # 1 old	AGTAAAGACAA	CGCGAAGGGTGA
Translation +1	S K R Q R E G	*
WT, G1 # 21	AGTAAAGACAA	CGCGAAGGGTGA
Translation +1	S K R Q R E G	*
WT, G1 # 5	AGTAAAGACAA	CGCGAAGGGTGA
Translation +1	S K R Q R E G	*
WT, G1 # 25	AGTAAAGACAA	CGCGAAGGGTGA
Translation +1	S K R Q R E G	*
WT, G1 # 9	AGTAAAGACAA	CGCGAAGGGTGA
Translation +1	S K R Q R E G	*
WT G1 # 17	AGTAAAGACAA	CGCGAAGGGTGA
Translation +1	S K R Q R E G	*
WT, G1 # 5 old	AGTAAAGACAA	CGCGAAGGGTGA
Translation +1	S K R Q R E G	*
WT Genel #13	AGTAAAGACAA	CGCGAAGGGTGA
Translation +1	S K R Q R E G	*
WT G1 #1	AGTAAAGACAA	CGCGAAGGGTGA
Translation +1	S K R Q R E G	*
TA014, G1 #15	AGTAAAGACAA	CGCGAAGGGTGA
Translation +1	S K R Q R E G	*
TA014, G1 #19	AGTAAAGACAA	CGCGAAGGGTGA
Translation +1	S K R Q R E G	*
TA014, G1 # 23	AGTAAAGACAA	CGCGAAGGGTGA
Translation +1	S K R Q R E G	*
TA014, G1 #27	AGTAAAGACAA	CGCGAAGGGTGA
Translation +1	S K R Q R E G	*
TA014, G1 # 2 old	AGTAAAGACAA	CGCGAAGGGTGA
Translation +1	S K R Q R E G	*
TA014, G1 # 3	AGTAAAGACAA	CGCGAAGGGTGA
Translation +1	S K R Q R E G	*
TA014, G1 # 31	AGTAAAGACAA	CGCGAAGGGTGA
Translation +1	S K R Q R E G	*
TA014, G1 # 6 old	AGTAAAGACAA	CGCGAAGGGTGA
Translation +1	S K R Q R E G	*
TA014, G1 # 7	AGTAAAGACAA	CGCGAAGGGTGA
Translation +1	S K R Q R E G	*

Appendix E: The nucleotide and amino acid sequences of glutathione synthetase (GS) (G1) from all the cloned sequences taken from AS-HK014 resistant TA014 strain and parental wildtype.

		20	40	60	80
G2	ATGGTGTTAA	ATGGTGTTAA	ATGGTGTTAA	ATGGTGTTAA	ATGGTGTTAA
Translation +1	M	V	L	K	L
Consensus	ATGGTGTTAA	ATGGTGTTAA	ATGGTGTTAA	ATGGTGTTAA	ATGGTGTTAA
Translation +1	M	V	L	K	L
WT, G2 #2	ATGGTGTTAA	ATGGTGTTAA	ATGGTGTTAA	ATGGTGTTAA	ATGGTGTTAA
Translation +1	M	V	L	K	L
WT, G2 #22	ATGGTGTTAA	ATGGTGTTAA	ATGGTGTTAA	ATGGTGTTAA	ATGGTGTTAA
Translation +1	M	V	L	K	L
WT, G2 #6	ATGGTGTTAA	ATGGTGTTAA	ATGGTGTTAA	ATGGTGTTAA	ATGGTGTTAA
Translation +1	M	V	L	K	L
WT, G2 #3 old	ATGGTGTTAA	ATGGTGTTAA	ATGGTGTTAA	ATGGTGTTAA	ATGGTGTTAA
Translation +1	M	V	L	K	L
WT, G2 #7 old	ATGGTGTTAA	ATGGTGTTAA	ATGGTGTTAA	ATGGTGTTAA	ATGGTGTTAA
Translation +1	M	V	L	K	L
WT, G2 #30	ATGGTGTTAA	ATGGTGTTAA	ATGGTGTTAA	ATGGTGTTAA	ATGGTGTTAA
Translation +1	M	V	L	K	L
WT, G2 #10	ATGGTGTTAA	ATGGTGTTAA	ATGGTGTTAA	ATGGTGTTAA	ATGGTGTTAA
Translation +1	M	V	L	K	L
WT, G2 #14	ATGGTGTTAA	ATGGTGTTAA	ATGGTGTTAA	ATGGTGTTAA	ATGGTGTTAA
Translation +1	M	V	L	K	L
WT, G2 #28	ATGGTGTTAA	ATGGTGTTAA	ATGGTGTTAA	ATGGTGTTAA	ATGGTGTTAA
Translation +1	M	V	L	K	L
TA014, G2 #4 old	ATGGTGTTAA	ATGGTGTTAA	ATGGTGTTAA	ATGGTGTTAA	ATGGTGTTAA
Translation +1	M	V	L	K	L
TA014, G2 #8	ATGGTGTTAA	ATGGTGTTAA	ATGGTGTTAA	ATGGTGTTAA	ATGGTGTTAA
Translation +1	M	V	L	K	L
TA014, G2 #8 old	ATGGTGTTAA	ATGGTGTTAA	ATGGTGTTAA	ATGGTGTTAA	ATGGTGTTAA
Translation +1	M	V	L	K	L
TA014, G2 #4	ATGGTGTTAA	ATGGTGTTAA	ATGGTGTTAA	ATGGTGTTAA	ATGGTGTTAA
Translation +1	M	V	L	K	L
TA014, G2 #24	ATGGTGTTAA	ATGGTGTTAA	ATGGTGTTAA	ATGGTGTTAA	ATGGTGTTAA
Translation +1	M	V	L	K	L
TA014, G2 #16	ATGGTGTTAA	ATGGTGTTAA	ATGGTGTTAA	ATGGTGTTAA	ATGGTGTTAA
Translation +1	M	V	L	K	L
TA014, G2 #12	ATGGTGTTAA	ATGGTGTTAA	ATGGTGTTAA	ATGGTGTTAA	ATGGTGTTAA
Translation +1	M	V	L	K	L
TA014, G2 #28	ATGGTGTTAA	ATGGTGTTAA	ATGGTGTTAA	ATGGTGTTAA	ATGGTGTTAA
Translation +1	M	V	L	K	L
TA014, G2 #20	ATGGTGTTAA	ATGGTGTTAA	ATGGTGTTAA	ATGGTGTTAA	ATGGTGTTAA
Translation +1	M	V	L	K	L

		100	120	140	160	180
G2	GCAGGACCCG	GCAGGACCCG	GCAGGACCCG	GCAGGACCCG	GCAGGACCCG	GCAGGACCCG
Translation +1	A	G	P	G	R	V
Consensus	GCAGGACCCG	GCAGGACCCG	GCAGGACCCG	GCAGGACCCG	GCAGGACCCG	GCAGGACCCG
Translation +1	A	G	P	G	R	V
WT, G2 #2	GCAGGACCCG	GCAGGACCCG	GCAGGACCCG	GCAGGACCCG	GCAGGACCCG	GCAGGACCCG
Translation +1	A	G	P	G	R	V
WT, G2 #22	GCAGGACCCG	GCAGGACCCG	GCAGGACCCG	GCAGGACCCG	GCAGGACCCG	GCAGGACCCG
Translation +1	A	G	P	G	R	V
WT, G2 #6	GCAGGACCCG	GCAGGACCCG	GCAGGACCCG	GCAGGACCCG	GCAGGACCCG	GCAGGACCCG
Translation +1	A	G	P	G	R	V
WT, G2 #3 old	GCAGGACCCG	GCAGGACCCG	GCAGGACCCG	GCAGGACCCG	GCAGGACCCG	GCAGGACCCG
Translation +1	A	G	P	G	R	V
WT, G2 #7 old	GCAGGACCCG	GCAGGACCCG	GCAGGACCCG	GCAGGACCCG	GCAGGACCCG	GCAGGACCCG
Translation +1	A	G	P	G	R	V
WT, G2 #30	GCAGGACCCG	GCAGGACCCG	GCAGGACCCG	GCAGGACCCG	GCAGGACCCG	GCAGGACCCG
Translation +1	A	G	P	G	R	V
WT, G2 #10	GCAGGACCCG	GCAGGACCCG	GCAGGACCCG	GCAGGACCCG	GCAGGACCCG	GCAGGACCCG
Translation +1	A	G	P	G	R	V
WT, G2 #14	GCAGGACCCG	GCAGGACCCG	GCAGGACCCG	GCAGGACCCG	GCAGGACCCG	GCAGGACCCG
Translation +1	A	G	P	G	R	V
WT, G2 #28	GCAGGACCCG	GCAGGACCCG	GCAGGACCCG	GCAGGACCCG	GCAGGACCCG	GCAGGACCCG
Translation +1	A	G	P	G	R	V
TA014, G2 #4 old	GCAGGACCCG	GCAGGACCCG	GCAGGACCCG	GCAGGACCCG	GCAGGACCCG	GCAGGACCCG
Translation +1	A	G	P	G	R	V
TA014, G2 #8	GCAGGACCCG	GCAGGACCCG	GCAGGACCCG	GCAGGACCCG	GCAGGACCCG	GCAGGACCCG
Translation +1	A	G	P	G	R	V
TA014, G2 #8 old	GCAGGACCCG	GCAGGACCCG	GCAGGACCCG	GCAGGACCCG	GCAGGACCCG	GCAGGACCCG
Translation +1	A	G	P	G	R	V
TA014, G2 #4	GCAGGACCCG	GCAGGACCCG	GCAGGACCCG	GCAGGACCCG	GCAGGACCCG	GCAGGACCCG
Translation +1	A	G	P	G	R	V
TA014, G2 #16	GCAGGACCCG	GCAGGACCCG	GCAGGACCCG	GCAGGACCCG	GCAGGACCCG	GCAGGACCCG
Translation +1	A	G	P	G	R	V
TA014, G2 #12	GCAGGACCCG	GCAGGACCCG	GCAGGACCCG	GCAGGACCCG	GCAGGACCCG	GCAGGACCCG
Translation +1	A	G	P	G	R	V
TA014, G2 #28	GCAGGACCCG	GCAGGACCCG	GCAGGACCCG	GCAGGACCCG	GCAGGACCCG	GCAGGACCCG
Translation +1	A	G	P	G	R	V
TA014, G2 #20	GCAGGACCCG	GCAGGACCCG	GCAGGACCCG	GCAGGACCCG	GCAGGACCCG	GCAGGACCCG
Translation +1	A	G	P	G	R	V

[illegible]

[illegible]

[illegible]

[illegible]

[illegible]

[illegible]

[illegible]

	1,640	1,660
G2	GTTGCGGCTCTTGATTCTCTAGCGGTGTTACCGTAA	
Translation +1	V A A L D S L A V V P *	
Consensus	GTTGCGGCTCTTGATTCTCTAGCGGTGTTACCGTAA	
Translation +1	V A A L D S L A V V P *	
WT, G2 # 2	GTTGCGGCTCTTGATTCTCTAGCGGTGTTACCGTAA	
Translation +1	V A A L D S L A V V P *	
WT, G2 # 22	GTTGCGGCTCTTGATTCTCTAGCGGTGTTACCGTAA	
Translation +1	V A A L D S L A V V P *	
WT, G2 # 6	GTTGCGGCTCTTGATTCTCTAGCGGTGTTACCGTAA	
Translation +1	V A A L D S L A V V P *	
WT, G2 # 3 old	GTTGCGGCTCTTGATTCTCTAGCGGTGTTACCGTAA	
Translation +1	V A A L D S L A V V P *	
WT, G2 # 7 old	GTTGCGGCTCTTGATTCTCTAGCGGTGTTACCGTAA	
Translation +1	V A A L D S L A V V P *	
WT, G2 # 30	GTTGCGGCTCTTGATTCTCTAGCGGTGTTACCGTAA	
Translation +1	V A A L D S L A V V P *	
WT, G2 # 10	GTTGCGGCTCTTGATTCTCTAGCGGTGTTACCGTAA	
Translation +1	V A A L D S L A V V P *	
WT, G2 # 14	GTTGCGGCTCTTGATTCTCTAGCGGTGTTACCGTAA	
Translation +1	V A A L D S L A V V P *	
WT, G2 # 26	GTTGCGGCTCTTGATTCTCTAGCGGTGTTACCGTAA	
Translation +1	V A A L D S L A V V P *	
TA014, G2 # 4 old	GTTGCGGCTCTTGATTCTCTAGCGGTGTTACCGTAA	
Translation +1	V A A L D S L A V V P *	
TA014, G2 # 8	GTTGCGGCTCTTGATTCTCTAGCGGTGTTACCGTAA	
Translation +1	V A A L D S L A V V P *	
TA014, G2 # 8 old	GTTGCGGCTCTTGATTCTCTAGCGGTGTTACCGTAA	
Translation +1	V A A L D S L A V V P *	
TA014, G2 # 4	GTTGCGGCTCTTGATTCTCTAGCGGTGTTACCGTAA	
Translation +1	V A A L D S L A V V P *	
TA014, G2 # 24	GTTGCGGCTCTTGATTCTCTAGCGGTGTTACCGTAA	
Translation +1	V A A L D S L A V V P *	
TA014, G2 # 16	GTTGCGGCTCTTGATTCTCTAGCGGTGTTACCGTAA	
Translation +1	V A A L D S L A V V P *	
TA014, G2 # 12	GTTGCGGCTCTTGATTCTCTAGCGGTGTTACCGTAA	
Translation +1	V A A L D S L A V V P *	
TA014, G2 # 28	GTTGCGGCTCTTGATTCTCTAGCGGTGTTACCGTAA	
Translation +1	V A A L D S L A V V P *	
TA014, G2 # 20	GTTGCGGCTCTTGATTCTCTAGCGGTGTTACCGTAA	
Translation +1	V A A L D S L A V V P *	

Reference List

- Acestor, N, Zikova, A, Dalley, RA, Anupama, A, Panigrahi, AK & Stuart, KD. (2011). Trypanosoma brucei mitochondrial respiratome: composition and organization in procyclic form. *Mol Cell Proteomics*, **10**, M110.
- Aksoy, S. (2003). Control of tsetse flies and trypanosomes using molecular genetics. *Vet Parasitol*, **115**, 125-145.
- Aksoy, S, Maudlin, I, Dale, C, Robinson, AS & O'Neill, SL. (2001). Prospects for control of African trypanosomiasis by tsetse vector manipulation. *Trends Parasitol*, **17**, 29-35.
- Al-Salabi, MI & de Koning, HP. (2005). Purine nucleobase transport in amastigotes of Leishmania mexicana: involvement in allopurinol uptake. *Antimicrob Agents Chemother*, **49**, 3682-3689.
- Albert, MA, Haanstra, JR, Hannaert, V, Van, RJ, Opperdoes, FR, Bakker, BM & Michels, PA. (2005). Experimental and in silico analyses of glycolytic flux control in bloodstream form Trypanosoma brucei. *J Biol Chem*, **280**, 28306-28315.
- Allsopp, R. (2001). Options for vector control against trypanosomiasis in Africa. *Trends Parasitol*, **17**, 15-19.
- Alsford, S, Eckert, S, Baker, N, Glover, L, Sanchez-Flores, A, Leung, KF, Turner, DJ, Field, MC, Berriman, M & Horn, D. (2012). High-throughput decoding of antitrypanosomal drug efficacy and resistance. *Nature*, **482**, 232-236.
- Ammon, HP & Wahl, MA. (1991). Pharmacology of Curcuma longa. *Planta Med*, **57**, 1-7.
- Arnold, K, Tran, TH, Nguyen, TC, Nguyen, HP & Pham, P. (1990). A randomized comparative study of artemisinin (qinghaosu) suppositories and oral quinine in acute falciparum malaria. *Trans R Soc Trop Med Hyg*, **84**, 499-502.
- Atsumi, T, Fujisawa, S & Tonosaki, K. (2005). Relationship between intracellular ROS production and membrane mobility in curcumin- and tetrahydrocurcumin-treated human gingival fibroblasts and human submandibular gland carcinoma cells. *Oral Dis*, **11**, 236-242.
- Bacchi, CJ. (1993). Resistance to clinical drugs in African trypanosomes. *Parasitol Today*, **9**, 190-193.
- Bacchi, CJ. (2009). Chemotherapy of human african trypanosomiasis. *Interdiscip Perspect Infect Dis*, **2009**, 195040.
- Baker, N, Alsford, S & Horn, D. (2011). Genome-wide RNAi screens in African trypanosomes identify the nifurtimox activator NTR and the eflornithine transporter AAT6. *Mol Biochem Parasitol*, **176**, 55-57.
- Balana-Fouce, R, Reguera, RM, Cubria, JC & Ordonez, D. (1998). The pharmacology of leishmaniasis. *Gen Pharmacol*, **30**, 435-443.

- Baldwin, SA, Beal, PR, Yao, SY, King, AE, Cass, CE & Young, JD. (2004). The equilibrative nucleoside transporter family, SLC29. *Pflugers Arch*, **447**, 735-743.
- Barennes, H, Balima-Koussoube, T, Nagot, N, Charpentier, JC & Pussard, E. (2006). Safety and efficacy of rectal compared with intramuscular quinine for the early treatment of moderately severe malaria in children: randomised clinical trial. *BMJ*, **332**, 1055-1059.
- Barrett, MP. (1999). The fall and rise of sleeping sickness. *Lancet*, **353**, 1113-1114.
- Barrett, MP, Boykin, DW, Brun, R & Tidwell, RR. (2007). Human African trypanosomiasis: pharmacological re-engagement with a neglected disease. *Br J Pharmacol*, **152**, 1155-1171.
- Barrett, MP, Burchmore, RJS, Stich, A, Lazzari, JO, Frasch, AC, Cazzulo, JJ & Krishna, S. (2003). The trypanosomiasis. *The Lancet*, **362**, 1469-1480.
- Barrett, MP, Zhang, ZQ, Denise, H, Giroud, C & Baltz, T. (1995). A diamidine-resistant *Trypanosoma equiperdum* clone contains a P2 purine transporter with reduced substrate affinity. *Mol Biochem Parasitol*, **73**, 223-229.
- Basselin, M, Lawrence, F & Robert-Gero, M. (1996). Pentamidine uptake in *Leishmania donovani* and *Leishmania amazonensis* promastigotes and axenic amastigotes. *Biochem J*, **315** (Pt 2), 631-634.
- Ben, SA, Zakraoui, H, Zaatour, A, Ftaiti, A, Zaafour, B, Garraoui, A, Olliaro, PL, Dellagi, K & Ben, IR. (1995). A randomized, placebo-controlled trial in Tunisia treating cutaneous leishmaniasis with paromomycin ointment. *Am J Trop Med Hyg*, **53**, 162-166.
- Besteiro, S, Williams, RAM, Coombs, GH & Mottram, JC. (2007). Protein turnover and differentiation in *Leishmania*. *International journal for parasitology*, **37**, 1063-1075.
- Bienen, EJ, Maturi, RK, Pollakis, G & Clarkson, AB, Jr. (1993). Non-cytochrome mediated mitochondrial ATP production in bloodstream form *Trypanosoma brucei brucei*. *Eur J Biochem*, **216**, 75-80.
- Blum, J, Nkunku, S & Burri, C. (2001). Clinical description of encephalopathic syndromes and risk factors for their occurrence and outcome during melarsoprol treatment of human African trypanosomiasis. *Trop Med Int Health*, **6**, 390-400.
- Bodenhamer, JE & Smilkstein, MJ. (1993). Delayed cardiotoxicity following quinine overdose: a case report. *J Emerg Med*, **11**, 279-285.
- Boland, ME, Brennand Roper, SM & Henry, JA. (1985). Complications of quinine poisoning. *The Lancet*, **325**, 384-385.
- Bridges, DJ, Gould, MK, Nerima, B, Maser, P, Burchmore, RJ & de Koning, HP. (2007a). Loss of the high-affinity pentamidine transporter is responsible for high levels of cross-resistance between arsenical and diamidine drugs in African trypanosomes. *Mol Pharmacol*, **71**, 1098-1108.

Bridges, DJ, Gould, MK, Nerima, B, Maser, P, Burchmore, RJ & de Koning, HP. (2007b). Loss of the high-affinity pentamidine transporter is responsible for high levels of cross-resistance between arsenical and diamidine drugs in African trypanosomes. *Mol Pharmacol*, **71**, 1098-1108.

Brochu, C, Wang, J, Roy, G, Messier, N, Wang, XY, Saravia, NG & Ouellette, M. (2003). Antimony uptake systems in the protozoan parasite *Leishmania* and accumulation differences in antimony-resistant parasites. *Antimicrob Agents Chemother*, **47**, 3073-3079.

Brown, SV, Hosking, P, Li, J & Williams, N. (2006). ATP synthase is responsible for maintaining mitochondrial membrane potential in bloodstream form *Trypanosoma brucei*. *Eukaryotic cell*, **5**, 45-53.

Brun, R, Blum, J, Chappuis, F & Burri, C. (2010). Human African trypanosomiasis. *Lancet*, **375**, 148-159.

Burri, C. (2010). Chemotherapy against human African trypanosomiasis: is there a road to success? *Parasitology*, **137**, 1987-1994.

Burri, C & Brun, R. (2003). Eflornithine for the treatment of human African trypanosomiasis. *Parasitology research*, **90**, 49-52.

Chang, K, Fong, D & Bray, R. (1985). Biology of *Leishmania* and Leishmaniasis. In *Leishmaniasis*. ed. Elsevier. pp. 1-30. Elsevier: Amsterdam, The Netherlands.

Changtam, C, de Koning, HP, Ibrahim, H, Sajid, MS, Gould, MK & Suksamrarn, A. (2010a). Curcuminoid analogs with potent activity against *Trypanosoma* and *Leishmania* species. *Eur J Med Chem*, **45**, 941-956.

Changtam, C, Hongmanee, P & Suksamrarn, A. (2010b). Isoxazole analogs of curcuminoids with highly potent multidrug-resistant antimycobacterial activity. *European journal of medicinal chemistry*, **45**, 4446-4457.

Chappuis, F, Sundar, S, Hailu, A, Ghalib, H, Rijal, S, Peeling, RW, Alvar, J & Boelaert, M. (2007). Visceral leishmaniasis: what are the needs for diagnosis, treatment and control? *Nat Rev Microbiol*, **5**, 873-882.

Chaudhuri, M, Ott, RD & Hill, GC. (2006). Trypanosome alternative oxidase: from molecule to function. *Trends Parasitol*, **22**, 484-491.

Chen, H, Zhang, ZS, Zhang, YL & Zhou, DY. (1999). Curcumin inhibits cell proliferation by interfering with the cell cycle and inducing apoptosis in colon carcinoma cells. *Anticancer Res*, **19**, 3675-3680.

Choudhuri, T, Pal, S, Agwarwal, ML, Das, T & Sa, G. (2002). Curcumin induces apoptosis in human breast cancer cells through p53-dependent Bax induction. *FEBS Lett*, **512**, 334-340.

Clarkson Jr, AB & Amole, BO. (1982). Role of calcium in trypanocidal drug action. *Science*, **216**, 1321-1323.

Connell, SR, Tracz, DM, Nierhaus, KH & Taylor, DE. (2003). Ribosomal protection proteins and their mechanism of tetracycline resistance. *Antimicrobial agents and chemotherapy*, **47**, 3675-3681.

- Coustou, V, Besteiro, S, Riviere, L, Biran, M, Biteau, N, Franconi, JM, Boshart, M, Baltz, T & Bringaud, F. (2005). A mitochondrial NADH-dependent fumarate reductase involved in the production of succinate excreted by procyclic *Trypanosoma brucei*. *J Biol Chem*, **280**, 16559-16570.
- Creek, DJ, Jankevics, A, Burgess, KEV, Breitling, R & Barrett, MP. (2012). IDEOM: An Excel interface for analysis of LC-MS based metabolomics data. *Bioinformatics*.
- Croft, SL, Barrett, MP & Urbina, JA. (2005). Chemotherapy of trypanosomiasis and leishmaniasis. *Trends Parasitol*, **21**, 508-512.
- Croft, SL & Coombs, GH. (2003). Leishmaniasis--current chemotherapy and recent advances in the search for novel drugs. *Trends Parasitol*, **19**, 502-508.
- Cunningham, ML, Zvelebil, MJ & Fairlamb, AH. (1994). Mechanism of inhibition of trypanothione reductase and glutathione reductase by trivalent organic arsenicals. *Eur J Biochem*, **221**, 285-295.
- Dahl, EL, Shock, JL, Shenai, BR, Gut, J, DeRisi, JL & Rosenthal, PJ. (2006). Tetracyclines specifically target the apicoplast of the malaria parasite *Plasmodium falciparum*. *Antimicrob Agents Chemother*, **50**, 3124-3131.
- Dardonville, C & Brun, R. (2004). Bisguanidine, bis(2-aminoimidazoline), and polyamine derivatives as potent and selective chemotherapeutic agents against *Trypanosoma brucei rhodesiense*. Synthesis and in vitro evaluation. *J Med Chem*, **47**, 2296-2307.
- de Koning, HP. (2001a). Transporters in African trypanosomes: role in drug action and resistance. *Int J Parasitol*, **31**, 512-522.
- de Koning, HP. (2001b). Uptake of pentamidine in *Trypanosoma brucei brucei* is mediated by three distinct transporters: implications for cross-resistance with arsenicals. *Mol Pharmacol*, **59**, 586-592.
- de Koning, HP. (2008). Ever-increasing complexities of diamidine and arsenical crossresistance in African trypanosomes. *Trends Parasitol*, **24**, 345-349.
- de Koning, HP, Anderson, LF, Stewart, M, Burchmore, RJ, Wallace, LJ & Barrett, MP. (2004). The trypanocide diminazene aceturate is accumulated predominantly through the TbAT1 purine transporter: additional insights on diamidine resistance in african trypanosomes. *Antimicrob Agents Chemother*, **48**, 1515-1519.
- de Koning, HP, Bridges, DJ & Burchmore, RJ. (2005). Purine and pyrimidine transport in pathogenic protozoa: from biology to therapy. *FEMS Microbiol Rev*, **29**, 987-1020.
- de Koning, HP, Gould, MK, Sterk, GJ, Tenor, H, Kunz, S, Luginbuehl, E & Seebeck, T. (2012). Pharmacological validation of *Trypanosoma brucei* phosphodiesterases as novel drug targets. *Journal of Infectious Diseases*.

- de Koning, HP & Jarvis, SM. (1997). Hypoxanthine uptake through a purine-selective nucleobase transporter in *Trypanosoma brucei* procyclic cells is driven by protonmotive force. *Eur J Biochem*, **247**, 1102-1110.
- de Koning, HP. (2007). Pyrimidine transporters of trypanosomes - a class apart? *Trend Parasitology*, **23**, 190.
- Delespaulx, V & de Koning, HP. (2007). Drugs and drug resistance in African trypanosomiasis. *Drug Resist Updat*, **10**, 30-50.
- Denise, H & Barrett, MP. (2001). Uptake and mode of action of drugs used against sleeping sickness. *Biochem Pharmacol*, **61**, 1-5.
- Denninger, V, Figarella, K, Schonfeld, C, Brems, S, Busold, C, Lang, F, Hoheisel, J & Duszenko, M. (2007a). Troglitazone induces differentiation in *Trypanosoma brucei*. *Exp Cell Res*, **313**, 1805-1819.
- Denninger, V, Figarella, K, Schonfeld, C, Brems, S, Busold, C, Lang, F, Hoheisel, J & Duszenko, M. (2007b). Troglitazone induces differentiation in *Trypanosoma brucei*. *Exp Cell Res*, **313**, 1805-1819.
- Desjeux, P. (2004). Leishmaniasis: current situation and new perspectives. *Comp Immunol Microbiol Infect Dis*, **27**, 305-318.
- Docampo, R & Moreno, SNJ. (1996). The role of Ca²⁺ in the process of cell invasion by intracellular parasites. *Parasitology Today*, **12**, 61-65.
- Drain, J, Bishop, JR & Hajduk, SL. (2001). Haptoglobin-related protein mediates trypanosome lytic factor binding to trypanosomes. *J Biol Chem*, **276**, 30254-30260.
- Duszenko, M, Figarella, K, Macleod, ET & Welburn, SC. (2006). Death of a trypanosome: a selfish altruism. *Trends Parasitol*, **22**, 536-542.
- Efferth, T, Dunstan, H, Sauerbrey, A, Miyachi, H & Chitambar, CR. (2001). The anti-malarial artesunate is also active against cancer. *Int J Oncol*, **18**, 767-773.
- Eintracht, J, Maathai, R, Mellors, A & Ruben, L. (1998). Calcium entry in *Trypanosoma brucei* is regulated by phospholipase A2 and arachidonic acid. *Biochemical Journal*, **336**, 659.
- el Kouni, MH. (2003). Potential chemotherapeutic targets in the purine metabolism of parasites. *Pharmacol Ther*, **99**, 283-309.
- Fahey, RC & Newton, GL. (1983). Occurrence of low molecular weight thiols in biological systems.
- Fairlamb, AH, Carter, NS, Cunningham, M & Smith, K. (1992). Characterisation of melarsen-resistant *Trypanosoma brucei* with respect to cross-resistance to other drugs and trypanothione metabolism. *Mol Biochem Parasitol*, **53**, 213-222.
- Fairlamb, AH, Henderson, GB, Bacchi, CJ & Cerami, A. (1987). In vivo effects of difluoromethylornithine on trypanothione and polyamine levels in bloodstream

- forms of *Trypanosoma brucei*. *Molecular and biochemical parasitology*, **24**, 185-191.
- Fairlamb, AH, Henderson, GB & Cerami, A. (1989). Trypanothione is the primary target for arsenical drugs against African trypanosomes. *Proc Natl Acad Sci U S A*, **86**, 2607-2611.
- Fairlamb, AH, Quesne, SA, Hide, G, Mottram, JC, Coombs, GH & Holmes, PH. (1997). Polyamine metabolism in trypanosomes. *Trypanosomiasis and leishmaniasis: biology and control*, 149-161.
- Fernandez, MM, Malchiodi, EL & Algranati, ID. (2011). Differential effects of paromomycin on ribosomes of *Leishmania mexicana* and mammalian cells. *Antimicrob Agents Chemother*, **55**, 86-93.
- Ferreira, JF & Janick, J. (1996). Distribution of artemisinin in *Artemisia annua*. In *Progress in new crops*. ed. J. Janick. pp. 579-584. ASHS Press: Arlington, VA.
- Fidalgo, LM & Gille, L. (2011). Mitochondria and trypanosomatids: targets and drugs. *Pharm Res*, **28**, 2758-2770.
- Field, MC & Carrington, M. (2009). The trypanosome flagellar pocket. *Nat Rev Microbiol*, **7**, 775-786.
- Figurella, K, Uzcategui, NL, Beck, A, Schoenfeld, C, Kubata, BK, Lang, F & Duzenko, M. (2006). Prostaglandin-induced programmed cell death in *Trypanosoma brucei* involves oxidative stress. *Cell Death Differ*, **13**, 1802-1814.
- Fischer, C, Voss, A & Engel, J. (2001). Development status of miltefosine as first oral drug in visceral and cutaneous leishmaniasis. *Medical Microbiology and Immunology*, **190**, 85-87.
- Flanigan, TP, Ramratnam, B, Graeber, C, Hellinger, J, Smith, D, Wheeler, D, Hawley, P, Heath-Chiozzi, M, Ward, DJ, Brummitt, C & Turner, J. (1996). Prospective trial of paromomycin for cryptosporidiosis in AIDS. *Am J Med*, **100**, 370-372.
- Frezard, F, Martins, PS, Bahia, AP, Le, ML, de Melo, AL, Pimenta, AM, Salerno, M, da Silva, JB & Demicheli, C. (2008). Enhanced oral delivery of antimony from meglumine antimoniate/beta-cyclodextrin nanoassemblies. *Int J Pharm*, **347**, 102-108.
- Fumarola, L, Spinelli, R & Brandonisio, O. (2004a). In vitro assays for evaluation of drug activity against *Leishmania* spp. *Res Microbiol*, **155**, 224-230.
- Fumarola, L, Spinelli, R & Brandonisio, O. (2004b). In vitro assays for evaluation of drug activity against *Leishmania* spp. *Res Microbiol*, **155**, 224-230.
- Galarreta, BC, Sifuentes, R, Carrillo, AK, Sanchez, L, Amado, MRI & Maruenda, H. (2008). The use of natural product scaffolds as leads in the search for trypanothione reductase inhibitors. *Bioorganic & medicinal chemistry*, **16**, 6689-6695.
- Ganguly, NK. (2002). Oral miltefosine may revolutionize treatment of visceral leishmaniasis. *TDR News*, **68**.

- Garcia, LS. (2007). Diagnostic Medical Parasitology, 5Th Edition. *Shock*, **27**.
- Gasser, RA, Jr., Magill, AJ, Oster, CN, Franke, ED, Grogl, M & Berman, JD. (1994). Pancreatitis induced by pentavalent antimonial agents during treatment of leishmaniasis. *Clin Infect Dis*, **18**, 83-90.
- Gomes, DC, Alegrio, LV, Leon, LL & de Lima, ME. (2002). Total synthesis and anti-leishmanial activity of some curcumin analogues. *Arzneimittelforschung*, **52**, 695-698.
- Gonzalez, RJ & Tarloff, JB. (2001). Evaluation of hepatic subcellular fractions for Alamar blue and MTT reductase activity. *Toxicol In Vitro*, **15**, 257-259.
- Gray, JH, Owen, RP & Giacomini, KM. (2004). The concentrative nucleoside transporter family, SLC28. *Pflugers Arch*, **447**, 728-734.
- Griffith, OW. (1999). Biologic and pharmacologic regulation of mammalian glutathione synthesis. *Free Radic Biol Med*, **27**, 922-935.
- Griffith, OW & Mulcahy, RT. (1999). The enzymes of glutathione synthesis: gamma-glutamylcysteine synthetase. *Adv Enzymol Relat Areas Mol Biol*, **73**, 209-67, xii.
- Grondin, K, Haimeur, A, Mukhopadhyay, R, Rosen, BP & Ouellette, M. (1997). Co-amplification of the gamma-glutamylcysteine synthetase gene gsh1 and of the ABC transporter gene pgpA in arsenite-resistant *Leishmania tarentolae*. *EMBO J*, **16**, 3057-3065.
- Gulcubuk, A, Altunatmaz, K, Sonmez, K, Haktanir-Yatkin, D, Uzun, H, Gurel, A & Aydin, S. (2006). Effects of curcumin on tumour necrosis factor-alpha and interleukin-6 in the late phase of experimental acute pancreatitis. *J Vet Med A Physiol Pathol Clin Med*, **53**, 49-54.
- Haanstra, JR, van, TA, Kessler, P, Reijnders, W, Michels, PA, Westerhoff, HV, Parsons, M & Bakker, BM. (2008). Compartmentation prevents a lethal turbo-explosion of glycolysis in trypanosomes. *Proc Natl Acad Sci U S A*, **105**, 17718-17723.
- Haberkorn, A, Harder, A & Greif, G. (2001). Milestones of protozoan research at Bayer. *Parasitol Res*, **87**, 1060-1062.
- Haines, LR, Hancock, RE & Pearson, TW. (2003). Cationic antimicrobial peptide killing of African trypanosomes and *Sodalis glossinidius*, a bacterial symbiont of the insect vector of sleeping sickness. *Vector Borne Zoonotic Dis*, **3**, 175-186.
- Hammarton, TC, Clark, J, Douglas, F, Boshart, M & Mottram, JC. (2003). Stage-specific differences in cell cycle control in *Trypanosoma brucei* revealed by RNA interference of a mitotic cyclin. *J Biol Chem*, **278**, 22877-22886.
- Hassan, HF & Coombs, GH. (1988). Purine and pyrimidine metabolism in parasitic protozoa. *FEMS Microbiol Rev*, **4**, 47-83.
- Hayes, JD & McLellan, LI. (1999). Glutathione and glutathione-dependent enzymes represent a co-ordinately regulated defence against oxidative stress. *Free Radic Res*, **31**, 273-300.

- Hepburn, NC, Siddique, I, Howie, AF, Beckett, GJ & Hayes, PC. (1993). Hepatotoxicity of sodium stibogluconate in leishmaniasis. *Lancet*, **342**, 238-239.
- Hide, G & Tilley, A. (2001). Use of mobile genetic elements as tools for molecular epidemiology. *Int J Parasitol*, **31**, 599-602.
- Hien, TT & White, NJ. (1993). Qinghaosu. *Lancet*, **341**, 603-608.
- Holder, GM, Plummer, JL & Ryan, AJ. (1978). The metabolism and excretion of curcumin (1,7-bis-(4-hydroxy-3-methoxyphenyl)-1,6-heptadiene-3,5-dione) in the rat. *Xenobiotica*, **8**, 761-768.
- Ibrahim, H. (2009a). New therapeutic strategies against trypanosomiasis and leishmaniasis. University of Glasgow.
- Ibrahim, H. (2009b). New therapeutic strategies against trypanosomiasis and leishmaniasis. Thesis for the Degree of Doctor of Philosophy, Glasgow University.
- Ibrahim, HM, Al-Salabi, MI, El, SN, Quashie, NB, Alkhaldi, AA, Escalé, R, Smith, TK, Vial, HJ & de Koning, HP. (2011). Symmetrical choline-derived dications display strong anti-kinetoplastid activity. *J Antimicrob Chemother*, **66**, 111-125.
- Imaida, K, Tamano, S, Kato, K, Ikeda, Y, Asamoto, M, Takahashi, S, Nir, Z, Murakoshi, M, Nishino, H & Shirai, T. (2001). Lack of chemopreventive effects of lycopene and curcumin on experimental rat prostate carcinogenesis. *Carcinogenesis*, **22**, 467-472.
- IMBODEN, CA, Jr., COOPER, WC, COATNEY, GR & JEFFERY, GM. (1950). Studies in human malaria. XXIX. Trials of aureomycin, chloramphenicol, penicillin, and dihydrostreptomycin against the Chesson strain of *Plasmodium vivax*. *J Natl Malar Soc*, **9**, 377-380.
- Iqbal, M, Okazaki, Y & Okada, S. (2009). Curcumin attenuates oxidative damage in animals treated with a renal carcinogen, ferric nitrilotriacetate (Fe-NTA): implications for cancer prevention. *Mol Cell Biochem*, **324**, 157-164.
- Iqbal, M, Sharma, SD, Okazaki, Y, Fujisawa, M & Okada, S. (2003). Dietary supplementation of curcumin enhances antioxidant and phase II metabolizing enzymes in ddY male mice: possible role in protection against chemical carcinogenesis and toxicity. *Pharmacol Toxicol*, **92**, 33-38.
- Ishiyama, A, Otoguro, K, Namatame, M, Nishihara, A, Furusawa, T, Masuma, R, Shiomi, K, Takahashi, Y, Ichimura, M & Yamada, H. (2008). In Vitro and in Vivo Antitrypanosomal Activity of Two Microbial Metabolites, KS-505a and Alazopeptin. *The Journal of antibiotics*, **61**, 627-632.
- Iten, M, Matovu, E, Brun, R & Kaminsky, R. (1995). Innate lack of susceptibility of Ugandan *Trypanosoma brucei rhodesiense* to DL- α -difluoromethylornithine (DFMO). *Trop Med Parasitol*, **46**, 190-194.
- Iten, M, Mett, H, Evans, A, Enyaru, JC, Brun, R & Kaminsky, R. (1997). Alterations in ornithine decarboxylase characteristics account for tolerance of *Trypanosoma brucei rhodesiense* to D, L- α -difluoromethylornithine. *Antimicrobial agents and chemotherapy*, **41**, 1922-1925.

Jannin, J & Cattand, P. (2004). Treatment and control of human African trypanosomiasis. *Curr Opin Infect Dis*, **17**, 565-571.

Jeffrey, HC & Leach, RM. (1966). *Atlas of medical helminthology and protozoology*. Livingstone.

Jha, TK, Sundar, S, Thakur, CP, Bachmann, P, Karbwang, J, Fischer, C, Voss, A & Berman, J. (1999). Miltefosine, an oral agent, for the treatment of Indian visceral leishmaniasis. *N Engl J Med*, **341**, 1795-1800.

Jhingran, A, Chatterjee, M & Madhubala, R. (2008). Leishmaniasis: Epidemiological Trends and Diagnosis. *Leishmania after the Genome: Biology and Control*, Horizon Scientific Press/Caister Academic Press, Norfolk, UK, 1-14.

Jiang, J, Stoyanovsky, DA, Belikova, NA, Tyurina, YY, Zhao, Q, Tungekar, MA, Kapralova, V, Huang, Z, Mintz, AH, Greenberger, JS & Kagan, VE. (2009). A mitochondria-targeted triphenylphosphonium-conjugated nitroxide functions as a radioprotector/mitigator. *Radiat Res*, **172**, 706-717.

Joe, B, Rao, UJ & Lokesh, BR. (1997). Presence of an acidic glycoprotein in the serum of arthritic rats: modulation by capsaicin and curcumin. *Mol Cell Biochem*, **169**, 125-134.

Jordan, AM. (1986). *Trypanosomiasis control and African rural development*. Longman.

Jung, TT, Rhee, CK, Lee, CS, Park, YS & Choi, DC. (1993). Ototoxicity of salicylate, nonsteroidal antiinflammatory drugs, and quinine. *Otolaryngol Clin North Am*, **26**, 791-810.

Kaiser, M, Bray, MA, Cal, M, Bourdin, TB, Torreele, E & Brun, R. (2011). Antitrypanosomal activity of fexinidazole, a new oral nitroimidazole drug candidate for treatment of sleeping sickness. *Antimicrob Agents Chemother*, **55**, 5602-5608.

Kamleh, A, Barrett, MP, Wildridge, D, Burchmore, RJ, Scheltema, RA & Watson, DG. (2008). Metabolomic profiling using Orbitrap Fourier transform mass spectrometry with hydrophilic interaction chromatography: a method with wide applicability to analysis of biomolecules. *Rapid Commun Mass Spectrom*, **22**, 1912-1918.

Kang, P, Dalvie, D, Smith, E, Zhou, S & Deese, A. (2007). Identification of a novel glutathione conjugate of flutamide in incubations with human liver microsomes. *Drug Metab Dispos*, **35**, 1081-1088.

Kayser, O, Kiderlen, AF & Croft, SL. (2003). Natural products as antiparasitic drugs. *Parasitol Res*, **90 Suppl 2**, S55-S62.

Kedzierski, L. (2010). Leishmaniasis vaccine: where are we today? *Journal of global infectious diseases*, **2**, 177.

Killick-Kendrick, R. (2010). Education is key to controlling visceral leishmaniasis. *Bull World Health Organ*, **88**, 11-12.

- Kinnamon, KE, Steck, EA & Rane, DS. (1979). A new chemical series active against African trypanosomes: benzyltriphenylphosphonium salts. *J Med Chem*, **22**, 452-455.
- Koide, T, Nose, M, Ogihara, Y, Yabu, Y & Ohta, N. (2002a). Leishmanicidal effect of curcumin in vitro. *Biol Pharm Bull*, **25**, 131-133.
- Koide, T, Nose, M, Ogihara, Y, Yabu, Y & Ohta, N. (2002b). Leishmanicidal effect of curcumin in vitro. *Biological & pharmaceutical bulletin*, **25**, 131-133.
- König, J, Wyllie, S, Wells, G, Stevens, MF, Wyatt, PG & Fairlamb, AH. (2011). Antitumor quinol PMX464 is a cytotoxic anti-trypanosomal inhibitor targeting trypanothione metabolism. *Journal of Biological Chemistry*, **286**, 8523.
- Kreier, JPBJR. (1987). *Parasitic Protozoa* London.
- Kuttan, R, Sudheeran, PC & Josph, CD. (1987). Turmeric and curcumin as topical agents in cancer therapy. *Tumori*, **73**, 29-31.
- Lanteri, CA, Tidwell, RR & Meshnick, SR. (2008). The mitochondrion is a site of trypanocidal action of the aromatic diamidine DB75 in bloodstream forms of *Trypanosoma brucei*. *Antimicrob Agents Chemother*, **52**, 875-882.
- Le Roch, KG, Johnson, JR, Ahiboh, H, Chung, DW, Prudhomme, J, Plouffe, D, Henson, K, Zhou, Y, Witola, W, Yates, JR, Mamoun, CB, Winzeler, EA & Vial, H. (2008). A systematic approach to understand the mechanism of action of the bithiazolium compound T4 on the human malaria parasite, *Plasmodium falciparum*. *BMC Genomics*, **9**, 513.
- Lee, J, Im, YH, Jung, HH, Kim, JH, Park, JO, Kim, K, Kim, WS, Ahn, JS, Jung, CW, Park, YS, Kang, WK & Park, K. (2005). Curcumin inhibits interferon- α induced NF- κ B and COX-2 in human A549 non-small cell lung cancer cells. *Biochem Biophys Res Commun*, **334**, 313-318.
- Legros, D, Evans, S, Maiso, F, Enyaru, JC & Mbulamberi, D. (1999). Risk factors for treatment failure after melarsoprol for *Trypanosoma brucei* gambiense trypanosomiasis in Uganda. *Trans R Soc Trop Med Hyg*, **93**, 439-442.
- Legros, D, Ollivier, G, Gastellu-Etcheberry, M, Paquet, C, Burri, C, Jannin, J & Buscher, P. (2002). Treatment of human African trypanosomiasis--present situation and needs for research and development. *Lancet Infect Dis*, **2**, 437-440.
- Li, W, Mo, W, Shen, D, Sun, L, Wang, J, Lu, S, Gitschier, JM & Zhou, B. (2005). Yeast model uncovers dual roles of mitochondria in action of artemisinin. *PLoS Genet*, **1**, e36.
- Luque-Ortega, JR, Reuther, P, Rivas, L & Dardonville, C. (2010). New benzophenone-derived bisphosphonium salts as leishmanicidal leads targeting mitochondria through inhibition of respiratory complex II. *J Med Chem*, **53**, 1788-1798.
- Lutje, V, Seixas, J & Kennedy, A. (2010). Chemotherapy for second-stage Human African trypanosomiasis. *Cochrane Database Syst Rev*, CD006201.

Maheshwari, RK, Singh, AK, Gaddipati, J & Srimal, RC. (2006). Multiple biological activities of curcumin: a short review. *Life sciences*, **78**, 2081-2087.

Mancini, PE & Patton, CL. (1981). Cyclic 3',5'-adenosine monophosphate levels during the developmental cycle of *Trypanosoma brucei brucei* in the rat. *Mol Biochem Parasitol*, **3**, 19-31.

Manson-Bahr, PE. (1987). The Leishmaniasis in Biology and Medicine-clinical Aspects and Control. In *Diagnosis*. ed. W.Peters, K.-K.R. pp. 704-728. Academic press: London.

Manson-Bahr, PEC. (1974). Trypanosomiasis and Leishmaniasis with special reference to Chagas' disease. *Proceedings of the Royal Society of Medicine*, **67**, 966.

Markell, EK, John, DT & Krotoski, WA. (1999). *Markell and Voge's Medical Parasitology*. Saunders Company: USA.

Masamune, A, Suzuki, N, Kikuta, K, Satoh, M, Satoh, K & Shimosegawa, T. (2006). Curcumin blocks activation of pancreatic stellate cells. *J Cell Biochem*, **97**, 1080-1093.

Maser, P, Wittlin, S, Rottmann, M, Wenzler, T, Kaiser, M & Brun, R. (2012). Antiparasitic agents: new drugs on the horizon. *Curr Opin Pharmacol*.

Mathis, AM, Holman, JL, Sturk, LM, Ismail, MA, Boykin, DW, Tidwell, RR & Hall, JE. (2006). Accumulation and intracellular distribution of antitrypanosomal diamidine compounds DB75 and DB820 in African trypanosomes. *Antimicrobial agents and chemotherapy*, **50**, 2185-2191.

Matlashewski, G. (2001). Leishmania infection and virulence. *Med Microbiol Immunol*, **190**, 37-42.

Matovu, E, Stewart, ML, Geiser, F, Brun, R, Maser, P, Wallace, LJ, Burchmore, RJ, Enyaru, JC, Barrett, MP, Kaminsky, R, Seebeck, T & de Koning, HP. (2003a). Mechanisms of arsenical and diamidine uptake and resistance in *Trypanosoma brucei*. *Eukaryot Cell*, **2**, 1003-1008.

Matovu, E, Stewart, ML, Geiser, F, Brun, R, Maser, P, Wallace, LJ, Burchmore, RJ, Enyaru, JC, Barrett, MP, Kaminsky, R, Seebeck, T & de Koning, HP. (2003b). Mechanisms of arsenical and diamidine uptake and resistance in *Trypanosoma brucei*. *Eukaryot Cell*, **2**, 1003-1008.

Matthews, KR. (2005). The developmental cell biology of *Trypanosoma brucei*. *J Cell Sci*, **118**, 283-290.

Meister, A. (1981). Metabolism and functions of glutathione. *Trends in Biochemical Sciences*, **6**, 231-234.

Merschjohann, K, Sporer, F, Steverding, D & Wink, M. (2001). In vitro effect of alkaloids on bloodstream forms of *Trypanosoma brucei* and *T. congolense*. *Planta Med*, **67**, 623-627.

- Mishra, S, Karmodiya, K, Surolia, N & Surolia, A. (2008). Synthesis and exploration of novel curcumin analogues as anti-malarial agents. *Bioorganic & medicinal chemistry*, **16**, 2894-2902.
- Mohammed, MH. (2000). *Physiology of Animal*. Dar Alketab Aljamae: UEA.
- Molina Portela, MP, Raper, J & Tomlinson, S. (2000). An investigation into the mechanism of trypanosome lysis by human serum factors. *Mol Biochem Parasitol*, **110**, 273-282.
- Moreno, B, Urbina, JA, Oldfield, E, Bailey, BN, Rodrigues, CO & Docampo, R. (2000). ³¹P NMR spectroscopy of *Trypanosoma brucei*, *Trypanosoma cruzi*, and *Leishmania major*. Evidence for high levels of condensed inorganic phosphates. *J Biol Chem*, **275**, 28356-28362.
- Moreno, SN, Docampo, R & Vercesi, AE. (1992). Calcium homeostasis in procyclic and bloodstream forms of *Trypanosoma brucei*. Lack of inositol 1, 4, 5-trisphosphate-sensitive Ca²⁺ release. *Journal of Biological Chemistry*, **267**, 6020.
- Moreno, SNJ & Docampo, R. (2003). Calcium regulation in protozoan parasites. *Current opinion in microbiology*, **6**, 359-364.
- Moreno, T, Pous, J, Subirana, JA & Campos, JL. (2010). Coiled-coil conformation of a pentamidine-DNA complex. *Acta Crystallogr D Biol Crystallogr*, **66**, 251-257.
- Mukherjee, A, Padmanabhan, PK, Sahani, MH, Barrett, MP & Madhubala, R. (2006). Roles for mitochondria in pentamidine susceptibility and resistance in *Leishmania donovani*. *Mol Biochem Parasitol*, **145**, 1-10.
- Murphy, MP. (2008). Targeting lipophilic cations to mitochondria. *Biochim Biophys Acta*, **1777**, 1028-1031.
- Nagajyothi, F, Zhao, D, Weiss, LM & Tanowitz, HB. (2012). Curcumin treatment provides protection against *Trypanosoma cruzi* infection. *Parasitol Res*.
- Nare, B, Wring, S, Bacchi, C, Beaudet, B, Bowling, T, Brun, R, Chen, D, Ding, C, Freund, Y, Gaukel, E, Hussain, A, Jarnagin, K, Jenks, M, Kaiser, M, Mercer, L, Mejia, E, Noe, A, Orr, M, Parham, R, Plattner, J, Randolph, R, Rattendi, D, Rewerts, C, Sligar, J, Yarlett, N, Don, R & Jacobs, R. (2010). Discovery of novel orally bioavailable oxaborole 6-carboxamides that demonstrate cure in a murine model of late-stage central nervous system african trypanosomiasis. *Antimicrob Agents Chemother*, **54**, 4379-4388.
- Navin, TR, Arana, BA, Arana, FE, Berman, JD & Chajon, JF. (1992). Placebo-controlled clinical trial of sodium stibogluconate (Pentostam) versus ketoconazole for treating cutaneous leishmaniasis in Guatemala. *J Infect Dis*, **165**, 528-534.
- Naylor, S, Mason, RP, Sanders, JK, Williams, DH & Moneti, G. (1988). Formaldehyde adducts of glutathione. Structure elucidation by two-dimensional nmr spectroscopy and fast-atom-bombardment tandem mass spectrometry. *Biochemical Journal*, **249**, 573.

- Newman, DJ & Cragg, GM. (2007). Natural Products as Sources of New Drugs over the Last 25 Years. *Journal of natural products*, **70**, 461-477.
- Newton, BA. (1974). Introduction. In *Trypanosomiasis and Leishmaniasis with special reference to Chagas' disease*.
- Nose, M, Koide, T, Ogihara, Y, Yabu, Y & Ohta, N. (1998). Trypanocidal effects of curcumin in vitro. *Biol Pharm Bull*, **21**, 643-645.
- Notarbartolo, M, Poma, P, Perri, D, Dusonchet, L, Cervello, M & D'Alessandro, N. (2005). Antitumor effects of curcumin, alone or in combination with cisplatin or doxorubicin, on human hepatic cancer cells. Analysis of their possible relationship to changes in NF-kB activation levels and in IAP gene expression. *Cancer Lett*, **224**, 53-65.
- O'Neill, PM, Barton, VE & Ward, SA. (2010). The molecular mechanism of action of artemisinin--the debate continues. *Molecules*, **15**, 1705-1721.
- Olliaro, P, Lazdins, J & Guhl, F. (2002). Developments in the treatment of leishmaniasis and trypanosomiasis. *Expert Opin Emerg Drugs*, **7**, 61-67.
- Olliaro, PL & Bryceson, AD. (1993). Practical progress and new drugs for changing patterns of leishmaniasis. *Parasitol Today*, **9**, 323-328.
- Opigo, J & Woodrow, C. (2009). NECT trial: more than a small victory over sleeping sickness. *Lancet*, **374**, 7-9.
- Opperdoes, FR & Michels, PAM. (2008). The metabolic repertoire of Leishmania and implications for drug discovery. *Leishmania, after the genome, 1st edn* Caister Academic Press, Norfolk, UK, 123-158.
- Paila, YD, Saha, B & Chattopadhyay, A. (2010). Amphotericin B inhibits entry of Leishmania donovani into primary macrophages. *Biochem Biophys Res Commun*, **399**, 429-433.
- Pan, MH, Huang, TM & Lin, JK. (1999a). Biotransformation of curcumin through reduction and glucuronidation in mice. *Drug Metab Dispos*, **27**, 486-494.
- Pan, MH, Huang, TM & Lin, JK. (1999b). Biotransformation of curcumin through reduction and glucuronidation in mice. *Drug Metab Dispos*, **27**, 486-494.
- Pepin, J & Milord, F. (1994). The treatment of human African trypanosomiasis. *Advances in Parasitology*, **33**, 1-47.
- Perez-Arriaga, L, Mendoza-Magana, ML, Cortes-Zarate, R, Corona-Rivera, A, Bobadilla-Morales, L, Troyo-Sanroman, R & Ramirez-Herrera, MA. (2006). Cytotoxic effect of curcumin on Giardia lamblia trophozoites. *Acta Trop*, **98**, 152-161.
- Peters, W & Killick-Kendrick, R. (1987). *The leishmaniasis in biology and medicine. Vol. I. Biology and epidemiology. Vol. II. Clinical aspects and control* continued. Academic Press Inc.(London) Ltd.
- Phillipson, JD. (1994). Natural products as drugs. *Trans R Soc Trop Med Hyg*, **88** Suppl 1, S17-S19.

Polonio, T & Efferth, T. (2008). Leishmaniasis: drug resistance and natural products (review). *Int J Mol Med*, **22**, 277-286.

Porteous, CM, Logan, A, Evans, C, Ledgerwood, EC, Menon, DK, Aigbirhio, F, Smith, RA & Murphy, MP. (2010). Rapid uptake of lipophilic triphenylphosphonium cations by mitochondria in vivo following intravenous injection: implications for mitochondria-specific therapies and probes. *Biochim Biophys Acta*, **1800**, 1009-1017.

Priotto, G, Kasparian, S, Mutombo, W, Ngouama, D, Ghorashian, S, Arnold, U, Ghabri, S, Baudin, E, Buard, V, Kazadi-Kyanza, S, Ilunga, M, Mutangala, W, Pohlig, G, Schmid, C, Karunakara, U, Torreele, E & Kande, V. (2009). Nifurtimox-eflornithine combination therapy for second-stage African *Trypanosoma brucei* gambiense trypanosomiasis: a multicentre, randomised, phase III, non-inferiority trial. *Lancet*, **374**, 56-64.

Radhakrishna Pillai, G, Srivastava, AS, Hassanein, TI, Chauhan, DP & Carrier, E. (2004). Induction of apoptosis in human lung cancer cells by curcumin. *Cancer letters*, **208**, 163-170.

Rasmussen, HB, Christensen, SB, Kvist, LP & Karazmi, A. (2000). A simple and efficient separation of the curcumins, the antiprotozoal constituents of *Curcuma longa*. *Planta medica*, **66**, 396-398.

Raz, B, Iten, M, Grether-Buhler, Y, Kaminsky, R & Brun, R. (1997a). The Alamar Blue assay to determine drug sensitivity of African trypanosomes (*T.b. rhodesiense* and *T.b. gambiense*) in vitro. *Acta Trop*, **68**, 139-147.

Raz, B, Iten, M, Grether-Buhler, Y, Kaminsky, R & Brun, R. (1997b). The Alamar Blue assay to determine drug sensitivity of African trypanosomes (*T.b. rhodesiense* and *T.b. gambiense*) in vitro. *Acta Trop*, **68**, 139-147.

Rodenko, B, Al-Salabi, MI, Teka, IA, Ho, W, El-Sabbagh, N, Ali, JAM, Ibrahim, HMS, Wanner, MJ, Koomen, GJ & de Koning, HP. (2011). Synthesis of marine-derived 3-alkylpyridinium alkaloids with potent antiprotozoal activity. *ACS Medicinal Chemistry Letters*.

Rodgers, J. (2009). Human African trypanosomiasis, chemotherapy and CNS disease. *J Neuroimmunol*, **211**, 16-22.

Ross, CA, Sutherland, DV, Hide, G, Mottram, JC, Coombs, GH & Holmes, PH. (1997). Drug resistance in trypanosomatids. *Trypanosomiasis and leishmaniasis: biology and control*, 259-269.

Ross, MF, Da Ros, T, Blaikie, FH, Prime, TA, Porteous, CM, Severina, II, Skulachev, VP, Kjaergaard, HG, Smith, RAJ & Murphy, MP. (2006). Accumulation of lipophilic dications by mitochondria and cells. *Biochemical Journal*, **400**, 199.

Rowen, RJ. (2002). *Townsend Letter for Doctors and Patients*.
<http://www.townsendletter.com/Dec2002/artemisinin1202.htm>.

RUIZ, SF, CASILLAS, J, PAREDES, M, VELAZQUEZ, J & RIEBELING, QB. (1952). [Terramycin in malaria therapy]. *Pan Am Med Womans J*, **59**, 10-15.

- Saleheen, D, Ali, SA, Ashfaq, K, Siddiqui, AA, Agha, A & Yasinzai, MM. (2002). Latent activity of curcumin against leishmaniasis in vitro. *Biol Pharm Bull*, **25**, 386-389.
- Salmon, D, Vanwalleghem, G, Morias, Y, Denoeud, J, Krumbholz, C, Lhomm+®, F, Bachmaier, S, Kador, M, Gossmann, J & Dias, FBS. (2012). Adenylate Cyclases of *Trypanosoma brucei* Inhibit the Innate Immune Response of the Host. *Science*.
- Schnauffer, A, Clark-Walker, GD, Steinberg, AG & Stuart, K. (2005). The F1-ATP synthase complex in bloodstream stage trypanosomes has an unusual and essential function. *EMBO J*, **24**, 4029-4040.
- Schumann, BG, Jutzi, P & Roditi, I. (2011). Genome-wide RNAi screens in bloodstream form trypanosomes identify drug transporters. *Mol Biochem Parasitol*, **175**, 91-94.
- Seifert, K & Croft, SL. (2006). In vitro and in vivo interactions between miltefosine and other antileishmanial drugs. *Antimicrob Agents Chemother*, **50**, 73-79.
- Shahi, SK, Krauth-Siegel, RL & Clayton, CE. (2002). Overexpression of the putative thiol conjugate transporter TbMRPA causes melarsoprol resistance in *Trypanosoma brucei*. *Mol Microbiol*, **43**, 1129-1138.
- Sharma, RA, Gescher, AJ & Steward, WP. (2005a). Curcumin: the story so far. *Eur J Cancer*, **41**, 1955-1968.
- Sharma, RA, Gescher, AJ & Steward, WP. (2005b). Curcumin: the story so far. *Eur J Cancer*, **41**, 1955-1968.
- Simarro, PP, Diarra, A, Ruiz Postigo, JA, Franco, JR & Jannin, JG. (2011). The human African trypanosomiasis control and surveillance programme of the World Health Organization 2000-2009: the way forward. *PLoS Negl Trop Dis*, **5**, e1007.
- Simarro, PP, Franco, J, Diarra, A, Postigo, JA & Jannin, J. (2012). Update on field use of the available drugs for the chemotherapy of human African trypanosomiasis. *Parasitology*, **139**, 842-846.
- Singh, RK, Pandey, HP & Sundar, S. (2006). Visceral leishmaniasis (kala-azar): challenges ahead. *Indian J Med Res*, **123**, 331-344.
- Sleigh, MJ. (1976). The mechanism of DNA breakage by phleomycin in vitro. *Nucleic Acids Res*, **3**, 891-901.
- Smilkstein, MJ, Kulig, KW & Rumack, BH. (1987). Acute toxic blindness: unrecognized quinine poisoning. *Ann Emerg Med*, **16**, 98-101.
- Smith, RA & Murphy, MP. (2010). Animal and human studies with the mitochondria-targeted antioxidant MitoQ. *Ann N Y Acad Sci*, **1201**, 96-103.
- Soignet, SL, Tong, WP, Hirschfeld, S & Warrell, RP, Jr. (1999). Clinical study of an organic arsenical, melarsoprol, in patients with advanced leukemia. *Cancer Chemother Pharmacol*, **44**, 417-421.

- Stock, BH, Bend, JR & Eling, TE. (1986). The formation of styrene glutathione adducts catalyzed by prostaglandin H synthase. A possible new mechanism for the formation of glutathione conjugates. *Journal of Biological Chemistry*, **261**, 5959.
- Strickler, JE & Patton, CL. (1975). Adenosine 3',5'-monophosphate in reproducing and differentiated trypanosomes. *Science*, **190**, 1110-1112.
- Stuart, K, Brun, R, Croft, S, Fairlamb, A, Gurtler, RE, McKerrow, J, Reed, S & Tarleton, R. (2008). Kinetoplastids: related protozoan pathogens, different diseases. *J Clin Invest*, **118**, 1301-1310.
- Sugimoto, K, Hanai, H, Tozawa, K, Aoshi, T, Uchijima, M, Nagata, T & Koide, Y. (2002). Curcumin prevents and ameliorates trinitrobenzene sulfonic acid-induced colitis in mice. *Gastroenterology*, **123**, 1912-1922.
- Sundar, S. (2001). Drug resistance in Indian visceral leishmaniasis. *Trop Med Int Health*, **6**, 849-854.
- Sundar, S, Jha, TK, Thakur, CP, Engel, J, Sindermann, H, Fischer, C, Junge, K, Bryceson, A & Berman, J. (2002). Oral miltefosine for Indian visceral leishmaniasis. *N Engl J Med*, **347**, 1739-1746.
- Sundar, S, Rai, M, Chakravarty, J, Agarwal, D, Agrawal, N, Vaillant, M, Oliaro, P & Murray, HW. (2008). New treatment approach in Indian visceral leishmaniasis: single-dose liposomal amphotericin B followed by short-course oral miltefosine. *Clin Infect Dis*, **47**, 1000-1006.
- Tabor, CW & Tabor, H. (1984). Polyamines. *Annu Rev Biochem*, **53**, 749-790.
- Tagboto, S & Townson, S. (2001). Antiparasitic properties of medicinal plants and other naturally occurring products. *Adv Parasitol*, **50**, 199-295.
- Taladriz, A, Healy, A, Flores Peñúñez, EJ, Herrero Garcíüa, V, Riüos Martiüñez, C, Alkhaldi, AAM, Eze, AA, Kaiser, M, de Koning, HP & Chana, A. (2012). Synthesis and Structure-Activity Analysis of New Phosphonium Salts with Potent Activity against African Trypanosomes. *Journal of Medicinal Chemistry*.
- TDR. (2002). Sixteenth Programme Report, Progress 2001-2002. Geneva: WHO.
- TDR. (2009). Tropical disease research annual report. WHO.
- Teka, IA, Kazibwe, AJ, El-Sabbagh, N, Al-Salabi, MI, Ward, CP, Eze, AA, Munday, JC, Maser, P, Matovu, E, Barrett, MP & de Koning, HP. (2011). The diamidine diminazene aceturate is a substrate for the high-affinity pentamidine transporter: implications for the development of high resistance levels in trypanosomes. *Mol Pharmacol*, **80**, 110-116.
- Tevis, DS, Kumar, A, Stephens, CE, Boykin, DW & Wilson, WD. (2009). Large, sequence-dependent effects on DNA conformation by minor groove binding compounds. *Nucleic Acids Res*, **37**, 5550-5558.

Thakur, CP, Kanyok, TP, Pandey, AK, Sinha, GP, Zaniewski, AE, Houlihan, HH & Olliaro, P. (2000). A prospective randomized, comparative, open-label trial of the safety and efficacy of paromomycin (aminosidine) plus sodium stibogluconate versus sodium stibogluconate alone for the treatment of visceral leishmaniasis. *Trans R Soc Trop Med Hyg*, **94**, 429-431.

Van Der Meide, WF, Sabajo, LOA, Jensema, AJ, Peekel, I, Faber, WR, Schallig, HDFH & Fat, RFM. (2009). Evaluation of treatment with pentamidine for cutaneous leishmaniasis in Suriname. *International journal of dermatology*, **48**, 52-58.

Van Voorhis, WC. (1990). Therapy and prophylaxis of systemic protozoan infections. *Drugs*, **40**, 176-202.

van Weelden, SWH, Fast, B, Vogt, A, van der Meer, P, Saas, J, van Hellemond, JJ, Tielens, AGM & Boshart, M. (2003). Procyclic *Trypanosoma brucei* do not use Krebs cycle activity for energy generation. *Journal of Biological Chemistry*, **278**, 12854-12863.

van Zandbergen, G, Linder, CGK, Heussler, V & Duszenko, M. (2010). Programmed cell death in unicellular parasites: a prerequisite for sustained infection? *Trends in parasitology*, **26**, 477-483.

Vickerman, K. (1985). Developmental cycles and biology of pathogenic trypanosomes. *British medical bulletin*, **41**, 105-114.

Vickerman, K, Myler, PJ & Stuart, KD. (1993). African trypanosomiasis.. ed. 3.

Vickerman, K. (1974). The Ultrastructure of Pathogenic Flagellates. In *Ciba Foundation Symposium 20 - Trypanosomiasis and Leishmaniasis (with Special Reference to Chagas' Disease)*. pp. 171-198. John Wiley & Sons, Ltd..

Vincent, IM, Creek, D, Watson, DG, Kamleh, MA, Woods, DJ, Wong, PE, Burchmore, RJ & Barrett, MP. (2010). A molecular mechanism for eflornithine resistance in African trypanosomes. *PLoS Pathog*, **6**, e1001204.

Vincent, IM, Creek, DJ, Burgess, K, Woods, DJ, Burchmore, RJ & Barrett, MP. (2012). Untargeted Metabolomics Reveals a Lack Of Synergy between Nifurtimox and Eflornithine against *Trypanosoma brucei*. *PLoS Negl Trop Dis*, **6**, e1618.

Visser, N & Opperdoes, FR. (1980). Glycolysis in *Trypanosoma brucei*. *Eur J Biochem*, **103**, 623-632.

Wadhone, P, Maiti, M, Agarwal, R, Kamat, V, Martin, S & Saha, B. (2009). Miltefosine promotes IFN-gamma-dominated anti-leishmanial immune response. *J Immunol*, **182**, 7146-7154.

Walter, RD, Nordmeyer, JP & Konigk, E. (1974). Adenylate cyclase from *Trypanosoma gambiense*. *Hoppe Seylers Z Physiol Chem*, **355**, 427-430.

Wang, CC. (1995). Molecular mechanisms and therapeutic approaches to the treatment of African trypanosomiasis. *Annu Rev Pharmacol Toxicol*, **35**, 93-127.

- Wang, YJ, Pan, MH, Cheng, AL, Lin, LI, Ho, YS, Hsieh, CY & Lin, JK. (1997). Stability of curcumin in buffer solutions and characterization of its degradation products. *J Pharm Biomed Anal*, **15**, 1867-1876.
- Ward, CP, Wong, PE, Burchmore, RJ, de Koning, HP & Barrett, MP. (2011). Trypanocidal furamidine analogues: influence of pyridine nitrogens on trypanocidal activity, transport kinetics, and resistance patterns. *Antimicrob Agents Chemother*, **55**, 2352-2361.
- Warren, KS & Mahmoud, AAF. (1984). *Tropical and geographical medicine*. McGraw-Hill.
- Welburn, SC, Fevre, EM, Coleman, PG, Odiit, M & Maudlin, I. (2001). Sleeping sickness: a tale of two diseases. *Trends Parasitol*, **17**, 19-24.
- White, NJ. (2004). Antimalarial drug resistance. *J Clin Invest*, **113**, 1084-1092.
- WHO. (1995). Model Prescribing Information: Drugs Used in Parasitic Diseases, 2nd Edition
Parasitic Diseases. Geneva: WHO.
- WHO. (2007). Report on Leishmaniasis and HIV co-infection. Geneva. World Health Organisation.
- WHO. (2010). Control of the Leishmaniases, Report of a meeting of the WHO export committee. Geneva.
- Wilairatana, P, Chanthavanich, P, Singhasivanon, P, Treeprasertsuk, S, Krudsood, S, Chalermrut, K, Phisalaphong, C, Kraisintu, K & Looareesuwan, S. (1998). A comparison of three different dihydroartemisinin formulations for the treatment of acute uncomplicated falciparum malaria in Thailand. *Int J Parasitol*, **28**, 1213-1218.
- Wolf, LR, Otten, EJ & Spadafora, MP. (1992). Cinchonism: two case reports and review of acute quinine toxicity and treatment. *J Emerg Med*, **10**, 295-301.
- Xiao, Y, McCloskey, DE & Phillips, MA. (2009). RNA interference-mediated silencing of ornithine decarboxylase and spermidine synthase genes in *Trypanosoma brucei* provides insight into regulation of polyamine biosynthesis. *Eukaryot Cell*, **8**, 747-755.
- Yakuob, AA, Gustafsson, LL, Ericsson, O & Hellgren, U. (1995). *Handbook of Drugs for Tropical Parasitic Infections*. Taylor and Francis Publication: UK.
- Yardley, V & Croft, SL. (2000). A comparison of the activities of three amphotericin B lipid formulations against experimental visceral and cutaneous leishmaniasis. *Int J Antimicrob Agents*, **13**, 243-248.
- Yarlett, N, Goldberg, B, Nathan, HC, Garofalo, J & Bacchi, CJ. (1991). Differential sensitivity of *Trypanosoma brucei* rhodesiense isolates to in vitro lysis by arsenicals. *Exp Parasitol*, **72**, 205-215.
- Yi, ZB, Yan, Y, Liang, YZ & Bao, Z. (2007). Evaluation of the antimicrobial mode of berberine by LC/ESI-MS combined with principal component analysis. *J Pharm Biomed Anal*, **44**, 301-304.

Yun, O, Priotto, G, Tong, J, Flevaud, L & Chappuis, F. (2010). NECT is next: implementing the new drug combination therapy for *Trypanosoma brucei* gambiense sleeping sickness. *PLoS neglected tropical diseases*, **4**, e720.

Zhou, J, Shen, J, Liao, D, Zhou, Y & Lin, J. (2004). Resistance to drug by different isolates *Trypanosoma evansi* in China. *Acta Trop*, **90**, 271-275.